Clinical Utility of Molecular Subtyping of Pancreatic Cancer

Stephan Ben Dreyer

BMSc, MBChB, MRCS

Submitted in fulfilment of the requirements for the Degree of Doctor of Philosophy

Wolfson Wohl Cancer Research Centre

Institute of Cancer Sciences

College of Medical, Veterinary and Life Sciences

University of Glasgow

December 2018

Abstract

Background: Pancreatic Cancer remains a dismal disease with the worst survival outcomes of any solid organ malignancy. The most common form is Pancreatic Ductal Adenocarcinoma (PDAC) which has a 5-year survival of only 5% and a median survival in the region of 6 months after diagnosis. The majority of patients present with metastatic or locally advanced disease that is unsuitable for surgical resection. The only potential curative treatment is surgery, yet only around 15 – 20% of patients undergo surgical resection. Of these, half of patients develop disease recurrence at 1 year, and only around 20% survive 5 years after surgery. These figures demonstrate that current treatment strategies are inadequate and better therapies and treatment selection tools are urgently needed.

Recent large-scale next generation sequencing studies of pancreatic cancer have revealed a small set of consistent mutations found in most pancreatic cancer genomes, and beyond that a low prevalence of targetable mutations for current therapies. Transcriptomic analysis has revealed molecular subtypes with significant differences in gene expression and molecular pathways. This may explain the failure of conventional clinical trial designs to show any meaningful survival benefit, except in small and undefined patient sub-groups. With the development of next generation sequencing technology, genomic sequencing and analysis can be performed in a clinically meaningful turnaround time. This can identify therapeutic targets in individual patients and personalise treatment selection. Incorporating pre-clinical discovery and molecularly guided therapy into clinical trial design has the potential to significantly improve outcomes in this lethal malignancy.

Aims: The aims of this PhD thesis are: 1. examine the clinical and pathological features of molecular subtypes of PDAC to identify novel biomarkers to select patients for surgical resection; 2. investigate therapeutic opportunities targeting DNA damage response machinery; and 3. develop clinical strategies to translate these findings into personalised clinical trials.

Results: Early recurrence after surgery, particularly liver metastases, and metastatic presentation were strongly associated with gene expression sets that define the squamous subtype of PDAC *(P* < 0.001). Lung recurrence, localised disease and long-term survival were associated with the classical pancreatic subtype and an anti-tumour immune response *(P* < 0.001). Patients with tumours of the body and tail of pancreas had

significantly worse survival than those with pancreatic head tumours (12.1 *versus* 22.0 months; $P = 0.001$). Location in the body and tail was associated with the squamous subtype of PDAC. Body and tail PDACs are enriched for gene programmes involved in tumour invasion and epithelial-to-mesenchymal transition, as well as features of poor antitumour immune response.

In three independent PDAC cohorts (total participants = 1184) the relationship between aberrant expression of pro-metastatic proteins S100A2 and S100A4 and survival was assessed. High expression of either S100A2 or S100A4 were independent poor prognostic factors in a training cohort of 518 participants and two independent validation cohorts (Glasgow, $n = 198$; German, $n = 468$). A preoperative nomogram incorporating S100A2 and S100A4 expression predicted survival as well as nomograms derived using post-operative clinicopathological variables.

DNA damage response (DDR) deficient cell lines and xenograft models were highly sensitive to Cisplatin and PARP inhibitors. A novel transcriptional signature of replication stress was generated and associated with the squamous subtype in both cell lines and bulk tumour samples. This signature predicted differential responses to cell cycle inhibitors of ATR, WEE1, CHK1, CDK4/6 and PLK4. Response to these inhibitors were independent of DDR status, but strongly associated with replication stress. These findings were used to inform the design of a phase Ib / II clinical trial targeting DDR deficiency and Replication Stress using PARP and ATR inhibitors in PDAC. A tissue acquisition protocol using endoscopic ultrasound guided biopsies for next generation sequencing was designed and allowed multi-omic characterisation of PDAC. This has been implemented within the *PRECISION-Panc* master protocol to allow molecular profiling of all patients, irrespective of disease stage, and facilitate precision medicine trials in PDAC.

Conclusions: Significant phenotypic differences exist between molecular subtypes of PDAC and these differences informed the design of novel selection tools for surgical resection. Proof of concept data demonstrates DDR deficiency and increased Replication Stress to be attractive targets in PDAC. Therapeutic vulnerabilities extend beyond platinum chemotherapy and can be targeted with novel small molecule inhibitors, with independent biomarkers that predict response to agents targeting either DDR or replication stress. This has led to the design and development of personalised medicine trials via the *PRECISION-Panc* platform targeting DDR and Replication stress that will open in early 2019.

Table of Contents

List of Tables

List of Figures

List of Publications

Publications directly resulting from this thesis

Dreyer SB, *et al.* Precision Oncology in Surgery: Patient selection for operable Pancreatic Cancer. *Annals of Surgery. Accepted November 2018* **[IF 9.2]**

Dreyer SB, *et al*. Defining the molecular pathology of pancreatic body and tail adenocarcinoma. *British journal of Surgery. 2018. 105:2. E183 – 191.* **[IF 5.9]**

Dreyer SB, Chang DK, Bailey P, Biankin AV. Pancreatic Cancer Genomes: Implications for clinical management and therapeutic development. *Clin Cancer Res. 2017 Apr 1;23(7):1638-164* **[IF 10.2]**

Preface

Pancreatic Ductal Adenocarcinoma (PDAC) remains a highly lethal malignancy with as few as 7% of patients surviving 5 years after diagnosis. There has been little progress over the last 5 decades in the management of the disease, with only a small number of clinical studies demonstrating incremental therapeutic benefit. Recently, however, the 'omics' revolution has led to an unprecedented wealth of knowledge into the molecular pathology of cancer. Next-generation sequencing of large cohorts of patients, along with in-depth molecular characterisation of representative pre-clinical models, has started to reveal key molecular processes and therapeutic opportunities in PDAC. Yet, this progress is still to make any significant clinical impact and improve survival rates and quality of life for patients.

Molecular subtyping of cancer has been widely adopted in an attempt to generate insights into different clinical disease patterns of histologically indistinguishable tumour subtypes. Recent molecular characterisation of PDAC revealed that there exist unique molecular subtypes of the disease, associated in part with histological variants. Molecular subtyping is only of benefit if it informs patient management strategies or therapeutic development. Furthermore, the clinical spectrum of the disease varies greatly. For example, patients with metastatic disease can present with rapidly progressive disease (often in the context of liver metastases), whereas patients with lung metastases can have significantly more indolent disease progression. There are molecular mechanisms likely underpinning these observations that, to date, have not been explored, explained or exploited.

This thesis aims to begin to close the gap between our understanding of the molecular pathology of PDAC and how it relates to clinical disease patterns and therapeutic opportunities within the disease. This was approached by building on the large molecular and clinical data generated as part of the International Cancer Genome Consortium's Pancreatic Cancer project, led by the Australian Pancreatic Genome Initiative. By overlaying prospectively collected clinical data with in-depth molecular analyses, this piece of work aims to build on next generation sequencing data to improve the clinical management of PDAC and define therapeutic strategies for patients that can rapidly be translated into clinical practice to impact patient outcomes.

The first results chapter explores the clinicopathological phenotypes of molecular subtypes of pancreatic cancer in order to relate different clinical disease patterns with underlying

tumour biology. This was performed by examining genomic and transcriptomic features of tumours that are associated with different recurrence patterns following surgery or disease stage at time of presentation in $n = 456$ participants. This was further investigated by addressing the different outcomes seen clinically in tumours of the tail of the pancreas compared to head by investigating the difference in transcriptomic profiles between these groups.

Chapter 4 investigates the concept of 'biologically borderline resectable' PDAC by identifying molecular features of poor prognosis and early recurrence following resection. By building on data generated in the previous section, biomarkers of poor prognosis, associated with clinically relevant molecular subtypes are identified. These are investigated as predictive biomarkers in 1184 patients who underwent surgery for pancreatic cancer and a pre-operative prognostic nomogram that predicts early recurrence was generated and validated.

Chapter 5 builds on the incremental benefits seen in platinum-based chemotherapy and explores therapeutic response biomarkers targeting DNA damage response deficiency. A novel signature of Replication Stress is generated and applied as a predictive therapeutic response biomarker for novel targeted agents. The association between DNA damage repair deficiency, replication stress and molecular subtypes are examined, which generates a therapeutic hypothesis to target these sub-groups of patients. This has led to the design of a Phase Ib / II trial investigating the clinical response of a combination of agents targeting DNA damage repair deficiency and replication stress in metastatic disease, of which the PhD candidate is a principal investigator.

Chapter 6 and 7 address the challenges of molecular profiling for all patients with pancreatic cancer in a clinically relevant manner to inform personalised treatment. By designing and implementing an endoscopic ultrasound guided biopsy protocol, all patients irrespective of disease stage can undergo profiling with success rates that are clinically acceptable. This has been adopted in numerous centres across the United Kingdom to allow patient enrolment into the *PRECISION-Panc* master protocol and allow entry into precision oncology clinical trials. The work presented in this thesis has thus far contributed to 3 peer-reviewed publications in high impact clinical and scientific journals. Most importantly, the impact of this thesis is demonstrated by the translation of numerous concepts generated from this body of work into clinical trials via the *PRECISION-Panc* clinical trial platform, of which the thesis author is a co-investigator.

Acknowledgement

The work presented in this thesis was undertaken at the Institute of Cancer Sciences, Wolfson Wohl Cancer Research Centre, University of Glasgow; and the West of Scotland Pancreatic Unit, Glasgow Royal Infirmary.

This work would not have been possible without a Clinical Research Fellowship award from Cancer Research UK (Clinical Training Award: C596/A20921). My utmost gratitude and thanks go to the countless volunteers and donors that selflessly raises funds every day to provide the medical science community with the financial backing required.

I would like to thank my colleagues at both the Wolfson Wohl Cancer Research Institute and Glasgow Royal Infirmary for their support and encouragement over the last 4 years. I am very grateful for the mentorship and support from Mr Nigel Jamieson and Professor Colin McKay over the last 4 years. In the lab, I am extremely grateful for the help and advice provided by Viola Paulus-Hock, Eirini Lampraki, Rosie Upstill Goddard, Marc Jones, Kim Moran-Jones, Liz Musgrove, Lisa Evers, Jen Morton, Dario Beraldi, Susie Cooke, Derek Wright, John Marshall, Sancha Martin, Giussy Caligiuri, Dr Fraser Duthie and all the staff at the Beatson BSU/BRU. I am very grateful for the support of The Glasgow Precision Oncology Laboratory and NHS GGC biorepository for their support in sample processing and sequencing. I would also like to thank Judith Dixon, and the other members of the *PRECISION-Panc* collaborative, for the hard work and dedication to translate some of the findings from this thesis into clinical trials for patients.

A special thank you to the staff members of the Endoscopy unit and Theatre E at Glasgow Royal Infirmary for the enthusiasm, support, phone calls, tissue samples and countless blood samples over the last 4 years. I would also like to thank the clinical members of the West of Scotland Pancreatic Unit for their continued advice and clinical support, especially Mr Euan Dickson, Mr Ross Carter, Mr Kyle Mitchell and Sister Elspeth Cowan.

I am very grateful for the unfailing support of my supervisors, Dr David Chang and Prof Andrew Biankin. A special thanks for providing me with the opportunity and guidance not just to perform the work presented in thesis, but more importantly to see the bigger picture.

I would like to use this opportunity thank my family and friends for their support, not just in the last 4 years, but throughout my career. A special thanks to Ben, Alix, Richard and

Frieda-Elsje for your love and support over the years. A special mention to Joshua and Luke, who with the help of a little bit of dry ice, has been the only family members I've convinced that science can be fun! To my parents, Ma and Pa, who have provided me with countless opportunities even when it means standing by the side of a rugby pitch in the cold rain every Saturday. I am especially grateful for the values of hard work and resilience and the passion you have inspired to make other people's lives better. A special mention my grandfather, Oupa Ben, who has inspired the surgeon-scientist philosophy in me and my late aunt Marietjie, who made me realise that just because a problem is challenging doesn't mean it's not worth solving.

Suzanne, thank you for your amazing support, encouragement and understanding over the last 4 years. Thanks for the great (work) trips and adventures. Without your help this would not have been possible. Isla, thank you for being the best thing ever.

Author's Declaration

I declare that I am the sole author if this thesis. The work presented here is my own, unless otherwise acknowledged. This thesis has not been submitted for a degree or diploma at any other institution.

Stephan B Dreyer

December 2018

Definitions/Abbreviations

5-FU	5-fluorouracil
°C	Degrees Celsius
ADEX	aberrantly differentiated endocrine exocrine
AJCC	American Joint Committee on Cancer
APGI	Australian Pancreatic Genome Initiative
ATM	Ataxia Telangiectasia Mutated
ATR	Ataxia Telangiectasia and Rad3 related
BRCA	breast cancer (1 / 2) susceptibility protein
BTPC	body and tail pancreatic cancer
CA 19-9	carbohydrate antigen 19-9
CDK4/6	cyclin-dependant kinases 4/6
Chk1	checkpoint kinase 1
COSMIC	catalogue of somatic mutations in human cancer
CTLA-4	cytotoxic T-lymphocyte associated protein 4
DDR	DNA damage response
DNA	deoxyribonucleic acid
DP	distal pancreatectomy
DSB	double strand DNA break
DSS	disease specific survival
ECOG	Eastern cooperative oncology group
EDTA	Ethylenediaminetetraacetic acid
EMT	epithelial to mesenchymal transition
EUS	endoscopic ultrasound
FFPE	formalin fixed, paraffin embedded
FNA	fine needle aspirate
G	gravity
g	gram
GPOL	Glasgow Precision Oncology Laboratory
γH2AX	gamma H2AX
GP	gene programme
Gy	gray
H&E	Haematoxylin and Eosin
HRD	homologous recombination deficient
KRAS	Kirsten rat sarcoma viral oncogene homolog
ICGC	International Cancer Genome Consortium
IPMN	intraductal papillary mucinous neoplasm
L	litre
LAPC	locally advanced pancreatic cancer
M	milli
MDT	multi-disciplinary team
MMR	DNA mismatch repair
n	nano

NGS	next generation sequencing
PANiN	pancreatic intra-epithelial neoplasm
PARP	poly ADP ribose polymerase
PBS	phosphate buffered saline
PC	pancreatic cancer
PD-1	programmed death-1
PD-L1	programmed death ligand-1
PDAC	pancreatic ductal adenocarcinoma
PDCL	patient derived cell line
PDX	patient derived xenograft
PLK4	polo like kinase 4
PNET	Pancreatic neuroendocrine tumour
PRIMUS	pancreatic cancer individualised multi-arm umbrella study
PS	performance status
RNA	ribonucleic acid
RNAseq	RNA sequencing
RPA	replication protein A
S100A2	S100 calcium binding protein A2
S100A4	S100 calcium binding protein A4
SSB	single strand DNA break
ssDNA	single stranded DNA
TNM	Tumour, lymph Node and Metastasis classification of malignant tumours
WEE1	WEE1 G2 checkpoint kinase
WGS	whole genome sequencing
μ	micro

1 Introduction

1.1 Pancreatic Cancer

1.1.1 Disease Burden

Despite significant advances in many common cancers, pancreatic cancer (PC) remains a highly lethal malignancy with almost no improvement in survival for the past 5 decades. PC is currently the 10th most common cancer in Western societies and has overtaken breast cancer to become the 3rd leading cause of cancer death in 2018 (Siegel et al., 2018). Malignancies of the pancreas can be divided into those of exocrine and endocrine cancers depending on the cell of origin. This thesis focuses on the highly lethal cancers of exocrine origin, pancreatic ductal adenocarcinoma (PDAC) and its variants, which constitutes > 90% of pancreatic cancer.

The almost universal fatality of the disease and recalcitrance to therapy, has led to PC to become a major research priority. Currently, around 9900 patients are diagnosed with PC annually in the United Kingdom, with 9200 deaths per annum (Figure 1-1) (CRUK, 2018). As a result, only around 5 – 7% of patients survive 5 years after diagnosis (Garrido-Laguna and Hidalgo, 2015, Hidalgo, 2010, Dreyer et al., 2017). The current median survival for metastatic disease is only 6 – 9 months, depending on the patient's performance status and ability to tolerate cytotoxic chemotherapy (Hidalgo, 2010, Garrido-Laguna and Hidalgo, 2015). These statistics highlight the fact that PC remains the most lethal solid organ malignancy, and progress in this disease lags behind other more common cancers such as lung, breast and colorectal.

Estimated New Cases

Males			Females		
Prostate	164,690	19%	Breast	266,120	30%
Lung & bronchus	121,680	14%	Lung & bronchus	112,350	13%
Colon & rectum	75,610	9%	Colon & rectum	64,640	7%
Urinary bladder	62,380	7%	Uterine corpus	63,230	7%
Melanoma of the skin	55,150	6%	Thyroid	40,900	5%
Kidney & renal pelvis	42,680	5%	Melanoma of the skin	36,120	4%
Non-Hodgkin lymphoma	41,730	5%	Non-Hodgkin lymphoma	32,950	4%
Oral cavity & pharynx	37,160	4%	Pancreas	26,240	3%
Leukemia	35,030	4%	Leukemia	25,270	3%
Liver & intrahepatic bile duct	30,610	4%	Kidney & renal pelvis	22,660	3%
All Sites	**856,370**	**100%**	**All Sites**	**878,980**	**100%**

Estimated Deaths

Males			Females		
Lung & bronchus	83,550	26%	Lung & bronchus	70,500	25%
Prostate	29,430	9%	Breast	40,920	14%
Colon & rectum	27,390	8%	Colon & rectum	23,240	8%
Pancreas	23,020	7%	Pancreas	21,310	7%
Liver & intrahepatic bile duct	20,540	6%	Ovary	14,070	5%
Leukemia	14,270	4%	Uterine corpus	11,350	4%
Esophagus	12,850	4%	Leukemia	10,100	4%
Urinary bladder	12,520	4%	Liver & intrahepatic bile duct	9,660	3%
Non-Hodgkin lymphoma	11,510	4%	Non-Hodgkin lymphoma	8,400	3%
Kidney & renal pelvis	10,010	3%	Brain & other nervous system	7,340	3%
All Sites	**323,630**	**100%**	**All Sites**	**286,010**	**100%**

Figure 1-1 Top 10 Cancer types by incidence and estimated deaths in the USA, 2018. Pancreatic Cancer is believed to become the 3rd most common cause of cancer death in Western Societies in 2018. Adapted from Siegel *et al.* (Siegel et al., 2018)

1.1.2 Pancreatic Anatomy and Physiology

The pancreas is a relatively inaccessible retroperitoneal organ, situated behind the stomach and surrounded by major vascular structures such as the portal vein. It is sub-divided into the head, neck, body and tail with the uncinate process extending from the head. Originally derived from embryonic endoderm, the pancreas is a mixed endocrine and exocrine gland with important homeostatic functions. The majority of the pancreatic parenchyma consists of cells involved in exocrine function and are arranged in lobular acini that drain into a ductal system. Endocrine cells such as the glucagon-producing alpha and insulin producing beta cells are scattered throughout in areas known as the islets of Langerhans. This thesis is focused on cancer of the exocrine pancreas (PDAC) which is thought to originate from exocrine cells.

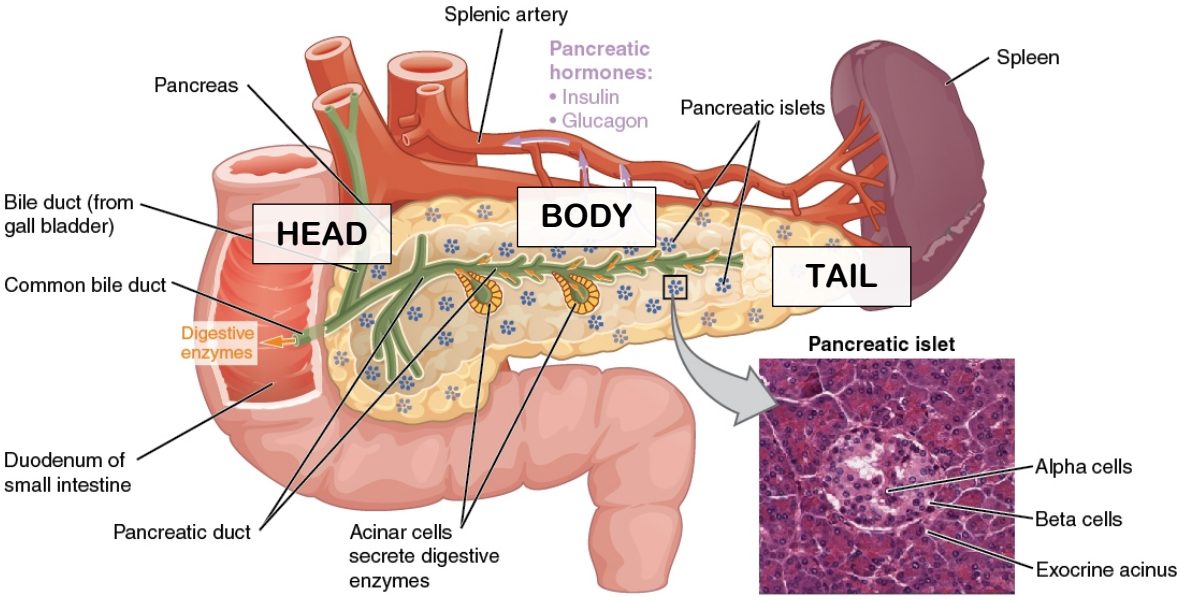

Figure 1-2 Anatomy of the Pancreas. Acinar cells secrete enzymes crucial for digestion and is secreted via the ductal system into the duodenum. Pancreatic islets are scattered throughout the pancreatic parenchyma and produces endocrine hormones such as insulin. *Adapted from Boora.info Human Anatomy reference.*

1.1.3 Pathophysiology of PDAC development

Studies in humans and genetically engineered mouse models (GEMMs) have revealed 3 common routes of PDAC development from pre-invasive lesions (Maitra et al., 2005). These includes Pancreatic Intraepithelial Neoplasm (PanIN), Intra-Ductal Papillary Mucinous Neoplasm (IPMN) and Mucinous Cystic Neoplasms (MCN). The most common route is via the gradual accumulation of genetic and histological features of PDAC via PanIN (Hruban et al., 2005, Maitra et al., 2005). These undergo gradual morphological progression from PanIN-1A, B, PanIN-2 and PanIN-3 (carcinoma-in-situ) (Hruban et al., 2005, Maitra et al., 2005). Studies in GEMMs have revealed that this progression is coupled with mutations in key cancer genes such as *KRAS* and *TP53* (Hingorani et al., 2003). Development of PDAC via IPMN appears to be more complex, and the majority of IPMNs do not progress to invasive malignancy. The underlying genomic mechanisms that differ during the development of IPMN PDAC are still to be fully delineated but may involve different epigenetic profiles to that of PDAC derived from PanINs (Roy et al., 2015). Furthermore, there is growing evidence that IPMN is associated with a global 'field-change' in the pancreatic duct, and that PDAC can originate out with the IPMN (Felsenstein et al., 2018).

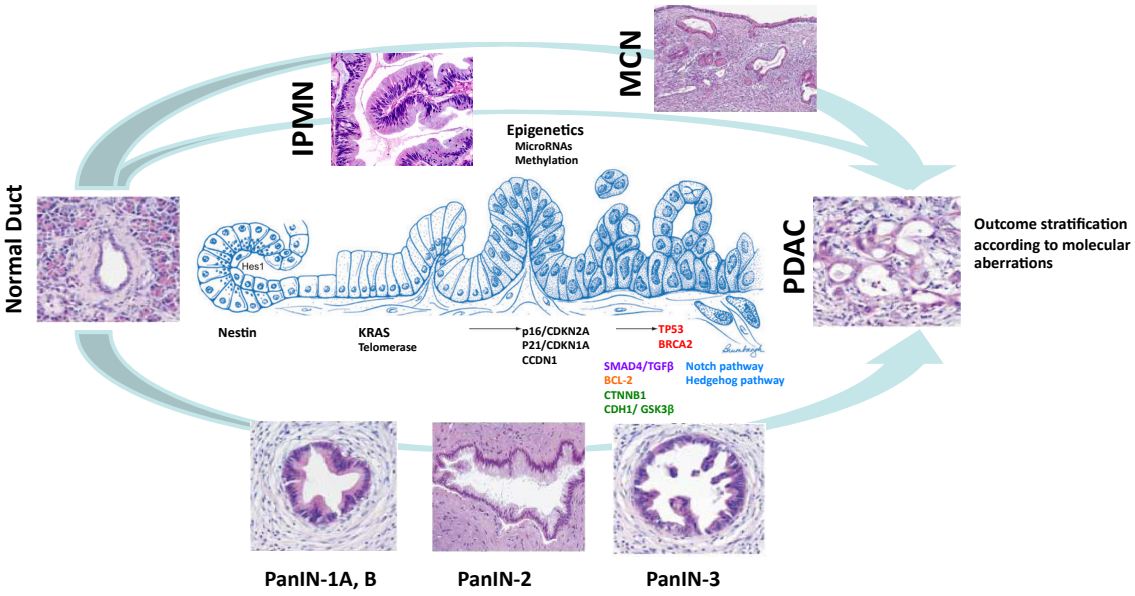

Figure 1-3 Development of PDAC from pre-invasive lesions. PDAC develops most commonly via the PanIN stepwise progression model with gradual accumulation of genetic and morphological features. The earliest genetic event is believed to be activating oncogenic *KRAS* mutations, followed by mutations in *CDKN2A*, *TP53* and loss of *SMAD4*. IPMN and MCN associated PDAC develops via different morphological pathways, but often share similar genetic mutations. Epigenetic modification of gene expression has significant impact on the molecular and phenotypic subtype of the tumour and is addressed in this thesis. Adapted from (Hruban et al., 2000)

1.1.4 Diagnosis

Current diagnosis of PDAC is usually achieved using cross-sectional non-invasive imaging with histological confirmation using samples obtained at endoscopic ultrasonography (EUS), or occasionally endoscopic retrograde cholangiopancreatography (ERCP). Most patients will be referred for transabdominal ultrasound (USS) or computed tomography (CT) if PDAC is suspected. Standard non-invasive USS is of limited value in the majority of patients, but can demonstrate an obstructed biliary tree, which in the absence of cholelithiasis is highly suggestive of malignancy. Contrast-enhanced multi-dimensional CT is the gold standard imaging procedure in suspected PDAC. A pancreas specific protocol can achieve accurate diagnosis in up to 97% of cases (Catalano et al., 2003, Chang et al., 2009b). Magnetic resonance imaging (MRI) can be a useful tool in patients with cystic disease of the pancreas, or in those where a contrast allergy prevents CT imaging with contrast (Hanninen et al., 2005).

Patients with suspected or proven neoplasms following cross-sectional imaging can undergo invasive imaging (EUS) with accompanying histological assessment to confirm

diagnosis (Chang et al., 2009b). This is currently recommended for all patients with suspected PDAC in the UK, to ensure accurate diagnosis prior to morbid treatments such as surgery or systemic chemotherapy. EUS allows accurate visualisation of the pancreas and biliary system, and characterisation of lesions, cysts and other abnormalities with high specificity and sensitivity, even in small tumours (Chang et al., 2009b). The recent development of fine needle core biopsies allows accurate histological diagnosis, whilst is facilitating more intricate molecular analyses of treatment naive PDAC (Valero et al., 2016, Bang et al., 2017, Artifon et al., 2017, Gleeson et al., 2016, Rodriguez et al., 2016). This is beginning to open the door for precision medicine strategies for patients with all stages of PDAC, but further refinement in biomarker and assay selection is required before this becomes widely utilised outside of clinical trials.

1.1.5 Treatment

Current treatment strategies for PDAC depends on the stage of the disease and the patient's performance status. Treatment decisions are made by a multidisciplinary team based upon multiple patient and tumour factors. The mainstay of therapy is surgery for the minor proportion of patients with localised, resectable disease. Systemic chemotherapy is used in the adjuvant, neoadjuvant and advanced disease settings. As of yet, individual tumour biology does not alter clinical decision making. This, however, is likely to change over the next decade, and this thesis is entirely focused on bridging the chasm between tumour biology and therapeutic selection in PDAC.

1.1.5.1 Surgical Management of PDAC

For PDAC, the only possibility of cure at present is surgical resection. However, only 20% of patients are deemed, based on cross-sectional imaging, to have operable disease. In reality, only 10 – 15% of patients undergo resection in most centres due to the rapid progression of the disease in some cases, and the morbidity associated with surgery resulting in many patients being unsuitable for resection (Hidalgo, 2010). Despite what is believed to be curative resection, 80% of patients will still succumb from PDAC, with around 50% developing recurrence within 1 year after surgery (Groot et al., 2017, Groot et al., 2018). This reflects a major treatment failure in these patients and suggests that many harbour metastatic disease at the time of surgery that is not detectable by current imaging modalities. Furthermore, surgery is associated with morbidity in around 40% of patients, and up to 50% of patients are unable to undergo systemic adjuvant chemotherapy post-surgery (Schniewind et al., 2006). This in turn leaves any micro metastatic disease

untreated and leads to early recurrence. Currently there are no recognised biomarkers or prognostic tools in widespread clinical practice that predict those patients that will develop early recurrence prior to surgical resection, and thus many patients undergo morbid surgical procedures with little or no benefit. On the other hand, patients with good prognosis do benefit from surgical resection, even in the setting of locally advanced disease. These patients often do not undergo surgery due to the position of the tumour making surgery high risk or technically impossible, but can have long term survival benefit following surgical resection (Gemenetzis et al., 2018). Currently, clinical tools such as cross-sectional imaging do not provide the clinician with sufficient information regarding each patient's individual tumour biology, and thus molecular selection markers for surgery are urgently needed.

Surgical treatment depends on the anatomical location and stage of PDAC. The most common surgical procedure is the Whipple's pancreaticoduodenectomy (PD). Resection of the pancreatic head, duodenum and common bile duct (CBD) is performed in conjunction with pylorus-preserving or classical PD. This is followed by reconstruction, either with pancreaticojejunostomy or pancreaticogastrostomy. Patients with tumours of the body and tail are treated with distal, or left sided, pancreatectomy (DP) which requires no reconstruction. Occasionally, total pancreatectomy is required to achieve clear margins or if multiple lesions (e.g. IPMN) are found within the pancreas. This is, however, associated with significant mortality, up to 10%, even in high volume units (Hartwig et al., 2016, Kulu et al., 2009).

The major surgical challenges of PD and DP involve dissecting the pancreas and malignant tissue in its entirety from the major vessels safely and with tumour free margins. Margin involvement is a major prognostic indicator of poor survival in PDAC, and, in experienced centres, is likely a reflection of the tumour's biology rather than technical expertise (Chang et al., 2009a, Jamieson et al., 2010, Jamieson et al., 2013). Extended lymphadenectomy appears to have no survival benefit yet results in significantly increased morbidity (Tol et al., 2014). The most common complicating factor in PD is tumour involvement of the portal (PV) or superior mesenteric vein (SMV) requiring vascular resection and reconstruction. Due to the pancreas' anatomical location, tumours of the head and uncinate process commonly involve these vessels and may preclude surgical resection. However, if venous resection and reconstruction is performed this does not appear to significantly reduce long term survival and oncological outcomes but is associated with increased morbidity and mortality following surgery (Tseng et al., 2006). Tumours of the neck and

body often involve the coeliac axis and its branches and precludes resection in most patients. Arterial resection for PDAC is a controversial topic, but in selected patients with locally advanced disease this can lead to long term survival (Gemenetzis et al., 2018). However, this is associated with significantly increased morbidity and mortality (Hartwig et al., 2016, Gemenetzis et al., 2018). Thus, novel patient selection tools are crucial to avoid futile high-risk surgery, whilst offering patients with favourable prognosis the opportunity for survival benefit from surgical resection.

1.1.5.2 Neoadjuvant Therapy

Neoadjuvant therapy for PDAC is gaining popularity throughout many centres due to a number of clinical and biological factors. The high incidence of resection margin involvement in surgery for borderline resectable or locally advanced PDAC has led to attempts to reduce margin positivity through neoadjuvant chemo- and radiotherapy (Jamieson et al., 2013, Jamieson et al., 2010, Chang et al., 2009a). Numerous studies are demonstrating significant reduction in margin positivity following a period of neoadjuvant therapy and in patients with initial borderline resectable (BR) disease survival is similar as in resectable PDAC (Hidalgo, 2010, Gillen et al., 2010, Tang et al., 2016, He et al., 2018, Hackert et al., 2016, Gemenetzis et al., 2018, Murphy et al., 2018). Furthermore, initial results suggest neoadjuvant therapy has survival benefits in patients undergoing resection for PDAC (Mokdad et al., 2017, He et al., 2018, Murphy et al., 2018). This is particularly the case for those with near complete or complete pathological response to therapy (Chatterjee et al., 2012, Zhao et al., 2012, Chun et al., 2011, He et al., 2018). Treatment of micro metastatic disease prior to surgery allows systemic control, whilst ensuring that the majority of patients can complete therapy. Only 50% of patients complete adjuvant chemotherapy due to the morbidity and long recovery period of surgery, and thus administering systemic therapy prior to surgery has advantages in a tumour type that for the majority of patients is systemic from early in the disease process (Schniewind et al., 2006). Furthermore, the period of neoadjuvant therapy allows a course of ‘biological’ selection during which patients with aggressive and significant systemic disease will progress and manifest as metastatic or locally aggressive disease. Thereby, reducing resection rates in cases where surgery is likely futile, and instead concentrated on patients that are most likely to benefit.

The enthusiasm for neoadjuvant therapy is hampered, however, by the increased difficulty during surgical dissection and damage to underlying vasculature which may increase

morbidity. Biomarkers of response and the optimal combination of chemo-, immune- and radiotherapy is far from defined and requires urgent investigation in order to prevent patients that may benefit from surgery being treated with ineffective systemic treatments upfront. Patients who present with resectable disease that is biologically aggressive will benefit from a period of neoadjuvant therapy and 'biological' selection. This thesis attempts to answer some of these questions in order to improve patient selection for therapy.

1.1.5.3 Adjuvant Therapy

Adjuvant therapy for PDAC has developed greatly over the last 2 decades. The European Study Group for Pancreatic Cancer (ESPAC) trials have largely focused on treatment in the adjuvant setting and made significant strides into improving outcomes after surgery for PDAC. ESPAC-1 demonstrated a survival benefit in using Fluorouracil (5-FU) in the adjuvant setting, over no chemotherapy, and with a survival benefit over chemoradiotherapy (Neoptolemos et al., 2004). Gemcitabine has recently been used as the adjuvant therapy of choice, following the ESPAC-3 trial which demonstrated that, in comparison with 5-FU, Gemcitabine has similar survival with fewer treatment related complications (Neoptolemos et al., 2010). Recently, this has been superseded by the ESPAC-4 trial which demonstrated a median survival of 28.0 months in the Gemcitabine plus Capecitabine group, compared with 25.5 months in the Gemcitabine only group (Neoptolemos et al., 2017). The estimated 5-year survival was 28.8% for the Gemcitabine plus Capecitabine group versus 16.3% for the Gemcitabine only group (Neoptolemos et al., 2017). As a result, Gemcitabine plus Capecitabine is now the recommended adjuvant chemotherapy for patients undergoing resection of PDAC. Yet, even with these advances the 5-year survival remains very low in comparison with other cancer subtypes, with few options for patients once the disease recurs. There remains significant scope for improving therapeutics and patient selection to improve the long-term survival for patients undergoing resection for PDAC. In particular, biomarker directed adjuvant and maintenance therapy for selected patients can potentially lead to long term survival benefits.

1.1.5.4 Treatment of Advanced disease

Unfortunately, the majority (around 80%) of patients with PDAC presents with either metastatic or locally advanced disease. For these patients, current therapeutic options are limited. Systemic chemotherapy is currently offered to patients who are fit enough to

tolerate the treatment. After the PRODIGE 4/ACCORD 11 trial, FOLFIRINOX (a combination containing Folinic acid, Fluorouracil, Irinotecan and Oxaliplatin) has become the recommended chemotherapy regime for patients with metastatic disease (Conroy et al., 2011). In comparison with Gemcitabine, FOLFIRINOX demonstrated improved overall survival of 11.1 versus 6.8 months. However, currently this is only recommended for patients with Eastern cooperative Oncology Group (ECOG) performance status (PS) 0 – 1, with patients with a poorer PS being offered Gemcitabine or no treatment. Furthermore, patients have very limited options at disease progression, with no proven 2nd line therapy options when disease progression occurs on primary systemic chemotherapy.

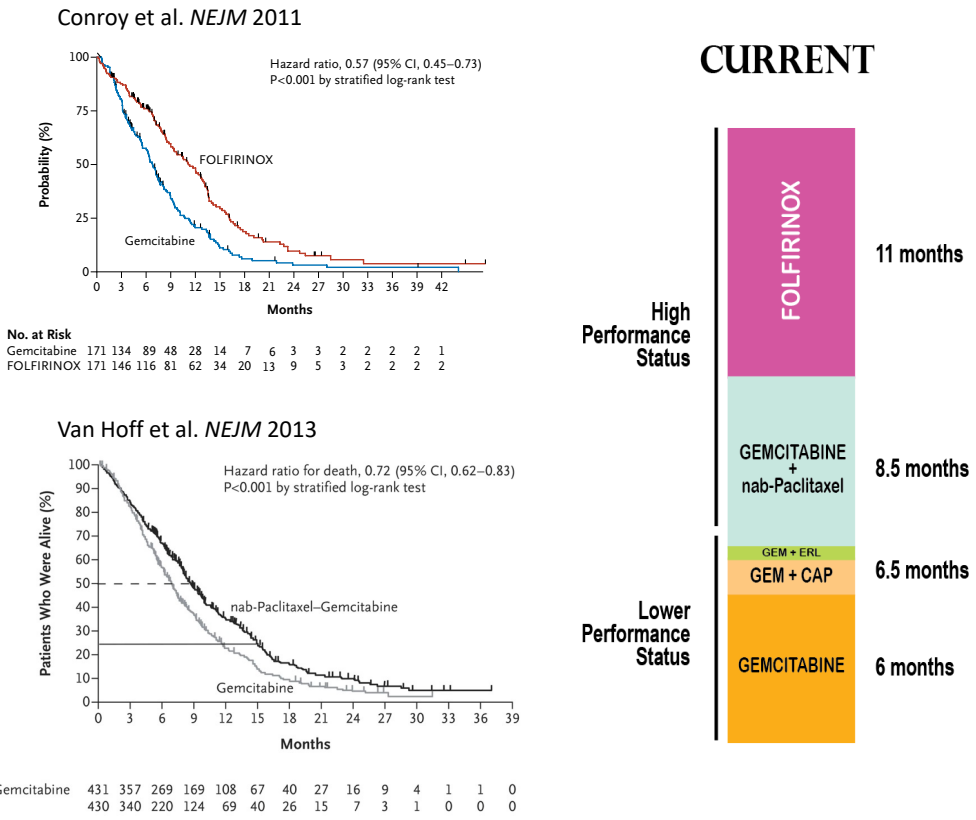

Figure 1-4 Current management of metastatic PDAC. Patients with advanced, metastatic PDAC are treated with systemic, cytotoxic chemotherapy based on performance status. Kaplan-Meier survival curves indicates median overall survival taken from randomised control trials that have influenced management of metastatic PDAC (Von Hoff et al., 2013, Conroy et al., 2011). The coloured bar chart demonstrates the therapeutic options available for metastatic PDAC based on performance status, with median overall survival from randomised studies indicated on the side. This highlights the urgent need for better therapies, based on underlying molecular biology of individual PDAC, to inform treatment decisions.

In locally advanced PDAC (LAPC), patients with a good PS are offered FOLFIRINOX and chemoradiotherapy, with some patients undergoing surgical exploration and resection after completion if there has been no disease progression or a good response to therapy

(Hackert et al., 2016, Hartwig et al., 2016, Balaban et al., 2016, Gemenetzis et al., 2018). There are a number of local therapies, such as irreversible electroporation, for unresectable disease that are currently being trialled with mixed results, and at present these are not recommended outside of clinical trials (He et al., 2014). It appears that there are a subgroup of patients with LAPC that can achieve long-term survival after a period of chemo – and radiotherapy prior to surgical exploration (Gemenetzis et al., 2018). Furthermore, patients with unresected LAPC often have longer survival than many 'resectable' PDAC that undergo pancreatectomy (Gemenetzis et al., 2018, Biankin et al., 2009). This suggests that there may be an underlying biological difference between these patient groups and requires further investigation to identify patients with LAPC that benefit from surgical resection, even in the setting of arterial resection.

1.1.5.5 Treatment Summary

Currently, treatment stratification in PDAC is based upon patient fitness, cross-sectional and endoscopic imaging with histological confirmation (Figure 1-5). The development of the cancer multi-disciplinary meeting (MDT) has led to a standardisation of treatment for patients in high volume units, that is based on evidence and national guidelines. Unfortunately, despite many endeavours, PDAC still remains a dismal disease. Treatment selection, based simply on imaging and limited histological modalities, does not allow for a tailored treatment approach. The 'omics' revolution has initiated the natural evolution of medicine and cancer care into the era of personalised medicine. There have been major advances in our knowledge and understanding of the underlying molecular changes that initiate and drive cancers, including PDAC. Yet, the exact phenotypic consequences of the inter-patient molecular heterogeneity of the disease and how that can inform treatment strategies is far from fully investigated.

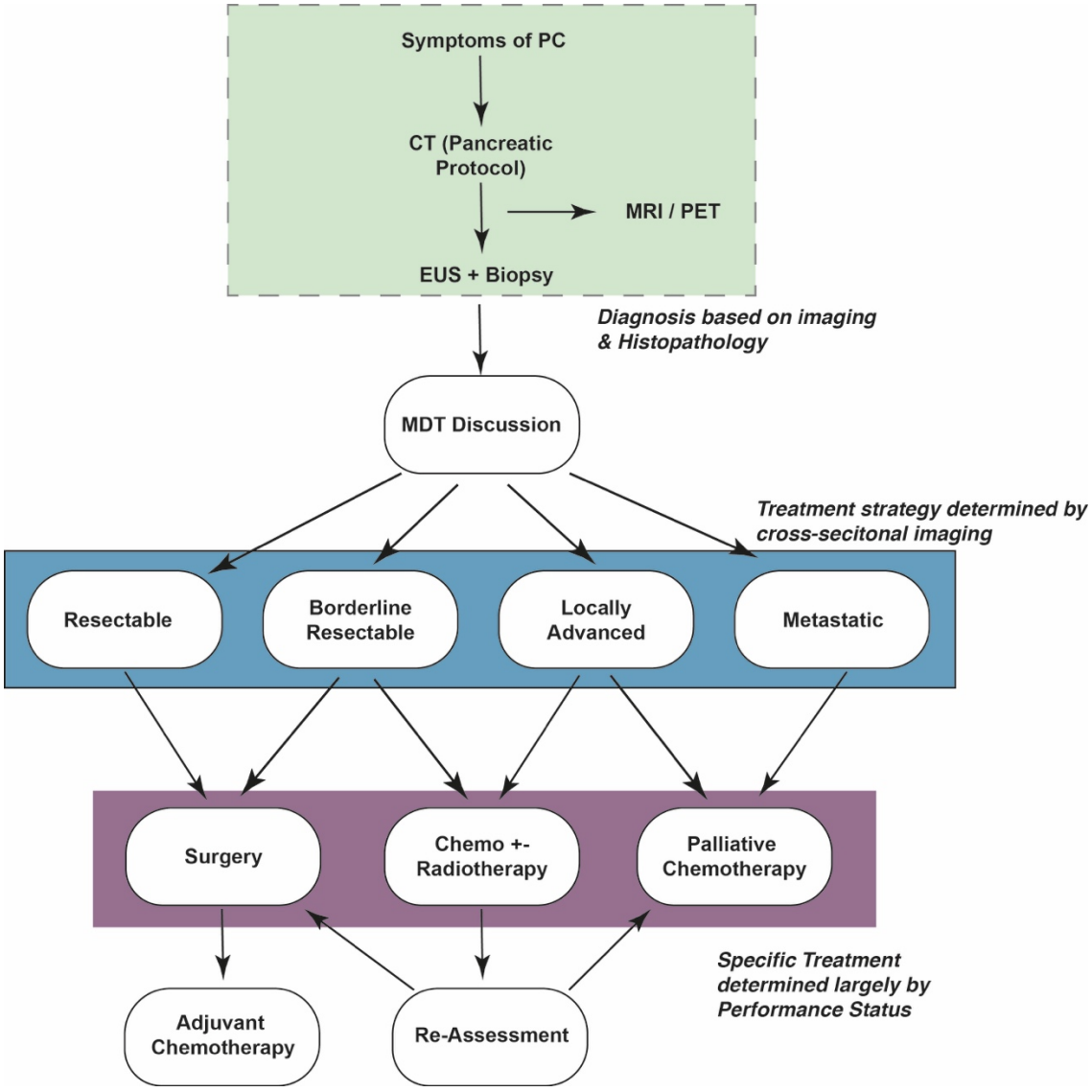

Figure 1-5 Patient flow diagram during diagnosis and treatment of PDAC. Patients are diagnosed using cross-sectional imaging, EUS and histopathology. MDT discussion determines current clinical stage of tumour and treatment strategy is based initially only on cross-sectional imaging. Specific treatments, including chemotherapy choice or whether to proceed with surgery, is exclusively determined by performance status in current clinical practice.

1.3 Molecular Landscape of PDAC

1.3.1 Somatic driver events

The inter-tumour heterogeneity of PDAC was first revealed after exome sequencing and single nuclear polymorphisms (SNP) microarrays demonstrated the genetic landscape of PDAC consists of a small number of frequently mutated genes, followed by a long tail of infrequent mutations (Jones et al., 2008). These segregate into 12 core signalling pathways that contribute to processes described as the hallmarks of cancer, including *KRAS* signalling, DNA damage control, WNT/Notch signalling and TGF-β signalling (Jones et al., 2008, Hanahan and Weinberg, 2011).

The Australian Pancreatic Cancer Genome Initiative (APGI), as part of The International Cancer Genome Consortium (ICGC), comprehensively analysed the genomic, transcriptomic and epigenetic changes of PDAC and has increased our understanding of the underlying molecular heterogeneity. Whole exome sequencing and copy number analysis in 99 resected PDACs, confirmed the presence of frequently mutated genes (*KRAS, TP53, CDKN2A, SMAD4, MLL3, TGFBR2, ARID1A* and *SF3B1*), and revealed mutations in DNA damage repair (*ATM)*, chromatin modification (*EPC1* and *ARID2*) and axon guidance in SLIT/ROBO signalling (Figure 1-6) (Biankin et al., 2012).

Whole genome sequencing (WGS) and copy number alterations revealed distinct chromosomal instability patterns and processes that underlie somatic mutagenesis, and structural variation analysis identified novel driver mutations (*KDM6A* and *PREX2*) not previously described in PDAC (Waddell et al., 2015). *KDM6A*, a SWI/SNF interacting partner involved in demethylation of lysine residues on histone, was found in 18% of patients, and is associated with a poor prognostic sub-type of PDAC (Bailey et al., 2016). Mutations in *RNF43* may offer therapeutic opportunities for WNT signalling antagonists in selected patients (Jiang et al., 2013). Importantly, whole genome and copy number analyses demonstrated novel putative read-outs of DNA damage response (DDR) deficiency, identifying a greater proportion of patients with DDR deficiency in PDAC than when based on simple mutations alone (Figure 1-6) (Waddell et al., 2015).

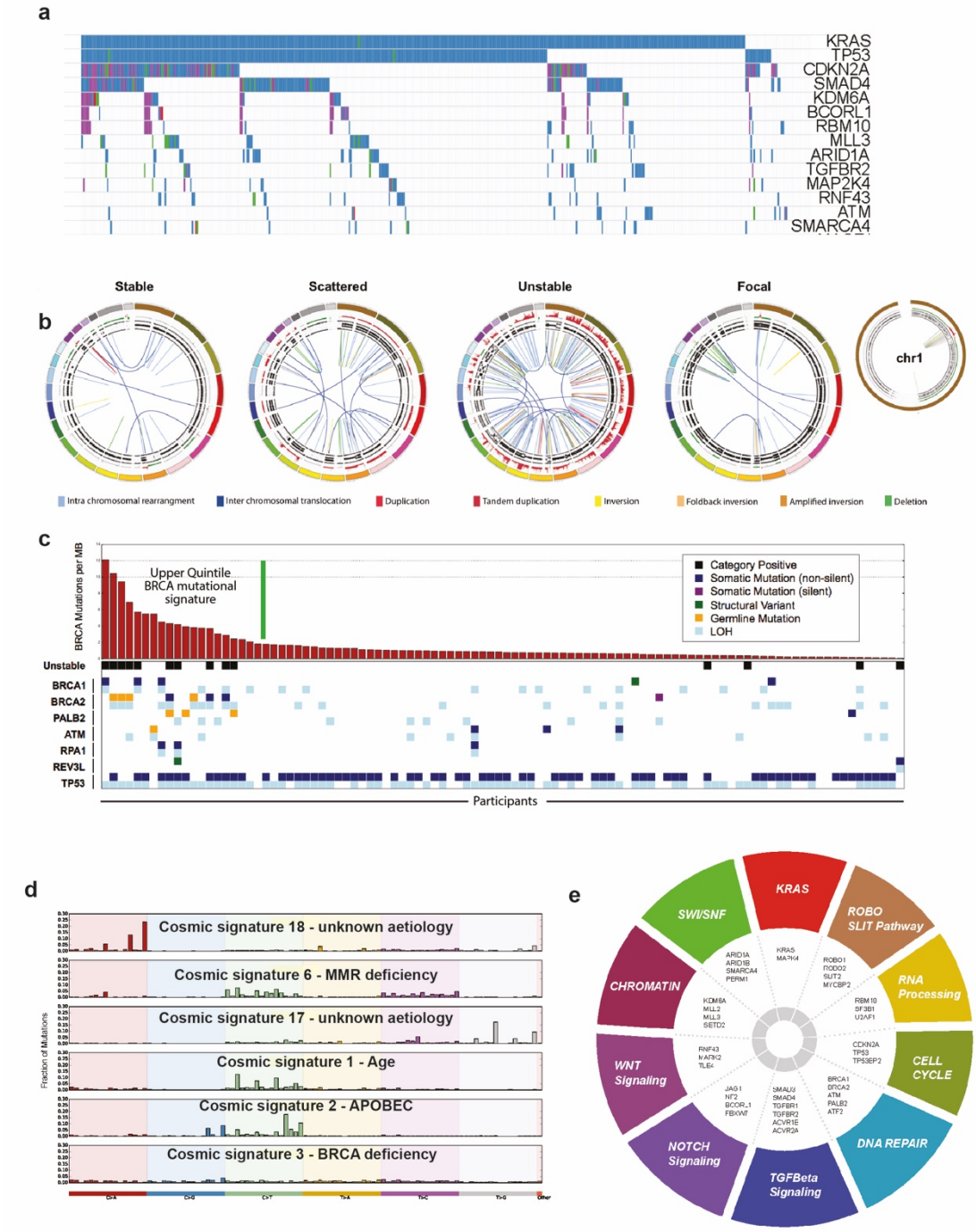

Figure 1-6 Whole genome characterisation of PDAC. a, Somatic mutations in the most commonly mutated genes in 456 samples. **b,** Subtypes of PDAC based on the number and pattern of chromosomal structural variants. The coloured outer rings are chromosomes, the following ring represents copy number changes (red equals gain, green equals loss), the following represents allele frequency, the inner lines represent chromosome structural re-arrangements. **c,** Defining the DDR deficient subtype using mutations in genes and other measures of DDR deficiency (mutational signatures and genomic instability): Cosmic *BRCA* mutational signature (defined as *BRCA* signature mutations per MB), ranked by prevalence and relationship to unstable genomes and point mutations within *BRCA* pathway genes. Taking into account germline & somatic mutations in well-defined DDR genes, unstable genomes and the *BRCA* mutational signature, DDR deficiency prevalence increases to 24% (green bar separates upper quintile of *BRCA mutational* signature prevalence). **d,** Examples of Cosmic mutational signatures defined by base substitutions in the human genome seen in PDAC, including the *BRCA* mutational signature. Overall, there are 6 possible types of base substitutions (C>A, C>G, C>T, T>A, T>C, T>G) and incorporating information on the bases 5' and 3' to each mutated base, along with the type of base substitution results in 96 possible combinations and generates a signature of somatic mutagenesis. **d,** Mutated

genes and the pathways where they occur in PDAC. Adapted from Dreyer et al. 2017 (Dreyer et al., 2017)

Resected PDAC that underwent WGS demonstrated 4 sub-types based on the number and pattern of chromosomal structural variants (Waddell et al., 2015). Tumours were classified as stable (≤50 structural variations), locally rearranged (a significant focal event on 1 or 2 chromosomes), scattered (moderate range of chromosomal damage, <200 structural variations) and unstable (> 200 structural variations). The 'unstable' sub-type occurred in 14% and the scale of genomic instability (up to 558 structural variations) suggests significant defects in DNA maintenance, particularly in the homologous recombination (HR) pathway (Figure 1-6) (Waddell et al., 2015, Tutt et al., 1999).

Somatic point mutational signatures (COSMIC signatures) within a cancer genome reflect the underlying processes contributing to mutagenesis, and to date, 4 have been associated with PDAC (*BRCA* mutational signature, Old Age, DNA mismatch repair deficiency, APOBEC family of cytidine deaminases) (Alexandrov et al., 2013, Chang et al., 2014a). WGS and analysis demonstrated that 10 of the 14 patients with unstable genomes were within the top quintile of *BRCA* mutational signature prevalence (Waddell et al., 2015). These were associated with germline and somatic mutations in *BRCA1, BRCA 2* and *PALB2* (Waddell et al., 2015). Mutations in other genes crucial to DNA maintenance, such as *ATM, RPA1, XRCC4* and *XRCC6*, were found in those with unstable genomes or a *BRCA* mutational signature, although most only occurred once making it difficult to draw conclusions (Waddell et al., 2015). These findings suggest significant overlap between unstable genomes, high ranking *BRCA* mutational signature and mutations in key DDR genes (Figure 1-6). Suggesting these can be utilized as putative biomarkers of DDR deficiency to direct therapy in selected patient sub-groups in clinical trials, as functional consequences of point mutations alone can be difficult to interpret (Waddell et al., 2015).

More recently, a novel informatics tool assessed ploidy, copy number changes and chromothripsis (a phenomenon at which up to thousands of clustered chromosomal re-arrangements occur as a single event) in PDAC, challenging the model of stepwise progression from PanIN to invasive PDAC (Notta et al., 2016). Approximately 65% of tumours demonstrated evidence of at least one chromothriptic event, and most copy number changes appear to occur after such catastrophic genetic events (Notta et al., 2016). By analysing the genomes of two PDAC tumours in detail, the authors demonstrated evidence of chromothripsis leading to loss of tumour suppressors *CDKN2A, TP53* and

SMAD4 (Notta et al., 2016). This suggest a proportion of PDAC tumours may not follow the stepwise progression model and could explain the rapid clinical progression of the disease in some patients. Chromothripsis leads to significant genetic instability and subsequently worse clinical outcomes for patients whose tumours had at least one such event (Notta et al., 2016). This highlights the potential implications in early disease detection and screening programs in PDAC.

1.3.2 Transcriptome

An integrated molecular analysis of ICGC PDAC donors identified 4 sub-types based on transcriptional networks that define gene programs within the tumour epithelial component and the microenvironment (Bailey et al., 2016). Sub-types were termed squamous, pancreatic progenitor, aberrantly differentiated endocrine exocrine (ADEX) and immunogenic and correlated with histopathological findings and long-term outcomes (Bailey et al., 2016).

The squamous sub-type was so-called as it is enriched for gene programs described in squamous like tumours of breast, bladder, lung and head and neck cancer (Hoadley et al., 2014). These co-segregated with histopathological adeno-squamous tumours and gene programs associated with inflammation, hypoxia response, metabolic programming and TGF-β signalling (Bailey et al., 2016). MYC pathway activation was enriched in this sub-type and correlates with a previous study demonstrating MYC activation in adeno-squamous PDAC and poor outcome (Bailey et al., 2016, Witkiewicz et al., 2015). Hypermethylation and downregulation of genes involved in pancreatic endodermal differentiation (*PDX1, MNX1, GATA6, HNF1B*) appeared to contribute to loss of endodermal identity and epithelial to mesenchymal transition (EMT) (Bailey et al., 2016). Mutations in *KDM6A* and *TP53* associate with other squamous epithelial tumours, and this class was associated with poor survival in PDAC with EMT (Hanahan and Weinberg, 2011, Fischer et al., 2015, Zheng et al., 2015).

In contrast with the squamous sub-type, the pancreatic progenitor sub-type is associated with better survival and is primarily defined by pathways and networks involved in pancreatic endodermal differentiation (Bailey et al., 2016). The progenitor class demonstrated increased expression of the apomucins *MUC1* and *MUC5AC*, both associated with the pancreatico-biliary subtype of intra-ductal papillary mucinous

neoplasms (IPMN) and was associated with invasive IPMN cancer histologically (Figure 1-7) (Bailey et al., 2016).

Within the progenitor class, perhaps the most exciting finding was the immunogenic sub-type which was defined by enrichment for pathways involved in immune cell infiltration and associated immune signalling pathways (Bailey et al., 2016). Transcriptomic evidence of infiltrating cytotoxic $CD8^+$ T cells, regulatory T and B cells along with expression of cytotoxic T-lymphocyte-associated protein 4 (CTLA-4) and programmed cell death 1 (PD-1) immune checkpoint pathways suggests immune suppression that can be targeted with checkpoint blockade in this class (Bailey et al., 2016). Expression signatures of immune cells predicted outcome, specifically macrophage infiltration and T cell co-inhibition associated with poor survival (Bailey et al., 2016). This provides rationale for using transcriptome analysis for identifying patients that may benefit from immunotherapy in PDAC.

Collisson *et al.* categorised PDAC, using transcriptional analysis, into quasi-mesenchymal (QM-PDA), classical and exocrine subtypes (Collisson et al., 2011). The QM-PDA sub-group was associated with worse overall survival and overlaps with the squamous sub-type described by Bailey *et al.* (Figure 1-7) (Collisson et al., 2011, Bailey et al., 2016). Collisson further described an endocrine sub-type that overlaps directly with the Bailey ADEX class (Bailey et al., 2016, Collisson et al., 2011). These were enriched for gene programs in endocrine and exocrine development and appears to be a sub-group of the progenitor class (Collisson et al., 2011, Bailey et al., 2016). Criticism of the ADEX and endocrine sub-groups suggest that these are defined by large amount of normal pancreas in low cellularity tumours. However, methylation patterns of the ADEX class correlates with other PDACs and patient derived cell lines demonstrated gene enrichment profiles that fall within the ADEX class, suggesting this is a genuine feature of the tumour epithelium (Bailey et al., 2016).

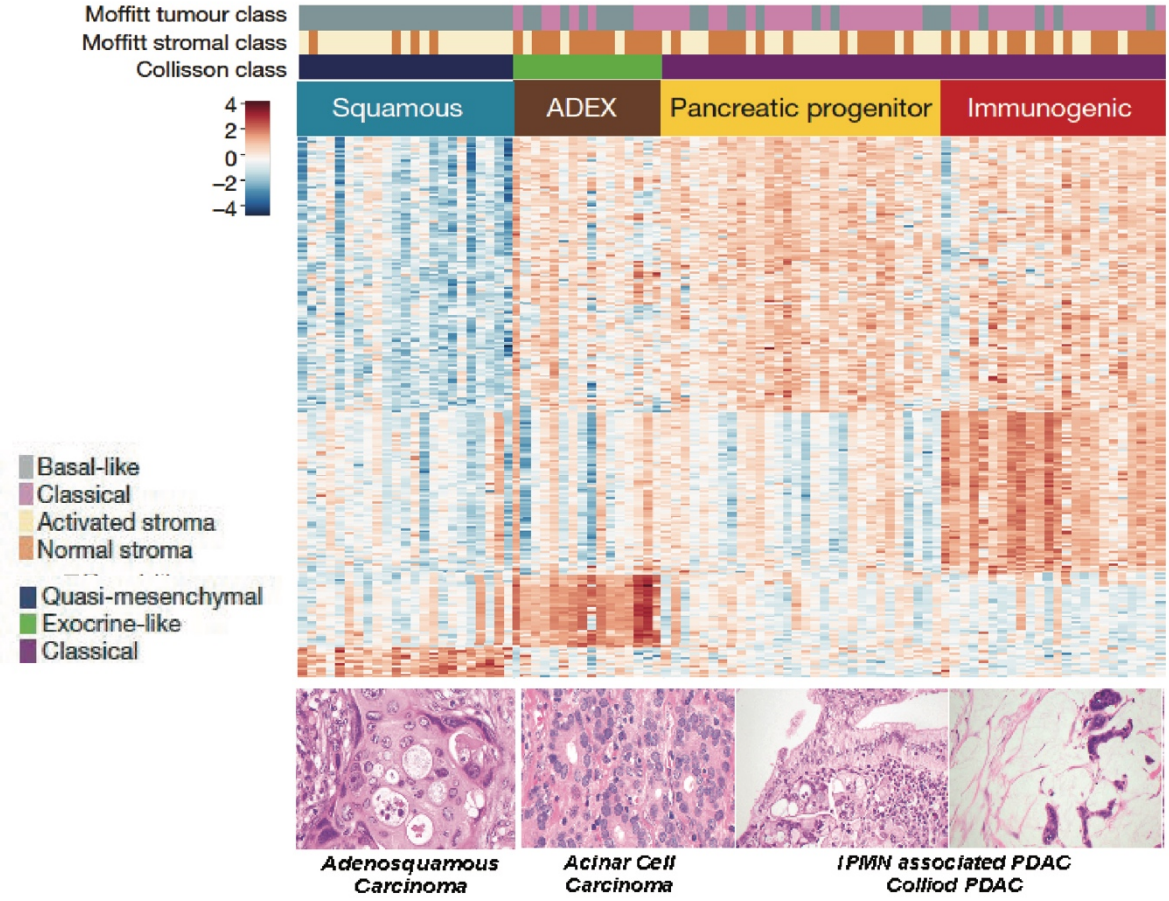

Figure 1-7 Molecular subtypes of PDAC. Transcriptional networks reveal 4 PDAC sub-types: Squamous (blue), ADEX (aberrantly differentiated endocrine and exocrine; brown); pancreatic progenitor (yellow), and immunogenic (red). Bailey subtypes aligned with Moffit tumour and stromal class, and Collisson classes. Adapted from Dreyer et al. 2017 (Dreyer et al., 2017)

Moffitt *et al.* performed virtual microdissection to differentiate the stromal and epithelial components of PDAC and minimize the confounding impact normal pancreatic tissue may confer (Moffitt et al., 2015). They described two sets of gene programs that define either an activated or normal stroma (Moffitt et al., 2015). The activated stroma was associated with a worse prognosis and enriched for genes previously associated with poor survival including *MMP9, MMP11* and Wnt family members (Moffitt et al., 2015). Defining gene expression within the epithelial component revealed 2 sub-types, named basal and classical (Moffitt et al., 2015). The classical sub-type was associated with improved prognosis and overlapped with the Collisson classical and Bailey progenitor sub-types (Figure 1-7) (Moffitt et al., 2015, Collisson et al., 2011, Bailey et al., 2016).

Comparing the basal with the QM-PDA sub-type, described by Collisson *et al.*, revealed that the QM-PDA classification considers gene programs from the basal epithelial and activated stroma classes (Collisson et al., 2011, Moffitt et al., 2015). A recent study by Puelo et al. demonstrated that by examining the transcripts from formalin fixed and paraffin-embedded PDAC that the squamous and classical pancreatic (which encompasses progenitor, ADEX and immunogenic) are recapitulated (Puleo et al., 2018). Immune infiltrates in the classical pancreatic subtype allowed stratification termed Pure Classical and Immune Classical (Puleo et al., 2018). Furthermore, they describe two distinct stromal subtypes termed Activated and Desmoplastic which demonstrated features of both the squamous and classical pancreatic subtypes (Puleo et al., 2018). The stroma and local immune response are strongly associated with outcome and response to therapy and classifying tumours purely on epithelial gene expression is unlikely to fully account for all molecular processes in the disease. This suggests that expression or transcriptomic classification should incorporate gene signatures from both the microenvironment and tumour epithelium to fully account for the molecular pathology of PDAC. The Collisson, and hence Bailey, classification incorporates key stromal, immune and epithelial elements that reflect tumour biology and prognosis. Currently, it is accepted that 2 distinct transcriptomic subtypes exist with varying molecular and clinical features (Figure 1-8). In this body of work these will be referred as the Squamous (also known as basal or Quasi-Mesenchymal) and Classical Pancreatic (also known as Pancreatic Progenitor, which incorporates the ADEX and Immunogenic classes) subtypes.

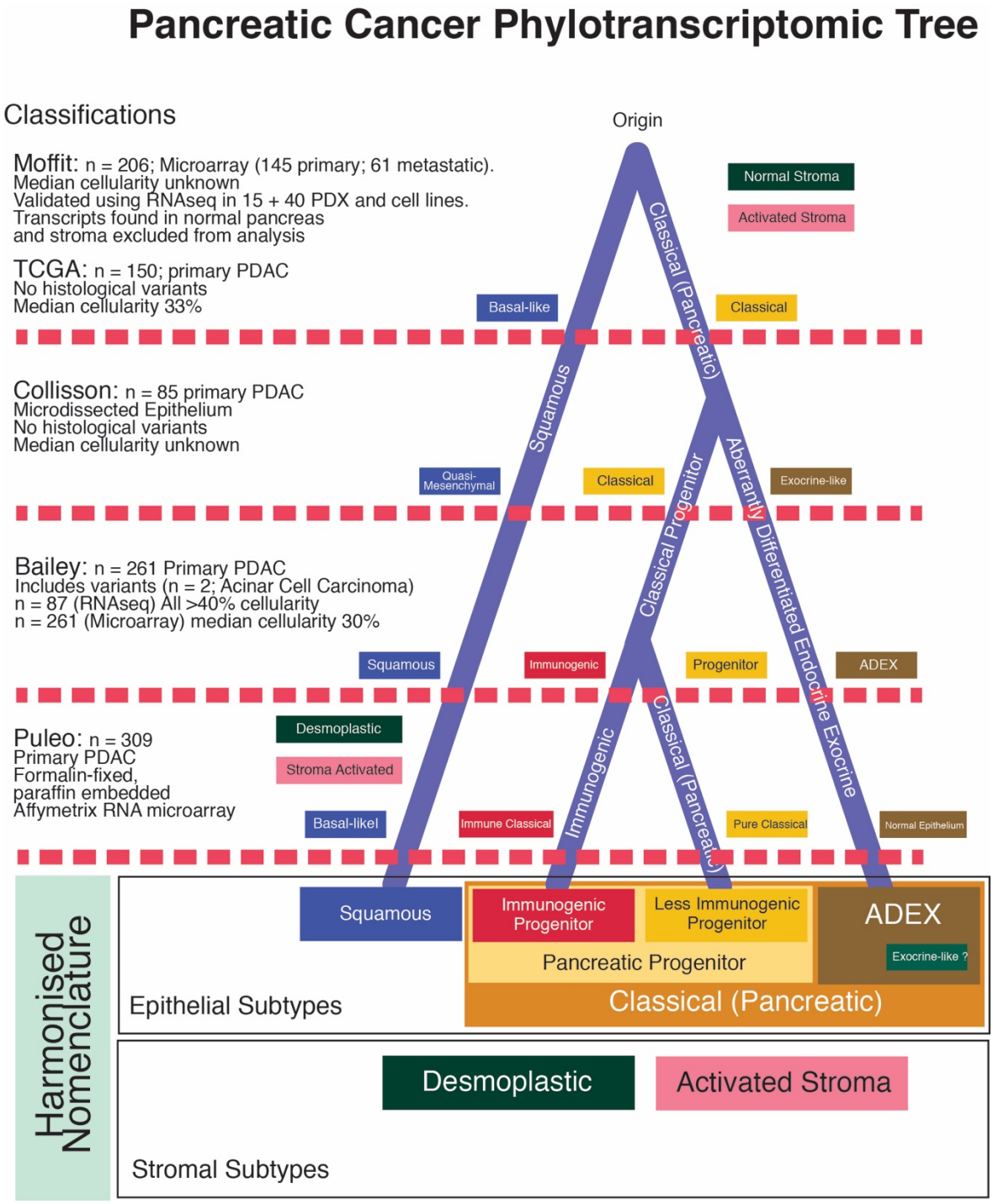

Figure 1-8 Transcriptomic Subtypes of PDAC. Incorporating the transcriptomic subtypes described by Moffit, Collisson and Bailey into a common nomenclature of molecular subtypes of PDAC. Two broad subtypes, the squamous and Classical Pancreatic exist. The Classical Pancreatic subtype can be further subdivided into a spectrum of tumours based on parallel lineages of pancreatic development. The exact relationship between stromal subtypes and epithelial subtypes have not been discerned and requires further investigation. However, as therapies targeting the tumour microenvironment develop, will likely play a role in future therapeutic development.(Figure from Collisson et al., 2019)

1.3.3 Inherited & Familial PDAC

Up to 10% of PDAC cases are due to inherited susceptibility and 20% of these form part of well-known cancer syndromes such as Familial Adenomatous Polyposis (FAP), Hereditary Non-Polyposis Colorectal Cancer (HNPCC), Familial Multiple Mole Melanoma (FMMM), Li Fraumeni syndrome, Hereditary Breast and Ovarian Cancer (HBOC) syndrome, or Peutz-Jegher syndrome (Klein, 2013). Hereditary pancreatitis appears to increase the risk of PDAC, particularly in the setting of *PRSS1, SPINK1* and potentially *CPA1* mutations (Roberts et al., 2016, Klein, 2013). Roberts *et al*. reaffirmed known PDAC susceptibility genes such as *ATM*, *BRCA2*, *CDKN2A* and *PALB2*, but also revealed rare germline variants that likely play a role in the disease (Roberts et al., 2016, Zhen et al., 2015). Importantly, several novel Familial PDAC susceptibility genes were identified and are involved in DNA damage response or chromosomal stability processes. Newly identified mutations in *BUB1B, CPA1, FANCC* and *FANCG* may thus predispose these patients to sensitivity for chemotherapeutics targeting the DNA damage response pathway (Roberts et al., 2016). This study illustrated the challenges in identifying and defining low prevalence PDAC susceptibility mutations and further work to delineate these associations and their therapeutic implications is required.

1.3.4 Intra-tumoural Heterogeneity in PDAC

There is growing evidence that individual tumours are composed of multiple clonal sub-sets with different mutations resulting in various levels of intra-tumoural heterogeneity (ITH) (Gerlinger et al., 2012, McGranahan and Swanton, 2015, Yap et al., 2012, Yachida and Iacobuzio-Donahue, 2013, Greaves and Maley, 2012, Andor and Graham, 2016, Navin et al., 2011, Campbell et al., 2008). Comparative sequencing of multiple PDAC lesions suggests that most somatic mutations occur in the primary tumour ('founder' mutations) prior to metastatic dissemination, and 'progressor' mutations occur during further clonal evolution (Yachida et al., 2010). Multiple, three-dimensionally spaced samples sequenced from primary tumours suggest multiple sub-clones within the primary tumour, which results in metastases originating from specific primary tumour sub-clones and thus ITH selects for metastatic sub-clones (Yachida et al., 2010). Phylogenetic relationships between primary tumours and metastases are distant suggesting that metastatic clones undergo significant evolution to obtain the survival advantage required for disease dissemination (Campbell et al., 2010, Moffitt et al., 2015). However, many of these studies were done in patients that have been exposed to systemic chemotherapy. Recently, it has been shown

that in chemo-naïve patients, the intra-tumoural heterogeneity between primary PDAC and metastatic lesions is limited (Makohon-Moore et al., 2017). Very importantly, driver mutations and thus targets for tailored therapy appear to be almost identical in all metastatic lesions for individual patients (Makohon-Moore et al., 2017). The majority of ITH thus appears to be in passenger mutations, yet, there are likely sub-clones that have differences in driver gene mutations that are not detectable at such a low frequency and will likely lead ultimately to treatment resistance.

The findings from these studies suggest that PDAC harbours ITH, but this probably is not significantly different amongst driver mutations in the chemo-naïve setting (Campbell et al., 2010, Yachida et al., 2010, Yap et al., 2012, Gerlinger et al., 2012, Swanton, 2012, Fisher et al., 2013, Makohon-Moore et al., 2017). The likely evolution during chemotherapy, however, will allow more distant genetic dissemination amongst tumour clones and thus may prove a challenge to treat in the 2nd line setting. This requires extensive further investigation in an attempt to assess the impact of ITH in treatment-naïve and post-therapy patients and how this will impact precision medicine initiatives.

1.3.5 Molecular therapeutic targets in PDAC

A deeper understanding of the molecular pathology of PDAC has led to the identification of multiple candidate targets both for novel and for repurposing therapeutic strategies (Figure 1-9). Most actionable targets occur at low prevalence in PDAC, and therefore molecularly-guided, personalised treatment approaches are essential to allow selection of appropriate participants for specific therapies. The low prevalence of these targets explains why studies of targeted therapies in unselected PDAC participants have not been successful (Biankin et al., 2015). However, several opportunities, supported by our increasing appreciation of the molecular pathology of PDAC are emerging. At present, the most promising is targeting DNA damage response (DDR) deficiency and immunotherapy strategies in defined patient sub-groups (Dreyer et al., 2017).

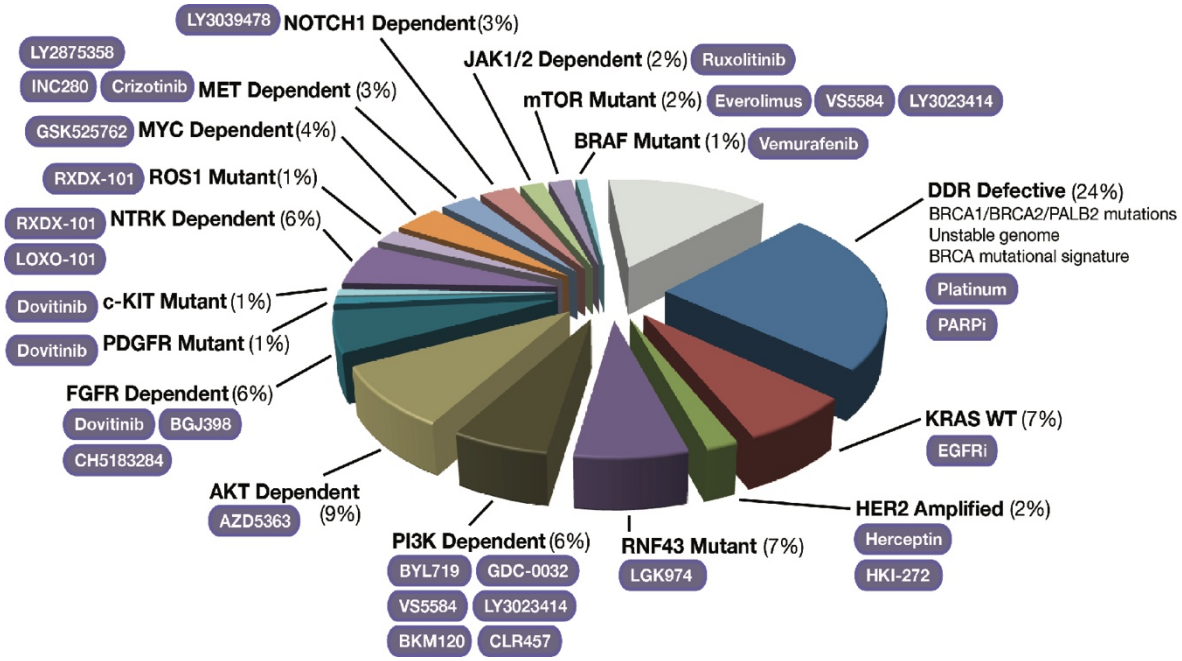

Figure 1-9 The PDAC actionable genome. Based on genomic aberrations, showing therapeutic opportunities for existing and emerging therapies in PDAC. It is important to note that whilst these targets exist, the functional consequences and potential therapeutic responsiveness to agents that target them, are largely unknown. Adapted from Dreyer et al. 2017 (Dreyer et al., 2017)

1.3.6 Targeting DNA damage response deficiency and replication stress

1.3.6.1 DNA damage response pathways

DNA damage can occur spontaneously during the normal cell cycle and replication, as a result of exposure to exogenous agents or due to inherited or acquired deficiencies in a number of DNA maintenance and replication mechanisms. DNA damage mechanisms include formation of DNA crosslinks or DNA breaks including single strand (SSB) and double strand breaks (DSB), base mismatches, insertions or deletions and bulky adduct formation (Ciccia and Elledge, 2010, Lord and Ashworth, 2012). This in turn results in DNA damage that can result in genomic instability and replication stress, which can be driven by oncogene activation (e.g. *CCNE1* and *Myc*) (Macheret and Halazonetis, 2018, Lord and Ashworth, 2012). SSBs can be secondary to reactive oxygen species release in normal cellular mechanisms and DNA replication errors during cell replication (Lord and Ashworth, 2012). This leads to replication stress and genomic instability and several mechanisms exist in order to repair DNA damage and restore the integrity of the genome (Ciccia and Elledge, 2010, Zhang et al., 2016a).

DSBs are potentially devastating to cell viability and unrepaired DSBs can progress to gross chromosomal abnormalities, mutations and cell death (Kennedy and D'Andrea, 2006). DSBs are repaired by two main repair mechanisms, namely homologous recombination (HR) and non-homologous end joining (NHEJ) (Kennedy and D'Andrea, 2006, Lord and Ashworth, 2012). HR aims to restore the original DNA sequence at the site of damage during the S and G2 phases of cell cycle (Lord and Ashworth, 2012, Kennedy and D'Andrea, 2006, Weber and Ryan, 2015). HR removes the section of DNA surrounding the DSB and aligns it with a homologous sequence of DNA that has been synthesised from a 'sister' chromatid template (Kennedy and D'Andrea, 2006, Lord and Ashworth, 2012). Crucial to this process are the BRCA 1, BRCA 2, partner & localiser of BRCA 2 (PALB 2), Ataxia Telangiectasia Mutated (ATM) and RAD 51 proteins (Lord and Ashworth, 2012, Kennedy and D'Andrea, 2006). Loss of function mutations in these genes can lead to homologous recombination deficiency (HRD) and can be detected using a variety of mutational and structural genomic signatures (Waddell et al., 2015, Davies et al., 2017, Alexandrov et al., 2013). NHEJ occurs during the entire cell cycle and repairs DSBs by directly joining the ends of DSBs together (Lord and Ashworth, 2012). This can result in the deletion or insertion of base pairs and hence result in further mutations, suggesting HR is a superior mechanism of DNA repair (Kennedy and D'Andrea, 2006). HRD results in an inability to repair DSBs which in turn sensitises to treatment by both platinum and PARP-inhibitors, the latter in a manner known as synthetic lethality (Bryant et al., 2005, Davies et al., 2017, Fong et al., 2010, Lord et al., 2015, Matulonis et al., 2016, McCabe et al., 2006, O'Connor, 2015).

1.3.6.2 Synthetic Lethality

The concept of synthetic lethality is based on compensatory mechanisms of DNA maintenance pathways that are required for cell viability (Kaelin, 2005, Lord et al., 2015). When considering two DDR pathways, if a defect within either DDR pathway exists this may be compatible with cell viability as the other pathway compensates. However, synthetic lethality exists if defects within both pathways are not compatible with cell viability (Kaelin, 2005). This concept is opening the door to a number of targeted therapies in appropriate sub-groups and does not only provide the potential to improve tumour response, but also reduce side effects. DDR deficiency in tumour cells would thus allow non-tumour cells to be unaffected by inhibition in a synthetically lethal approach and potentially reduce toxicity. The best proven example of synthetic lethality thus far are

PARP-inhibitors, but this concept is opening the door to many more new targeted agents, particularly novel strategies targeting DDR deficiency (Lord et al., 2015).

1.3.6.3 Therapeutic targets of DNA damage response deficiency in PDAC

Increasingly cohort studies and anecdotal reports of exceptional responders are identifying candidate molecular targets for current and novel therapeutic strategies in PDAC, including those targeting DDR deficiency (Chang et al., 2014b). Up to 24% of PDAC demonstrate defects in DDR that can potentially be targeted with DNA damaging agents or DDR targeted agents through synthetic lethality (Waddell et al., 2015, Lord et al., 2015). Integrated genomic readouts of DDR deficiency are emerging as potentially more appropriate than using point mutations in selected DDR genes alone and can identify patients that will respond to platinum-based therapy, PARP inhibition or novel agents that target DDR pathways (Table 1-1) (Waddell et al., 2015). A significant proportion of patients with PDAC harbour heterozygous mutations in DDR pathways with unknown functional consequences. The term *BRCAness* refers to tumours in which HR deficiency exist, without evidence of a germline *BRCA1* or *BRCA2* mutation (Lord and Ashworth, 2016). These can potentially be identified by the Cosmic *BRCA* mutational signature or an unstable genome, and can be associated with mutations in *ATM, ATR, PALB2* and potentially others such as *RPA1* (Lord and Ashworth, 2016, Waddell et al., 2015). The clinical benefit of targeting heterozygous somatic or germline mutations in PDAC using synthetic lethality strategies is yet to be determined. The degree of haplosufficiency, which refers to the level of function if only a single copy of a gene exists, for several DDR genes are undefined at present and there exists no consensus on the relevance of assessing the 2nd allele to predict therapeutic sensitivity for the majority of genes involved in DDR. Thus, developing other genomic readouts or surrogates of DDR or HR deficiency may be more beneficial as biomarkers of therapeutic response.

The evidence for the efficacy of platinum-based therapy in PDAC is ever increasing in the neoadjuvant, adjuvant and palliative settings (Ciliberto et al., 2013, Conroy et al., 2011, Oettle et al., 2013, Rombouts et al., 2016, Strobel and Buchler, 2016, Hackert et al., 2016). Exceptional responders to platinum therapy are well documented, yet biomarkers of response require to be tested in prospective clinical trials (Waddell et al., 2015, Chang et al., 2014b). *BRCA1* and *BRCA2* germline carriers are known to respond to platinum and PARP-inhibitors in multiple tumour types including PDAC (Lord and Ashworth, 2012, Lord and Ashworth, 2016, Pishvaian et al., 2017). Platinum resistance, however, is

common and can occur after secondary *BRCA1* or *BRCA2* mutations, or other mechanisms (Barber et al., 2013, Edwards et al., 2008, Lord and Ashworth, 2013, Norquist et al., 2011, Patch et al., 2015, Sakai et al., 2008, Pishvaian et al., 2017). Thus, identifying therapeutic targets after platinum resistance develops is crucial since platinum-based chemotherapy is now recommended in patients with good performance status with PDAC.

Table 1-1 Known mutated gene targets in DNA damage response pathways in PDAC

Gene symbol	Therapeutic	Rationale	References	Estimated prevalence in PDAC (%)
ARID1A	ATR inhibitor / PARP inhibitor / Platinum	Pre-clinical models	(Shen et al., 2015, Williamson et al., 2016)	16
ATM	ATR inhibitor / PARP inhibitor / Platinum	Clinical Trials / Case reports / Pre-clinical models	(Reaper et al., 2011, Biankin et al., 2012, Kim et al., 2014, Fokas et al., 2014, Weber and Ryan, 2015, Mohni et al., 2015, Valero et al., 2015, Karnitz and Zou, 2015, Bang et al., 2015)	10
ATR	PARP-inhibitor / ATM inhibitor	Pre-clinical models	(Weber and Ryan, 2015)	1
BRCA1 ***BRCA2***	Platinum / PARP inhibitor / ATR inhibitor	Clinical trials / Case reports / Pre-clinical models	(Bryant et al., 2005, Kennedy and D'Andrea, 2006, Waddell et al., 2015, Lord et al., 2015, Zhen et al., 2015, Lord and Ashworth, 2016)	7
PALB2	Platinum / PARP inhibitor	Case reports / Pre-clinical models	(Waddell et al., 2015, Villarroel et al., 2011, Lord and Ashworth, 2016)	2
RAD51 / RAD51C	PARP-inhibitors	Clinical trials / Pre-clinical models	(McCabe et al., 2006, Swisher et al., 2016)	1
RPA1	Platinum / PARP-inhibitor	Pre-clinical models	(Waddell et al., 2015, McCabe et al., 2006)	3

1.3.7 Replication stress in PDAC

Novel agents, targeting cell cycle checkpoint activation, such as ATR, CHK1 and WEE1 inhibitors have demonstrated significant potential in early pre-clinical studies, however their role and patient selection markers require further investigation (Reaper et al., 2011, Fokas et al., 2012, Prevo et al., 2012, Huntoon et al., 2013, Fokas et al., 2014, Weber and Ryan, 2015, Krajewska et al., 2015). This holds promise for *ATM* deficient PDAC, which can occur in up to 8% of patients and is associated with familial pancreatic cancer, as normal DDR mechanisms become reliant on Ataxia Telangiectasia and Rad3 related (ATR) signalling following ATM down regulation (Weber and Ryan, 2015). Mutations in *ATM* (found in 8% of the ICGC cohort) may predict sensitivity to targeted DNA damaging

agents (e.g. PARP-inhibitors or ATR inhibitors), however it remains to be determined whether ATM mutations, gene expression, transcriptional signatures or immunohistochemistry is the ideal biomarker of response in this patient sub-group (Bang et al., 2015). There is growing evidence that mutations in chromatin remodelling pathways (e.g. *ARID1A* mutations) can be targeted using PARP- or ATR-inhibitors (Lord et al., 2015, Shen et al., 2015, Reaper et al., 2011, Weber and Ryan, 2015, Bang et al., 2015, Williamson et al., 2016). These mutations are associated with the poor prognostic squamous sub-type and may provide a therapeutic strategy to target this sub-set of patients (Bailey et al., 2016).

Replication stress can be defined as the slowing or stalling of the DNA replication fork which makes the cell vulnerable to DNA damage in the form of single strand DNA breaks (Dobbelstein and Sorensen, 2015, Zeman and Cimprich, 2014). Many external factors such as ultraviolet light, hypoxia, radiation, oncogene activation and chemotherapeutics result in stalling DNA polymerases at sites of DNA damage and thus initiates the replication stress response (Fokas et al., 2014). Fork stalling leads to single stranded DNA and is coated by Replication Protein A (RPA) (Zeman and Cimprich, 2014). This in turn leads to a cascade of repair mechanisms via the activation of ATR, checkpoint kinase 1 (CHK1) and WEE1 (Chanoux et al., 2009, Dobbelstein and Sorensen, 2015, Zeman and Cimprich, 2014). A significant proportion of cancer cells exhibit defects in DDR that manifests as replication stress, particularly through loss of ATM/P53 signalling. In these cells, there is a potential loss of G1/S checkpoint control, and DDR may be solely dependent on G2 / M checkpoint activation in an ATR-dependent manner (Fokas et al., 2014, Fokas et al., 2012, Dobbelstein and Sorensen, 2015). ATR is crucial to sensing stalled replication forks and SSBs and via CDK1, activates WEE1 which in turn results in cell cycle arrest at the G2 checkpoint (Geenen and Schellens, 2017). This allows for DNA damage repair prior to subsequent mitosis (Geenen and Schellens, 2017). This suggests that ATR, CHK1 or Wee1 inhibition can potentially sensitise cells, with increased replication stress, to DNA damage in a synthetically lethal manner whilst not affecting normal tissue cells and hence reducing toxicity.

At present no reliable biomarkers of response exist for cell cycle checkpoint inhibitors. This requires urgent further investigation, to determine patients who will benefit from these agents in PDAC. This is also of particular interest in patients treated with Platinum chemotherapy, who subsequently develop treatment resistance and disease progression as

replication stress may persist after platinum resistance (Drean et al., 2017, Leijen et al., 2016b, Pishvaian et al., 2017, Sakai et al., 2008).

1.3.7.1 Immunotherapy in PDAC

Achieving significant advances in PDAC will require multi-modal therapeutic strategies to target the epithelial, stromal and immune components of the tumour. Transcriptomic analyses have identified sub-groups of tumours with differential stromal and immune responses. Of great interest, is the immunogenic sub-type that demonstrates enriched gene expression in immune gene sets such as PD-1/PD-L1 and CTLA-4 (Bailey et al., 2016).

The mutational burden in tumours with mismatch repair (MMR) deficiency is increased in PDAC (Humphris et al., 2016). Mutations in MMR genes (*MSH2, MLH1)* and a recently described MMR mutational signature (Alexandrov et al., 2013) are associated with MMR deficiency and the highest tumour mutational burden (TMB) in around 1% of PDAC (Humphris et al., 2016). Immune checkpoint inhibitors have shown great promise in melanoma, colorectal and non-small cell lung cancer, particularly in those tumours with hypermutation and MMR deficiency (Le et al., 2015, Rizvi et al., 2015, Hamid et al., 2013). Recent analysis suggests that MMR and *BRCA* mutational signatures correlate with antitumour immune responses in PDAC (Connor et al., 2016). These were associated with increased mutational burden, yet, immune responses were dampened by increased expression of immune checkpoint activity (Connor et al., 2016). These findings suggested that neoantigen load contributes to antitumour cytolytic activity, a requirement for immunotherapy response, however increased expression of PD-1, CTLA-4 and IDO-1 leads to immune resistance (Connor et al., 2016). A recent study, however, has demonstrated that the quality of neoantigens appear to be more important than the quantity in determining anti-tumour immune response in PDAC (Balachandran et al., 2017). Crucially, neoantigens that have predicted reactivity to microbial neo-epitopes were associated with T-cell responses and long-term survival in PDAC (Balachandran et al., 2017). Yet, neoantigen number by itself did not, suggesting that high quality neoantigens are predictive of T-cell responses in PDAC (Balachandran et al., 2017). This suggests that increased neoantigen load, secondary to high TMB, increases the likelihood that the tumour presents high quality neoantigens and thus anti-tumour immune responses. To date, the results of immune checkpoint blockade have not been encouraging in PDAC (Foley et al., 2015). This data, however, implies that in a selected subset of patients, immune

therapies such as PD-1/PD-L1 and CTLA-4 checkpoint blockade can induce significant and durable clinical responses.

Targeting immune signalling pathways can prime immune responses in non-immunogenic tumours and enhance sensitivity to checkpoint blockade and chemotherapy (Steele et al., 2016, Nywening et al., 2016, Winograd et al., 2015, Jiang et al., 2016). Inhibition of CXCR2, focal adhesion kinase 1 and stimulation of CD40 leads to enhanced T-cell tumour infiltration and checkpoint blockade response (Steele et al., 2016, Jiang et al., 2016, Winograd et al., 2015). Inhibiting the CCR2-CCL2 axis modulates both T and non-T cell immune mechanisms, potentially leading to enhanced response in combination with cytotoxic chemotherapy (Nywening et al., 2016). Intriguingly, it appears that myeloid cell depletion is crucial to inducing durable anti-tumour immune responses (Nywening et al., 2016, Zhang et al., 2017, Steele et al., 2016). With increasing immunotherapies becoming available and entering clinical trials, there is an urgent need to identify biomarkers of response in order to stratify patients to effective immunotherapy combinations at appropriate time-points in the tumour life-span.

1.4 Molecular Profiling of PDAC

The major progress in the understanding of the genomic heterogeneity and stratified therapy for PDAC brings exceptional challenges. The advances in next generation sequencing allows whole genome sequencing to be completed within 2 weeks of tissue sampling and allow rapid translation of molecular data to select patient therapy in the clinic (Roth et al., 2013, Sjoquist et al., 2014, Chantrill et al., 2015). Tissue sampling from PDAC remains a technical challenge, even with the advance of radiological and endoscopic techniques. Yet, recently the LEAP trial demonstrated the feasibility of obtaining core biopsies from patients with metastatic disease (Poplin et al., 2013). Somatic mutations can be detected by EUS-guided fine needle aspiration of advanced PDAC and thus allow stratification of treatment (Valero et al., 2015). However, these methods simply consider somatic mutation detection which in itself may not be sufficient for identifying functional mutations and molecular subtypes that predict response to therapy.

Circulating tumour cells (CTCs) and circulating free tumour DNA (cfDNA) provide an attractive form of liquid biopsy for patients with advanced PDAC to allow molecular characterisation and biomarker identification (Khoja et al., 2012, Kurihara et al., 2008). CTCs have been shown to be prognostic indicators in metastatic breast, prostate and

colorectal cancer (Kurihara et al., 2008, Riethdorf et al., 2007, Cristofanilli et al., 2005, Yagata et al., 2008, Khoja et al., 2012, Cohen et al., 2008, de Bono et al., 2008). CTCs have been shown to allow molecular profiling by immunohistochemistry analysis (Khoja et al., 2012). Yet, it remains to be seen how CTCs compare with primary biopsy and whether these novel liquid biopsies can be used for identifying genomic biomarkers to stratify treatment decisions.

A significant challenge in stratified medicine in PDAC is obtaining and returning molecular analysis results to the clinic in an acceptable timeframe (Chantrill et al., 2015). This is particularly challenging in PDAC, a disease that progresses rapidly, especially in patients that present with metastatic disease. This often leads to deterioration of patients' performance status and can result in patients not being offered treatment due to worsening condition or death (Chantrill et al., 2015). Furthermore, failure rate using standard diagnostic formalin fixed paraffin embedded (FFPE) biopsies for molecular profiling is as high as 30 – 40% which makes recruitment to clinical trials exceptionally challenging (Zill et al., 2015). To combat this, a novel approach to molecular profiling is required and incorporated into standard clinical care for patients with PDAC. A proportion of this PhD thesis is dedicated to developing these strategies in order to facilitate personalised medicine in a practical, clinically relevant time-frame for patients.

1.5 Summary

Genomic analyses have improved our understanding of the complex molecular pathology of PDAC. Studies are revealing molecular sub-sets of patients that can have durable responses to specific therapies and clinical strategies are being developed to incorporate this into practice. Treatment resistance, however, remains a significant problem even in those that respond initially. Extensively characterized pre-clinical models are crucial to identify novel therapeutic targets, responsive molecular patient sub-sets and dissect out treatment resistance mechanisms in PDAC. Successful translation of large-scale genomic discoveries requires novel clinical approaches to develop and incorporate personalised medicine into PDAC and improve outcomes in this lethal disease.

1.6 Aims and Hypothesis

It is **hypothesised** that clinical disease patterns that are encountered, such as metastatic pattern and early disease recurrence, co-segregate with molecular subtypes of PDAC. Furthermore, sub-groups of patients (e.g. DDR deficiency) are believed to respond preferentially to novel targeted therapy and that molecular subtypes may harbour therapeutic vulnerabilities that require urgent exploration. The **overall aim** of this thesis is to define the clinical utility of molecular subtyping of pancreatic cancer to inform treatment stratification and therapeutic development. The **specific aims** are:

1. Assess the clinicopathological features of molecular subtypes of PDAC to identify prognostic subgroups and explore the utility of molecular subtyping in informing patient selection for surgical resection.

2. Define the clinical utility of candidate biomarkers of poor prognostic PDAC (S100A2 and S100A4) in predicting early recurrence and poor outcome following surgery.

3. Develop novel biomarkers of DNA damage response deficiency and Replication Stress and investigate the relationship of these with molecular subtypes and therapeutic response to novel agents in PDAC.

4. Develop clinical trials that target DDR deficiency and Replication Stress in PDAC.

5. Develop a tissue acquisition protocol using endoscopic ultrasound guided biopsies that allows molecular profiling for all patients with PDAC, irrespective of disease stage.

2 Methods and Materials

2.1 Clinical Patient Cohorts

2.1.1 Ethical Approval

Ethical approval was obtained both locally and at contributing institutions. Full ethical approval was obtained for all studies involving human samples (see ethical approval numbers below).

2.1.2 Ethical approval numbers

Australian Pancreatic Genome Initiative / International Cancer Genome Consortium cohorts:

Sydney South West Area Health Service Human Research Ethics Committee, Western Zone, protocol number 2006/54

Sydney Local Health District Human Research Ethics Committee, protocol number X11-0220

Northern Sydney Central Coast Health Human Research Ethics Committee, protocol number 0612-251M

Sydney West Area Health Service Human Research Ethics Committee (Westmead Campus), protocol number HREC2002/3/4.19

South East Sydney Illawarra Area Health, Northern Hospital Network HREC- protocol number 05/321

South East Sydney Illawarra Area Health HREC- Southern Section, protocol number 05/54

Glasgow cohort:

West of Scotland Research Ethics Service (WoSRES) committee, NHS Greater Glasgow and Clyde. Molecular profiling of pancreatic cancer for improved prediction of Survival. Research Ethics Committee reference number: 07/S0704/26

German cohort:

Ethikkommission an der Technischen Universität Dresden (Approval number EK59032007) and Ethik-Kommission der FAU (Approval number 170_16 B)

***PRECISION-Panc* Endoscopic ultrasound training cohort (called the EUS cohort)**

Ethical approval was obtained for collecting additional research biopsies from patients undergoing endoscopic ultrasound guided (EUS) biopsies for investigation of possible pancreatic cancer. Ethical approval number: 17/WS/0085. Fully informed consent was obtained or all patients from which additional biopsies were taken. Samples were anonymised at point of collection with only PhD candidate able to identify patients from research samples.

2.1.3 Description of Cohorts

2.1.3.1 The International Cancer Genome Consortium cohort

Patients were recruited prospectively through the Australian Pancreatic Cancer Genome Initiative (APGI) as part of the International Cancer Genome Consortium (ICGC). Informed consent and human research ethics approvals were obtained in each contributing clinical centre. Contributing patients were restricted to those with resectable, chemo- and radiotherapy naïve pancreatic ductal adenocarcinoma who underwent either Whipple's pancreaticoduodenectomy, total or distal pancreatectomy. Following surgical resection, histopathological analysis from a pancreatic pathologist was performed and specimens with macroscopic evidence of tumour were snap frozen as a source of tumour DNA, along with samples of duodenum, stomach or spleen as a source of germline DNA. Standard histopathological processing was performed and a diagnosis of PDAC was confirmed independently by 2 Consultant Pathologists with a specialist interest in pancreatic cancer. Clinical and pathological data were collected for each patient, with strict audit to ensure clinical data accuracy at a standard expected of a clinical trial.

The ICGC cohort totalled 456 patients that underwent molecular profiling of some description (discussed in greater detail later in this thesis). These largely form part of the Australian Pancreatic Genome Initiative (APGI) cohort, which was utilised as the training set for biomarker and clinical evaluation (see below).

2.1.3.2 Training and Validation cohorts for biomarker investigation (see Chapter 4)

Detailed clinicopathological and outcome data were obtained for three cohorts of patients, totaling 1184 consecutive, unselected patients with a diagnosis of operable pancreatic ductal adenocarcinoma who underwent pancreatic resection with curative intent. Cohorts were obtained in collaboration with Dr Christian Pilarsky (German Cohort), Dr Nigel Jamieson (Glasgow Cohort) and the Australian Pancreatic Genome Initiative (APGI cohort).

These originated from teaching hospitals associated with the Australian Pancreatic Cancer Genome Initiative (APGI) (www.pancreaticcancer.net.au), Australia; the West of Scotland Pancreatic unit, Glasgow Royal Infirmary, United Kingdom; and the Technical University of Dresden, Dresden, Germany (Table 1). The three cohorts consisted of a **training cohort** of **518 patients** accrued prospectively through the **APGI** for the International Cancer Genome Consortium (ICGC; www.icgc.org)(Hudson et al., 2010) and **2 independent validation cohorts** of **198** and **468 patients** from **Glasgow** and **Germany** respectively (part of these cohorts were used for previous studies) (Biankin et al., 2012, Waddell et al., 2015, Jamieson et al., 2012, Bailey et al., 2016, Mann et al., 2012, Chang et al., 2009a, Murphy et al., 2008, Biankin et al., 2009) in accordance with the TRIPOD Type 3 model development approach and REMARK (Reporting Recommendations for Tumor Marker Prognostic Studies) criteria (Collins et al., 2015) The patients in all 3 cohorts were treated after 1998 with more modern approaches such as multi-modality therapy, and some of the patients were part of Phase III randomized-controlled trials such as ESPAC-3 (Neoptolemos et al., 2010). All cohorts displayed clinical and pathological features that are consistent with the expected clinical behavior of PDAC and are similar to published PDAC cohorts worldwide (Schnelldorfer et al., 2008, Cameron et al., 2006). The diagnosis and all pathological features were reviewed centrally by at least one specialist pancreatic histopathologist, and the date and cause of death was obtained from Central Cancer Registries and treating clinicians.

2.1.3.3 The *PRECISION-Panc* EUS training cohort

As part of the development of the *PRECISION-Panc* clinical trial platform tissue collection and processing workflow, a cohort of ***n* = 90 patients** were used as a training set for development of the endoscopic ultrasound (EUS) biopsy protocol. Patients were identified at first presentation to the local (West of Scotland Pancreatic Unit, Glasgow Royal

Infirmary) tertiary pancreatic surgery department. Patients with a pancreatic mass suspicious of malignancy (including pancreatic adenocarcinoma, pancreatic neuroendocrine tumour, intra-ductal papillary mucinous neoplasm (IPMN), cholangiocarcinoma) were included. Patients were informed using a patient information sheet and consultation with the PhD candidate on the process of additional EUS biopsy samples for research purposes including genomic sequencing. All patients gave informed. (see Chapter 7).

2.2 Next Generation Sequencing and Analysis

2.2.1 DNA and RNA extraction

2.2.1.1 ICGC Cohort

Tumour samples for the ICGC cohort used for clinical analyses (Chapter 3) were collected as bulk tumour samples or generated from patient derived xenografts. Bulk and PDX extractions of the ICGC cohort were performed principally by Marc Jones, and other members of Professor Biankin's laboratory team, prior to PhD candidate starting his research fellowship. Tissue samples representative of invasive tumour were snap frozen and cryopreserved at -80°C. Fresh frozen tumour samples underwent full face cryosection to confirm tumour presence and epithelial cellularity estimate. Macro dissection was performed prior to DNA and RNA extraction to enrich for tumour epithelium.

DNA and RNA extraction were performed using the AllPrep® DNA/RNA Mini Kit (Qiagen, Cat. No. 80004) according to manufacturer's protocol and as previously described (Bailey et al., 2016, Waddell et al., 2015). Briefly, on dry ice, frozen tumour tissue was crushed and placed within falcon tube and appropriate volume of RLT® buffer (Qiagen) and 2-mercaptoethanol (Aldrich) was added. This was homogenised immediately, and samples were frozen and stored at -80°C until further processing. After thawing at room temperature, tubes were centrifuged, and supernatant transferred to AllPrep® DNA columns (Qiagen). The larger tissue fragments were discarded. The supernatant (maximum 600µl for each tube) was centrifuged (10000 g x 30 secs) and the AllPrep® DNA column kept in collection tube for further processing. RNA was extracted from the supernatant flow through by adding 900µl 100% Ethanol per 600µl supernatant that was originally added to DNA column. This was loaded (700µl maximum per column) to AllPrep® RNA columns and spun for 2 minutes at 10 000g until all flow through was processed. Qiagen

RPE® buffer was added to the RNA column and spun at 10 000g for 2 mins. The flow through was discarded and this was repeated. The column was briefly spun to discard any residual ethanol, and this was discarded. The column was placed in new collection tube and 50µl RNA-free water (Qiagen) was added to the centre of the column. After incubation for 1 minute, the column was centrifuged and the resulting flow-through (RNA) was stored at -80°C.

DNA was purified by adding 500µl AW1® buffer (Qiagen) to each DNA column and centrifuged for 2 mins at 10 000g. This was repeated using buffer AW2® (Qiagen) and the flow through discarded. The column was transferred to a 1.5ml collection tube and 100µl pre-heated (70°C) buffer was added to the centre of DNA column membrane, incubated and centrifuged at 10 000g for 2 mins. The resulting flow through (DNA) was stored and quantified using the Nanodrop® 2000 spectophotometer.

2.2.1.2 Patient Derived Cell Lines

PDCLs were extracted principally by Marc Jones, as well as the PhD candidate and members of the Glasgow Precision Oncology laboratory. DNA and RNA were extracted from the PDCLs using the AllPrep® DNA/RNA Mini Kit (Qiagen, Cat. No. 80004) according to manufacturer's protocol and as previously described (Bailey et al., 2016, Waddell et al., 2015). The correct number of cells (no more than 1 x 10^7) were counted and a cell pellet generated in a centrifuge tube. The supernatant was removed, and the cells disrupted using 600µl Buffer RLT Plus (AllPrep® DNA/RNA Mini Kit). The lysate was homogenised and transferred to an AllPrep® DNA spin column and centrifuged. The DNA spin column was stored at 4°C whilst the RNA was extracted. The remaining steps were performed as described above. DNA and RNA were quantified using Nanodrop® 2000 spectophotometer and stored at -80°C.

2.2.1.3 EUS biopsies

Patients were sedated and received analgesia as standard (Midazolam, Fentanyl and local anaesthetic throat spray) for EUS and underwent initial endoscopy and ultrasound assessment of the pancreaticobiliary tract. Patients with evidence of a mass suspicious of a pancreaticobiliary neoplasm were biopsied as standard. This was followed by 1 – 3 additional samples for research purposes. Biopsies were taken using a fanning technique with a variety of EUS needles (discussed in Chapter 7). Diagnostic specimens were

processed as standard using local collection protocols. This involved expelling all biopsies from the same lesion in a single pot of methanol based buffered preservative solution (ThinPrep Preservcyte, Hologic, inc. Cat no: 85093-001). Additional research biopsies that were preserved in methanol fixative and embedded in FFPE was processed in a similar fashion. An additional venous blood sample (4-5mls) were collected in standard EDTA blood tubes (e.g. BD Vacutainer® K2EDTA tube, Cat no. KFK171) as a source of germline DNA.

2.2.1.4 Collecting fresh frozen EUS biopsies

All EUS biopsies presented in this thesis (except EUS 16 – collected by Dr David Chang) was collected and processed by the PhD candidate. EUS biopsies underwent cryopreservation to enable next generation sequencing including RNA and whole genome sequencing. This is a novel protocol designed by the PhD candidate and not previously described. Additional biopsies (1 – 3) were expelled in 5 – 10ml of PBS in a 50ml collection tube. This was gently swirled to allow excess blood to separate from the biopsy material. This was passed via a 70 μm nylon mesh cell strainer (Fisherbrand®, Cat No. 22363548) and the biopsy tissue transferred onto a metal histology mounting slide. This allowed the biopsies to lie in a flat level plane, which enable cryosection at a later stage. The metal slide was transferred onto dry ice and the biopsies mounted in optimal cutting temperature (OCT) compound (VWR chemicals™, Cat No. 361603E) immediately. After the OCT has set, the mounted block and biopsies were removed from the mounting slide, placed in pre-labelled plastic cassette and transported to secure cold storage at -70 °C.

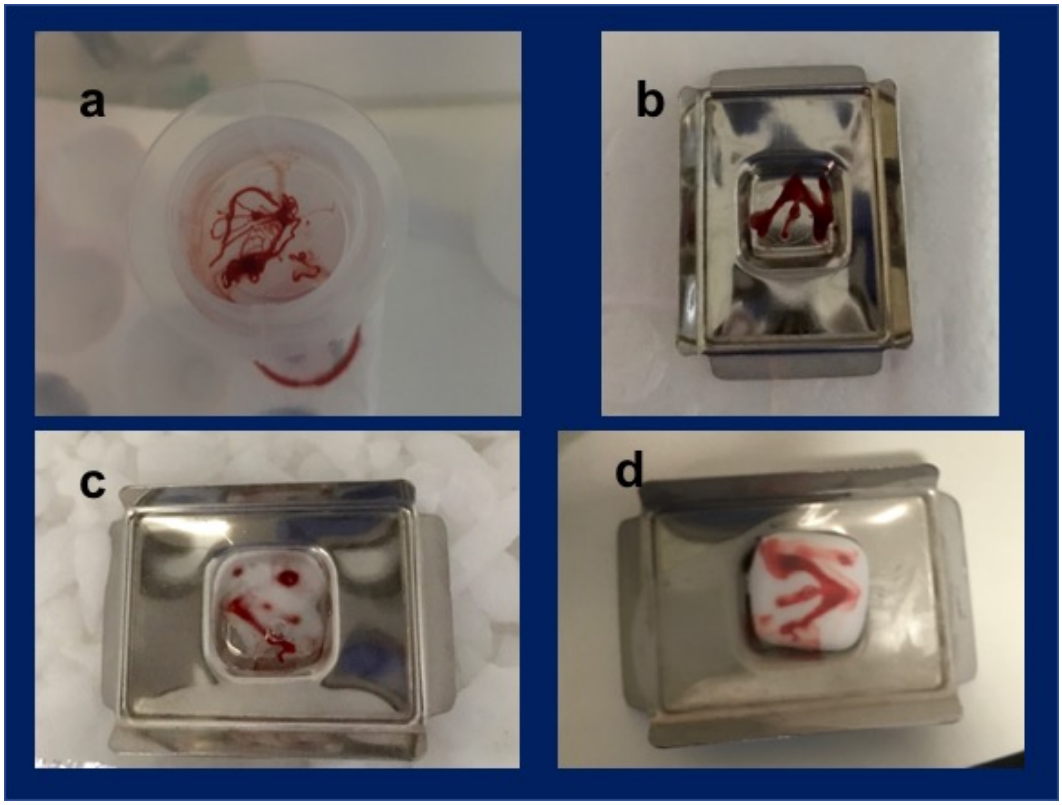

Figure 2-1 Cryopreservation of EUS biopsy samples. A) Biopsies are decanted onto a cell strainer to allow separation of blood and fluid from biopsy material. **B)** Biopsies are laid flat on a metal mounting slide to facilitate cryosection at a later stage. **C)** Metal slide is placed directly on dry ice and OCT added to freeze and mount. **D)** Completed OCT block containing flat mounted EUS biopsies.

2.2.1.5 Extraction of fresh frozen EUS biopsies

All fresh frozen EUS biopsy extractions were performed by the PhD candidate. Fresh frozen EUS biopsies underwent histological analysis prior to DNA extraction, provided the diagnostic specimen was conclusive. In cases where uncertainty remained regarding the diagnosis, the fresh frozen specimens were reprocessed and embedded in FFPE to be used as diagnostic samples. Cryosections were performed by the Beatson Institute of Cancer research histopathology unit. Sections were stained with haematoxylin and eosin (H&E) followed by formal assessment by a Consultant Pathologist with an interest in pancreatic cancer. Regions with tumour epithelium were marked on H&E slides and histological cellularity determined. Macro dissection was performed to enrich for tumour epithelium in the frozen specimens. This involved overlaying the marked H&E slide with the OCT frozen block, whilst keeping the frozen tissue on dry ice. The corresponding marked areas were dissected using a fresh scalpel blade for DNA and RNA extraction.

DNA and RNA extractions were performed using the AllPrep® DNA/RNA micro Kit from Qiagen© (Cat. no 80284). Briefly, on ice, 600µl of RLT Plus solution (AllPrep® Micro Kit) was added to macro dissected tissue and disrupted using a rotor-stator homogenizer (Polytron® PT1200E, KINEMETICA) in a glass test tube. The lysate underwent freezing and thawing to allow complete lysis followed by centrifuging to separate the supernatant from tissue fragments. The supernatant was added to an AllPrep® DNA spin column, centrifuged and stored at 4°C for extraction. 600 µl of Ethanol was added to the flow-through (containing RNA and protein) and added to an RNA spin column and centrifuged. This was followed by buffer washing of the spin column multiple times. RNA was isolated by eluting the RNA from the column using RNase-free water directly to the spin column (30 - 50µl) and centrifuging for 1 minute at 8 000 x g. DNA was isolated by buffer washing the DNA column and eluting the column with warmed elution buffer EB (AllPrep® Micro Kit). DNA and RNA were quantified using the Nanodrop® 2000 spectophotometer. DNA and RNA were stored at -80°C until sequencing.

2.2.1.6 *PRECISION-Panc* clinical trial EUS biopsies

Patients enrolled in the *PRECISION-Panc* master protocol that underwent molecular profiling from EUS biopsies had samples preserved in methanol fixative and embedded in FFPE. The commercial fixative used may vary from site to site, provided it is a methanol fixative (similar to ThinPrep PreservCyte, Hologic, inc. Cat no: 85093-001). The *PRECISION-Panc* protocol requests patients to have a minimum of 3, but ideally 5, EUS biopsies collected and fixed in the same pot. Samples are then transferred to local pathology laboratory, where it is processed and embedded in formalin fixed paraffin embedded (FFPE) block for histological diagnosis followed by DNA and RNA extraction.

EUS biopsies are processed into FFPE blocks by retrieving all ‘micro-biopsies’ from the preservative pot using dedicated filter paper (CellPath^{TM} tissuewrap). To avoid contamination, human fibrin or serum are not be used to make cell clots. These are next fixed for 12 to 24 hours in formalin and embedded as a paraffin block using standard histological techniques. Diagnostic H&E slide is taken, followed by cellularity estimation by dedicated Consultant Pathologist. An assessment on suitability for extraction and sequencing (sufficient tissue volume and tumour cellularity) is made by a consultant pathologist with significant experience in these techniques.

2.2.1.7 Extraction of FFPE biopsies

Formalin fixed EUS biopsies underwent DNA extraction by the NHS Greater Glasgow & Clyde Molecular Genetics Laboratory. Extraction in a clinically approved facility was selected as this ensures appropriate quality control for clinical trial enrolment and future treatment stratification. Sample extraction is performed using 2 – 4 10μM tissue curls using the Maxwell® 16 FFPE Plus LEV DNA Purification Kit (Cat No. AS1135). The Maxwell® 16 System offers automation and walk-away purification that saves time and labour by eliminating reagent preparation, pipetting and centrifugation steps. Briefly, samples are prepared by centrifuging tissue curls and adding Proteinase K and Incubation buffer (included in Maxwell® Kit Cat No. AS1135). This is incubated at 70°C overnight followed by the addition of lysis buffer. The sample is now ready for DNA purification and is added to the Maxwell® FFPE Plus LEV DNA cartridge. Automated extraction and elution are performed using elution buffer supplied in the extraction kit.

2.2.1.8 Extraction of germline DNA from blood

All germline DNA extractions were performed by the PhD candidate, except the *PRECISION-Panc* clinical trial specimens which were extracted in the NHS Greater Glasgow & Clyde Molecular Genetics Laboratory. Germline DNA was obtained by venous blood preserved in standard diagnostic EDTA blood tubes. DNA was extracted using the DNeasy Blood Mini kit from Qiagen© (Cat no. 69504). Briefly, 200 μl of whole blood is added to 20 μl of Qiagen protease in a 1.5ml microcentrifuge and incubated at 56°C for 10 minutes. 200μl of Ethanol is added, and the mixture applied to a DNA spin column. This was centrifuged, followed by buffered washing of the DNA column. DNA was isolated by elution with buffer AE (DNeasy Blood Mini Kit, Qiagen©). DNA yield was quantified using the Nanodrop® 2000 spectophotometer and stored at -80°C until sequencing.

2.2.2 Library preparation and Sequencing

Sequencing libraries were created with Lisa Evers (Laboratory Technician) and the Glasgow Precision Oncology Laboratory sequencing team.

2.2.2.1 Whole-genome library preparation.

Whole-genome libraries were generated using either the Illumina TruSeq DNA LT sample preparation kit (Illumina, Part no. FC-121–2001 and FC-121–2001) or the Illumina TruSeq

DNA PCR-free LT sample preparation kit (Illumina, Part no. FC-121–3001 and FC-121–3002) according to the manufacturer's protocols. If available, 1µg of DNA was used as input for fragmentation to ~300 base pairs (bp). In the EUS sequencing cohort lower quantities of DNA (down to 500ng) was used for whole genome sequencing. Quantification of libraries for clustering was performed using the KAPA Library Quantification Kit - Illumina/ Universal (KAPA Biosystems, Part no. KK4824) in combination with the Life Technologies Viia 7 real time PCR instrument.

2.2.2.2 RNA sequencing library generation and sequencing.

RNA sequencing libraries for patient derived cell lines were generated using TruSeq Stranded Total RNA kits (catalogue no. RS-122-2203). Due to the relative low input of the RNA obtained from EUS biopsy samples, RNA sequencing libraries for these were performed using the KAPA RNA HyperPrep kit with Riboerase (KAPABIOSYSTEMS©, KK8561) designed for small input samples on Illumina® systems. Depending on the sample size up to 1µg of RNA was used to produce libraries. cDNA was synthesized from the enriched and fragmented RNA using Invitrogen's SuperScript II Reverse Transcriptase (catalogue number 18064) and random primers. This was converted into double stranded DNA and subjected to 15 cycles of PCR to produce RNA-seq libraries ready for sequencing. Prior to sequencing, libraries were examined for quality and quantity using an Agilent BioAnalyser and Caliper's LabChip GX (part no. 122000) instruments using the DNA High Sensitivity Reagent kit (product no. CLS760672).

2.2.2.3 Targeted, Whole genome and RNA sequencing.

Sequencing was performed by the Glasgow Precision Oncology Laboratory sequencing facility. This is a state-of-the-art purpose-built facility and has recently obtained Good Clinical Laboratory Practice (GCLP) accreditation to allow clinically valid sample sequencing. Sequencing was performed on Illumina platforms according to the manufacturer's instructions. All sequencing runs were subjected to quality control according to approved Glasgow Precision Oncology Laboratory standard operating procedures.

2.2.3 Data Analysis

Upfront bulk tumour DNA and RNA sequencing alignment, processing and initial analysis of the ICGC cohort was performed by the Australian Pancreatic Genome Initiative as part

of the International Cancer Genome Consortium (Bailey et al., 2016, Waddell et al., 2015, Biankin et al., 2012). RNA sequencing analysis of the PDCLs were performed by Dr Rosie Upstill-Goddard (post-doctoral bioinformatician) and Dr Peter Bailey (Senior Lecturer). RNA sequencing analyses and gene set enrichment presented in Chapter 3 was performed by Dr Rosie Upstill-Goddard and the PhD candidate. All RNA sequencing analyses of EUS biopsies were performed by Dr Rosie Upstill-Goddard. Whole genome analysis of EUS biopsies were performed by Dr Dario Beraldi (staff bioinformatician) and targeted sequencing analysis was performed by the Glasgow Precision Oncology Laboratory automated pipeline which was overseen by Dr Susie Cooke and Dr John Marshall. Interpretation and application of sequencing analyses with clinical and pathological data was performed by PhD candidate.

2.2.3.1 Targeted sequencing

Detailed somatic and germline variants were obtained for the ICGC cohort. This was correlated with clinical and pathological data as described in Chapter 3. Samples underwent either whole exome or whole genome sequencing with analysis generating reports on copy number variation, Single nucleotide substitutions and insertions/deletions, structural variations and germline mutations. These analyses were completed prior to starting this PhD project, and were obtained from the ICGC prior to correlating with clinical and pathological data. Detailed description of genome analyses these as been previously published (Bailey et al., 2016, Biankin et al., 2012, Waddell et al., 2015).

Targeted panel sequencing was analysed using the Glasgow Precision Oncology laboratory genome analysis pipeline (EUS cohort). Analysis generated read-outs on somatic point mutations and copy number variations. The data processing has been handled using the workflow manager snakemake (version 4.3.0). Custom scripts have been written in R version 3.5.0 and python 3.6.3. Sequence reads in fastq format were trimmed to remove low quality ends using bbduk version 37.98 and aligned to the human reference genome GRCh38 using bwa mem version 0.7.15. Read pairs mapping to the same location were marked using picard MarkDuplicates version 2.18.0. Read and alignment qualities were assessed using FastQC (version 0.11.7) and samtools stats.

Single nucleotide variants and short insertions and deletions were detected with Mutect2 in the Genome Analysis Toolkit version 4.0.4.0. Tumour somatic variants were distinguished from germline variants by contrasting calls in each tumour sample against the matched

normal sample. Putative artefact calls were filtered against a set of somatic variants detected in a pool of blood normal samples. The resulting variants were annotated with VEP version 91 using the *--flag_pick* option to flag the most biologically relevant annotation for each variant. Copy number variants were detected with the R package FACETS version 0.5.14. The source of polymorphic sites was dbSNP version 150. Note that FACETS also provide estimates of tumour purity and ploidy.

2.2.3.2 Whole Genome Sequencing

The circular maps of the genomic variants were plotted using the R package circlize.

The single nucleotide variants and short insertions somatic variants displayed for each gene and library (i.e. for the drawing of the oncoplot) were detected as described above. Only variants with frequency greater than 5% and passing all the mutect filters and having significant impact on the underlying transcript were retained. However, for the *KRAS* gene this selection was relaxed, and any variant was used for plotting.

Whole genome analysis was performed on selected EUS samples and PDCLs. For these, Substitutions and indels were called using a consensus calling approach that included qSNP, GATK and Pindel. The details of call integration and filtering, and verification using orthogonal sequencing and matched sample approaches are as previously described (Nones et al., 2014, Waddell et al., 2015, Patch et al., 2015). The Somatic structural variant pipeline was identified using the qSV tool for PDCLs. Structural variants were identified with manta version 1.3.2. Putative artefact variants were filtered against a set of variants detected in the same pool of normal samples above.

A detailed description of its use has been recently published (Waddell et al., 2015, Nones et al., 2014). Mutational signatures were defined for genome-wide somatic substitutions, as previously described (Waddell et al., 2015).

2.2.3.3 RNA-sequencing, alignment and differential expression

Bulk RNAseq expression data, for the ICGC cohort, were obtained from Bailey *et al.* and the ICGC portal (Bailey et al., 2016). For the PDCLs and EUS cohort RNA sequencing reads were aligned to the GRCh37 genome build using STAR (Dobin et al., 2013). Counts for known genes were generated using the function featureCounts in the R/Bioconductor package “Rsubread”(Liao et al., 2014). The R/Bioconductor package “DESeq2” was used

to normalize count data between samples and to identify differentially expressed genes (Love et al., 2014). Expression data were normalized using the rlog transform in the DESeq2 package and these values were used for all downstream analyses.

Heatmaps were generated using the R package ComplexHeatmap (Gu et al., 2016). Genes with differential expression with log fold change > 2 and $P \leq 0.05$ were included in differential heatmaps. Boxplots were generated using the R package ggpubr.

2.2.3.4 Gene set enrichment analysis

The R package clipper (Martini et al., 2013) was used to identify pathways and/or processes showing significant change between PDCL subtypes. Pathways and/or processes identified by clipper analysis were selected for signature generation. Subtype specific gene signatures representing each pathway and/or process were generated by selecting significant genes in a given graph. Gene weights in each signature represent estimated Z-scores generated from Student t-test p-values with direction of change provided by the t-test statistic. The 'sig.score' function from the R package genefu (Haibe-Kains et al., 2012) was used to calculate a specific signature score in a given sample using the signatures generated for each pathway and/or process.

The package 'ConsensusClusterPlus'(Wilkerson and Hayes, 2010) was used to classify PDCLs according to the expression signatures defined in Bailey *et al*.. Gene sets representing PDAC subtypes were generated as previously described. Gene Ontology and pathway enrichment analysis was performed using the R package 'dnet' and/or the ClueGO/CluePedia Cytoscape (Bindea et al., 2013, Bindea et al., 2009) plugins as indicated.

2.2.3.5 Replication Stress signature generation

The replication stress signature was generated by the PhD candidate, Dr David Chang (supervisor), Dr Rosie Upstill-Goddard and Dr Peter Bailey. In order to define subtype specific signatures that can inform therapeutic development, differentially expressed genes were compared to genes associated with gene ontology (GO) terms using the R package 'dnet'. Significantly expressed GO terms involved in DNA damage response and cell cycle control were selected. Differential expression of each selected GO term was applied to each individual PDCL that underwent RNA sequencing. This in turn, was used to generate a composite score by totalling the score for each selected GO term. This was termed the

replication stress signature. Generation of signature score for bulk tumour samples followed the same methodology (Chapter 5).

2.3 Assessment of S100A2 and S100A4 expression with survival

2.3.1.1 Tissue Microarray construction

The effect of biomarker protein expression with clinical outcome was assessed using tissue microarrays (TMA) generated from 3 distinct areas per tumour. Tumour areas were assessed using diagnostic haematoxylin and eosin (H&E) stained tissue sections by specialist Consultant Pathologists with an interest in Pancreatic Cancer (Dr Fraser Duthie (Glasgow), Prof Anthony Gill (APGI), Prof James Kench (APGI), Dr Angela Chou (APGI)). For biomarker evaluation, TMA sections were cut at 4μm and mounted on adhesive glass slides prior to incubation at 60°C overnight.

2.3.1.2 S100A2 Immunohistochemistry

Prior to antibody staining, unmasking was performed using DAKO S2367 target retrieval solution (Dako corporation) for 5 minutes. Immunostaining was performed using the DAKO autostainer and TMA sections were incubated with anti-S100A2 mouse monoclonal antibody, 1:50 dilution, (clone DAK-S100A2/1; Dako Corporation, Glostrup, Denmark) for 60 minutes. As part of a standardised biomarker discovery and development process, initial cut-offs were generated using earlier training/discovery cohorts, then validated using independent validation cohorts. S100A2 and S100A4 expression analysis was performed in an early training cohort of PDAC to define the optimal expression for analysis (Biankin et al., 2009). S100A2 expression was defined using intensity (0 – 3+) in the proportion of epithelial tumour cells (0 – 100%) (Figure 2-2). High S100A2 expression was defined as cytoplasmic staining with intensity 3+ in >30% of cells. Expression was dichotomised as high and low based on previous work by Dr David Chang and Professor Andrew Biankin (supervisors). Appropriate positive and negative controls were used.

2.3.1.3 S100A4 Immunohistochemistry

Antigen retrieval involved using the DAKO S1699 solution (DAKO corporation) in 100°C water bath for 15 minutes followed by immunostaining using the DAKO autostainer. Anti-S100A4 rabbit polyclonal antibody (NeoMarkers, Cat. #RB-1804, Fremont, CA, USA)

with a dilution of 1:100 was incubated for 60 minutes**.** As part of a standardised biomarker discovery and development process, initial cut-offs were generated using earlier training/discovery cohorts, then validated using independent validation cohorts. S100A2 and S100A4 expression analysis was performed in an early training cohort of PDAC to define the optimal expression for analysis (Biankin et al., 2009). Positive S100A4 expression was defined as either nuclear and/or cytoplasmic staining of any intensity in > 1% of epithelial tumour cells (Figure 2-2) (Biankin et al., 2009). All samples were dichotomised as positive and negative for analysis based on preliminary work by Dr David Chang and Professor Andrew Biankin (supervisors). Appropriate positive and negative controls were used.

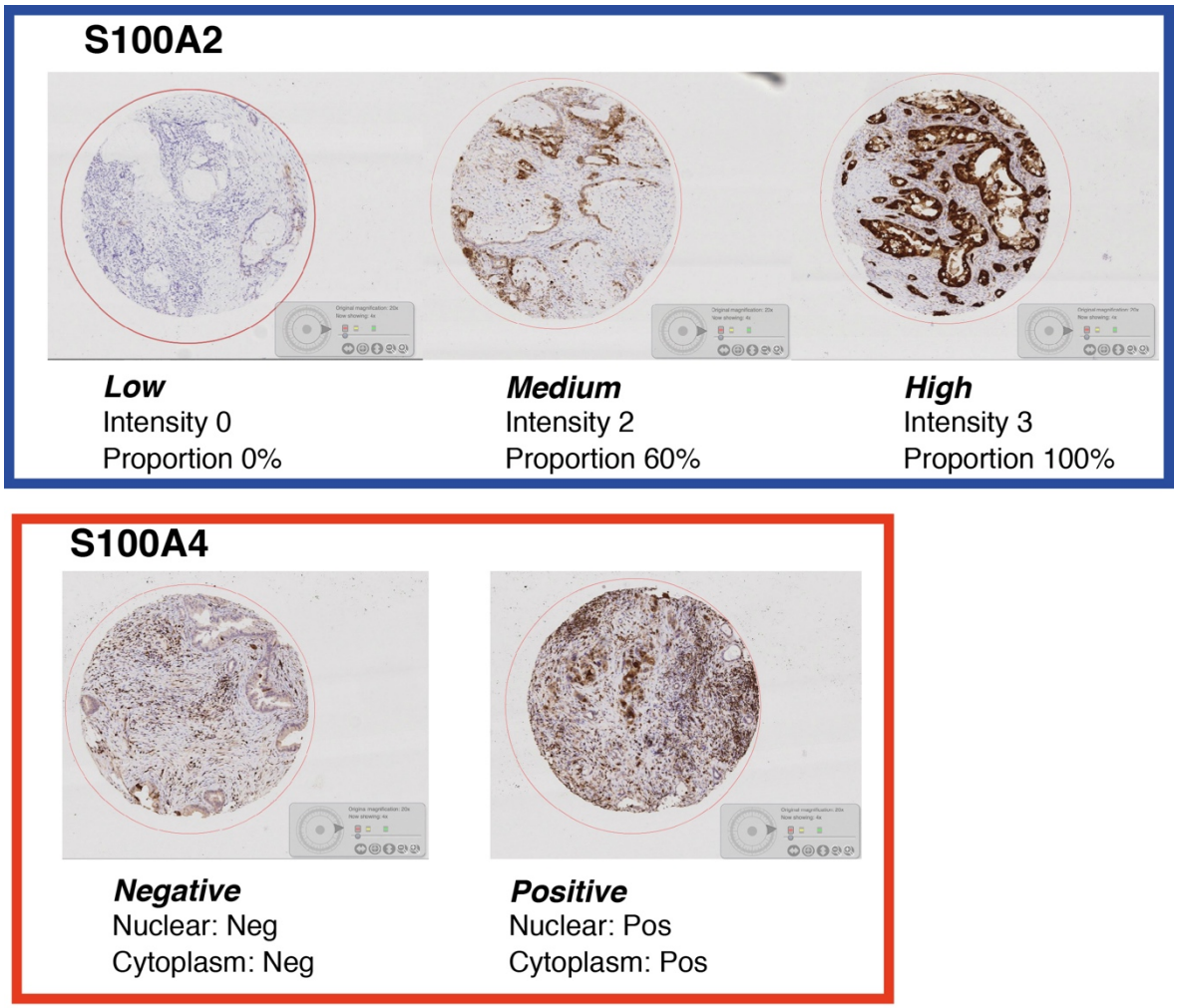

Figure 2-2 S100A2 and A4 expression analysis. Representative images of S100A2 and A4 IHC demonstrating typical appearance of high S100A2 (intensity 3+ in > 30% of epithelial cells) and positive S100A4 (any positive nuclear or cytoplasmic staining > 1% epithelial cells) expression.

2.3.1.4 EUS fine needle aspirates (FNA) and Cell Block Construction for biomarker evaluation

EUS-FNA samples were collected and processed as per the standard diagnostic pathway using endoscopic and cytohistological techniques according to local practice. These were collected prior to the availability of new EUS biopsy needles that were used for the *PRECISION-Panc* EUS cohort described previously. Formalin-fixed EUS-FNA tissue fragments or cell block preparations were embedded in paraffin, sectioned (4 μm) and H&E stained as standard. Staining for S100A2 and S100A4 were performed as described above and compared with corresponding resection specimen from 17 consecutive patients undergoing both EUS-FNA and pancreatectomy.

2.3.1.5 Immunohistochemistry scoring

All TMA cores were double scored, with each individual assessor blinded to the other's result. This included the PhD candidate, as well as Dr David Chang (supervisor) and Dr Fraser Duthie (Consultant Pancreatic Pathologist). All samples were scored by a Consultant Pathologist as one of the blinded assessors. Some samples were scored historically by collaborators Prof James Kench, Prof Anthony Gill and Dr Angela Chou (all 3 of whom are consultant pathologists associated with the APGI).

2.3.1.6 Tripod Checklist for Biomarker evaluation

In order to ensure an appropriate standard for biomarker prediction model development, the tripod checklist was followed as a quality assurance guide (Collins et al., 2015). The TRIPOD checklist is presented below, along with the appropriate steps acknowledged. Those marked n/a does not apply to this study or the patient cohorts.

Table 2-1 TRIPOD checklist: Prediction model development and validation

Section/Topic			Checklist Item	Performed
Title and abstract				
Title	1	D;V	Identify the study as developing and/or validating a multivariable prediction model, the target population, and the outcome to be predicted.	Yes
Abstract	2	D;V	Provide a summary of objectives, study design, setting, participants, sample size, predictors, outcome, statistical analysis, results, and conclusions.	Yes
				Introduction
Background and objectives	3a	D;V	Explain the medical context (including whether diagnostic or prognostic) and rationale for developing or validating the multivariable prediction model, including references to existing models.	Yes

	3b	D;V	Specify the objectives, including whether the study describes the development or validation of the model or both.	Yes
				Methods
Source of data	4a	D;V	Describe the study design or source of data (e.g., randomized trial, cohort, or registry data), separately for the development and validation data sets, if applicable.	Yes
	4b	D;V	Specify the key study dates, including start of accrual; end of accrual; and, if applicable, end of follow-up.	Yes
Participants	5a	D;V	Specify key elements of the study setting (e.g., primary care, secondary care, general population) including number and location of centres.	Yes
	5b	D;V	Describe eligibility criteria for participants.	Yes
	5c	D;V	Give details of treatments received, if relevant.	Yes
Outcome	6a	D;V	Clearly define the outcome that is predicted by the prediction model, including how and when assessed.	Yes
	6b	D;V	Report any actions to blind assessment of the outcome to be predicted.	
Predictors	7a	D;V	Clearly define all predictors used in developing or validating the multivariable prediction model, including how and when they were measured.	Yes
	7b	D;V	Report any actions to blind assessment of predictors for the outcome and other predictors.	Yes
Sample size	8	D;V	Explain how the study size was arrived at.	Yes
Missing data	9	D;V	Describe how missing data were handled (e.g., complete-case analysis, single imputation, multiple imputation) with details of any imputation method.	Yes
Statistical analysis methods	10a	D	Describe how predictors were handled in the analyses.	Yes
	10b	D	Specify type of model, all model-building procedures (including any predictor selection), and method for internal validation.	Yes
	10c	V	For validation, describe how the predictions were calculated.	Yes
	10d	D;V	Specify all measures used to assess model performance and, if relevant, to compare multiple models.	Yes
	10e	V	Describe any model updating (e.g., recalibration) arising from the validation, if done.	N/A
Risk groups	11	D;V	Provide details on how risk groups were created, if done.	Yes
Development vs. validation	12	V	For validation, identify any differences from the development data in setting, eligibility criteria, outcome, and predictors.	Yes
				Results
Participants	13a	D;V	Describe the flow of participants through the study, including the number of participants with and without the outcome and, if	N/A

			applicable, a summary of the follow-up time. A diagram may be helpful.	
	13b	D;V	Describe the characteristics of the participants (basic demographics, clinical features, available predictors), including the number of participants with missing data for predictors and outcome.	Yes
	13c	V	For validation, show a comparison with the development data of the distribution of important variables (demographics, predictors and outcome).	Yes
Model development	14a	D	Specify the number of participants and outcome events in each analysis.	Yes
	14b	D	If done, report the unadjusted association between each candidate predictor and outcome.	Yes
Model specification	15a	D	Present the full prediction model to allow predictions for individuals (i.e., all regression coefficients, and model intercept or baseline survival at a given time point).	Yes
	15b	D	Explain how to the use the prediction model.	Yes
Model performance	16	D;V	Report performance measures (with CIs) for the prediction model.	Yes
Model-updating	17	V	If done, report the results from any model updating (i.e., model specification, model performance).	N/A
				Discussion
Limitations	18	D;V	Discuss any limitations of the study (such as nonrepresentative sample, few events per predictor, missing data).	Yes
Interpretation	19a	V	For validation, discuss the results with reference to performance in the development data, and any other validation data.	Yes
	19b	D;V	Give an overall interpretation of the results, considering objectives, limitations, results from similar studies, and other relevant evidence.	Yes
Implications	20	D;V	Discuss the potential clinical use of the model and implications for future research.	Yes
				Other information
Supplementary information	21	D;V	Provide information about the availability of supplementary resources, such as study protocol, Web calculator, and data sets.	N/A
Funding	22	D;V	Give the source of funding and the role of the funders for the present study.	Yes

2.3.2 Survival Analysis

Survival analyses and nomogram generation were performed by the PhD candidate in collaboration with Dr Mark Pinese (Post-Doctoral bioinformatician, Garvan Institute, Sydney).

2.3.2.1 Statistical Analysis

The influence of clinicopathological variables on survival was assessed with Cox proportional hazards regression, and the differences in outcome between predefined subgroups was evaluated using the log-rank test (Bland and Altman, 2004). Where multiple cohorts were included in a single model, baseline hazard was always stratified by cohort throughout the procedure. On the basis of exploratory analysis, age was modelled with a cohort interaction term in the combined models; no other substantive variable to cohort interactions were identified. *P*-values of less than 0.05 were considered statistically significant. Statistical analysis was performed using SPSS (Version 22.0; IBM SPSS Statistics, IBM Corporation, Armonk, NY). Model fitting and nomogram generation was performed using R 3.4.0 (The R Project for Statistical Computing, Vienna, Austria). Disease-specific survival (DSS) was used as the primary endpoint for the APGI and Glasgow cohorts. Patients succumbing to other causes were right censored in the analysis. As the majority of patients with PDAC unfortunately succumb to disease, even after seemingly curative resection (Groot et al., 2017), overall survival (OS) was used for the German cohort, as disease-specific survival was not available.

2.3.3 Prognostic Nomograms

2.3.3.1 MSKCC Nomogram Evaluation

The published Memorial Sloan Kettering Cancer Centre (MSKCC) nomogram (Brennan et al., 2004) was applied to the APGI, Glasgow, and German cohorts, yielding per-patient estimates of linear risk score and 6-, 12- and 24-month survival probabilities. Some variables in the MSKCC nomogram were not collected in the current cohorts and were imputed to the mean value of that variable reported for the MSKCC nomogram derivation cohort (Table 2-2).

Table 2-2 Availability of MSKCC prognostic variables in the validation cohorts.

	Cohorts		
MSKCC Variable	APGI	Glasgow	German
Portal vein involvement	Absent	Absent	Absent
Splenectomy	Absent	Absent	Absent

Back pain	Absent	Absent	Absent
Weight loss	Absent	Absent	Absent
Posterior margin involvement	Absent	Absent	Absent
Number of nodes involved	97.7%	Absent	Absent
Number of nodes not involved	95.4%	Absent	Absent
Patient sex	Complete	Complete	Absent
Tumor longest axis length	99.2%	Complete	43.8%
Tumor location (head vs body / tail)	Complete	Complete	87.2%
Histological grade	99.6%	Complete	95.5%
Margin involvement	Complete	Complete	97.2%
T Stage	Complete	Complete	99.8%
Age at diagnosis	Complete	Complete	Complete

2.3.3.2 Nomogram Construction

Two Cox proportional hazard models were fit to the APGI training cohort data, one containing conventional clinicopathological variables available post-operatively (age, tumour size, T-stage, tumour location, vascular invasion, perineural invasion, margin status, presence of lymph node metastases, and differentiation), and the other containing only variables assessable pre-operatively (age, tumour size, tumour location, and S100A2 and S100A4 status). Patient sex was not included in models due to its known poor prognostic value in PDAC (Brennan et al., 2004). To improve the clinical utility of the nomogram, follow-up was truncated at 24 months to focus prognosis prediction in this most clinically critical period following surgery. To simplify generation and application of the predictive nomograms, violations of the proportional hazards assumption were

addressed by stratifying the baseline hazard by predictive variables, rather than introducing interaction with a time-dependent stratum.

2.3.3.3 Nomogram Testing

Nomograms were tested for discrimination and calibration against validation cohorts (Glasgow and Germany) using established methods (Altman and Royston, 2000, Gerds and Schumacher, 2006). Variability of the Brier score assessment of overall fit was estimated using 5,000 bootstrap rounds (Altman and Royston, 2000, Gerds and Schumacher, 2006).

2.4 Pre-clinical cell line and animal models

2.4.1 Patient Derived Cell lines (PDCLs)

Patient derived cell lines (PDCLs) were generated as part of the APGI's contribution to the ICGC project. All cell line experiments presented in this thesis was performed by the PhD candidate unless otherwise stated. Primary, treatment naïve, resectable PDAC were collected and processed as previously described (Waddell et al., 2015). PDCLs were cultured at 37°C either in normal oxygen or hypoxic conditions (Table 2-3, Table 2-4).

2.4.1.1 Cell culture – general principles

Cell culture was performed in an appropriate cell culture facility with strict infection control. Tissue culture reagents were sterilised prior to use (0.22μM Stericup filter unit, Merck Millipore, catalogue no. SCGPU05RE) and stored either at 4°C or frozen (-20°C) if appropriate. Cells were cultured to 80 – 90% confluence and passaged into appropriate fractions (e.g. 1:3), depending on the growth characteristics of each individual cell line, either once or twice weekly. This was performed by washing cells with phosphate buffered saline (PBS) and detached using PBS containing 0.04 mg / ml EDTA (Thermo Scientific, catalogue no. 15040-066). Cell lines, when not in use, were cryopreserved (-80°C) in a solution of 10% DMSO in fetal bovine serum (FBS). All cell lines were routinely tested for Mycoplasma contamination using MycoAlert PLUS Mycoplasma Detection Kit (Lonza, catalogue no. LT07-318), and discarded if positive.

Table 2-3 Media formulations for patient derived cell lines

REAGENT	Final concentration	SOURCE	Cat IDENTIFIER
HPAC modified media formulation			
DMEM/F12		Life Technologies	#11320-074
HEPES (1M)	15 mM	Life Technologies	#15630106
FBS (filtered)	8%	Hyclone; Thermo Scientific	#SH30084.03
hEGF (1 mg/L)	10 ng/mL	Life Technologies	#PHG0311L
Hydrocortisone (1 mg/mL in EtOH)	40 ng/mL	Sigma	#H0888-1G
Insulin (100 IU/mL) ActRapid	0.1 IU/mL	Life Technologies	#12585014
Glucose solution 10%	0.12%	Sigma	#G8644
M199/F12 media formulation			
M199	50%	Life Technologies	#31150-022
F12 HAM	50%	Life Technologies	#21765-029
HEPES	15mM	Life Technologies	#15630-049
Glutamine	2 mM	Life Technologies	#25030024
EGF	20ng/mL	Life Technologies	#PHG0311L
Hydrocortisone	40ng/mL	Sigma	#H0888-1G
apo-Transferrin	5ug/mL	Sigma	#T1147-500mg
Insulin ActRApid 1(00 IU/mL)	0.2 IU/mL	Life Technologies	#12585014
Glucose solution 10%	0.06%	Sigma	#G8644
FBS (filtered)	7.5%	Hyclone; Thermo Scientific	#SH30084.03
Tri-iodotyronine (0.1 ug/mL)	0.5 pg/mL	Sigma	#T6397-100mg
MEM vitamins (100x)	1x	Life Technologies	#11120037
O-phosphoryl ethanolamine	2 ug/mL	Sigma	#P0503-1g
IMDMrich media formulation			
IMDM		Life Technologies	#21980-065
FBS (filtered)	20%	Hyclone; Thermo Scientific	#SH30084.03
EGF	20 ng/mL	Life Technologies	#PHG0311L
apo-Transferrin	2.5 ug/mL	Sigma	#T1147-500mg
Insulin ActRapid (100 IU/mL)	0.2 IU/mL	Life Technologies	#12585014
MEM vitamins (100 x)	0.5x	Life Technologies	#11120037
DMEM and KSFM media formulation			
DMEM		Life technologies	#41965-039
FBS (filtered)	10%	Hyclone; Thermo Scientific	#SH30084.03
KSFM+EGF+BPE stock	Add 134mL of stock		
KSFM+EGF+BPE stock			
KSFM	Add all KSFM supplements to 500mL of KSFM media	Life technologies	#17005-059
KSFM supplements (BPE and EGF)		Life technologies	#37000-015
Mayo cell line media formulation			
DMEM/F12		Life technologies	#11320-074
FBS (filtered)	10%	Hyclone; Thermo Scientific	#SH30084.03
HEPES	15mM	Life Technologies	#15630-049

Table 2-4 Patient derived cell line media and culture conditions

Cell line	Media formulation	Incubator $C0^2$ (%)
TKCC-2.1	M199/F12	2%
TKCC-05	HPAC modified	5%
TKCC-06	HPAC modified	5%
TKCC-07	M199/12	5%
TKCC-09	M199/12	5%
TKCC-10	M199/12	5%
TKCC-12	M199/12	5%
TKCC-14	M199/12	5%
TKCC-15	M199/F12	2%
TKCC-16	M199/F12	2%
TKCC-17	M199/F12	2%
TKCC-18	IMDMrich	2%
TKCC-19	IMDMrich	2%
TKCC-22	IMDMrich	2%
TKCC-26	M199/F12	2%
TKCC-27	M199/F12	2%
Mayo	Mayo	5%
PacaDD	DMEM and KMSF	5%

2.4.1.2 Irradiation of cells

At 24 hours after seeding, cells were processed and fixed for immunofluorescence analysis. Designated time point replicates were exposed to 4 Gray (Gy) ionising radiation (IR) and processed for analysis at 2, 4 and 20 hours after exposure. Cells were irradiated using an XStrahl RS225 radiation unit. X-rays were delivered at 195kV with a current of 15mA. This provides a dose rate of 1.5mGy per minute at a distance of 400mm from the source.

2.4.1.3 Gamma H2AX and Replication Protein A foci formation assay

Immunofluorescence analysis of foci of phosphorylated proteins within the DNA damage response pathway was assessed to determine baseline replication defects. Phosphorylated Replication Protein A (pRPA) was used as a measure of replication stress. RPA is phosphorylated and recruited to sites of stalled replication forks and thus represent functional consequences of replication stress (Dobbelstein and Sorensen, 2015). Gamma H2AX (γH2AX), a marker of double strand DNA breaks (DSBs), was used as a functional

marker of homologous recombination (HR) deficiency and thus DNA damage repair deficiency (Dobbelstein and Sorensen, 2015, Paull et al., 2000).

Following irradiation, cells were fixed by removing media and washing with normal saline. Each well was treated with 50µl of nuclear extraction buffer (NEB) (Table 2-5) to allow for nuclear staining only, followed by washing with PBS. This was followed by addition of 100µl of 4% Paraformaldehyde (MERCK, P6148-500G) for 10 minutes, followed by washing with PBS. Cells were then treated with bovine serum albumin (BSA) blocking buffer (5% BSA, 0.3% TRITON-X in PBS) for 1 hour at room temperature or overnight at 4ºC. After washing with PBS, cells were stained with primary antibodies at a dilution of 1:1000 with anti-pRPA32 (S4/S8, Bethyl Laboratories Inc.) and anti-γH2AX (Ser139, MERCK) for 1 hour. Secondary antibodies used were (green) Alexa Fluor® 488 goat anti-mouse IgG (MERCK, Cat No. AP124JA4) and (red) Cy3 goat anti-rabbit IgG (MERCK, Cat no. AP132C). After washing with PBS, 100µl of DAPI (InvitrogenTM, Cat No. D3571) at concentration of 300nM were added as a nuclear stain and after 2 hours this was exchanged for 100ml PBS and plates were sealed.

Table 2-5 Nuclear extraction buffer

Compound	Volume	Cat No. (Sigma-Aldrich)
10mM Pipes pH 6.8	2.5ml (0.2M Pipes)	P1851
100mM NaCL	1ml (5M NaCl)	S3014
300mM Sucrose	7.5ml (2M sucrose)	S0389
3mM $MgCl_2$	150µl (1M $MgCl_2$)	M8266
1mM EGTA pH8	500µl (0.1M EGTA)	E3889
0.5% Triton X-100	250µl	T8787
H_2O	38.1ml	

2.4.1.4 Quantification and statistical analysis

Confocal imaging was performed using the Opera Phenix™ high content screening system (PerkinElmer) with assistance from Dr Grant McGregor. Initial screen was performed at 5x followed by high resolution imaging at 63x magnification using a water objective, at

wavelengths of 405nm (DAPI), 488nm (Alexa) and 561nm (Cy3). A minimum of 320 cells (median 980, range 322 - 1886), in biological triplicates, were analysed for each time point.

Image analysis was performed using Columbus™ Image data storage and analysis system (PerkinElmer Inc, Waltham, MA). Statistical analysis was performed using GraphPad Prism 6 (GraphPad Software Inc, La Jolla CA).

2.4.1.5 Reverse Phase Protein Array (RPPA)

RPPA analysis was performed by Dr Bryan Serrels (post-doctoral scientist) as part of a wider analysis of differential protein expression in the PDCLs. Analysis was performed by Dr Bryan Serrels and Dr Peter Bailey, with application and interpretation of results by PhD candidate. Briefly, Samples were lysed in RIPA lysis buffer (50mM Tris-HCL at pH7.4, 150mM Sodium Chloride, 5mM EGTA, 0.1% SDS, 1% NP40, 1% Deoxycholate, supplemented protease and phosphatase inhibitor tablets; Roche Applied Science Cat. #: 05056489001 and 04906837001) for 30 min on ice and cleared by centrifugation for 15 min at 4°C. Protein concentration was determined using a Bradford assay (Sigma) and all samples were normalized to 2mg/ml. 4x SDS sample buffer (40% Glycerol, 8% SDS, 0.25M Tris-HCL, pH 6.8. 1/10th vol/vol 2-mercaptoethanol) was added to each sample, followed by incubation at 80°C for 5 mins. Serial dilutions (1, 0.5, 0.25, 0.125) were prepared and samples were printed onto Avid nitrocellulose coated glass slides (Grace Biolabs) using an Aushon 2470 microarrayer (Aushon Biosystems), with 2 technical replicates per sample. Slides were processed as follows: 4 x 15 min washes with dH20, incubated with antigen retrieval agent (Reblot strong, Millipore) for 15 min, 3 x 5 min washes with PBS, incubated with superblock TBST (ThermoFisher Scientific) for 10 min, 3 x 5 min washes with TBST, incubated with primary antibodies (all 1:200) diluted in superblock TBST for 60 mins, 3 x 5 min washes with TBST, blocked with superblock TBST for 10 mins, 3 x 5 min washes with TBST, incubated with anti-rabbit dylight 800 secondary Ab (1:2000 in superblock TBST)(Cell Signalling Technologies) for 30 mins, 3 x 5 min washes with TBST, 1 x 5 min wash with dH20, slides spun at 2000rpm for 5mins and allowed to air dry in the dark. An additional slide was stained with FAST Green FCF for normalization against total protein: 3 x 5min washes with dH20, incubated for 15 mins in 1% NaOH, slides rinsed 20 x in dH20, incubated for 10 min in dH20, incubated in de-stain (30% methanol, 7% glacial acetic acid, 63% dH20) for 15 min, incubated for 3 mins in FAST green staining solution (0.0025%w/v FAST green in de-stain), rinsed 20 x in

dH20, incubated for 15 mins in de-stain solution, rinsed 20 x in dH20, spun at 2000rpm for 5 mins and allowed to air dry in the dark. All steps were performed at room temperature with agitation. Slides were visualized using an Innopsys 710AL infra-red microarray scanner and signals quantified using MAPIX microarray image analysis software (Innopsys). All signals were within the linear range of detection with an R^2 vlaue >0.9. Final output is the median value for each dilution series, background subtracted and normalized for protein loading.

2.4.1.6 Small interfering RNA (siRNA) screen

As part of an extensive collaboration, the siRNA screen was performed on PDCLs by Dr Chris Lord's team (The Institute of Cancer Research, London) and subsequent analysis by Dr Peter Bailey and Dr Rosie Upstill-Goddard. After optimization of culture and experimental conditions, each PDCL was reverse transfected in a 384 well-plate format with a custom siGENOME siRNA library (Dharmacon, USA) designed to target 714 kinase coding genes, 256 protein phosphatase coding genes, 722 genes implicated in energy metabolism, 73 tumor suppressor genes and 166 genes involved in the repair of DNA damage. Only genes involved in DNA damage and replication was assessed in this PhD thesis. Each well in the 384 well-plate arrayed library contained a SMARTpool of four distinct siRNA species targeting different sequences of the target transcript. Each plate was supplemented with non-targeting siCONTROL and siPLK1 siRNAs (Dharmacon, USA). Cell viability was estimated five days after transfection using a luminescent assay detecting cellular ATP levels (CellTitre-Glo, Promega). Luminescence values were processed using the cellHTS2 R package (Boutros et al., 2006). To evaluate the effect of each siRNA pool on cell viability, we log2 transformed the luminescence measurements and then centred these to the median value for each plate. The plate-centred data were scaled to the median absolute deviation (MAD) of the library as a whole to produce robust Z-scores. All screens were performed in triplicate. Screens judged to have poor dynamic range (Z' factor < 0)(Zhang et al., 1999) or poorly correlated replicates ($r < 0.7$) were excluded during an evaluation of screen quality. Z scores were adjusted using a quantile normalization(Parrish and Spencer, 2004).

Genes with functional dependency, so called siRNA "hits", were identified by calculating the median absolute deviation of normalized Z-scores for a given siRNA across all samples and identifying sample Z scores greater than or equal to 2 x the median absolute deviation. This analysis generated a "seed" matrix (n siRNA hits x m samples) which was used as

starting input for the Randon Walk with Restart (RWR) algorithm as implemented by the R package dnet (Fang and Gough, 2014). This algorithm was used to identify functionally important subnetworks associated with cell viability from a curated protein-protein interaction network STRING v 10 (Szklarczyk et al., 2015). Considering the complex nature of topological features of human interactome data, we introduce a randomization-based test to evaluate the candidate interactors utilizing 1000 topologically matched random networks. Candidate interactors that remain significant (i.e., p edge<0.05) were identified and a consensus subnetwork was constructed by collapsing all sample-specific results. The resulting network was visualized using RedeR (Castro et al., 2012).

2.4.1.7 *In Vitro* Cytotoxicity assays

Cells were detached from culture flasks and centrifuged. 4ml of media was added to the cell pellet and single cell suspensions created. Cells were counted using cell counting chambers (Nexcellon Bioscience, SD1000) and the Cellometer Auto 1000 automated cell counter (Nexcellon Bioscience). The desired cell concentration was then created by resuspending in appropriate volumes of media. Cell number per well was optimised to ensure 90% confluence in control wells at time of assay completion (Table 2-6). Cells were seeded on 96 well plates (Costar®, Corning Incorporated) and allowed to adhere for 24 hours.

Cells were treated with increasing doses of Cisplatin (Accord Healthcare), AZD6738 (Astrazeneca®), AZD1775 (Astrazeneca®) and AZD7762 (Astrazeneca®) for 72hours (Table 2-7). Cells were treated with BMN-673 (Pfizer Inc.), Rucaparib (Clovis Oncology), CFI-400945 (Cayman Chemical) and Palbociclib (Pfizer Inc.) for a total of 9 days, with repeated dosing every 72 hours in conjunction with changing cell media (Table 2-7). Actinomycin D (Sigma), drug vehicle (DMSO) and media only controls were performed on each individual plate. Dr Eirini Maria-Lampraki (PhD student) and Clara Paris (student intern, supervised by PhD candidate) assisted in performing some of the cytotoxicity assays.

Table 2-6 Optimised cell number for cell viability cytotoxicity assays

PDCL	Cells / Well 72-hour assay	Cells / Well 216-hour assay
TKCC 02.1	4 x 10^3	500
TKCC 05	2.5 x 10^3	
TKCC 06	1 x 10^4	
TKCC07	12.5 x 10^3	
TKCC 10	2.5 x 10^3	750
TKCC 15	7.5 x 10^3	250
TKCC 17	1.5 x 10^4	
TKCC 18	4 x 10^3	500
TKCC 22	7.5 x 10^3	2000
TKCC 26	1 x 10^4	
MAYO 4636	7.5 x 10^3	2000
MAYO 5289	6 x 10^3	3000
MAYO 4911	7.5 x 10^3	
PaCadd137	7.5 x 10^3	
Panc08.13	4 x 10^3	

Table 2-7 Agents used in cell viability cytotoxicity assays

Agent	Mechanism of Action	Solvent	Assay duration (hrs)	Manufacturer
Cisplatin	Platinum	PBS	72	Accord Healthcare
AZD6738	ATR inhibitor	1% DMSO in PBS	72	Astrazeneca®
AZD1775	WEE1 inhibitor	1% DMSO in PBS	72	Astrazeneca®
AZD7762	CHK1 inhibitor	1% DMSO in PBS	72	Astrazeneca®
BMN-673	PARP inhibitor	1% DMSO in PBS	216	Pfizer Inc
Rucaparib	PARP inhibitor	1% DMSO in PBS	216	Clovis Oncology
CFI-400945	PLK4 inhibitor	10% DMSO in PBS	216	Cayman Chemicals
Palbociclib	CDK4/6 inhibitor	1% DMSO in PBS	216	Pfizer Inc

Cell viability was determined using CellTiter 96® Aqueous non-radioactive cell proliferation assay composed of solutions of a tetrazolium compound [3-(4,5-

dimethylthiazol-2-yl)-5-(3-carboxymethoxyphenyl)-2-(4-sulfophenyl)-2H-tetrazolium, inner salt; MTS] and an electron-coupling reagent (phenazine methosulfate; PMS) (Promega, Madison, WI, USA). The assay was performed at an absorbance of 490 nm using an ELISA plate reader (Tecan Trading AG) after 1 hour of incubation with MTS. Background absorbance was corrected for by wells containing medium alone and the absorbance was normalised to a scale of 0% (complete cell death by actinomycin D (5 - 10μg/ml) to 100% (no drug). At least 3 biological repeats were performed for each experiment. EC50 calculation, statistical analysis and dose response curves were generated using GraphPad Prism 6 (GraphPad Software Inc, La Jolla CA).

2.5 Animal based studies

2.5.1 Approvals / Licencing

Animal procedures were carried out according to the Home Office guidance on the Operation of Animals (Scientific Procedures) Act 1986. All investigators involved in animal work were appropriately trained with a personal home office licence (PhD candidate number: IA6DD319C). All procedures were approved under appropriate project licences (PPl numbers 70/8438 and PBC2386EB).

Mice were housed in the Beatson Institute of Cancer Research animal facility. All were kept in a specific pathogen-free environment, with an appropriate 12-hour day and night cycle. Cages were individually ventilated and maintained to a high standard, with access to food and water 24 hours a day. Animals were monitored at least 3 times per week, this was increased when on treatment and indicated according to project licence guidance. Mice were euthanised by carbon dioxide asphyxiation and cervical dislocation at the completion of each experiment. All animal numbers were annually reported as per home office guidance.

2.5.2 Patient Derived Xenografts

2.5.2.1 Implantation

Patient derived xenografts (PDX) of PDAC were generated and comprehensively characterised as part of the ICGC project (Biankin et al., 2012, Waddell et al., 2015, Bailey et al., 2016). BALB/c nude mice were anaesthetised and a single PDX fragment was inserted sub-cutaneous into the right flank according to standard operating procedure. All

xenografts presented in this thesis were implanted by the PhD candidate. Briefly, animals were anaesthetised using sealed Isoflurane inhalation unit. Once fully anaesthetised, animals were transferred onto a heated operating unit, with a mouthpiece providing ongoing Isoflurane anaesthesia and oxygen. All mice were confirmed to be fully anaesthetised and received injection of Buprenorphine (0.01mg/ml) at a dose of 0.25 µl/g as post-operative analgesia. A 2-3mm incision is made in the right flank followed by implantation of a 2mm x 2mm x 2mm tumour fragment. A Matrigel plug (around 50µl) is injected in the tumour cavity and incision is closed with Mikron autoclip 9mm surgical stapler. Mice were allowed to wake naturally and kept under close observation post-operatively. All received Rimadyl (Carprofen) as oral analgesia 24 hours prior and 72 after procedures.

2.5.2.2 PDX monitoring

PDX models were grown to 150mm^3 (volume = length^2 x width / 2), at this point each PDX was randomised to a different treatment regime. Responsive PDXs were treated once tumour size returned to 150mm^3, up to a maximum of three rounds. Resistant models were treated after a treatment break of 2 weeks in accordance with current clinical treatment regimes, up to a maximum of 2 rounds. Each experiment was terminated once tumour volume reached end-point (750mm^3), in accordance with home office animal welfare regulations.

2.5.2.3 PDX model selection

PDX models were selected based on recently described (Waddell et al., 2015) putative biomarkers of DDR deficiency. Candidate DDR mutations were confirmed using Sanger sequencing prior to implantation.

2.5.2.4 Sanger sequencing of PDX models

A DDR deficient (PDX 2179) and DDR proficient (PDX 2133) bulk tumour PDX model were selected for implantation. In order to confirm the revived and expanded PDX population contained the mutation of interest, targeted Sanger sequencing was performed. A polymerase chain reaction (PCR) product was created, amplified and sequenced. DNA was extracted from each of the revived PDX tumours using the AllPrep kit by Qiagen, of which multiple fragments for implantation were harvested.

PCR amplification of the gene region of interest was performed using Platinum *Pfx*® DNA polymerase (Invitrogen, Cat No. 11708-013) and Veriti® 96 well thermo-cycler (Applied Biosystems). The PCR amplification mix was constructed at a volume of 50 µl (Table 2-8).

Table 2-8 PCR amplification composition

Component	Volume (µl)
10X *Pfx* Amplification buffer	5
10mM dNTP mixture	1.5
50mM MgSO4	1
Primer Mix (10uM)	1.5
Template DNA (10pg – 200ng)	>1
Platinum *Pfx* DNA polymerase	0.4
Autoclaved, distilled water	To 50

Primers were designed using Primer-Blast (http://www.ncbi.nlm.nih.gov/tools/primer-blast/) after determining DNA sequence surrounding target mutation. Primers were manufactured by Invitrogen® (Table 2-9). A three-step cycling reaction was done through 30 cycles at a temperature gradient from 52 - 60°C to determine optimum amplification temperature. This was found to be 54°C and further amplification reactions for these primers were done at this temperature. A three-step reaction was performed for 30 cycles at 94°C for 15 seconds (denature step), 54°C for 30 seconds (annealing step) and 68°C for 38 seconds.

In the case of PDX 2179, the primer was designed to target the pathogenic, high consequence, somatic splice site mutation in *BRCA1* (position 41201216, base change A > G) with loss of 2nd allele (Waddell et al., 2015). For PDX 2133, primers were designed to confirm the presence of a mutation in *PALB2* (base change, 2451GACT>-) with no loss of 2nd allele or change in protein.

Table 2-9 Primers for Sanger sequencing of PDX models

	PDX 2179 ***BRCA1***	**PDX 2133** ***PALB2***
Forward Amplification Primer	AAGGGAGGAAGGGAGGGAAG	TCG ACG GAA TGT TTA TGC AGC
Reverse Amplification Primer	TGGAGTCTTTTGGCACAGGT	AAA CTC GCA AAG CCA GCA TAC
Forward Sequencing Primer	GGCCTTATGGAGACTGATAACCA	GAC TCA ATG GGT GGA GGT GTT
Reverse Sequencing Primer	GGCATCCATAGGGACTGACAG	TAC GGT TGC GCC TGA TGA TAA

2.5.2.5 DNA separation using Agarose gel

Prior to Sanger sequencing, the amplified DNA fragments were isolated. Agarose gel was constructed using 3g UltraPure™ Agarose (Life Technologies) in 150ml of Tris Acetate-EDTA (TEA)® buffer (Sigma Life Science). A gel with 2% Agarose concentration was constructed to enable optimal separation of 500 - 600 base-pair (bp) DNA fragments. SYBR safe® DNA gel stain (Invitrogen by Life Technologies) was added and gel was allowed to set at room temperature. The DNA-PCR product was prepared by adding 10µl of 6x Orange DNA Loading Dye® (Thermo Scientific) to 50µl of DNA product. A 100bp DNA marker was constituted using 100bp solution (Invitrogen), 6x Orange DNA Loading Dye® (Thermo Scientific) and TEA® buffer. Once the gel was set, the DNA products and marker were placed in appropriate channels.

The gel was run at 120V for 60mins. Using BioRad Chemidoc® ultra-violet (UV) imaging system, the DNA bands were imaged. In PDX 2179, the first run did not demonstrate distinct bands at 500 – 600bp (representative of PCR product). Thus, this was cut from gel and DNA re-isolated. A repeat PCR amplification was performed using the sequencing primers as previously described. A repeat DNA extraction gel (120V, 400mA) was run and DNA bands visualised using ultra-violet light reader with 100bp marker.

2.5.2.6 DNA Gel Extraction

Under UV guidance the DNA band at 580bp was cut from the gel and purified using QIAquick® Gel Extraction kit (Qiagen, Cat no. 28115). Briefly, QC buffer was added 3 volumes to weight of gel and incubated at 50°C until gel fully dissolves. Ispropanol was added at 1 volume per weight of gel, centrifuged in DNA column (Qiagen) and repeated. Since the product was to be used for sequencing, 500µl buffer QG® (Qiagen) was added and centrifuged. The DNA column was washed using 750 µl PE buffer® (Qiagen) and centrifuged. The resulting flow through was discarded and the DNA isolated by eluting with 50µl buffer EB® (Qiagen), incubating for 1-2minutes and centrifuging for 1 minute. The flow through (extracted DNA) was labelled and quantified using Nanodrop® 2000 spectrophotometer prior to Sanger sequencing. Sanger sequencing was performed within the Beatson Institute of Cancer Research's Molecular Technology service using an Applied Biosystems 3130xl (16 capillary) sequencer.

2.5.3 Patient derived cell line xenografts

Early passage patient derived cell lines (PDCLs) were selected for sub-cutaneous implantation to generate cell line xenografts in CD-1 nude mice. PDCLs were cultured to 80 – 90% confluence as previously described. Cells were washed with PBS and detached using PBS containing 0.04 mg / ml EDTA (Thermo Scientific, catalogue no. 15040-066). Once detached, the cells were counted and resuspended in PBS according to a pre-determined concentration. This was then combined with an equal volume of Matrigel at 1:1 ratio to generate the desired cell concentration. These were stored on ice for less than 30 minutes prior to implantation.

Using an injection technique, 1x 10^6 were implanted into the right flank of CD-1 nude mice. Cell line xenografts were allowed to grow following transplantation until established and were of sufficient size to be measured with a high level of accuracy (volume at least 50mm^3). This is lower than used for bulk tumour PDXs, as preliminary experiments demonstrated rapid disease progression once a size of 150mm^3 is reached that makes therapeutic evaluation not feasible. In each arm, 5 mice were implanted with 1 million cells after preliminary experiments demonstrated this produces satisfactory growth in selected PDCLs.

2.5.4 Treatment Regimens

Upon tumour threshold, mice were treated with either Cisplatin, Gemcitabine, Olaparib, AZD6738, saline (control) or combinations of these (Table 2-10, Table 2-11). As PDXs were reaching threshold, treatment allocation was done on a random basis, using a random number generator. Each PDX was treated with the subsequent treatment regimen upon reaching threshold depending on the random order generated for that round. This ensured no bias in selecting PDXs to treatments. PBS (control) was allocated during every second round of treatments. All treatments were administered by Beatson small animal unit staff as per protocol.

Treatment cycles were completed after 4 weeks. If tumour response was observed, then further cycles were only given if tumour growth returned to threshold (150mm^3). In cases where no significant response was seen, a 2-week treatment break was given to all animals and then a 2nd cycle restarted. The maximum number of cycles that each animal was exposed to was 3 cycles.

Table 2-10 PDX treatment agents

Agent	Mechanism of Action	Solvent	Cat No	Manufacturer
Cisplatin	Platinum	PBS	PL20075/0123	Accord Healthcare
AZD6738	ATR inhibitor	10% DMSO + 40% Propylene Glycol	Under MTA	Astrazeneca®
Olaparib	PARP inhibitor	10 % DMSO + 9% Cyclodextrin	Under MTA	Astrazeneca®
Gemcitabine		PBS	S1146	Selleckchem
Vehicles for Agents				
Cyclodextrin			C4767	Sigma
Propylene Glycol			P4347	Sigma
Methylcellulose			M0252	Sigma

Table 2-11 PDX treatment regimens

Agents	Dose	4-week Cycle
Control	10μl/g	IP, Monday and Thursday, weeks
Cisplatin	6mg/kg IV	IV, day 1 and 14
Gemcitabine	140mg/kg IP	IP, Mondays and Thursdays, 4 weeks
Olaparib	50mg/kg oral gavage	Oral gavage, Monday to Friday, 4 weeks
Olaparib + **Cisplatin**	50mg/kg (Olaparib) 70mg/kg (Cisplatin)	Oral gavage, Monday to Friday, 4 weeks IV, day 1 and 14
AZD6738	25mg/kg oral gavage	Oral gavage, daily, 4 weeks
AZD6738 + **Cisplatin**	25mg/kg (AZD6738) 70mg/kg (Cisplatin)	Oral gavage, daily, 4 weeks IV, day 1 and 14

IV – intravenous (tail injection); IP – intra-peritoneal injection

2.5.4.1 Monitoring of animals on treatment

Mice were monitored at least 3 times per week which included measurement of tumour volume and assessment of the condition of the animal using weight and body conditioning score. Tumour volume was calculated using the formula volume = 0.5 x Length^2 x Width and normalised to 100% on the first day (day 0) of the first cycle of treatment. In an effort to standardise measurements, tumour volume was measured by the PhD candidate at all times, apart from exceptional circumstances. During these times, a trained colleague (Viola Paulus-Hock) performed all measurements who were very familiar with all of the animals involved in the experiment. Mice were weighed 2 – 3 times per week depending on weight loss and treatment schedule. If weight loss reached 20% and body conditioning score reached level 3 the animal was euthanised.

2.5.4.2 Statistical analysis

Response to therapy was measured using published methodology (Rottenberg et al., 2007, Waddell et al., 2015). Briefly, twice weekly tumour measurements were used to calculate tumour volume. Comparison was made by standardising volume to 100% on day 0 of treatment regime. PDX growth was averaged across each treatment arm using percentage change in tumour volume. Growth curves were generated using GraphPad Prism 6 (GraphPad Software Inc, La Jolla CA), with each data point charted with the standard error of mean.

3 Clinicopathological features of Molecular subtypes of PDAC

3.1 Introduction

Clinical disease patterns for patients with PDAC vary significantly between, as yet, undefined subgroups of patients. Patients may present with loco-regional disease or disseminated metastatic disease. Furthermore, patients have different clinical disease progression patterns, with significant differences in outcome for patients with different disease recurrence patterns following surgery (Suenaga et al., 2014, Sperti et al., 1997, Van den Broeck et al., 2009, Groot et al., 2017). Liver metastases, either as recurrence or *de novo* metastatic disease at presentation, is associated with poor outcomes (Groot et al., 2017). The majority of patients develop liver metastases within 12 months after upfront surgery, suggesting that metastatic disease is already present at the time of resection in most patients (Groot et al., 2017, Sperti et al., 1997, Suenaga et al., 2014). On the other hand, lung metastases are associated with prolonged survival amongst metastatic patients (Groot et al., 2017). These differences suggest that significant biological differences exist between these patient groups. Biological markers that predict patterns of disease progression may inform treatment approaches and provide more accurate patient selection for surgery or neoadjuvant therapy.

There are meaningful differences in outcome between PDAC located in the head, as compared to those of the body and tail of the pancreas (BTPC) (Artinyan et al., 2008, Brennan et al., 1996, Watanabe et al., 2004, Sener et al., 1999, Lau et al., 2010, de Rooij et al., 2016). Approximately 15% of PDAC occur in the body and tail of the pancreas and differences in outcome has been largely attributed to late presentation in comparison with tumours of the pancreatic head (Artinyan et al., 2008, Brennan et al., 1996, Watanabe et al., 2004, Lau et al., 2010). Pancreatic tumours of the head and uncinate process often present with jaundice, and thus thought to present earlier in the disease process. BTPC usually presents with weight loss and pain, symptoms more in keeping with advanced disease (Watanabe et al., 2004). Yet, previous studies suggest that TNM stage at presentation is not significantly different between the two tumour locations (Sohn et al., 2000). The molecular pathology of PDAC has been intensely studied recently, yet, the genetic and molecular characteristics between PDAC of the head and BTPC, and other disease patterns, have not been elucidated. The poor prognosis and high rates of early

recurrence in BTPC, provides an opportunity to identify potential molecular features associated with these differences in clinical disease patterns.

Genomic analyses have revealed distinct molecular subtypes of PDAC based on transcriptomic profiles that are beginning to inform clinical characteristics such as prognosis (Bailey et al., 2016, Collisson et al., 2011, Moffitt et al., 2015). Bailey *et al.* described a poor prognostic 'squamous' subtype that is enriched with histopathological adeno-squamous tumours, *TP53* mutations (Fang et al., 2017) and gene programs associated with inflammation, hypoxia response, metabolic reprogramming, MYC pathway activation and TGF-β signalling (Bailey et al., 2016). The squamous subtype is characterised by hypermethylation and downregulation of genes involved in pancreatic endodermal differentiation (*PDX1, MNX1, GATA6, HNF1B*) (Bailey et al., 2016). The squamous subtype is enriched for mutations and loss of key epigenetic regulators (e.g. *KDM6A*) which may contribute to the loss of the endodermal identity of these tumours (Bailey et al., 2016). Using expression patterns of immune cell populations within the tumour microenvironment, Bailey *et al.* demonstrated evidence of immune avoidance in the squamous subtype (Bailey et al., 2016). The incidence of the squamous subtype was around 25% in the resected ICGC cohort, yet the prevalence in all stages of PDAC has not been fully investigated but may be as high as 50% in more advanced disease. The squamous subtype (Bailey et al., 2016) (also termed basal (Moffitt et al., 2015) or Quasi-Mesenchymal (Collisson et al., 2011)) is consistently described when subtyping PDAC with a strong association with survival (Bailey et al., 2016, Moffitt et al., 2015, Collisson et al., 2011). The clinicopathological characteristics of these tumours, and how they relate to their molecular pathology is yet to be elucidated and understood.

This chapter examines the clinicopathological features associated with specific molecular subtypes of PDAC and investigates the molecular characteristics of specific disease patterns in the ICGC cohort (n = 275 patients). Clinical and pathological disease patterns were correlated with genomic and transcriptomic analyses with the aim of defining the molecular features underpinning specific disease patterns in PDAC. The results demonstrate a strong association of the squamous subtype with metastatic disease, particularly with liver metastases. Next, the molecular pathology of body & tail PDAC was investigated revealing an association with molecular features of aggressive disease and immune evasion with BTPC. These results suggest that molecular features underlie specific disease patterns and can potentially be used as biomarkers to inform clinical decision making and treatment selection.

3.2 Results

In order to investigate the clinical and pathological features of molecular subtypes of PDAC, an in-depth clinical analysis of patients that underwent molecular profiling as part of the ICGC PDAC cohort was performed. Detailed clinical and pathological data, acquired prospectively to the standard expected for a clinical trial, was correlated with next generation sequencing data (Bailey et al., 2016, Biankin et al., 2012, Waddell et al., 2015). Clinically relevant disease patterns, e.g. primary tumours that develop lung metastases, were defined and comparative molecular analyses performed to reveal candidate molecular processes that underlie these patterns which inform future biomarker and therapeutic development.

3.2.1 Clinical disease patterns of Molecular subtypes

3.2.1.1 Clinical features of the ICGC transcriptome cohort

The Australian Pancreatic Genome Initiative (APGI) acquired biospecimen and clinicopathological data for 518 primary resectable, chemo naïve, PDAC (termed the **APGI cohort)** (Figure 3-1). Of these, 456 were selected to form The International Cancer Genome Consortium (ICGC) cohort (termed the **ICGC cohort**) which underwent integrated genomic characterisation as previously described (Figure 3-1) (Bailey et al., 2016, Waddell et al., 2015, Biankin et al., 2012).

Tumours underwent both genomic and transcriptomic analyses, with the sequencing strategy determined primarily by tumour cellularity (Figure 3-1). Those that underwent molecular subtyping (termed the **ICGC transcriptome cohort,** n = 275 in total) consisted of PDAC that had transcriptomic analysis performed and had clinicopathological features consistent with other cohorts of resected PDAC (Table 3-1). Depending on tumour cellularity, molecular subtyping was performed using either RNA sequencing (n = 96) or gene expression micro-array (n = 266) and subtyped as described in Bailey *et al.* (Bailey et al., 2016). In total, 87 patients had both RNAseq and micro-array analysis. In this section of Chapter 3, the ICGC transcriptome cohort is used to correlate molecular data (gene expression and molecular subtypes) with detailed clinicopathological data to investigate the association of clinical disease patterns with molecular pathology.

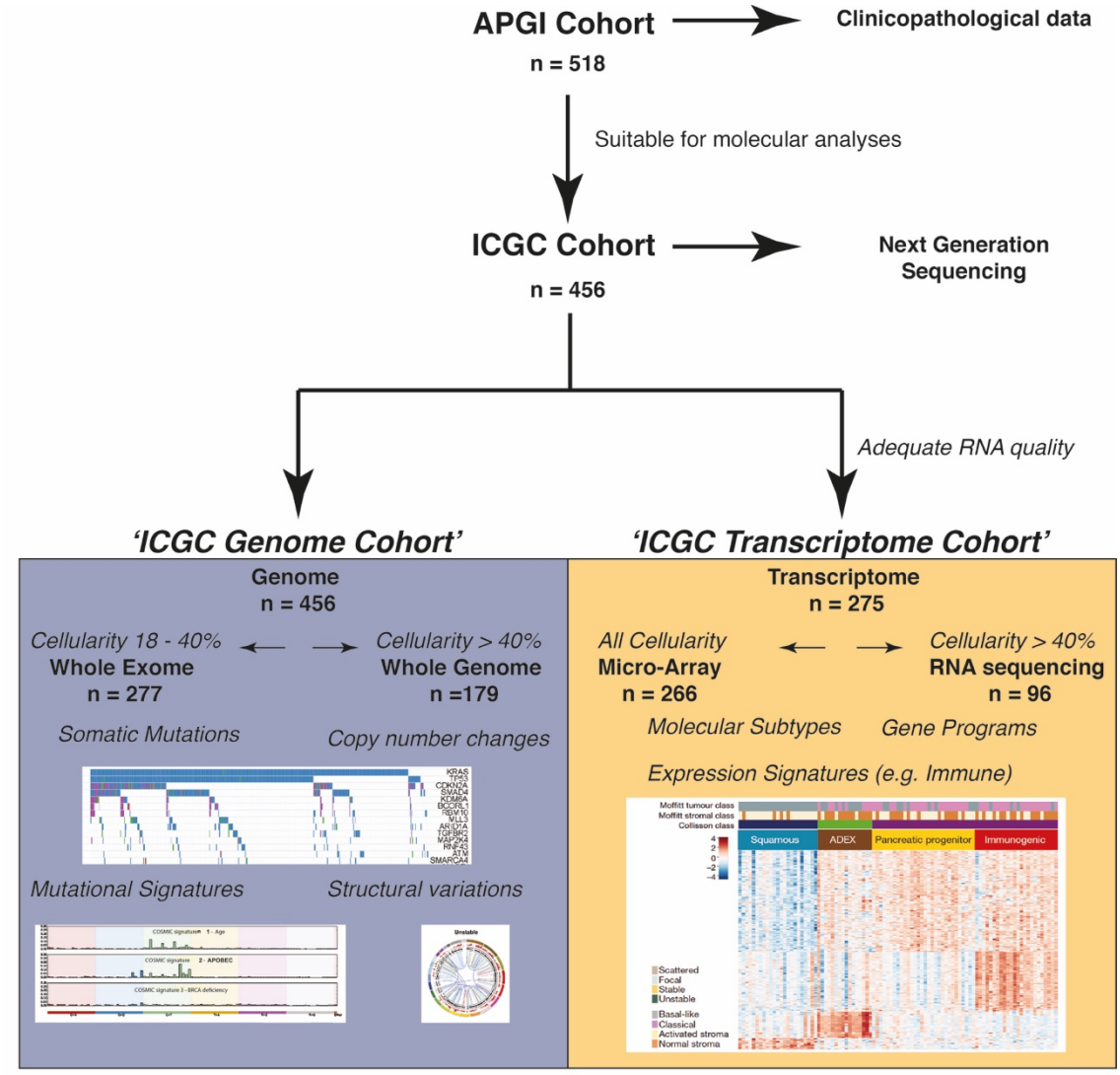

Figure 3-1 Genomic and Transcriptomic profiling strategy of the ICGC cohort. The APGI acquired data and biospecimens on 518 PDACs, of which 456 were suitable for next generation sequencing. These all (*n* = 456) underwent exome or whole genome sequencing (called the ICGC genome cohort). Transcriptomic analysis was performed using either RNA sequencing (RNAseq) or gene expression micro-array based on cellularity and adequate RNA quality of the sample in a selection (*n* = 275) of PDACs (called the ICGC transcriptome cohort). Tumour cellularity > 40% allowed whole genome sequencing, whilst RNAseq was performed in tumours with sufficient cellularity (>40%) and quality RNA.

The ICGC transcriptome cohort (*n* = 275) was representative of published resected PDAC cohorts (Table 3-1). Validated prognostic features were associated with disease specific survival (DSS), such as nodal status (*P* = 0.002), tumour grade (*P* = 0.003), tumour size (*P* = 0.003), positive resection margin (*P* = 0.002), perineural (*P* = 0.001) and vascular (*P* < 0.001) invasion, as well as completion of adjuvant chemotherapy (P < 0.001). When accounting for molecular subtype, however, many of these factors are associated with prognosis only in the Classical Pancreatic subtype. This includes N-stage (*P* = 0.008 in the Classical vs *P* = 0.453 in the Squamous), tumour grade (*P* = 0.030 vs *P* = 0.673) and

resection margin status ($P = 0.002$ vs $P = 0.514$) (Table 3-1). This suggests that molecular features play a more significant role in prognosis and disease progression than standard pathological features in the squamous subtype. To further investigate this, a survival analysis of the molecular subtypes was performed. In comparison with the Classical Pancreatic subtype, Squamous subtype PDAC was associated with significantly worse survival after pancreatectomy in both the RNAseq (median survival 13.3 vs 23.7 months, $P = 0.010$) and micro-array cohorts (median survival 14.9 vs 22.0 months, $P = 0.001$) (Figure 3-2).

Table 3-1 Patient characteristics for the ICGC transcriptome cohort stratified by molecular class. Disease specific survival (DSS, in months) is demonstrated for each variable in all patients and molecular subtypes. *P* -value calculated using log-rank test. † Median survival not reached.

	All Patients			Classical Pancreatic			Squamous		
Variables	***n* = 275 No. (%)**	**Median DSS**	***P***	***n* = 196 No. (%)**	**Median DSS**	***P***	***n* = 79 No. (%)**	**Median DSS**	***P***
Sex									
Male	142 (52.6)	18.4	0.074	99 (51.6)	19.8	0.121	43 (55.1)	29.6	0.467
Female	128 (47.4)	23.7		93 (48.4)	29.0		35 (44.9)	24.8	
Age (years)									
Mean	66.7			67.0			66.1		
Median	68.0			68.0			67.0		
Range	34.0 – 90.0			37.0 – 90.0			34.0 – 90.0		
Outcome									
Follow-up (months)	2.8 – 81.0			7.5 – 81.0			2.8 – 79.0		
Median follow-up (months)	42.0			46.5			39.0		
Death PC	194 (70.5)			134 (68.7)			60 (76.9)		
Death other	17 (6.2)			10 (5.1)			7 (9.0)		
Death Unknown	3 (1.1)			3 (1.5)			0 (0.0)		
Alive	59 (21.5)			48 (24.6)			11 (13.9)		
Lost to FU	2 (0.7)			1 (0.5)			1 (1.3)		
Stage (AJCC 7th)									
I	19 (7.1)	15.0	0.142	13 (6.8)	15.0	0.008	6 (7.7)	†	0.320
II	238 (88.5)	20.7		172 (90.0)	25.0		66 (8.5)	14.0	
III	1 (0.4)	21.5		0 (0.0)	-		1 (1.3)	11.0	
IV	11 (4.0)	13.0		6 (3.1)	13.0		5 (6.4)	21.5	
T Stage (AJCC 7th)									
T1	6 (2.2)	73.0	0.293	6 (3.1)	73.0	0.561	0 (0.0)	-	0.225
T2	40 (14.9)	20.0		30 (15.7)	19.8		10 (12.8)	23.7	
T3	220 (81.8)	19.6		154 (80.6)	25.0		66 (84.6)	14.0	
T4	3 (1.1)	20.3		1 (0.5)	20.3		2 (2.6)	14.1	
N Stage (AJCC 7th)									
N0	63 (23.5)	32.0	0.002	48 (25.1)	40.0	0.008	17 (12.8)	12.9	0.453
N1	205 (76.5)	19.3		143 (74.9)	20.7		61 (78.2)	15.0	
Grade / Differentiation									
I / Well	16 (6.0)	33.0	0.003	16 (8.4)	33.0	0.030	0 (0.0)	-	0.673
II / Moderate	160 (59.5)	23.0		125 (65.4)	26.5		35 (45.5)	15.0	
III / Poor	87 (32.3)	16.0		46 (24.1)	18.3		41 (53.2)	14.0	
IV/Undifferentiated	5 (1.9)	13.3		4 (2.1)	10.2		1 (1.3)	13.3	
Tumour size									
≤ 20mm	29 (10.8)	39.0	0.003	24 (12.6)	39.0	0.057	5 (6.5)	23.0	0.037
> 20 ≤ 40mm	169 (63.1)	20.2		119 (62.3)	23.0		50 (64.9)	17.0	
> 40mm	70 (26.1)	15.0		48 (25.1)	19.8		22 (28.6)	9.3	
Margins (R0=0mm)									
Clear	195 (72.5)	23.0	0.002	142 (74.3)	28.6	0.002	53 (67.9)	15.0	0.514
Involved	74 (27.5)	15.9		49 (25.7)	18.0		25 (32.1)	12.1	
Perineural Invasion									
Negative	47 (17.7)	33.3	0.001	25 (13.5)	40.0	0.006	19 (24.7)	23.0	0.028
Positive	218 (82.3)	18.3		160 (86.5)	20.3		58 (75.3)	12.1	
Vascular Invasion									
Negative	103 (39.5)	31.4	<0.001	77 (41.8)	37.5	<0.001	26 (33.8)	18.4	0.022
Positive	158 (60.5)	17.0		107 (58.2)	19.3		51 (66.2)	13.6	
Adjuvant Chemotherapy									
< 3 cycles	77 (35.3)	13.3	<0.001	49 (30.8)	14.0	0.009	28 (47.5)	10.0	0.007
≥ 3 cycles	141 (64.7)	27.0		110 (69.2)	31.4		31 (52.5)	17.7	

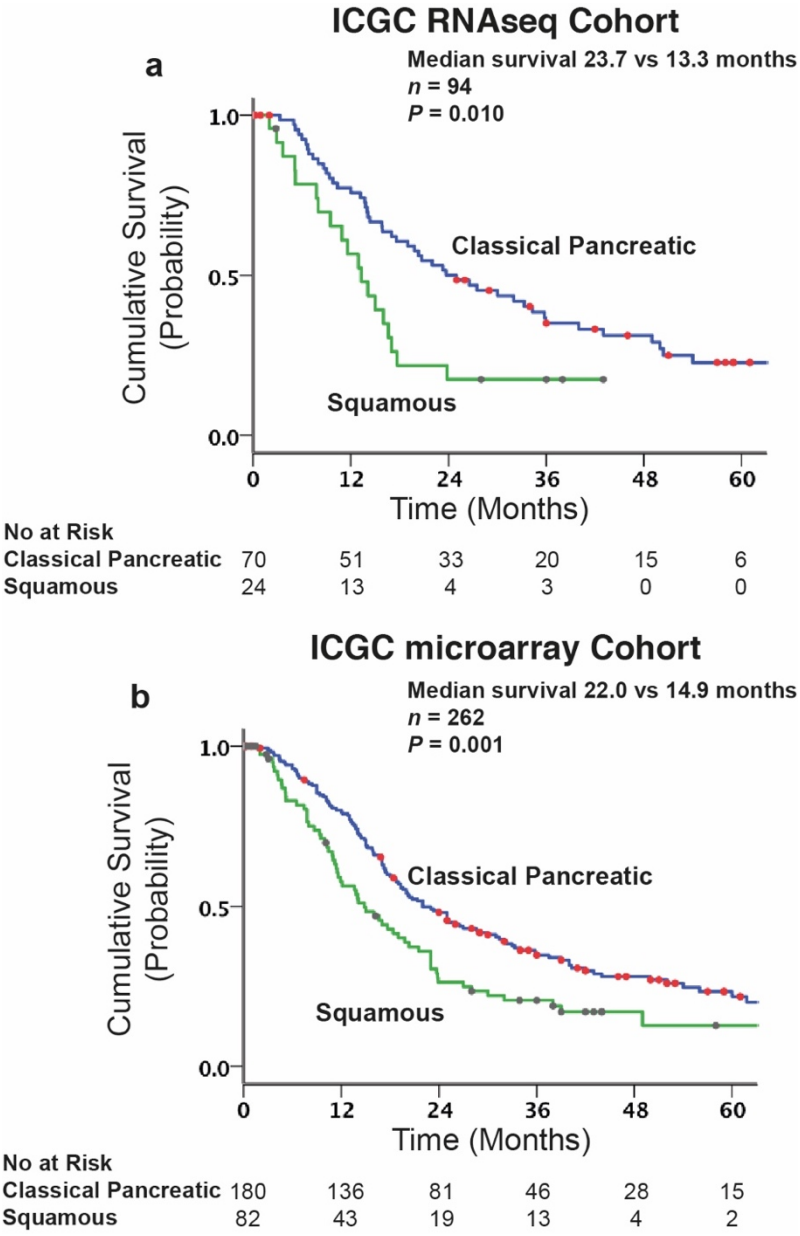

Figure 3-2 Kaplan-Meier survival analysis for ICGC cohort with transcriptomic analysis. Patients stratified based on molecular subtype in both the RNAseq (a) and micro-array (b) cohorts.

3.2.1.2 The impact of molecular subtyping on AJCC staging

Recently, there has been substantial interest to update the current AJCC staging system (AJCC 7th) for PDAC to improves its prognostic value (Allen et al., 2017, Strobel et al., 2015, Tarantino et al., 2017, van Roessel et al., 2018). Numerous studies demonstrated improved prognostic value in using tumour size, positive lymph node number and ratio, for resectable PDAC (Strobel et al., 2015, Tarantino et al., 2017, Allen et al., 2017, van Roessel et al., 2018). This led to a review and subsequent adjustment of the AJCC staging system for PDAC (AJCC 8th) which has recently been introduced into clinical practice (Allen et al., 2017). The main changes are that T-stage is now based on tumour size (T1 ≤

2cm, T2 > 2cm ≤ 4cm, T3 > 4cm, T4 still reflects coeliac or superior mesenteric arterial involvement) and N-stage on the number of positive lymph nodes harvested during surgical resection (N1 for 1 – 3 and N2 for 4 or more positive lymph nodes). TNM staging, however, only indirectly reflects tumour biology and thus may not accurately stage patients with aggressive disease. The ICGC cohort was acquired and analysed during the time period at which the AJCC 7th staging system was used, and to investigate the impact of molecular subtyping to the AJCC 8th staging system, the ICGC cohort was restaged using the new system.

A multivariate analysis model of known prognostic clinicopathological variables demonstrated that T stage (TIII vs TI/II; HR 2.33, 95% CI 1.37 – 4.07, *P* =0.003) and N stage (N2 vs N1/2; HR 1.64, 95% CI 1.12 -2.40, P = 0.011) remained independent prognostic factors. Including the molecular subtypes in the analysis showed that the squamous subtype remained a strong independent prognostic factor for DSS after surgery for PDAC (HR 1.73, 95% C.I. 1.15 – 2.61, *P* = 0.009) (Table 3-2).

Table 3-2 Univariate Cox regression analysis for ICGC transcriptome cohort.

	Univariate Analysis	
	HR (95% CI)	***P***
Age (> 70 years)	1.35 (1.01 – 1.80)	0.042
Grade (III / IV vs I / II)	1.71 (1.27 – 2.31)	< 0.001
Margin Involvement (Positive)	1.64 (1.20 – 2.23)	0.002
Vascular Invasion (Positive)	2.01 (1.47 – 2.75)	< 0.001
Perineural Invasion (Positive)	1.96 (1.29 – 2.98)	0.002
Lymph Node stage 8th N1	1.37 (0.92 – 2.04)	0.116
Lymph Node stage 8th N2	2.40 (1.60 – 3.61)	< 0.001
T stage (8th edition) T2	1.56 (0.92 – 2.63)	0.097
T stage (8th edition) T3	2.33 (1.37 – 4.07)	0.003
Adjuvant Chemotherapy (≥ 3 cycles)	0.51 (0.36 – 0.70)	< 0.001
Tumour Location (Body/Tail vs Head)	1.73 (1.22 – 2.47)	0.002
Subtype (Squamous vs Classical Pancreatic)	**1.80 (1.32 – 2.45)**	**< 0.001**

Table 3-3 Final multivariate Cox regression analysis model for the ICGC molecularly subtyped cohort

	Multivariate Analysis	
	HR (95% CI)	*P*
Age (> 70 years)	1.62 (1.15 – 2.29)	0.006
Grade (III / IV)	1.59 (1.08 – 2.35)	0.020
Perineural Invasion (Positive)	1.79 (1.07 – 3.00)	0.027
Lymph Node stage 8th N2	1.64 (1.12 – 2.40)	0.011
T stage (8th edition) T3	1.65 (1.15 – 2.38)	0.007
Adjuvant Chemotherapy (≥ 3 cycles)	0.48 (0.34 – 0.68)	<0.001
Subtype (Squamous)	**1.73 (1.15 – 2.61)**	**0.009**

To further investigate the value of the AJCC 8th staging system in the 2 broad molecular classes, Kaplan-Meier survival analyses were performed in each subtype. The new staging system proved to be prognostic in the Classical Pancreatic subtype based on N ($P < 0.001$) but not T ($P = 0.057$) stage (Figure 3-3). In contrast, T ($P = 0.037$) but not N ($P = 0.218$) stage was prognostic in the squamous subtype (Figure 3-3). In addition, margin status, a well validated predictor of recurrence in PDAC failed to demonstrate prognostic value in the squamous subtype ($P = 0.514$) (Figure 3-3).

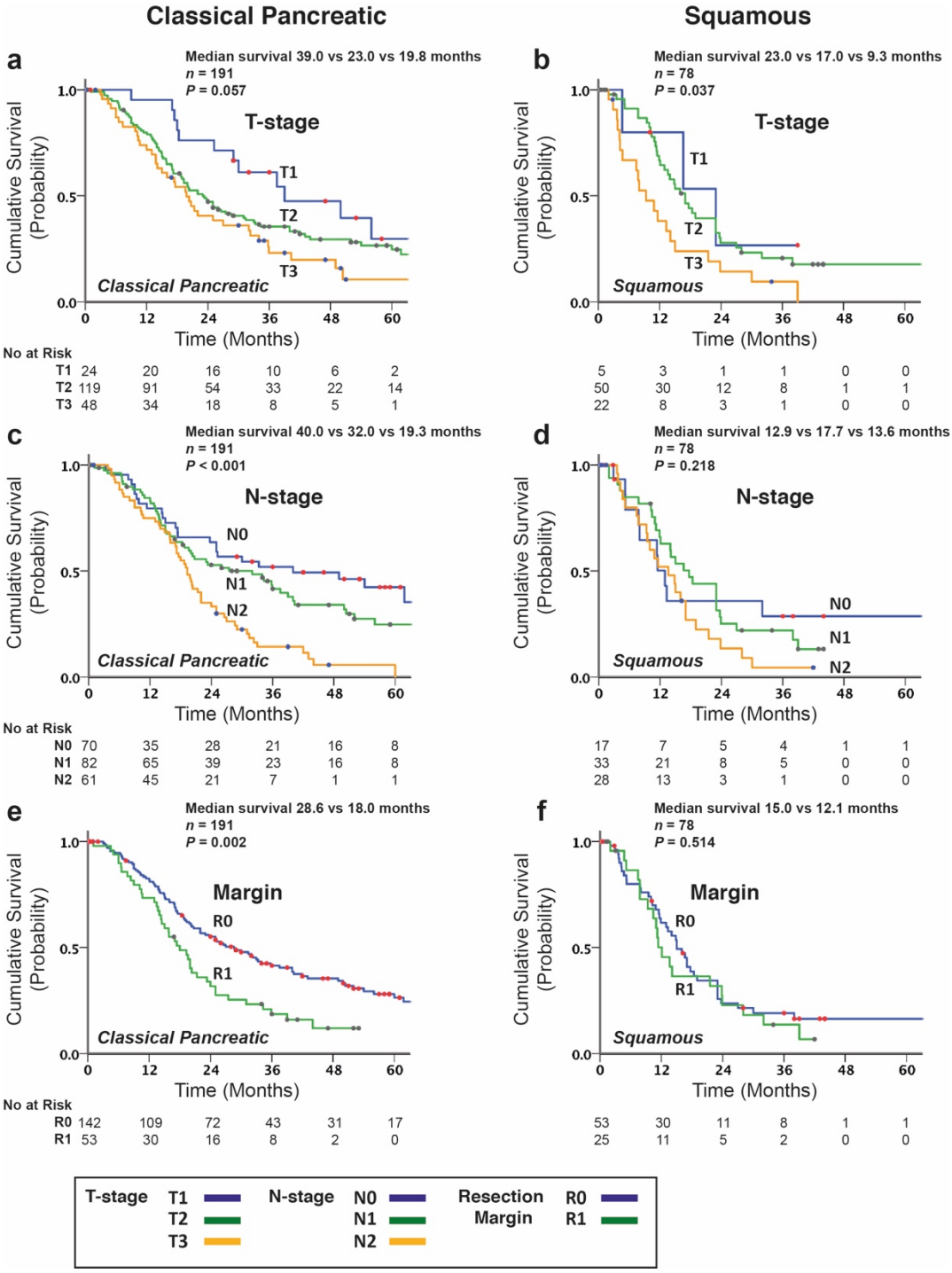

Figure 3-3 Kaplan-Meier survival curves for ICGC transcriptome cohort stratified by molecular subtype and pathological prognostic variable. The squamous subtype is a strong predictor of poor outcome, irrespective of disease stage. a) T-stage AJCC 8th staging system b) N-stage AJCC 8th edition c) Margin status (R0 = 0mm). In the squamous subtype, nodal metastases and resection margin status loses its prognostic value. This suggests that the squamous subtype is associated with a significantly worse survival, and that standard clinical and pathological features do not fully account for the differences seen,

These findings suggest that molecular classification of PDAC adds prognostic value in addition to standard clinicopathological variables. In particular, the prognostic value of margin status becomes irrelevant in the squamous subtype (Table 3-3, Figure 3-3). This is of great importance as many trials in the neoadjuvant setting and investigating surgical

techniques utilises margin status as a primary endpoint but may have little influence on long term survival in this patient subgroup. This data suggests that the squamous subtype is more likely to represent a pro-metastatic phenotype, as local disease control becomes less important than in the Classical Pancreatic subtype. To further investigate this and potential pathological factors driving a poor prognosis in the squamous subtype, an analysis of pathological and clinical features of each of the molecular subtypes was performed.

3.2.1.3 The squamous subtype is associated with high pathological grade and liver recurrence after pancreatectomy

Squamous subtype tumours are associated with poor tumour differentiation (also known as higher tumour grade) ($P < 0.001$), body and tail tumours ($P = 0.033$), and adenosquamous tumours ($P = 0.004$), but not with pathological T stage ($P = 0.467$), nodal status ($P = 0.520$), tumour size ($P = 0.334$) and margin status ($P = 0.838$) in the RNAseq set (Table 3-4). The classical subtype was associated with perineural invasion ($P = 0.027$), IPMN with invasion ($P = 0.014$) and mucinous tumours ($P = 0.010$).

The association between molecular subtypes and disease recurrence patterns was next investigated in the RNAseq set in the patients ($n = 65$) who developed recurrence. The squamous subtype was associated with liver recurrence ($P = 0.002$) (Table 3-4), and all (20/20) patients with squamous tumours in the RNAseq set developed and succumbed to distant metastatic disease (Table 3-4). There was no association between lung recurrence and transcriptomic subtypes in the RNAseq set ($P = 0.345$) (Table 3-4).

Table 3-4 Association between clinicopathological variables, tumour recurrence patterns and PDAC subtype ICGC RNAseq cohort (*n* = 96)

	Classical Pancreatic *n* = 71	Squamous *n* = 25	*P*-value (Chi-square)
T – stage (AJCC 7th)			
T I / II	11 (15.7%)	3 (12%)	0.467
T III / IV	59 (84.3%)	22 (88%)	
N – stage (AJCC 8th)			
N0	25 (35.7%)	8 (33.3%)	0.520
N1	45 (64.3%)	16 (66.7%)	
Tumour location			
Head	**60 (84.5%)**	**16 (64.0%)**	**0.033**
Body / Tail	**11 (15.5%)**	**9 (36.0%)**	
Grade / Differentiation			
I / II	**52 (74.3%)**	**5 (21.7%)**	**<0.001**
III / IV	**18 (25.7%)**	**18 (78.3%)**	
Perineural Invasion			
Negative	**9 (13.2%)**	**8 (34.8%)**	**0.027**
Positive	**59 (86.8%)**	**15 (65.2%)**	
Vascular space invasion			
Negative	31 (45.6%)	8 (34.8%)	0.256
Positive	37 (54.4%)	15 (65.2%)	
Size			
≤ 20mm	10 (14.3%)	1 (4.3%)	0.334
> 20 ≤ 40mm	38 (54.3%)	12 (52.2%)	
> 40mm	22 (31.4%)	10 (43.5%)	
Margin status (R0=0mm)			
Negative	58 (82.9%)	20 (83.3%)	0.615
Positive	12 (17.1%)	4 (16.7%)	
Histological subtype			
IPMN with invasion	**13 (18.3%)**	**0 (0%)**	**0.014**
Mucin	**14 (19.7%)**	**0 (0%)**	**0.010**
Adenosquamous	**2 (2.8%)**	**6 (24.0%)**	**0.004**
Acinar cell	2 (2.8%)	0 (0%)	0.545
PDAC - NOS	52 (73.2%)	19 (76.0%)	0.506
Local only Recurrence			
No	41 (91.1%)	20 (100%)	0.194
Yes	4 (8.9%)	0 (0%)	
Liver Recurrence			
No	**25 (56%)**	**3 (15%)**	**0.002**
Yes	**20 (44%)**	**17 (85%)**	
Lung Recurrence			
No	33 (73.3%)	13 (65.0%)	0.345
Yes	12 (26.7%)	7 (35.0%)	
Lung Recurrence (no liver)			
No	38 (84.4%)	18 (90.0%)	0.432
Yes	7 (15.6%)	2 (10.0%)	
Non-Liver Distant Recurrence			
No	**27 (65.9%)**	**18 (90.0%)**	**0.040**
Yes	**14 (34.1%)**	**2 (10.0%)**	

The association between recurrence pattern, pathological features and molecular subtype was further investigated in the ICGC transcriptome cohort that underwent micro-array gene expression analysis. As demonstrated in the RNAseq cohort, the squamous subtype is

associated with higher pathological grade (P <0.001), tumour location in the body / tail (P < 0.001) and histological adenosquamous tumours (P < 0.001). As seen in the RNAseq set, the Classical subtype was associated with IPMN with invasion (P = 0.029), however did not reach statistical significance in mucinous tumours (P = 0.084). In the 178 patients that developed recurrence, liver recurrence was associated with the squamous subtype (P = 0.032). Conversely, lung recurrence was more likely in the Classical Pancreatic group (P = 0.048) and particularly in those that develop lung recurrence without liver metastases (P = 0.016). In patients that develop lung, but no liver, metastases (n =31), 83% (n = 26) were the Classical Pancreatic subtype. This infers a strong association between molecular subtype and metastatic pattern in patients undergoing pancreatectomy.

Table 3-5 Association between clinicopathological variables and PDAC subtype in the ICGC mRNA micro-array cohort (*n* = 266)

	Classical Pancreatic *n* = 184	Squamous *n* = 82	*P*-value (Chi-square)
T - stage			
T I / II	34 (18.5%)	13 (15.9%)	0.370
T III / IV	150 (81.5%)	69 (84.1%)	
N - stage			
N0	44 (24.0%)	18 (22.0%)	0.419
N1	139 (76.0%)	64 (78.0%)	
Tumour location			
Head	**163 (88.6%)**	**57 (69.5%)**	**< 0.001**
Body / Tail	**21 (11.4%)**	**25 (30.5%)**	
Grade / Differentiation			
I / II	**135 (73.8%)**	**37 (45.7%)**	**<0.001**
III / IV	**48 (26.2%)**	**44 (54.3%)**	
Perineural Invasion			
Negative	29 (16.0%)	17 (21.3%)	0.198
Positive	152 (84%)	63 (78.8%)	
Vascular space invasion			
Negative	75 (42.1%)	26 (32.5%)	0.091
Positive	103 (57.9%)	54 (67.5%)	
Size			
≤ 20mm	22 (12.0%)	7 (8.6%)	0.430
> 20 ≤ 40mm	117 (63.9%)	49 (60.5%)	
> 40mm	44 (24.0%)	25 (30.9%)	
Margin			
Negative	138 (75.4%)	55 (67.1%)	0.104
Positive	45 (24.6%)	27 (32.9%)	
Histological subtype			
IPMN with invasion	**21 (11.4%)**	**3 (3.7%)**	**0.029**
Mucin	23 (12.5%)	5 (6.1%)	0.084
Adenosquamous	**2 (1.1%)**	**11 (13.4%)**	**<0.001**
Acinar cell	2 (1.1%)	0 (0%)	0.478
PDAC - NOS	155 (84.2%)	66 (80.5%)	0.279
Local only Recurrence			
No	102 (86.4%)	50 (83.3%)	0.365
Yes	16 (13.6%)	10 (16.7%)	
Liver Recurrence			
No	**66 (55.9%)**	**24 (40.0%)**	**0.032**
Yes	**52 (44.1%)**	**36 (60.0%)**	
Lung Recurrence			
No	**79 (66.9%)**	**48 (80.0%)**	**0.048**
Yes	**39 (33.1%)**	**12 (20.0%)**	
Lung Recurrence (no liver)			
No	**92 (78.0%)**	**55 (91.7%)**	**0.016**
Yes	**26 (22.0%)**	**5 (8.3%)**	
Non-Liver Distant Recurrence			
No	81 (68.6%)	48 (80.0%)	0.075
Yes	37 (31.4%)	12 (20.0%)	

In order to identify candidate molecular pathways associated with specific recurrence patterns, a gene ontology (GO) analysis in patients with liver and lung metastatic recurrence was performed. GO terms are generated by associating differential gene

expression across specific pathways to which they are functionally related (Balakrishnan et al., 2013). This allows an analysis of specific pathways that are differentially upregulated based upon mRNA expression in different subgroups (Balakrishnan et al., 2013). In this analysis, patients with liver recurrence and those with lung (no liver) recurrence were used as separate denominators to investigate upregulated molecular pathways in each disease pattern. This was performed using the molecular features of the primary tumour, instead of the secondary metastases, to identify candidate pathways that drive specific metastatic patterns and may inform clinical decisions and therapeutic development.

Liver recurrence was associated with upregulated molecular features of squamous differentiation (pathways related to Cornification, Keratin development and differentiation, Skin development) (Figure 3-4). Furthermore, gene pathways associated with an anti-tumour immune response were significantly downregulated in those that developed liver metastases (Figure 3-4). This implies that in those that develop liver recurrence, an immunosuppressive, pro-inflammatory micro-environment may promote liver dissemination (Nielsen et al., 2016, Steele et al., 2016). This has previously been demonstrated in mouse models of PDAC to be secondary to macrophage and neutrophil infiltration in the primary tumour and metastatic sites (Steele et al., 2016). These molecular features may guide clinical trials to enrich cohorts with these features to test anti-myeloid therapy (e.g. CXCR2 or CSF1R inhibitors) in trials.

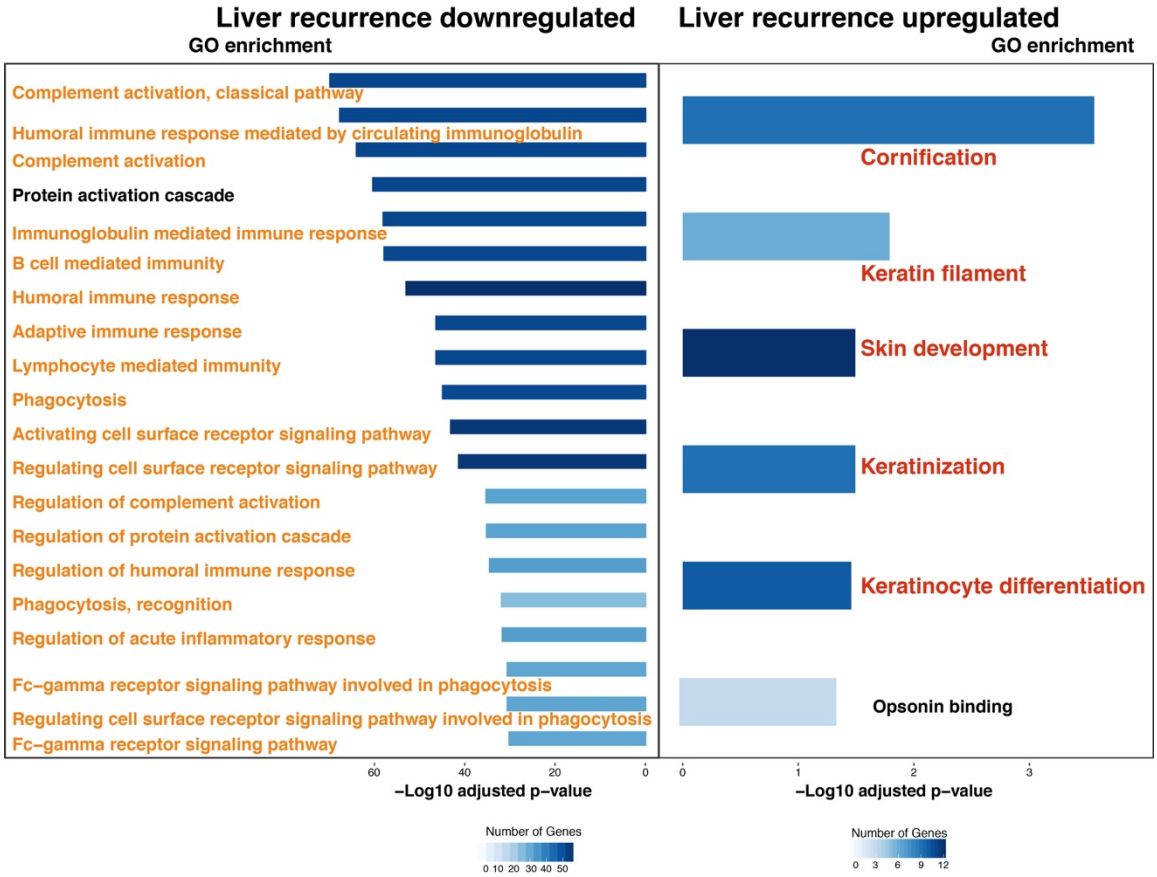

Figure 3-4 Gene Ontology enrichment terms in patients that developed liver recurrence following pancreatectomy for PDAC. Liver recurrence is significantly associated with squamous differentiation and immunosuppressive, pro-inflammatory pathways. In those that develop liver recurrence, there was significant down regulation in anti-tumour immune response pathways (**highlighted in orange, left half of figure**) suggesting that liver recurrence is associated with a pro-inflammatory, immunosuppressive primary tumour microenvironment. GO terms that were associated with mRNA expression demonstrates that features of squamous differentiation (**highlighted in red, right half of figure**) are upregulated in the patients with liver recurrence.

Next, a similar analysis of the patient group that develop lung, but no liver recurrence, was performed (Figure 3-5). This revealed that in primary tumours that develop lung metastases, there is significant downregulation (i.e. reduced mRNA expression) in pathways associated with squamous differentiation (Figure 3-5). This suggests that the squamous subtype is not associated with lung recurrence and this difference in tumour biology may partly explain the improved outcomes seen in those patients with only lung recurrence in comparison to those that develop liver metastases. The exact mechanism underlying this phenomenon was not investigated, but may be associated with the pro-inflammatory, myeloid rich, microenvironment in the squamous subtype, which in turn promotes liver metastases (Nielsen et al., 2016, Candido et al., 2018). In contrast, the Classical Pancreatic subtype does not appear to be associated with transcriptomic evidence of myeloid infiltration which may reduce the affinity for these primary tumours to

metastasise to the liver. To confirm this was beyond the data available for analysis here and requires further investigation using longitudinal studies in PDAC, with parallel well designed pre-clinical studies using genetically engineered mouse models or other approaches.

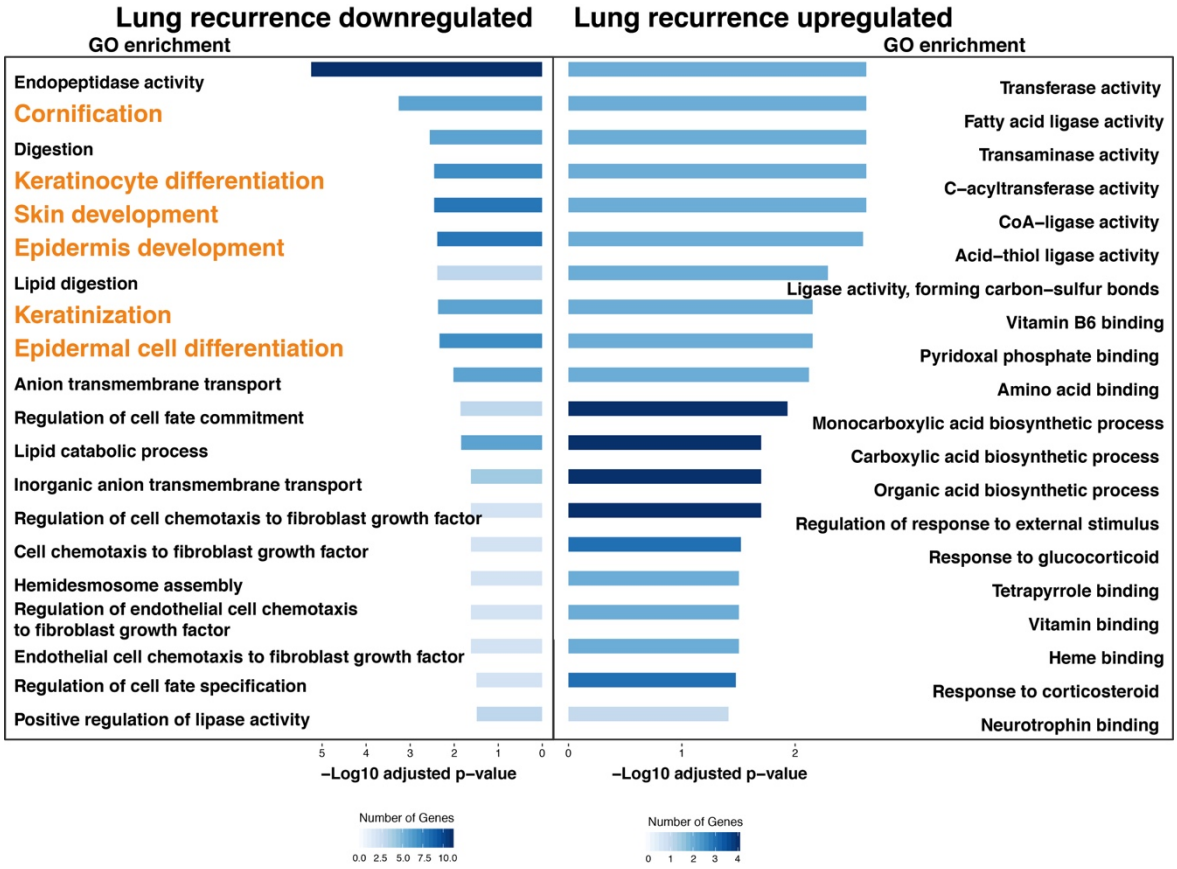

Figure 3-5 Gene Ontology enrichment terms in patients that developed lung recurrence following pancreatectomy for PDAC. Patients that develop lung recurrence has significant down regulation of pathways (based on mRNA expression) associated with squamous differentiation (highlighted in orange).

To further investigate the impact of disease pattern on patient outcome, a survival analysis was performed comparing disease specific survival in distinct disease pattern groups (Figure 3-6). Recurrence patterns were defined as;

1) local recurrence only
2) lung metastases (and no liver metastases)
3) Liver metastases (including other distant sites of recurrence)
4) Distant metastases without lung or liver recurrence (e.g. peritoneal).

Patients with local only and lung (no liver) recurrence had significantly better disease specific survival compared to liver and other distant recurrence patterns (median survival 23.0 vs 23.7 vs 13.6 vs 16.7 months, $P < 0.001$) (Figure 3-6). Liver metastases also developed earlier than other sites of recurrence (median time to recurrence 7.9 vs 12.9 vs 11.0 vs 10.0, $P < 0.001$) (Figure 3-6).

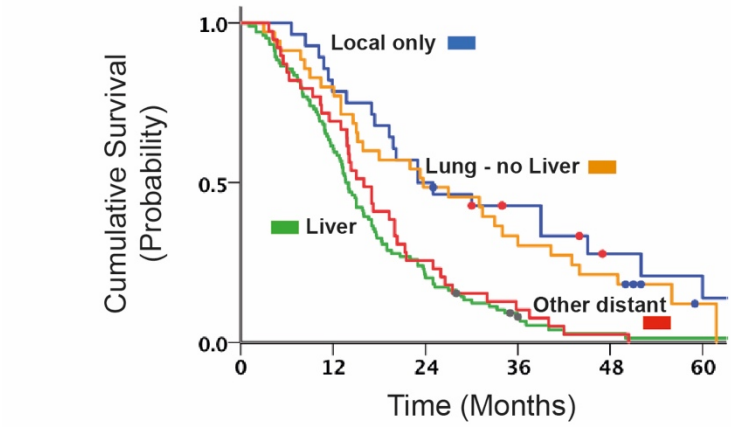

No at Risk							Disease Specific Survival $P < 0.001$	Recurrence Free Survival $P < 0.001$
Local only	28	22	14	9	4	3	23.0	12.9
Lung - no Liver	35	28	17	11	7	1	23.7	11.0
Liver	104	64	22	7	2	1	13.6	10.0
Other distant	39	27	10	4	1	0	16.0	7.9

Figure 3-6 Disease Specific Survival stratified by recurrence pattern in the ICGC cohort. This figure demonstrates that lung and local recurrence has significantly better outcome following surgery than those patients that present with metastatic disease in the liver or elsewhere. Survival stratified by site of recurrence in patients with disease recurrence only. Patients with local only and lung recurrence had significantly better DSS following pancreatectomy than those with liver or other distant sites of recurrence (DSS and RFS shown as median survival, *P* calculated using log rank test and tested for differences amongst groups).

Patients that developed local recurrence only had a similar margin positivity rate than the other sites (Table 3-6). However, in the ICGC cohort margin status was defined as 0mm, i.e. at the margin. This has been shown to be less prognostic than a clear margin of at least 1mm (Chang et al., 2009a, Jamieson et al., 2013, Jamieson et al., 2010). Unfortunately, detailed margin reports were not available for all participants in the ICGC cohort to define margin status using a 1mm cut-off.

Table 3-6 Resection margin status and recurrence patterns in the APGI cohort

	Local Only	Lung (no Liver)	Liver	Other distant	*P*-value (Chi-square)
Resection Margin Status (R0 = 0mm)					0.637
Clear	17 (60.7)	23 (65.7)	73 (71.6)	23 (59.0)	
Involved	11 (39.3)	12 (34.3)	29 (28.5)	15 (40.5)	

The data presented here correlates with other studies suggesting recurrence pattern to be intricately linked to prognosis following pancreatectomy for PDAC (Groot et al., 2018, Groot et al., 2017). Furthermore, margin status does not affect recurrence pattern in this cohort, in keeping with other studies (Sugiura et al., 2013, Yamamoto et al., 2017). This suggests that there are molecular and phenotypical features of the primary tumour that are associated with recurrence patterns and that this may explain the differences seen in prognosis between these. As a consequence, a further detailed analysis of molecular data and disease patterns was performed.

3.2.1.4 Squamous subtype is associated with metastatic disease at presentation

To further investigate the relationship between molecular subtype and clinical disease patterns, an independent unselected cohort of patients presenting with all stages of PDAC (the *PRECISION-Panc* EUS training cohort) underwent RNA sequencing and analysis. Patients presenting for diagnostic EUS and biopsy underwent additional biopsies for molecular profiling. In 35 consecutive patients with confirmed PDAC and sufficient fresh frozen biopsy tissue, RNA extraction and RNAseq was performed. Gene expression was normalised, and consensus clustering performed based on gene programs described in Bailey *et al*.(Bailey et al., 2016). Due to the relatively small cohort (n = 35), and the strong overlap between Pancreatic Progenitor, ADEX and Immunogenic subtypes, patients were subtyped as either Classical Pancreatic and Squamous (Figure 3-7). Since this cohort contained patients presenting with all stages of PDAC, molecular subtypes were correlated with stage at presentation (Figure 3-7). Out of 35 patients, 16 (46%) were classified as Classical Pancreatic and 19 (54%) Squamous (Figure 3-7). The squamous subtype was associated with *de novo* metastatic disease (n = 10, 53%) compared to the Classical Pancreatic subtype (n = 3, 19%) (P = 0.042, Chi square-test). In contrast, the Classical Pancreatic group was associated with locally advanced disease (50% vs 21%, P = 0.075, Chi square-test), however, this failed to reach significance due to low patient numbers. To further investigate the association of a metastatic phenotype and the squamous subtype,

gene expression analysis was performed by clustering gene programs based on disease stage at presentation. Patients presenting with *de novo* metastatic disease, had significant enrichment of Gene Programme 2 (GP2) expression in comparison with locally advanced ($P = 0.006$) and resectable ($P = 0.0058$) PDAC (Figure 3-7). GP2 is the strongest gene program that defines the squamous subtype, consisting of genes involved in invasion, inflammation and epithelial-to-mesenchymal transition (Bailey et al., 2016). This further strengthens the association of the squamous subtype with metastatic PDAC. Furthermore, these data also demonstrate an incidence of the squamous subtype at 54% in all stages of PDAC, compared to 29% in early resected disease which made up the ICGC cohort (Table 3-1, Figure 3-7). Suggesting that the squamous subtype is significantly more prevalent than first appreciated, when accounting for all stages of PDAC.

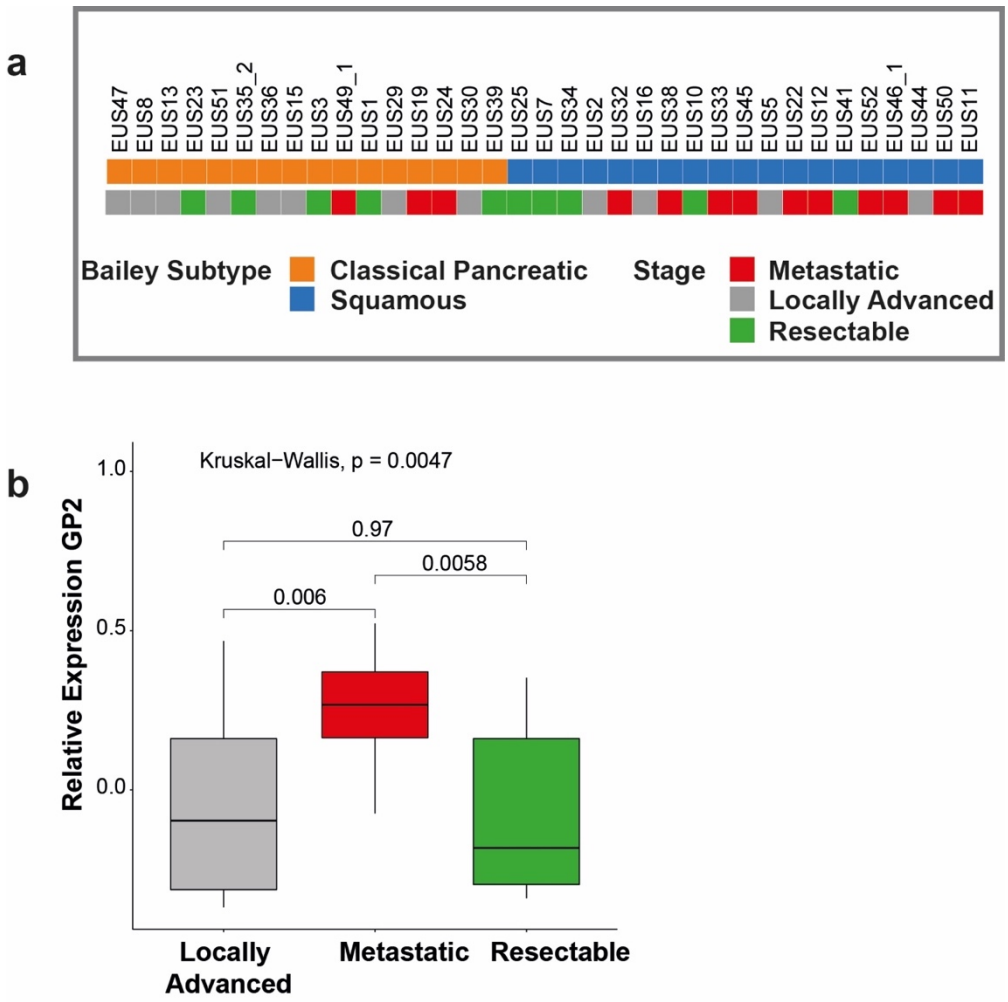

Figure 3-7 Molecular characterisation of EUS guided fine needle biopsies of PDAC. a) EUS guided biopsies from unselected, untreated patients ($n = 35$) presenting for diagnostic sampling, ranked from right to left based on GP2 gene set enrichment score. Coloured boxes indicate transcriptomic subtype and clinical stage at time of presentation. b) Boxplot

representing association of clinical stage and relative GP2 expression of EUS biopsy samples at time of presentation.

From the analysis presented so far in this chapter, there are a number of key concepts that arise (Figure 3-8):

- First, the squamous subtype is associated with a poor prognosis following surgery and appears to be more prognostic than a number of well validated pathological features.

- Second, body and tail cancers of the pancreas are more likely to be of squamous subtype and potentially explains the worse outcomes of these patients compared to those with cancers of the head and uncinate process. Third, the Classical Pancreatic subtype is associated with mucinous and IPMN malignancies whilst the squamous subtype is associated with adenosquamous tumours. This may explain the differences in outcome in these patients clinically, particularly the poor prognosis of adenosquamous PDAC, and relatively good prognosis in IPMN PDAC.

- Last, the squamous subtype is associated with liver recurrence whereas lung recurrence is associated with the Classical Pancreatic subtype. This likely explains the association between poor survival in patients that develop liver recurrence, and relatively longer survival in those that develop lung recurrence.

These central concepts are investigated further in this thesis. Next, in this chapter, the biological features of body and tail cancers are further explored in an attempt to apply the findings above. Chapter 4 explores the association between poor prognosis in the squamous subtype and is addressed by developing molecular prognostic tools to identify patients with aggressive tumour biology prior to treatment in order to better select patients for personalised therapy.

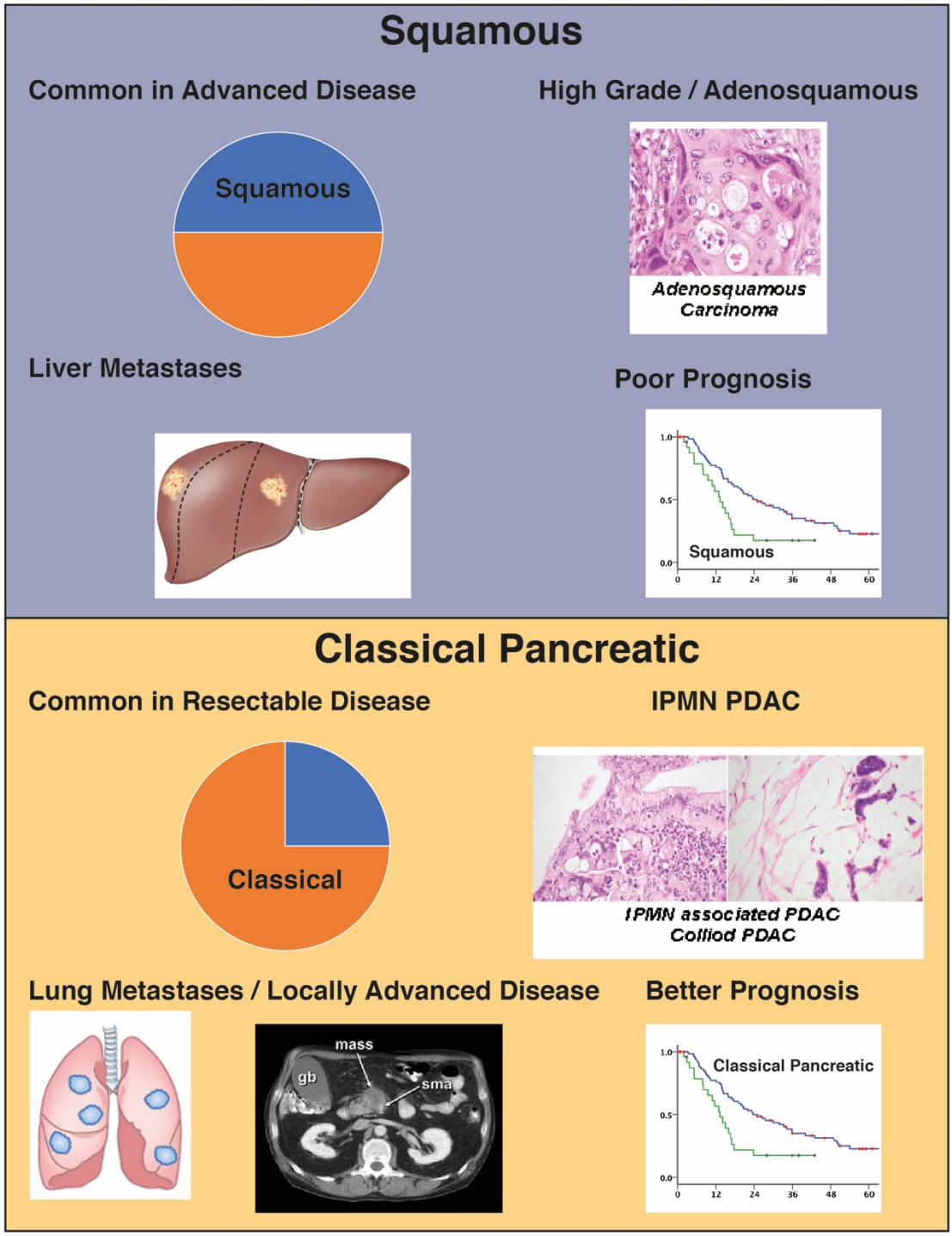

Figure 3-8 Clinical and Pathological Disease Patterns associated with Molecular subtypes of PDAC. The squamous subtype is associated with advanced disease, liver metastases, high pathological grade (poor differentiation) and adenosquamous differentiation. These are clinical features that have been associated and validated as poor prognostic markers of PDAC. The Classical Pancreatic subtype is associated with early stage disease and progresses more commonly via lung metastases and local progression in comparison to the squamous subtype. IPMN associated PDAC is strongly associated with the Classical Pancreatic subtype and these features have been previously validated as predictors of better prognosis in PDAC. These molecular subtypes may underlie the differences in prognosis seen with these routine clinical and histological prognosticators.

3.3 The molecular pathology of Body and Tail PDAC

There are meaningful differences in the outcomes of patients with PDAC located in the head, as compared to those of the body and tail of pancreas (BTPC) (Artinyan et al., 2008, Brennan et al., 1996, Watanabe et al., 2004, Sener et al., 1999, Lau et al., 2010, de Rooij et al., 2016, Mackay et al., 2018). Approximately 15% of PDAC occur in the body and tail and differences in outcome have largely been attributed to late presentation in comparison with tumours of the pancreatic head (Artinyan et al., 2008, Brennan et al., 1996, Watanabe et al., 2004, Lau et al., 2010). Pancreatic tumours of the body and tail are thought to present at an advanced stage and are more often associated with unresectable disease (Artinyan et al., 2008). BTPC usually presents with weight loss and pain, symptoms more in keeping with advanced disease (Watanabe et al., 2004). Yet, previous studies suggest that TNM stage after surgical resection is not significantly different between the two tumour locations (Sohn et al., 2000). Metastatic PDAC of the body and tail is associated with more sites of metastases, peritoneal metastases and appears to be associated with more aggressive biology clinically (Mackay et al., 2018). The molecular pathology of PDAC has been intensely studied recently, yet, the genetic and molecular differences between PDAC of the head and BTPC have not been well-defined. The poor prognosis and high rates of early recurrence in BTPC, provides an opportunity to identify potential molecular features associated with these clinical disease patterns and aggressive disease.

In this section of Chapter 3, the extended APGI cohort (n = 518), which includes the ICGC cohort (n = 456), is investigated for clinical and molecular differences between PDAC of the head (n = 426) and BTPC (n = 92). First, standard clinicopathological and prognostic features of BTPC is investigated in this cohort. Second, using extensive molecular characterisation of the ICGC cohort, molecular characteristics (including molecular subtype, gene programs and mutational signatures) associated with BTPC is investigated.

3.3.1 Results

3.3.1.1 Patient Cohort characteristics

Patient characteristics of the APGI cohort included for clinical analysis are summarised in Table 3-7. In total 518 patients' clinical data was acquired (APGI cohort), and molecular profiling performed as part of the APGI's contribution to the ICGC (ICGC cohort) (Figure 3-1). Of these, 456 PDACs underwent DNA sequencing, consisting of 179 whole genomes and 277 additional participants with whole exome sequencing. Ninety-six underwent

whole transcriptome RNA sequencing (RNAseq) and the others underwent transcriptomic characterisation using microarray gene expression analysis (n = 266) based on lower tumour epithelial contents.

Table 3-7 Patient characteristics for the APGI cohort stratified by primary tumour location

	Head			Body & Tail		
Variables	**n = 426 No. (%)**	**Median DSS (months)**	***P* value (Logrank)**	**n = 92 No. (%)**	**Median DSS (months)**	***P* value (Logrank)**
Sex						
Male	213 (50.0)	22.4	0.904	45 (48.9)	11.6	0.168
Female	213 (50.0)	121.0		47 (51.1)	13.0	
Age (years)						
Mean	66.5			67.8		
Median	68.0			70.5		
Range	28.0 – 88.0			28.0 – 86.0		
Outcome						
Follow-up (months)	18.0 – 164.0			32.0 – 136.0		
Median follow-up (months)	48.0			45.0		
Death PC	196 (46.0)			47 (51.1)		
Death other	10 (2.3)			5 (5.4)		
Death Unknown	0 (0.0)			0 (0.0)		
Alive	215 (50.5)			40 (43.5)		
Lost to FU	5 (1.2)			0 (0.0)		
Stage (AJCC 7th)						
I	**24 (5.7)**	**56.6**	**<0.001**	**8 (8.7)**	**51.9**	**0.018**
II	**400 (93.9)**	**21.0**		**74 (80.4)**	**13.0**	
III	**1 (0.2)**	**20.0**		**1 (1.1)**	**21.0**	
IV	**1 (0.2)**	**5.7**		**9 (9.8)**	**7.6**	
T Stage (AJCC 7th)						
T1	16 (3.8)	31.0	0.117	5 (5.4)	73.0	0.142
T2	34 (8.0)	32.0		14 (15.2)	15.8	
T3	375 (88.0)	21.0		72 (78.3)	11.6	
T4	1 (0.2)	20.0		1 (1.1)	21.0	
N Stage (AJCC 7th)						
N0	**134 (31.5)**	**25.2**	**0.004**	35 (38.9)	12.0	0.724
N1	**292 (68.5)**	**20.7**		55 (61.1)	13.0	
Grade						
I	**32 (7.5)**	**38.1**	**0.012**	9 (9.9)	15.8	0.903
II	**283 (66.6)**	**23.0**		57 (62.6)	12.1	
III	**107 (25.2)**	**17.0**		23 (25.3)	13.0	
IV	**3 (0.7)**	**13.0**		2 (2.2)	9.0	
Tumour size						
≤ 20mm	**92 (21.6)**	**32.0**	**0.007**	**9 (10.1)**	**72.6**	**0.001**
> 20 ≤ 40mm	**255 (60.0)**	**19.0**		**37 (41.6)**	**13.0**	
> 40mm	**78 (18.4)**	**17.0**		**43 (48.3)**	**11.1**	
Margins (R0 = 0mm)						
Clear	**285 (66.9)**	**25.2**	**<0.001**	53 (57.6)	14.0	0.152
Involved	**141 (33.1)**	**16.7**		39 (42.4)	11.4	
Perineural Invasion						
Negative	**94 (22.5)**	**29.7**	**0.020**	20 (22.5)	13.0	0.556
Positive	**324 (77.5)**	**20.0**		69 (77.5)	12.1	
Vascular Invasion						
Negative	**193 (46.8)**	**25.0**	**0.002**	**41 (47.1)**	**15.4**	**0.045**
Positive	**219 (53.2)**	**19.4**		**46 (52.9)**	**11.6**	
Adjuvant Chemotherapy						
< 3 cycles	**249 (58.7)**	**16.5**	**<0.001**	**61 (66.3)**	**9.3**	**0.013**
≥ 3 cycles	**175 (41.3)**	**29.9**		**31 (33.7)**	**17.0**	

3.3.1.2 Body and tail tumours of the pancreas have a significantly worse prognosis after pancreatectomy

In the APGI cohort, the majority of tumours (n = 426, 77%) were located in the head of the pancreas and 98 (23%) had BTPC. There was no difference in patient demographics between those presenting with head compared to body / tail tumours (Table 3-7). BTPC were more likely to be lower pathological stage (T I / II) (20.7% vs 11.7%; $P = 0.021$) (Table 3-8), yet significantly larger in size at time of resection (median maximum diameter 40 vs 30 mm, $P = 0.001$) (Table 3-8). Despite there being no discernible difference in well-defined clinical prognostic pathological variables except tumour size between the two groups (Table 3-8), patients presenting with body and tail tumours had a worse outcome (median survival 12.1 vs 22.0 months; $P = 0.001$) (Figure 3-9). Multivariate Cox regression survival analysis revealed that tumour location remained an independently prognostic variable (HR 1.72 (95% CI 1.01 – 1.62), $P < 0.001$) (Table 3-9). These data suggest that BTPC is associated with poor survival following surgery. Yet, standard prognostic, extensively validated, clinicopathological features do not appear to account for these findings.

Table 3-8 Clinicopathological variables and tumour location ICGC cohort. *Statistical difference calculated using ANOVA

	Head	Body / Tail	*P*-value (Chi-square)
T – stage (AJCC 7th edition)			
T I / II	**50 (11.7%)**	**19 (20.7%)**	**0.021**
T III / IV	**376 (88.3%)**	**73 (79.3%)**	
N – stage (AJCC 7th edition)			
N0	134 (31.5%)	35 (38.9%)	0.108
N1	292 (68.5%)	55 (61.1%)	
Grade			
I / II	303 (73.4%)	62 (71.3%)	0.390
III / IV	110 (26.6%)	25 (28.7%)	
Perineural Invasion			
Negative	94 (22.5%)	20 (22.5%)	0.561
Positive	324 (77.5%)	69 (77.5%)	
Vascular space invasion			
Negative	193 (46.8%)	41 (47.1%)	0.527
Positive	219 (53.2%)	46 (52.9%)	
Size			
≤ 20mm	**92 (21.6%)**	**9 (10.1%)**	**0.007**
> 20 ≤ 40mm	**255 (60.0%)**	**37 (41.6%)**	
> 40mm	**78 (18.4%)**	**43 (48.3%)**	
Median Diameter	**30mm**	**40mm**	**< 0.001***
Mean Diameter	**32mm**	**47mm**	**<0.001***
Margin (R0 = 0mm)			
R0	285 (66.9%)	53 (57.6%)	0.059
R1	141 (33.1%)	39 (42.4%)	
Adjuvant Chemotherapy			
< 3 cycles	249 (58.7%)	61 (66.3%)	0.109
≥ 3 cycles	175 (41.3%)	31 (33.7%)	

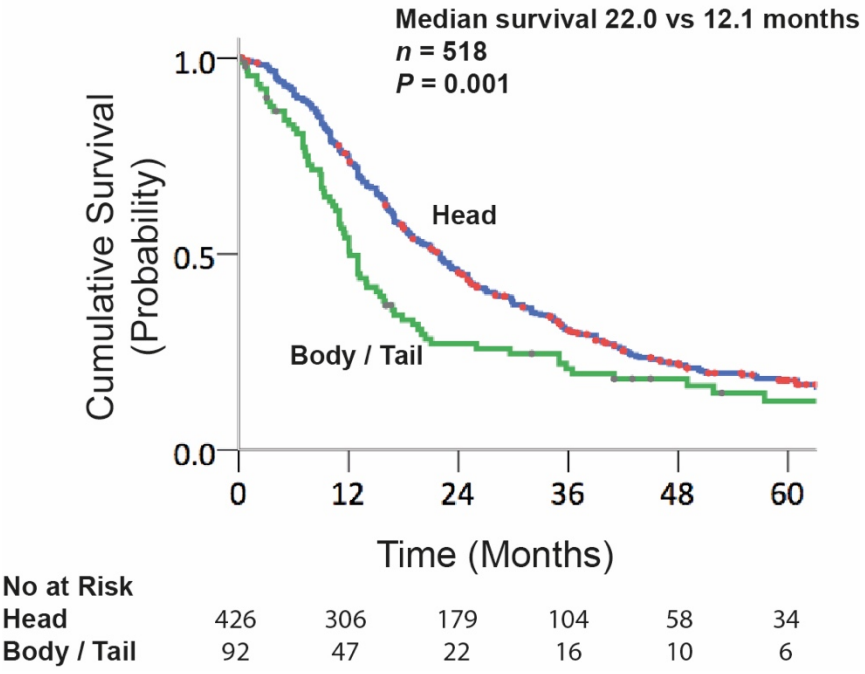

Figure 3-9 Kaplan-Meier survival curves for the APGI cohort. Survival stratified by tumour location. Patients presenting with BTPC had significantly worse DSS following pancreatectomy (*P* calculated using log rank test).

Table 3-9 Multivariate Survival model for the ICGC cohort, including tumour location

	Variable	Hazard Ratio (95% CI)	*P* Value
Clinicopathological variables and Tumour location (*n* = 465)	Differentiation (poor)	1.32 (1.04 – 1.67)	*0.023*
	T Stage (T3/4)	1.35 (0.96 – 1.89)	0.088
	Lymph Node Involvement	1.13 (0.89 – 1.44)	0.307
	Margin Involvement (Positive)	1.73 (1.38 – 2.17)	< 0.001
	Tumour Location (Body/Tail)	1.70 (1.29 0 2.22)	< 0.001
	Perineural Invasion (Positive)	1.15 (0.88 – 1.49)	0.305
	Vascular Invasion (Positive)	1.23 (0.97 – 1.55)	0.085
	Differentiation (poor)	1.32 (1.04 – 1.67)	0.024
	T Stage (T3/4)	1.37 (0.98 – 1.93)	0.068
	Margin Involvement (Positive)	1.75 (1.40 – 2.18)	<0.001
	Tumour Location (Body/Tail)	1.71 (1.31 – 2.24)	<0.001
	Perineural Invasion (Positive)	1.15 (0.89 – 1.49)	0.298
	Vascular Invasion (Positive)	1.27 (0.89 – 1.49)	0.298
	Differentiation (poor)	1.30 (1.03 – 1.65)	0.030
	T Stage (T3/4)	1.37 (0.97 – 1.92)	0.070
	Margin Involvement (Positive)	1.78 (1.43 – 2.22)	<0.001
	Tumour Location (Body/Tail)	**1.72 (1.31 – 2.26)**	**<0.001**
	Vascular Invasion (Positive)	1.30 (1.01 – 1.62)	0.019

3.3.1.3 Body and tail cancers are associated with the squamous subtype of PDAC

Cancers of the body and tail of pancreas co-segregated with the squamous subtype of pancreatic cancer in both the patients that underwent whole transcriptome sequencing (n = 96; P = 0.033), and those who underwent mRNA microarray sequencing (non-redundant set n = 266; P < 0.001) (Table 3-10). The prevalence of the squamous subtype was more than double than that observed in tumours located in the head in both the RNAseq (45% vs 21%) and micro-array (54% vs 26%) sets (Table 3-10).

Table 3-10 Association between tumour location and Bailey subtype

	Head	Body / Tail	*P*-value (Chi-square)
Molecular Subtype (RNA sequencing; *n* = 96)			
Classical Pancreatic	60 (78.9%)	11 (55.0%)	0.033
Squamous	16 (21.1%)	9 (45.0%)	
Molecular Subtype (micro-array; *n* = 266)			
Classical Pancreatic	163 (74.1%)	21 (45.7%)	< 0.001
Squamous	57 (25.9%)	25 (54.3%)	

In those patients that underwent WGS (n = 179), there was no association between tumour location and chromosomal structural variation subtypes as described by Waddel *et al.*(Waddell et al., 2015) (P = 0.211), however BTPC was associated with a *BRCA* mutational signature (COSMIC mutational signature 3) (P = 0.025) (Table 3-12). Based on the frequency of mutations per megabase (MB), COSMIC mutational signature 17

(unknown aetiology) (P = 0.002) was associated with BTPC. There was no association with COSMIC mutational signatures of loss of mismatch repair status (MMR, COSMIC mutational signature 6) (P = 0.619), oesophageal cancer (COSMIC mutational signature 18) (P = 0.976), deamination (COSMIC signature 1) (P = 0.287) nor COSMIC signature 2 (APOBEC) (P = 0.301) (Table 3-12).

Table 3-11 Tumour location and association with Structural variation subtypes (*n* = 179)

	Head	Body / Tail	*P*-value (Chi-square)
SV subtype			
Stable	20 (14.3%)	5 (15.2%)	0.211
Focal	46 (32.9%)	5 (15.2%)	
Scattered	61 (43.6%)	20 (60.6%)	
Unstable	13 (9.3%)	3 (9.1%)	

Table 3-12 Tumour location and association with mutational signatures (*n* = 179)

COSMIC Mutational Signature	Mean mutations per MB (*P* calculated by ANOVA table)		
	Head	Body / Tail	*P*
MMR (COSMIC signature 6)	1.34	0.73	0.619
Unknown aetiology (COSMIC signature 17)	**0.38**	**0.56**	**0.002**
Oesophageal Cancer (COSMIC signature 18)	0.51	0.51	0.976
Deamination (COSMIC signature 1)	1.80	1.98	0.287
APOBEC (COSMIC signature 2)	0.74	0.93	0.301
BRCA (COSMIC signature 3)	**1.41**	**2.17**	**0.025**

3.3.1.4 Body and tail Squamous PDAC is associated with extremely poor survival

Resected tumours were segregated by tumour location and transcriptomic subtype, as defined in Bailey *et al.*, to assess differences in outcome in squamous tumours of the head versus body and tail. Squamous tumours of the body and tail had an extremely poor

survival compared with the rest of the cohort (median survival 22 vs 5.2 months; $P < 0.001$) (Figure 3-10). These findings were recapitulated in the microarray set (median survival 25.0 vs 18.4 vs 15.9 vs 11.5 months, $P = 0.001$) (Figure 3-10).

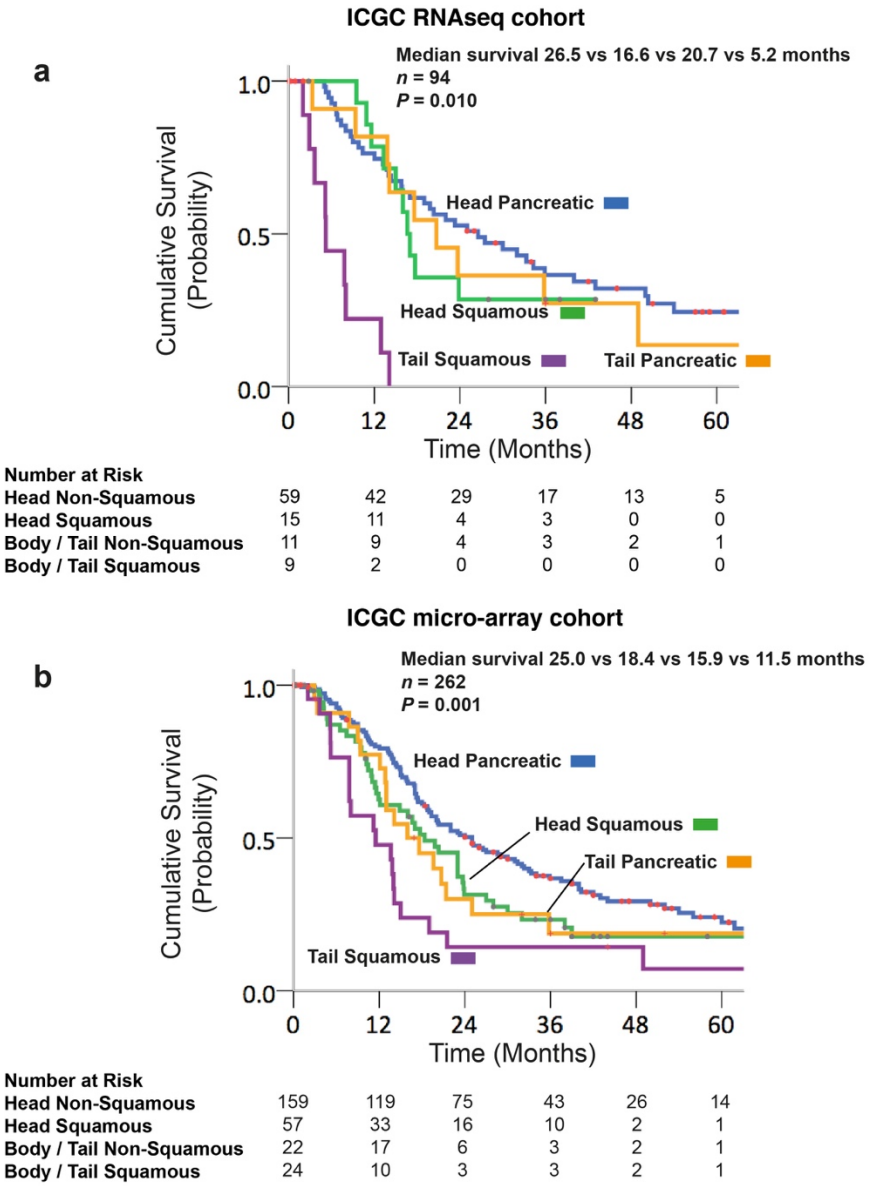

Figure 3-10 Kaplan-Meier survival curve stratified by Bailey subtype and tumour location in (a) RNAseq (*n* = 94) and (b) gene expression micro-array (*n* = 262) sets. In both patient cohorts, squamous BTPC is associated with very poor prognosis. In the RNAseq cohort, the median survival was only 5.2 months for this patient group.

3.3.1.5 Body and Tail PDAC is associated with molecular features of aggressive disease

Bailey *et al*. described 10 gene programs (GP) that discriminate the molecular attributes of the 4 transcriptomic subtypes of PDAC (Bailey et al., 2016). These are based on differential expression of genes related to molecular pathways underlying differences in

each subtype (Bailey et al., 2016). These can be described as gene sets that define each subtype (e.g. squamous) and can be utilised to identify candidate molecular processes specific to PDAC subsets, such as BTPC, and was further investigated.

Molecular subtypes of PDAC as defined by Bailey *et al*. correlated with tumour location and thus an in-depth analysis was performed comparing tumour location with gene programs (GP) that define the subtypes described by Bailey *et al*.(Bailey et al., 2016). BTPC was associated with gene networks involved in epithelial-to-mesenchymal transition (EMT), inflammation, hypoxia response, metabolic reprogramming, TP63 expression and squamous differentiation (gene program 2 (GP2)) (Figure 3-11, Figure 3-12) (Bailey et al., 2016). GP2 remained the highest differentiator defining the squamous subtype described by Bailey *et al.*(Bailey et al., 2016). *TP63* expression, a key feature of GP2, is associated with epithelial cell plasticity and EMT, particularly in the presence of *TP53* mutations (Engelmann and Putzer, 2014). The association with EMT is further enhanced by hypermethylation and subsequent down regulation of pancreatic endodermal genes driving a mesenchymal subtype, which is associated with a worse outcome in PDAC (Wang et al., 2017, Cancer Genome Atlas Research Network. Electronic address and Cancer Genome Atlas Research, 2017, Fischer et al., 2015, Zhang et al., 2018). GP2 is enriched for the expression of genes involved in inflammation and driving an immunosuppressive microenvironment, which can lead to immune-evasion of these tumours. In addition, S100A2 is highly expressed in GP2 (Figure 3-12) and is associated with poor outcome and a pro-metastatic phenotype in patients with resectable PDAC (further explored in Chapter 4). These molecular features that are associated with BTPC provide candidate biological mechanisms that likely contribute to the poor outcomes seen in these patients.

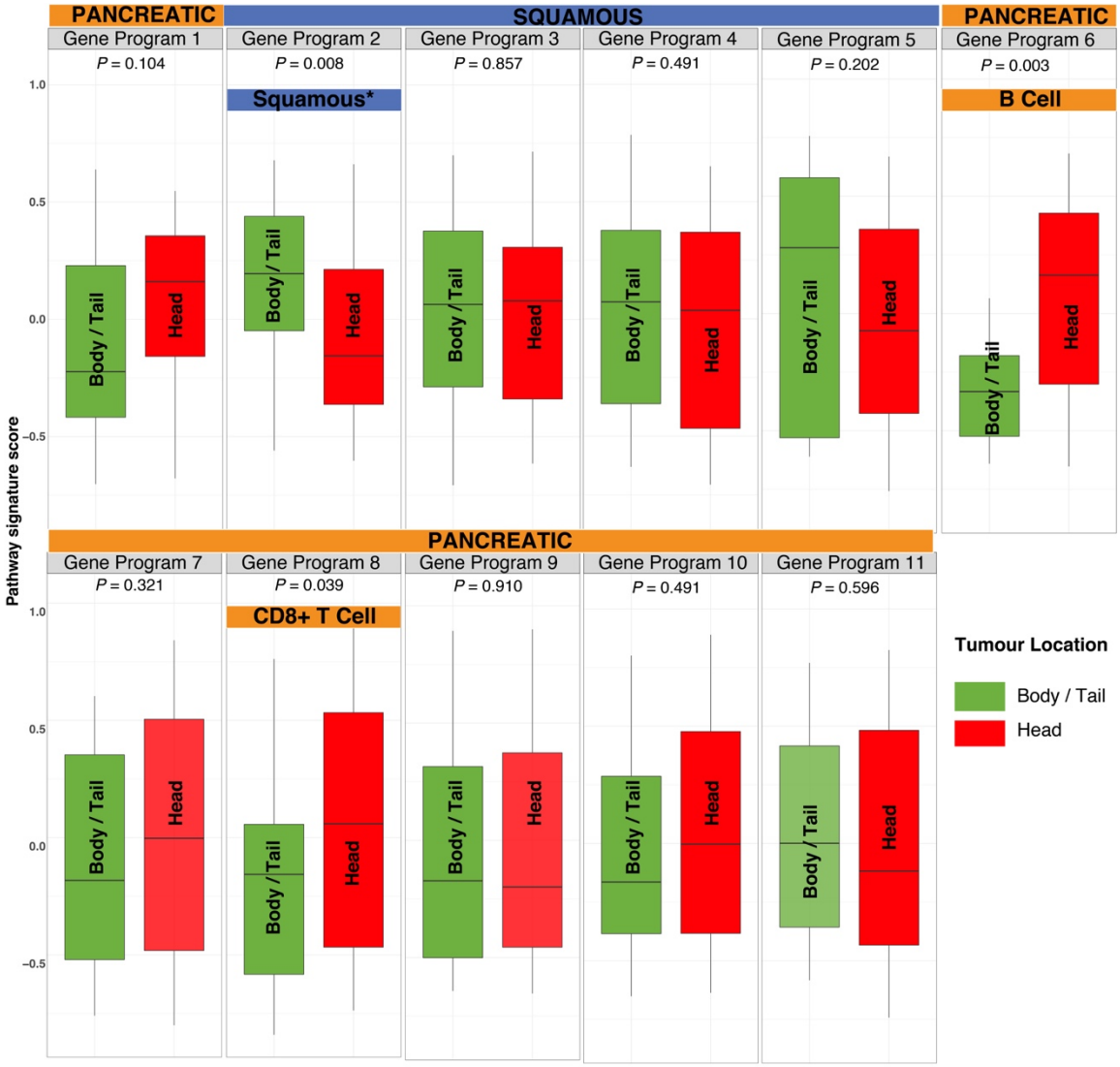

Figure 3-11 Association between Gene programs described by Bailey *et al.* and tumour location in the APGI cohort. BTPC is enriched for gene programs defining the squamous subtype (GP2), whilst gene programs reflecting an immune response (GPs 6 & 8) is relatively enriched in head tumours. Each GP is a composite score of significantly expressed genes defining the molecular subtypes defined by Bailey *et al*. Gene programs that define the Squamous (blue) and Classical Pancreatic (orange) are highlighted. Differential expression of each GP is stratified by tumour location. GP2, a strong gene classifier of the squamous subtype associated with squamous differentiation, inflammation and epithelial-mesenchymal transition, is enriched in the Body / Tail group (P = 0.008). GPs 6 (P = 0.003) and 8 (P = 0.039) are associated with an anti-tumour immune response and is differentially expressed in tumours located in the pancreatic head compared to those in the body / tail.

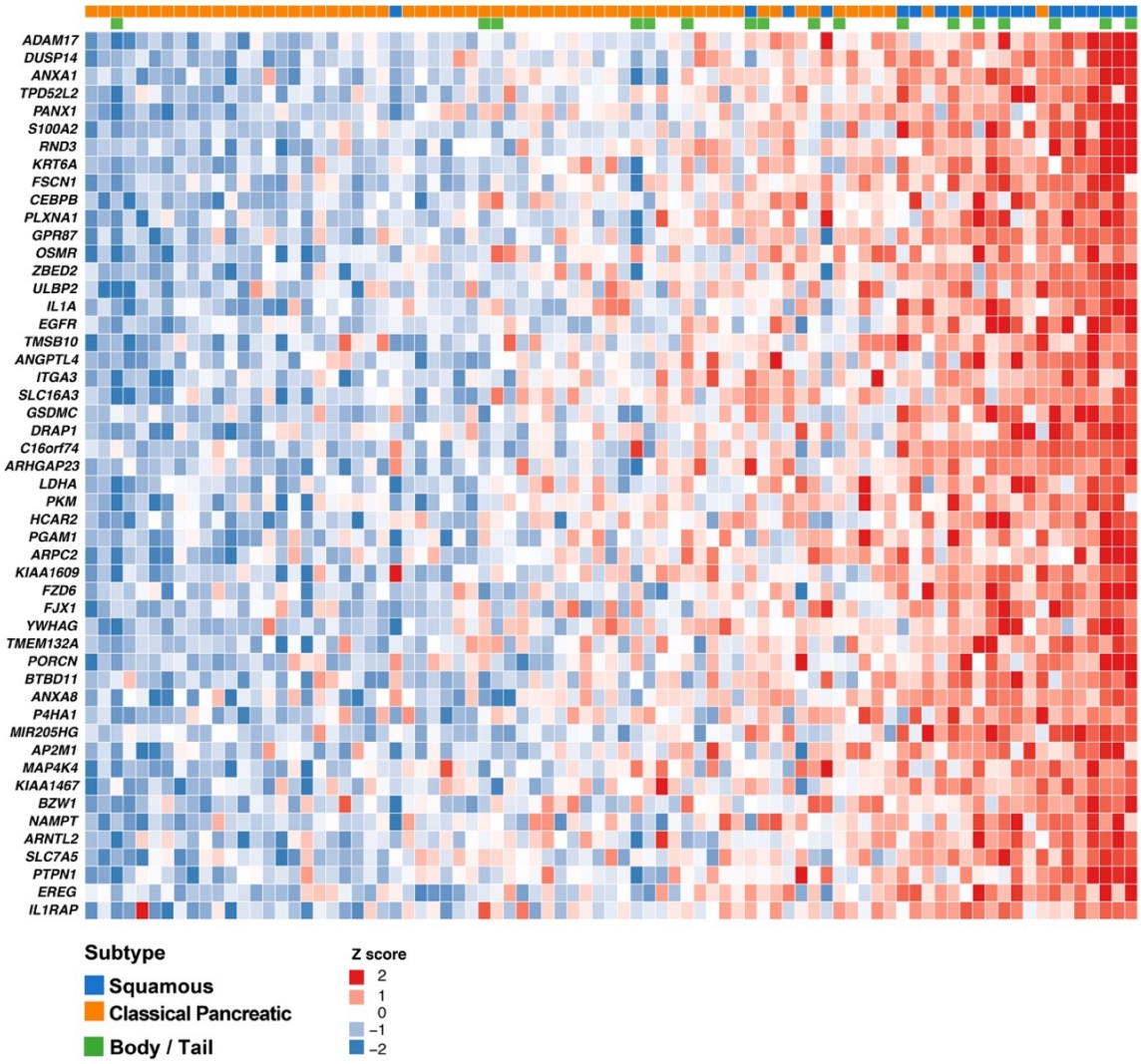

Figure 3-12 Heatmap of relative gene expression of gene program 2. Tumours located in the body or tail (marked by green box) are enriched for expression by gene program 2. Tumour subtype and location is shown on the top-bar. Tumours ranked from right to left based on highest to lowest score in GP2, demonstrating an association between BTPC and GP2.

3.3.1.6 Body / Tail PDAC is associated with an immunosuppressive tumour microenvironment

Based on transcriptomic analysis, head tumours were enriched for GPs 6 and 8 in comparison with BTPC (Figure 3-11). These GPs are associated with B cell (GP6) and $CD8^+$ T cell (GP8) signalling respectively (Bailey et al., 2016) (Figure 3-11, Figure 3-13, Figure 3-14,Table 3-13). These are features that define the Immunogenic subtype of PDAC, a sub-class of the Pancreatic Progenitor class described by Bailey *et al.* (Bailey et al., 2016). To further delineate the molecular characteristics that may underlie the differential expression of immune GPs in BTPC, a correlative analysis with immune specific gene signatures was performed (Bailey et al., 2016). These immune signatures are defined by expression patterns of specific immune cell populations found in the tumour

microenvironment (Bailey et al., 2016, Rooney et al., 2015). BTPC exhibited immune signatures corresponding to low dendritic cell infiltrate ($P = 0.005$), low co-stimulation of antigen presenting cells (APC) ($P = 0.041$) and a low Type II Interferon response ($P = 0.002$) (Table 3-13). These findings suggest that relative to head tumours, BTPC is associated with a dampened anti-tumour immune response and increased immune avoidance. Head tumours are relatively enriched for B cell signalling (GP6) and this has been shown to be associated with a better prognosis (Bailey et al., 2016). Similarly, BTPC lacks $CD8^+$ T cell signalling (GP8), suggesting an immunosuppressive tumour micro-environment (TME). This may reflect an increase in myeloid cell infiltration and tumour associated macrophage related immunosuppression and inflammation (Steele et al., 2016). The squamous subtype is enriched for macrophage and neutrophil signalling, which has been shown to contribute to the immunosuppressive microenvironment (Steele et al., 2016, Bailey et al., 2016). Therefore, the association between immunosuppression in BTPC may be secondary to the high prevalence of the squamous subtype in this subgroup of tumours. The relatively high expression of GP2 may drive this from tumour epithelium by the enrichment of pro-inflammatory signalling. In-depth analysis of the TME may reveal potential targets of novel immunotherapy agents in BTPC, including targeting the immune checkpoint and myeloid signalling axes (Steele et al., 2016).

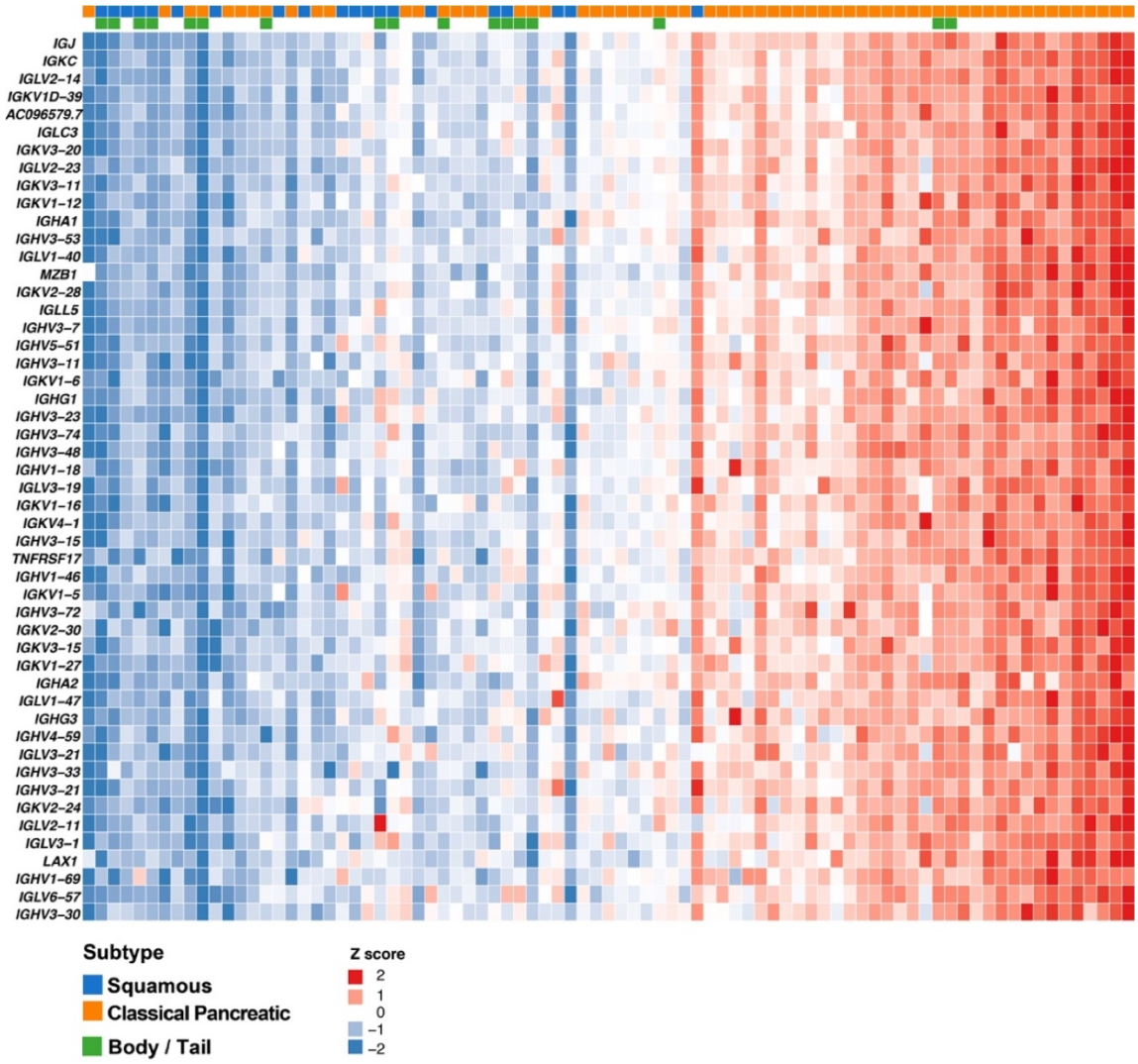

Figure 3-13 Heatmap of relative gene expression of gene program 6. Tumours located in the body or tail (marked by green box) are associated with reduced expression of genes associated with B cell infiltration into the tumour microenvironment. Bailey subtype and tumour location is shown on the top bar. Tumours are ranked from right to left based on GP6 expression, demonstrating the inverse relationship between BTPC and GP6 which is associated with B cell immune infiltrate.

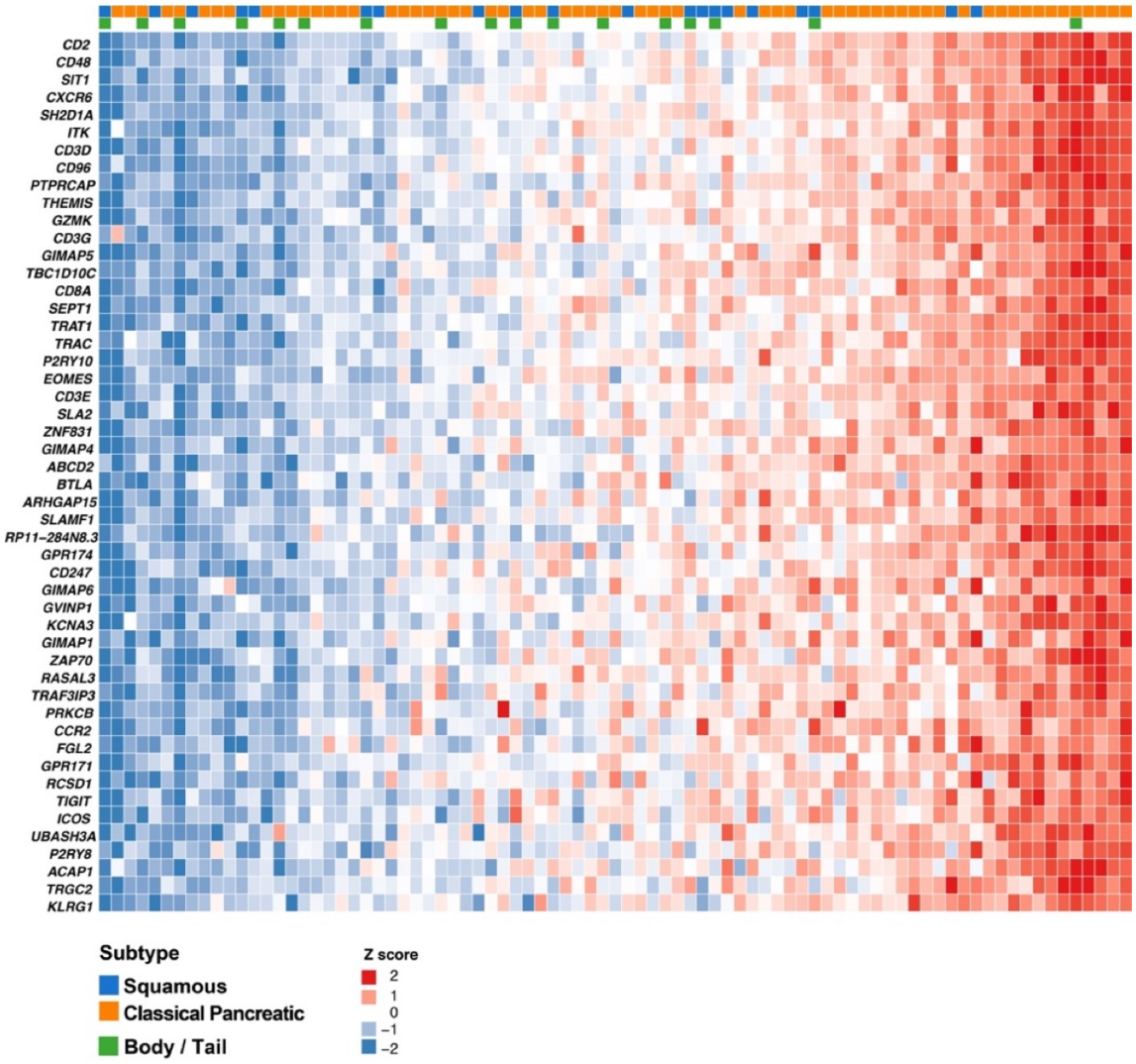

Figure 3-14 Heatmap of relative gene expression of gene program 8. Tumours located in the body or tail (marked by green box) are associated with reduced expression of genes associated with $CD8^+$ T cell infiltration into the tumour microenvironment. Bailey subtype and tumour location is shown on the top bar. Tumours are ranked from right to left based on GP8 expression, demonstrating the inverse relationship between BTPC and GP8. Demonstrating the dissociation between BTPC and gene expression associated with $CD8^+$ T cell tumour infiltrate.

Table 3-13 Tumour location and association with immune signatures of PDAC in RNAseq set (*n* = 96)

	Head	Body / Tail	*P*-value (Chi-square)
B Cells			
Low	50 (65.8%)	17 (85%)	0.078
High	26 (34.2%)	3 (15.0%)	
CD4 Reg T cells			
Low	50 (65.8%)	16 (80%)	0.172
High	26 (34.2%)	4 (20%)	
CD8 T cells			
Low	49 (64.5%)	17 (85%)	0.064
High	27 (35.5%)	3 (15%)	
Macrophages			
Low	26 (34.2%)	7 (35%)	0.572
High	50 (65.8%)	13 (65%)	
Neutrophils			
Low	55 (72.4%)	13 (65%)	0.349
High	21 (27.6%)	7 (35%)	
Natural Killer Cells			
Low	53 (69.7%)	14 (70%)	0.607
High	23 (30.3%)	6 (30%)	
Dendritic Cells			
Low	**49 (64.5%)**	**19 (95.0%)**	**0.005**
High	**27 (35.5%)**	**1 (5.0%)**	
MHC Class 1			
Low	50 (65.8%)	15 (75%)	0.309
High	26 (34.2%)	5 (25.0%)	
Co-Stimulation APC			
Low	**47 (61.8%)**	**17 (85.0%)**	**0.041**
High	**29 (38.2%)**	**3 (15.0%)**	
Co-Stimulation T Cells			
Low	53 (69.7%)	15 (75.0%)	0.436
High	23 (30.3%)	5 (25.0%)	
Co-Inhibition APC			
Low	51 (67.1%)	17 (85.0%)	0.095
High	25 (32.9%)	3 (15.0%)	
Co-Inhibition T cells			
Low	26 (34.2%)	9 (45.0%)	0.262
High	50 (65.8%)	11 (55.0%)	
Type I Interferon response			
Low	52 (68.4%)	14 (70.0%)	0.562
High	24 (31.6%)	6 (30.0%)	
Type II Interferon response			
Low	**46 (60.5%)**	**19 (95.0%)**	**0.002**
High	**30 (39.5%)**	**1 (5.0%)**	
Cytolytic activity			
Low	52 (68.4%)	15 (75.0%)	0.391
High	24 (31.6%)	5 (25.0%)	

3.3.1.7 The molecular and clinicopathological features of BTPC

In order to further delineate the transcriptomic differences between BTPC and PDAC of the head, a gene set enrichment analysis using gene ontology (GO) terms was performed.

This analysis reflects the transcriptomic differences in cellular pathways based upon differential gene expression between the two groups. This analysis demonstrated that, relative to tumours of the body and tail, head PDAC is enriched for a number of immune gene pathways including complement activation, humoral and adaptive immune response, B cell and lymphocyte mediated immunity (Figure 3-15). In contrast, BTPC is enriched for gene programs involved in squamous differentiation and inflammation (e.g. Cornification, Keratinocyte differentiation, Epidermal development and differentiation, Interleukin-6 production) (Figure 3-15). This further highlights the relative gene expression associated with an immunosuppressive and inflammatory environment of BTPC, whilst being enriched for the squamous subtype of PDAC (Figure 3-15).

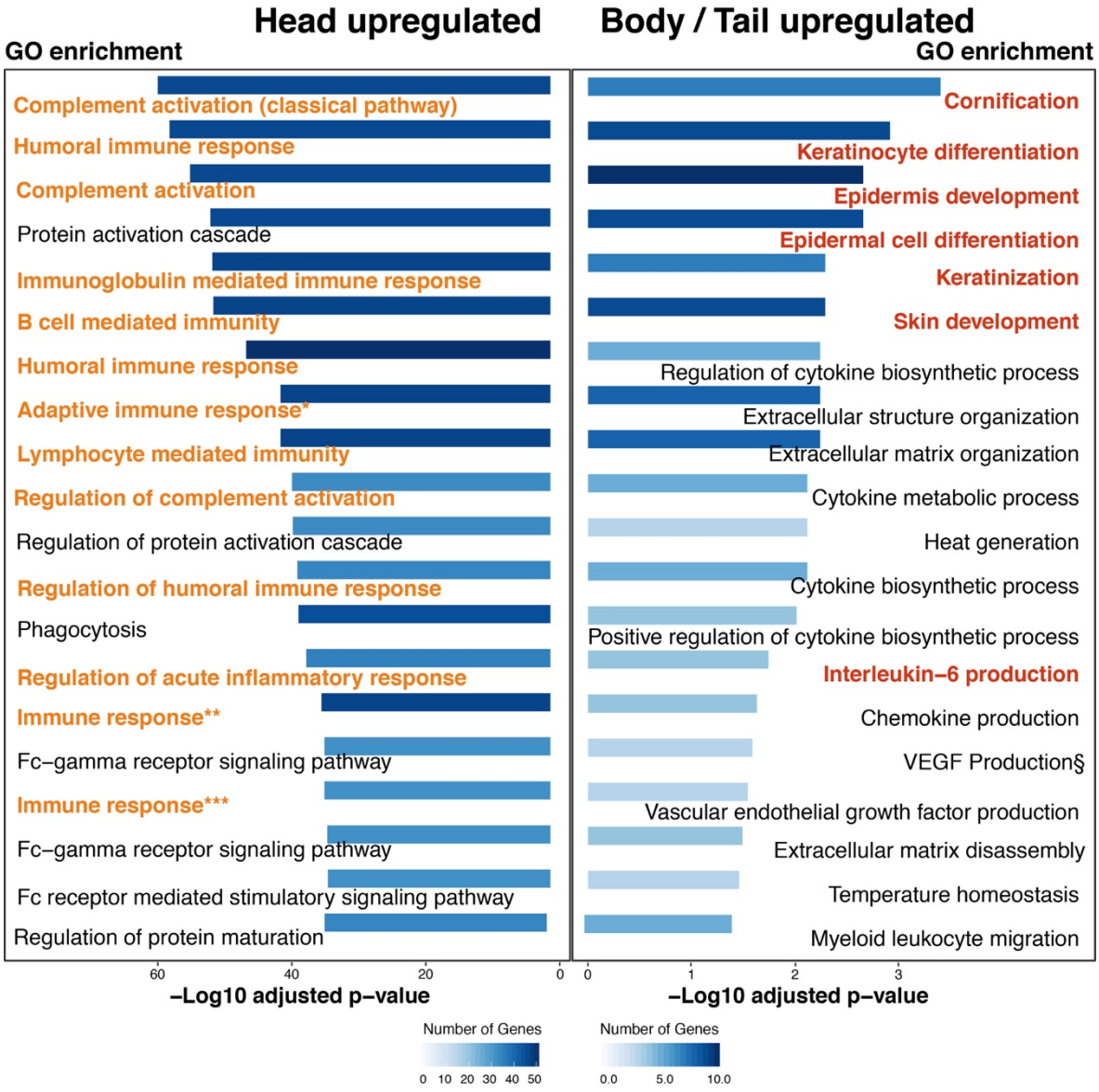

Figure 3-15 Gene ontology enrichment analysis of PDAC of the head and body / tail. BTPC is associated with a pro-inflammatory and relatively immunosuppressive environment, whilst expressing genes associated with squamous differentiation in PDAC. Relative to BTPC, tumours of the head are enriched for anti-tumour immune responses (orange). In contrast, BTPC is enriched

for pathways involved in squamous differentiation and inflammation (red). (*Adaptive immune response based on somatic recombination of immune receptors built from immunoglobulin superfamily domains; ** Immune response – activating cell surface receptor signalling pathway; ***Immune response – regulating cell surface receptor signalling pathway involved in phagocytosis; § Regulation of VEGF Production)

At present, the temporal sequence of genomic and epigenetic events leading to the progression to different PDAC subtypes has yet to be fully revealed. Although yet to be proven, the squamous subtype appears to be more 'advanced' on the molecular clock in comparison to other subtypes, and this may reflect an additional level of genomic instability, due to the accumulation of DNA damage, and molecular events that contribute to the unique transcriptome of these tumours (Bailey et al., 2016). Previous studies have found that these tumours are associated with mutations in epigenetic regulators and enriched for hypermethylation and downregulation of genes involved in pancreatic development (Bailey et al., 2016, Moffitt et al., 2015, Collisson et al., 2011). The results presented in this chapter suggest that BTPC is more likely to be of squamous subtype, suggesting that these are biologically more aggressive at time of diagnosis, or surgical resection, than cancer of the pancreatic head. Genes involved in inflammation, EMT and invasion are enriched in BTPC which are known molecular factors associated with poor prognosis. mRNA expression of the calcium binding protein S100A2, which accelerates tumour invasion, is higher in tumours located in BTPC, and is one of the most differentially expressed genes in GP2 (Figure 3-12). In chapter 4, the relationship between S100A2 expression and prognosis in PDAC is explored and is used to generate a novel molecular predictor of early recurrence in the form of a pre-operative molecular nomogram for operable PDAC.

It remains to be determined whether BTPC presents at a later stage of tumour evolution or whether these are biologically different and thus more likely to be squamous from the outset. However, some of our findings suggest that this may reflect the relative late presentation of BTPC and thus being more advanced, both clinically and molecularly (Figure 3-16). Firstly, tumours of the body and tail are larger in size which may reflect a biologically 'older' tumour. Secondly, BTPC correlates with molecular features that are driven by epigenetic events associated with chromosomal instability and epigenetic events that may drive intra-tumoural heterogeneity (Notta et al., 2016, Jamal-Hanjani et al., 2017). The exact sequence of these events in tumorigenesis and progression have yet to be elicited but may be associated with a later stage of the disease evolution. This requires large scale genomic and transcriptomic studies associated with high quality clinical data, which can be

investigated in parallel with international clinical trials such as *PRECISION-Panc* and *DIPLOMA* (Distal Pancreatectomy, Minimally invasive or open, for malignancy).

The relative immunosuppressive transcriptomic signalling seen in BTPC likely reflects the enrichment of squamous subtype in this cohort. Whether this is a true difference in the composition of the tumour microenvironment, particularly in relation to immune cell infiltrate, remains to be determined. Comparing gene programs and gene ontology with immune cell populations in bulk tumour will dissect the association between these signalling pathways and functional consequences of the TME. However, it is likely that the squamous subtype, and thus more likely BTPC, will be enriched for macrophage and neutrophil infiltration which in turn suppresses anti-tumour T cell responses. Further studies using immune cell immunohistochemistry and correlating with transcriptomic analysis is required to delineate this relationship.

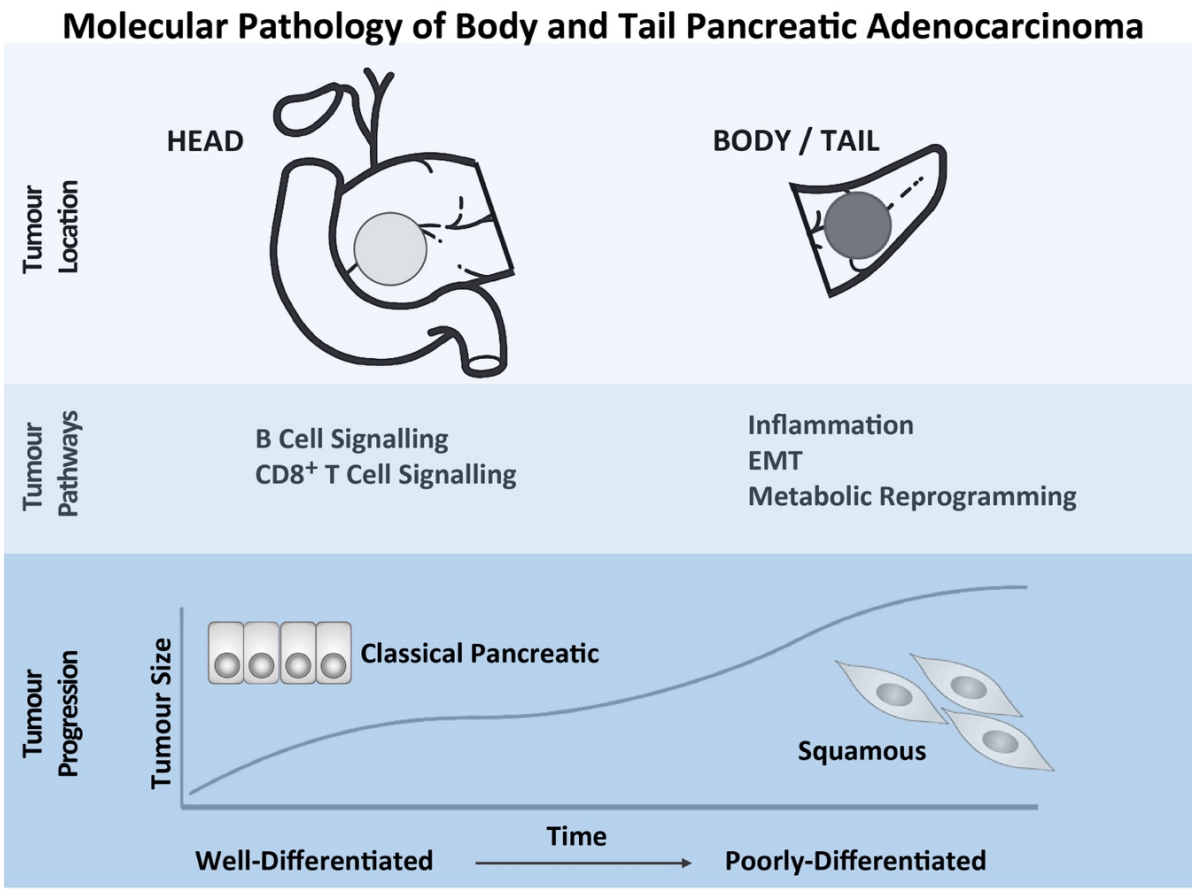

Figure 3-16 Graphical representation of the association between tumour location and differential transcriptional networks in the ICGC cohort. A potential theory of subtype evolution suggests that tumour size increases along the molecular clock, associated with dedifferentiation from pancreatic progenitor-like to squamous-like. This leads to EMT, inflammation and immunosuppression leading to a pro-metastatic phenotype.

3.4 Discussion

The data presented in this chapter suggests that the squamous subtype is associated with a pro-metastatic phenotype at time of presentation, and liver recurrence following pancreatectomy. Furthermore, PDAC of the body / tail is strongly associated with the squamous subtype and molecular features of aggressive disease. The underlying pathogenesis of these features are not yet elucidated but may be due to late presentation in comparison with PDAC of the head. Jaundice is a common presentation for head and uncinate process tumours, which can result in early presentation for these patients. BTPC, on the other hand, presents late with symptoms such as weight loss and pain that are features of poor outcomes. BTPC is found to be significantly larger than head PDAC, and this may reflect the late presentation of these tumours, if one considers tumour size to be related to time. This suggests that the 'older' a PDAC, the more likely it is to evolve into the squamous subtype. These data, however, was generated from a single cohort and larger scale studies are required to further address this and to fully understand the evolution from Classical Pancreatic to Squamous subtype.

The aggressive molecular features associated with BTPC results in poor clinical outcomes for these patients, even after attempted curative surgical resection. In the APGI cohort, patients with squamous subtype BTPC had extremely poor survival (median survival only 5.2 months in the RNAseq cohort, $P = 0.010$) in comparison with the rest of the resected cohort. This suggests that these patients may be better treated with a neoadjuvant approach to avoid futile surgery, as occult metastatic disease may manifest over this period. Due to the molecular features of aggressive disease associated to BTPC, one can also argue that, until molecular markers of early recurrence are better defined, all body and tail tumours are better served with a neoadjuvant approach to identify those patients that are likely to recur early. In order to better tailor surgical decision making for these patients, molecular selection strategies are urgently needed in PDAC. These are addressed in Chapter 4 of this PhD thesis.

This chapter reveals multiple novel findings in the relationship between molecular subtypes and clinicopathological features of PDAC. The squamous subtype is associated with histological features of aggressive disease, liver metastases and early recurrence following pancreatectomy. Furthermore, tumours located in the body and tail of the pancreas is associated with the squamous subtype and molecular characteristics that contribute to the worse outcomes seen in this patient group. The Classical Pancreatic

subtype, on the other hand, is associated with histological features that is known to predict better prognosis (e.g. IPMN cancers) and is subsequently associated with improved survival in this cohort. The association between lung metastases and classical pancreatic subtype reveals molecular process that may contribute to better outcomes in this patient group. These findings can potentially inform future biomarker and therapeutic development strategies to combat metastatic disease patterns in PDAC.

As we enter a molecular era, identifying patients that will benefit from potentially morbid procedures such as pancreatectomy is an important task for surgeons. Well-designed clinical trials, particularly in the operable and neoadjuvant setting, will allow detailed study of the temporal and spatial clonal evolution of PDAC, and may shed light on the relationship between disease progression along the molecular timeline of tumours. This will contribute to an expanding knowledge bank of molecular and clinical data, acquired from multiple initiatives globally, and will further delineate the relationship between tumour location, presentation stage and the molecular features of PDAC.

4 Predicting response to pancreatic resection: defining pro-metastatic and aggressive disease

4.1 Introduction

Whilst there is growing enthusiasm for using molecular selection markers to treat cancer with many systemic agents, only imaging is used to stage patients and assess suitability for operative resection. Similarly, either a surgery first, or neoadjuvant approach is often used without measures of individual tumour biology and risk of occult metastatic disease. This is exemplified in PDAC: surgical resection offers the only chance of cure, with chemotherapy adding modest benefit, but has significant morbidity and mortality risk. Even with complete resection and adjuvant chemotherapy, the five-year survival rate is ~20% (Neoptolemos et al., 2010, Regine et al., 2008, Oettle et al., 2007, Dreyer et al., 2017, Neoptolemos et al., 2017), with most failing due to metastatic disease and ~30% succumbing within one-year (Barugola et al., 2007, Iacobuzio-Donahue et al., 2009). This high metastatic failure rate indicates that current staging systems for PDAC are unable to effectively identify patients with occult metastases and aggressive disease, for whom resection brings potential morbidity and is of uncertain benefit. Hence, better selection methods are urgently needed.

Prognosis prediction tools such as nomograms have been developed for many cancer types to better inform treatment decisions. The most widely used tool in resectable PDAC is the prognostic nomogram developed at the Memorial Sloan-Kettering Cancer Centre (MSKCC) (Brennan et al., 2004)·(de Castro et al., 2009, White et al., 2006, Ferrone et al., 2005). However, these prognostic nomograms can only be applied after resection as they include clinicopathological variables that only become available after assessment of the resected specimen. Pancreatectomy is associated with mortality risk and significant morbidity that often leads to long recovery periods of 3-6 months after surgery with major implications on quality of life, often in the context of a short life expectancy (Heerkens et al., 2018, Schniewind et al., 2006).

Numerous molecular biomarkers with potential clinical utility have been studied in PDAC, but few have been independently validated (Garcea et al., 2005, Jamieson et al., 2011, Ansari et al., 2011). Aberrant expression of S100A2 and S100A4 calcium-binding proteins, both of which function to accentuate tumour aggressiveness and metastasis, are independently associated with poor survival in PDAC (Ai et al., 2008, Huang et al., 2016,

Biankin et al., 2009). Significant hypomethylation of S100A2 (with increased expression) was identified in the poor prognostic squamous subtype of PDAC (Bailey et al., 2016). This correlates with similar studies by Collison *et al.* and Moffitt *et al.*, both of which found S100A2 to be highly expressed in the poor prognostic Quasi-Mesenchymal and Basal subtypes respectively (Collisson et al., 2011, Moffitt et al., 2015). These poor prognostic subtypes overlap extensively, yet the genes used to define each vary between Bailey (n = 707), Collison (n = 62) and Moffitt (n = 50) classifiers. Only 8 genes overlap in all three classifiers, of which *S100A2* remains a strong predictor of the squamous subtype. The fact that *S100A2* remains significantly enriched within all 3 subtypes, even when using a small number of genes, suggests that its association with a poor prognostic subtype is biologically relevant.

In this chapter, the prognostic value of these two biologically relevant molecules as molecular prognostic biomarkers is investigated in 1184 patients from 3 independent patient cohorts. The aberrant expression of these biomarkers and prognosis in patients with resectable pancreatic cancer was investigated in a training set (n = 518) and form the basis of a biomarker-based pre-operative nomogram aimed at identifying those at high risk of early recurrence. This nomogram was validated in two further cohorts (n = 198 and 468), and the feasibility of its preoperative use was tested as proof-of-concept using pre-operative endoscopic ultrasound guided fine-needle aspiration biopsies (EUS-FNA).

4.2 Results

4.2.1 Patient cohorts

Three independent cohorts were used to investigate the association between S100A2 and S100A4 expression, and prognosis after pancreatectomy for PDAC. These consisted of primary resected PDAC and were called the APGI (n = 518), Glasgow (n = 198) and German (n = 468) cohorts totalling n = 1184 patients, making this one of the largest biomarker studies performed in PDAC to date. Patient characteristics for all three cohorts are summarized in Table 4-1.

The APGI cohort consisted of 518 patients, most of whom were treated after 1998 with modalities including adjuvant chemotherapy. There were 260 women and 258 men. The median age at diagnosis was 68 years and ranged from 28 to 88 years. The median follow-up for surviving patients was 47 months (range, 18 to 164 months). Eighty-nine patients (17.2%) were alive at the census date. Three hundred and ninety-four patients (76.1%) died from pancreatic cancer, thirty-one patients (6%) died of other causes, and three patients (0.6%) died of unknown causes. One patient (0.1%) was lost to follow-up. The median disease-specific survival was 17.9 months, with 3- and 5-year survival rates of 29% and 17% respectively. The majority of tumours were moderately differentiated (Grade II) (66%), followed by poor differentiation (Grade III) (25%), and only 8% of tumours were well differentiated (Grade I). Most tumours were located in the head of the pancreas (82.2%) and were more than 20 mm in maximal diameter (80.5%). Three hundred and thirty-eight out of 518 patients (65.3%) had resections with clear surgical margins using the R0 = 0 mm definition. Lymph node metastases were present in three hundred and forty-seven (67.2%) patients, perineural invasion was present in three hundred and ninety-three patients (77.5%), and vascular space invasion was present in two hundred and sixty-five patients (53.1%) (Table 4-1).

Factors associated with a significantly better survival included T1 and T2 tumours (median survival 34.4 vs 24.3 vs 18.3 months; P = 0.006) compared to T3 tumours, well or moderately differentiated tumours (median survival 21.2 vs 17.0 months; P = 0.036), absence of lymph node metastases (22.4 Vs 18.7 months; P = 0.009), absence of surgical margin involvement (23.7 Vs 15.4 months; P < 0.001), tumours of the pancreatic head (median survival 22.0 Vs 12.1 months; P < 0.001) compared with those of the body/tail, absence of vascular space invasion (23.0 Vs 17.0 months; P < 0.001), and absence of

perineural invasion(median survival 26.0 vs 18.3 months; *P = 0.016*). Univariate survival analysis and hazard ratios for the APGI cohort are presented in Table 4-2.

The Glasgow cohort consisted of 198 patients, which included 93 women and 105 men. The mean age at diagnosis was 63 years and range from 37 to 86 years. The median follow-up for surviving patients was 48 months (range, 35 to 84 months). Nine patients (4.5%) were alive at the census date. One hundred and seventy patients (85.9%) died from pancreatic cancer, nineteen patients (9.6%) died of other causes, and no patients were lost to follow-up. The median disease-specific survival was 17.0 months, with 3- and 5-year survival rates of 22% and 10% respectively. The majority of tumours were moderately differentiated (Grade II) (62%), followed by poor differentiation (Grade III) (32%), and only 6% of tumours were well differentiated (Grade I). All tumours were located in the head of the pancreas and most were more than 20 mm in maximal diameter (84.8%). 52 out of 198 patients (26.3%) had resections with clear surgical margins using the R0 = 1 mm definition. Lymph node metastases were present in one hundred and sixty-two (81.8%) patients, perineural invasion was present in one hundred and eighty-four patients (92.9%), and vascular space invasion was present in ninety-eight patients (49.5%) (Table 4-1).

Factors associated with a significantly better survival included female sex (median survival 20.4 vs 17.0 months, P = 0.036), well and moderately differentiated tumours (median survival 20.9 vs 13.4 months, P = 0.016), T1 and T2 tumours (median survival 33.5 Vs 17.8 months; P = 0.038) compared to T3 tumours, absence of lymph node metastases (31.0 Vs 18.8 months; P = 0.001), absence of surgical margin involvement (26.6 Vs 16.8 months; P = 0.002), and absence of vascular space invasion (23.1 Vs 16.3 months; P = 0.006). Univariate survival analysis and hazard ratios for the Glasgow cohort are presented in Table 4-3.

The German cohort consisted of 468 patients that were treated at three units (Universities of Dresden, Regensburg and Jena), which included 213 women and 255 men. The mean age at diagnosis was 64 years and range from 31 to 84 years. The median follow-up for surviving patients was 31.9 months (range, 0 to 137 months). Eighty-eight patients (18.8%) were alive at the census date. Accurate disease specific survival was not available for this cohort and since the majority of patients with PDAC succumb to the disease, overall survival was used for analysis. The median overall survival was 15.7 months, with 3- and 5-year survival rates of 25% and 11% respectively. The majority of tumours were poorly differentiated (Grade III) (51%), followed by moderate differentiation (Grade II) (44%),

and only 4% of tumours were well differentiated (Grade I). Three hundred and seventy-two tumours (91.2%) were located in the head of the pancreas and for those with accurate size documented, most were more than 20 mm in maximal diameter (83.4%). 340 out of 486 patients (74.7%) had documented resections with clear surgical margins using the R0 = 0 mm definition. Lymph node metastases were present in three hundred and eighteen (68.5%) patients, perineural invasion was documented positive in one hundred and eighty-five patients (58.0%), and vascular space invasion was present in sixty-eight patients (26.7%) (Table 4-1).

Factors associated with a significantly better survival included well to moderately differentiated tumours (median survival 21.1 vs 13.8 months; $P < 0.001$), absence of lymph node metastases (median survival 22.9 vs 15.4 months; $P = 0.008$), absence of surgical margin involvement (median survival 18.4 vs 12.9 months; $P = 0.002$) and absence of vascular space invasion (median survival 20.0 vs 14.6 months; $P = 0.016$). Univariate survival analysis and hazard ratios for the German cohort are presented in Table 4-4.

Table 4-1 Patient characteristics for APGI, Glasgow and German cohorts. *P* calculated using log rank test

	APGI Cohort *(Training Set)*			**Glasgow Cohort** *(Validation Set 1)*			**German Cohort** *(Validation Set 2)*		
Variables	**n = 518 No. (%)**	**DSS**	***P***	**n = 198 No. (%)**	**DSS**	***P***	**n = 468 No. (%)**	**DSS**	***P***
Sex									
Male	258 (49.8)	18.7		105 (53.0)	17.8		255 (54.5)	17.4	
Female	260 (50.2)	21.0	0.573	93 (47.0)	20.4	0.547	213 (45.5)	15.2	0.455
Age (years)									
Mean	66.7			62.5			64.2		
Median	68.0			63.9			66.0		
Range	28.0 – 88.0			37.4 – 86.0			31.0 – 84.0		
Outcome									
Follow-up (months)	18.0–163.8			35.0 – 84.0			0.0 – 137.8		
Median follow-up (months)	47.0			48.0			31.9		
Death PC	394 (76.1)			170 (85.9)					
Death other	31 (6.0)			19 (9.6)					
Death Unknown	3 (0.6)			0 (0.0)			380 (81.2)		
Alive	89 (17.2)			9 (4.5)			88 (18.8)		
Lost to FU	1 (0.1)			0 (0.0)					
Stage AJCC 7th									
I	32 (6.2)	51.9		1 (0.5)	----		25 (5.4)	26.0	
II	474 (91.5)	18.8		193 (97.5)	19.1		408 (87.3)	16.8	
III	2 (0.4)	20.0		4 (2.0)	11.3		8 (1.7)	6.8	
IV	10 (1.9)	6.0	<0.001	0 (0.0)	----	0.249	26 (5.6)	10.8	0.001
T Stage AJCC 7th									
T1	21 (4.1)	34.4		2(1.0)	11.1		11 (2.4)	24.8	
T2	48 (9.3)	24.3		14 (7.1)	33.5		60 (12.8)	18.2	
T3	447 (86.3)	18.3	0.033	178 (89.9)	18.0		385 (82.4)	16.4	
T4	2 (0.4)	20.0		4 (2.0)	11.3	0.119	11 (2.4)	6.8	0.010
N Stage AJCC 7th									
N0	169 (32.8)	22.4		36 (18.2)	31.0		146 (31.5)	22.9	
N1	347 (67.2)	18.7	0.008	162 (81.8)	18.5	0.001	318 (68.5)	15.4	0.008
Grade / Differentiation									
I / Well	41 (7.9)	35.4		12 (6.1)	23.2		18 (4.0)	24.7	
II / Moderate	340 (65.9)	21.0		122 (61.6)	20.4		196 (43.9)	20.9	
III / Poor	130 (25.2)	17.0	0.039	64 (32.3)	13.4	0.039	229 (51.2)	13.7	
IV / Undifferentiated	5 (1.0)	13.0					4 (0.9)	34.4	<0.001
Tumour size									
≤ 20mm	100 (19.5)	34.4		30 (15.2)	28.1		34 (16.6)	18.4	
> 20mm	414 (80.5)	17.0	<0.001	168 (84.8)	18.4	0.052	171 (83.4)	17.1	0.621
Margins									
Clear	338 (65.3)	23.7		52 (26.3)	26.6		340 (74.7)	18.4	
Involved	180 (34.7)	15.4	<0.0001	146 (73.7)	16.8	0.002	115 (25.3)	12.9	0.002
Tumour Location									
Head	426 (82.2)	22.0		198 (100.0)	19.1		372 (91.2)	18.2	
Others	92 (17.8)	12.1	0.001	0 (0.0)	----	----	36 (8.8)	16.9	0.414
Perineural Invasion									
Negative	114 (22.5)	26.0		14 (7.1)	18.2		134 (42.0)	19.2	
Positive	393 (77.5)	18.3	0.015	184 (92.9)	19.5	0.505	185 (58.0)	16.5	0.144
Vascular Invasion									
Negative	234 (46.9)	23.0		100 (50.5)	23.1		187 (73.3)	20.0	
Positive	265 (53.1)	17.0	< 0.001	98 (49.5)	16.3	0.006	68 (26.7)	14.6	0.016
S100A2 Expression									
Low	392 (77.3)	21.0		135 (68.2)	24.7		282 (70.5)	18.2	
High	115 (22.7)	15.0	0.023	63 (31.8)	13.0	<0.001	118 (29.5)	11.9	<0.001
S100A4 Expression									
Negative	169 (32.9)	29.9		61 (30.8)	26.4		142 (33.0)	22.0	
Positive	345 (67.1)	16.2	< 0.001	137 (69.2)	16.2	0.011	288 (72.0)	14.6	0.013

Adjuvant Chemotherapy									
≥ 3 cycles	206 (39.8)	27.1	<0.001	85 (42.9)	21.8	0.142	153 (32.7)	20.6	0.015
< 3 cycles	310 (59.8)	15.1		113 (57.1)	14.8		315 (67.3)	15.1	

Table 4-2 Univariate survival analysis for APGI cohort

Variable	Hazard Ratio (95% CI)	*P* Value
Differentiation (reference: Well / Moderate)		
Poor / Undifferentiated	1.27 (1.01 – 1.59)	0.041
Size (> 30mm)	1.45 (1.19 – 1.77)	<0.001
pT Stage T3 or T4 (reference: T1 or T2)	1.54 (1.13 – 2.10)	0.006
Age (> 65)	1.28 (1.04 – 1.56)	0.017
Lymph nodes positive	1.34 (1.08 – 1.66)	0.009
Resection margin involved	1.69 (1.37 – 2.07)	< 0.001
Location body / tail (reference: head)	1.53 (1.19 – 1.97)	0.001
Perineural invasion	1.35 (1.06 – 1.73)	0.016
Vascular invasion	1.45 (1.18 – 1.78)	<0.001
S100A2 positive	1.31 (1.04 – 1.65)	0.024
S100A4 positive	1.62 (1.30 – 2.02)	<0.001

Table 4-3 Univariate survival analysis for Glasgow cohort. Included head tumours only

Variable	Hazard Ratio (95% CI)	*P* Value
Differentiation (reference: Well / Moderate)		
Poor / Undifferentiated	1.47 (1.07 – 2.02)	0.017
Size (> 30mm)	1.38 (1.88 – 2.57)	<0.001
pT Stage T3 or T4 (reference: T1 or T2)	1.77 (1.02 – 3.07)	0.041
Age (> 65)	0.76 (0.56 – 1.03)	0.079
Lymph nodes positive	2.05 (1.34 – 3.13)	0.001
Resection margin involved	1.77 (1.24 – 2.54)	0.002
Perineural invasion	1.27 (0.64 – 2.49)	0.494
Vascular invasion	1.55 (1.14 – 2.10)	0.005
S100A2 positive	2.14 (1.56 – 2.96)	<0.001
S100A4 positive	1.54 (1.11 – 2.14)	0.009

Table 4-4 Univariate survival analysis for German cohort

Variable	Hazard Ratio (95% CI)	*P* Value
Differentiation (reference: Well / Moderate)		
Poor / Undifferentiated	1.57 (1.27 – 1.93)	<0.001
Size (> 30mm)	0.94 (0.68 – 1.29)	0.697
pT Stage T3 or T4 (reference: T1 or T2)	1.00 (0.76 – 1.33)	0.994
Age (> 65)	1.11 (0.87 – 1.41)	0.413
Lymph nodes positive	1.35 (1.08 – 1.69)	0.008
Resection margin involved	1.44 (1.14 – 1.80)	0.003
Location body / tail (reference: head)	1.17 (0.80 – 1.70)	0.415
Perineural invasion	1.20 (0.94 – 1.54)	0.145
Vascular invasion	1.45 (1.07 – 1.96)	0.017
S100A2 positive	1.69 (1.34 – 2.14)	<0.001
S100A4 positive	1.33 (1.06 – 1.67)	0.013

4.2.2 Elevated S100A2 Expression is associated with Poor Survival after Pancreatectomy

In all three cohorts, high expression of S100A2 calcium-binding protein was associated with poor survival after pancreatectomy. In the APGI cohort, expression of S100A2 was high in 115 of 507 patients (22.7%) (median survival 21.0 Vs 15.0 months; $P = 0.023$) (Figure 4-1). S100A2 expression was high in 63 out of 198 patients (31.8%) in the Glasgow cohort (median survival 24.7 vs 13 months; $P < 0.001$) and in 118 out of 400 patients (29.5%) in the German cohort (median survival 18.2 vs 11.9 months; $P < 0.001$) (Figure 4-1).

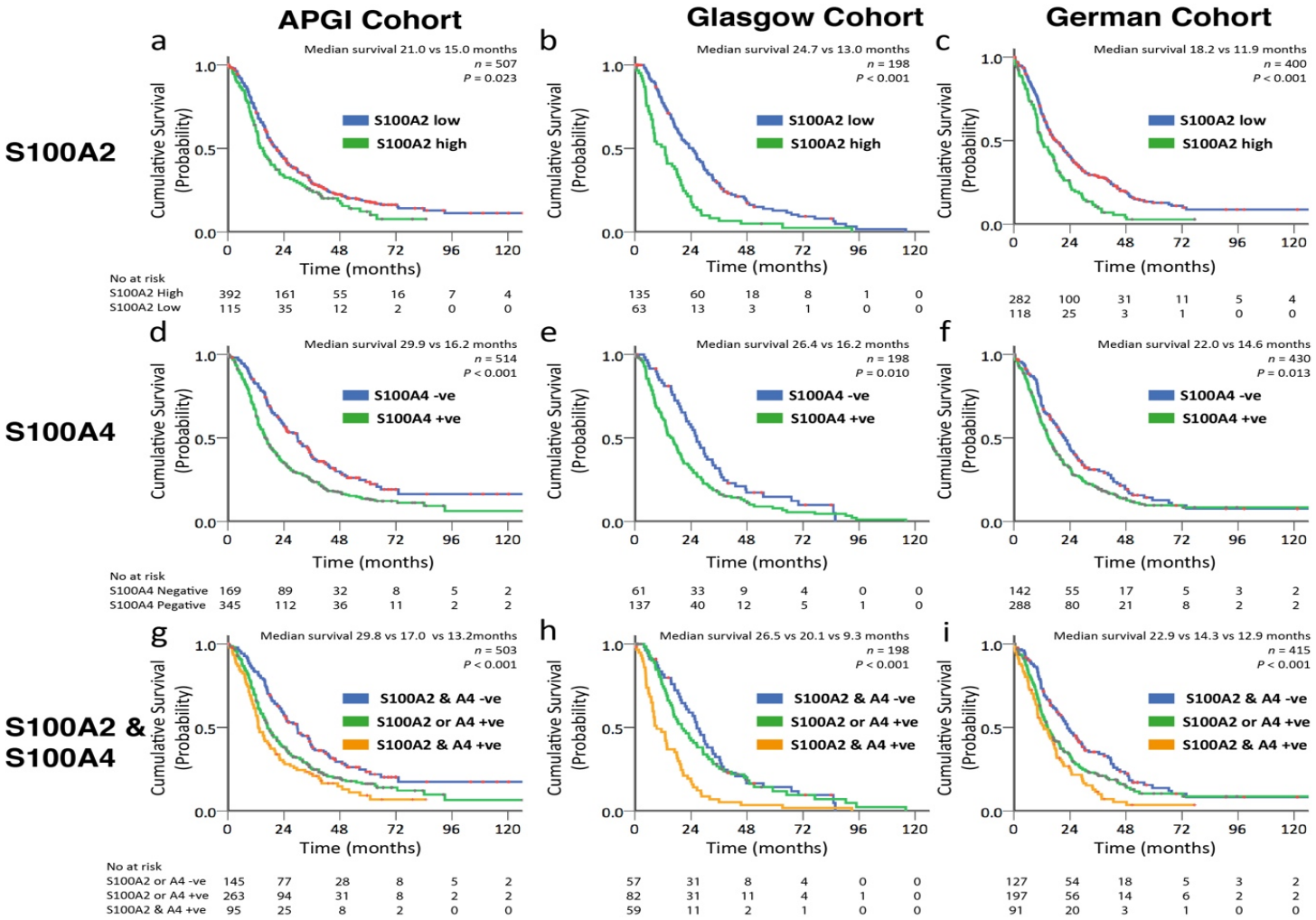

Figure 4-1 Kaplan-Meier survival curves for biomarker expression in all 3 cohorts. S100A2 expression is prognostic after surgery in the (a) APGI, (b) Glasgow, (c) German cohorts; S100A4 expression is prognostic in the (d) APGI, (e) Glasgow, (f) German Cohorts; S100A2 and S100A4 expression stratifies patient survival into 3 distinct prognostic groups (g) APGI cohort, (h) Glasgow and (i) German cohort.

High S100A2 expression remained a significant independent prognostic factor in a combined multivariate model of all 3 cohorts (Table 4-5; HR = 1.64, 95% CI 1.33 – 2.02 $P < 0.001$). This was also the case in the APGI (Table 4-6; HR 1.32, 95% CI 0.97 – 1.80, $P < 0.001$) and Glasgow (Table 4-7; HR 2.00, 95% CI 1.36 – 2.90, $P < 0.001$) cohorts, but not the German (Table 4-8; HR 1.48, 95% CI 0.95 – 2.29, $P = 0.076$) cohort. It is likely that this reflects reduced power or cohort-specific variable collinearities, as the influence of S100A2 expression on survival was not significantly different between cohorts (Likelihood ratio test, $\chi^2 = 4.86$, df = 2, $P = 0.09$). Furthermore, S100A2 was associated with poor survival in the German cohort (univariate cox regression (HR 1.69, 95% CI 1.34 – 2.14, $P < 0.001$) and log rank survival analysis (Table 4-4, Figure 4-1).

Table 4-5 Multivariate model for all cohorts combined. Baseline hazard stratified by cohort

Variable	Coefficient	Hazard Ratio (95% CI)	*P* Value
Differentiation (reference value: Well)			0.046
Moderate	0.057	1.06 (0.68 – 1.66)	
Poor / Undifferentiated	0.200	1.26 (0.76 – 1.96)	
Size along longest axis (cm, relative to 3.0cm)	0.127	1.14 (1.06 – 1.22)	< 0.001
pT Stage T3 or T4 (reference value: T1 or T2)	0.441	1.55 (1.13 – 2.14)	0.003
Age (decades, relative to 65)	0.210	1.23 (1.07 – 1.43)	0.271
Lymph nodes positive	0.024	1.02 (0.82 – 1.28)	0.127
Resection margin involved	0.512	1.67 (1.36 – 2.04)	< 0.001
Location tail (reference: head)	0.110	1.12 (0.79 – 1.57)	0.254
Perineural invasion	0.290	1.34 (1.03 – 1.73)	0.009
Vascular invasion	0.166	1.18 (0.97 – 1.43)	0.062
S100A2 positive	0.494	1.64 (1.33 – 2.02)	< 0.001
S100A4 positive			< 0.001
0 – 6 months post resection	0.707	2.03 (1.08 – 3.80)	
6 – 12 months post resection	0.724	2.06 (1.30 – 3.28)	
12 – 24 months post resection	0.520	1.68 (1.19 – 2.38)	
Over 24 months post resection	– 0.122	0.88 (0.63 – 1.25)	
Age:Cohort interaction (reference: APGI)			< 0.001
Glasgow	0.647	0.65 (0.52 – 0.81)	
German	0.945	1.06 (0.70 – 1.28)	

Table 4-6 Multivariate models for APGI cohort

Variable	Coefficient	Hazard Ratio (95% CI)	*P* Value
Differentiation (reference value: Well)			0.411
Moderate	0.287	1.33 (0.69 – 2.59)	
Poor / Undifferentiated	0.331	1.39 (0.68 – 2.83)	
Size along longest axis (cm, relative to 3.0cm)	0.050	1.05 (0.96 – 1.15)	0.013
pT Stage T3 or T4 (reference value: T1 or T2)	0.414	1.51 (0.99 – 2.30)	0.025
Age (decades, relative to 65)	0.212	1.24 (1.06 – 1.44)	0.003
Lymph nodes positive	– 0.143	0.87 (0.63 – 1.20)	0.965
Resection margin involved	0.548	1.73 (1.29 – 2.32)	< 0.001
Location tail (reference value: head)	0.279	1.32 (0.91 – 1.92)	0.052
Perineural invasion	0.081	1.08 (0.79 – 1.50)	0.210
Vascular invasion	0.248	1.28 (0.95 – 1.73)	0.049
S100A2 positive	0.275	1.32 (0.97 – 1.80)	0.017
S100A4 positive			0.018
0 – 6 months post resection	0.798	2.22 (0.84 – 5.86)	
6 – 12 months post resection	0.754	2.13 (1.08 – 4.17)	
12 – 24 months post resection	0.510	1.67 (1.00 – 2.76)	
Over 24 months post resection	0.051	1.05 (0.62 – 1.77)	

Table 4-7 Multivariate models for Glasgow cohort

Variable	Coefficient	Hazard Ratio (95% CI)	*P* Value
Differentiation (reference value: Well)			0.053
Moderate	– 0.241	0.79 (0.42 – 1.46)	
Poor / Undifferentiated	– 0.002	1.00 (0.52 – 1.93)	
Size along longest axis (cm, relative to 3.0cm)	0.366	1.44 (1.23 – 1.69)	< 0.001
pT Stage T3 or T4 (reference value: T1 or T2)	0.489	1.63 (0.93 – 2.85)	0.065
Age (decades, relative to 65)	– 0.246	1.78 (0.66 – 0.93)	0.007
Lymph nodes positive	0.164	1.18 (0.74 – 1.87)	0.020
Resection margin involved	0.560	1.80 (1.22 – 2.66)	0.022
Location head (reference value: tail)	ND*	ND*	ND*
Perineural invasion	– 0.108	0.90 (0.44 – 1.84)	0.541
Vascular invasion	0.189	1.21 (0.85 – 1.71)	0.132
S100A2 positive	0.688	2.00 (1.36 – 2.90)	< 0.001
S100A4 positive			0.048
0 – 6 months post resection	0.774	2.17 (0.74 – 6.39)	
6 – 12 months post resection	0.862	2.37 (0.97 – 5.79)	
12 – 24 months post resection	0.552	1.74 (0.94 – 3.22)	
Over 24 months post resection	– 0.152	0.86 (0.45 – 1.48)	

Table 4-8 Multivariate models for German cohort

Variable	Coefficient	Hazard Ratio (95% CI)	*P* Value
Differentiation (reference value: Well)			0.099
Moderate	0.339	1.40 (0.42 – 4.73)	
Poor / Undifferentiated	0.452	1.57 (0.47 – 5.30)	
Size along longest axis (cm, relative to 3.0cm)	0.128	1.14 (0.93 – 1.39)	0.075
pT Stage T3 or T4 (reference value: T1 or T2)	– 0.208	0.81 (0.34 – 1.96)	0.973
Age (decades, relative to 65)	0.223	1.25 (1.00 – 1.56)	0.041
Lymph nodes positive	0.162	1.18 (0.76 – 1.82)	0.579
Resection margin involved	0.474	1.61 (1.08 – 2.39)	0.077
Location head (reference value: tail)	– 0.051	0.95 (0.41 – 2.25)	0.963
Perineural invasion	0.443	1.56 (1.05 – 2.30)	0.021
Vascular invasion	ND*	ND*	ND*
S100A2 positive	0.391	1.48 (0.95 – 2.29)	0.076
S100A4 positive			0.340
0 – 6 months post resection	0.904	2.47 (0.71 – 8.61)	
6 – 12 months post resection	0.262	1.30 (0.62 – 2.71)	
12 – 24 months post resection	0.091	1.10 (0.58 – 2.07)	
Over 24 months post resection	– 0.440	0.64 (0.31 – 1.32)	

4.2.3 Positive S100A4 Expression is associated with Poor Survival after Pancreatectomy

Positive expression of S100A4 was associated with poor survival after pancreatectomy in all three cohorts. In the APGI cohort, 345 out of 514 patients (67.1%) with analysable tissue had positive expression of S100A4 and had a significantly worse outcome (median survival 29.9 Vs 16.2 months; $P < 0.001$) (Figure 4-1). These findings were recapitulated in the Glasgow cohort with 137 out of 198 patients (69.2%) with analysable tissue demonstrating positive expression of S100A4, that was again associated with poor outcome (median survival 26.4 Vs 16.2 months; $P = 0.010$) (Figure 4-1). In the German cohort, 288 out of 430 patients (72.0%) with positive S100A4 expression demonstrated significantly worse outcome (median survival 22.0 vs 14.6 months, $P = 0.013$) (Figure 4-1).

In a combined multivariate model, S100A4 remained strongly prognostic in a time dependent manner with its effect on prognosis decreasing after 24 months in both the combined (HR 2.06, 95% CI 1.30 – 3.28, $P < 0.001$ at 12 months), and individual models (Table 4-5, Table 4-6, Table 4-7, Table 4-8). This data suggests that S100A4 is a strong predictor of disease recurrence in the first 24 months after surgery, with its effect decreasing after this period. S100A4 was an independent prognostic factor in multivariate models in the APGI (Table 4-6, HR 2.13, 95% CI 1.08 – 4.17, $P = 0.018$ at 12 months) and Glasgow (Table 4-7, HR 2.37, 95% CI 0.97 – 5.79, $P = 0.048$ at 12 months) cohorts. Similar to S100A2, S100A4 was not significant in a multivariate model in the German

cohort (Table 4-8), however, was predictive in univariate cox regression (HR 1.33, 95% CI 1.06 – 1.67, $P = 0.013$) and log rank survival analysis (Table 4-4, Figure 4-1).

4.2.4 Expression of S100A2 and S100A4 Stratifies Patients into 3 Prognostic Groups

The combined prognostic effects of the two biomarkers were assessed independently in all three cohorts (Figure 4-2). This defined three distinct prognostic groups (Figure 4-1, Figure 4-3, Table 4-1)

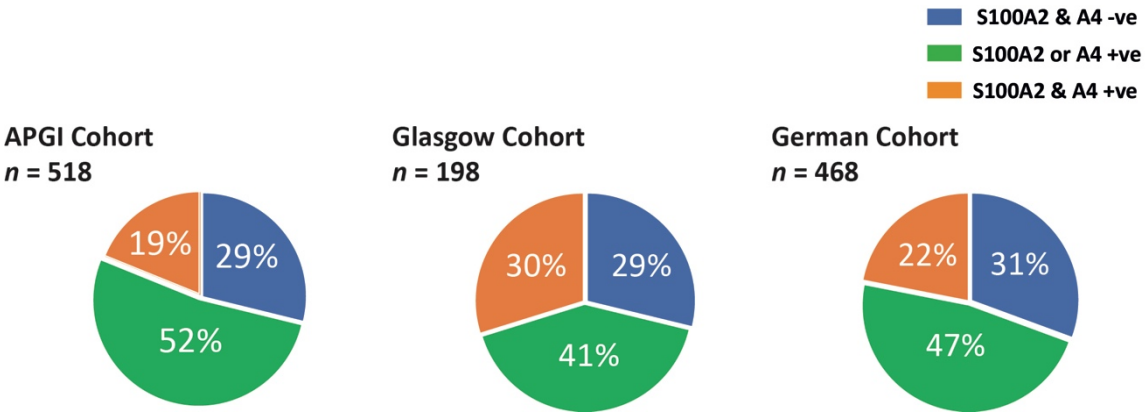

Figure 4-2 Biomarker expression profile in APGI, Glasgow and German cohorts

Patients with low or no expression of either S100A2 or S100A4 had the best prognosis, followed by patients with either high S100A2 or positive S100A4 expression (Figure 4-3). In the APGI cohort, patients with both biomarkers positive had the worst prognosis (median survival 29.8 vs 17.0 vs 13.2 months respectively, $P < 0.001$) (Figure 4-1). These findings were validated in the Glasgow (median survival 26.5 vs 20.1 vs 9.3 months; $P < 0.001$) and the German (median survival 22.9 vs 14.3 vs 12.9 months; $P < 0.001$) cohorts (Figure 4-1). When combining all 3 cohorts, patients with both biomarkers positive had a 12-month survival rate of only 54% after pancreatectomy, compared to 79% and 66% respectively in the biomarker negative or single biomarker positive groups (Figure 4-3).

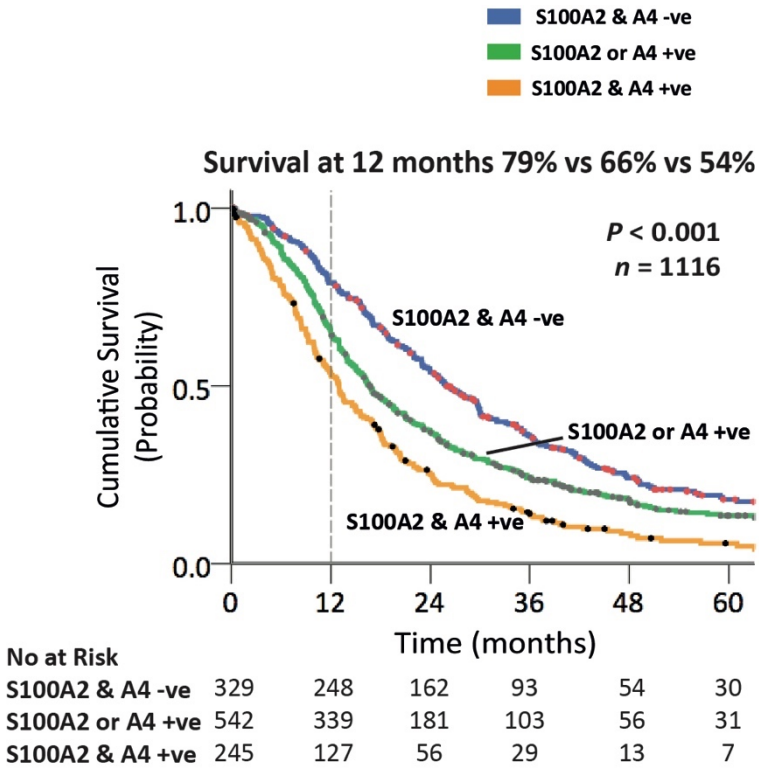

Figure 4-3 Kaplan-Meier survival curves for all 3 cohorts combined, stratified by biomarker expression (both negative, one positive, both positive). Patients with both biomarkers positive had a survival rate of only 54%, 26% and 6% at 1, 2 and 5 years respectively. This was found to be 79%, 54% and 18% in the biomarker negative and 66%, 38% and 14% in the single biomarker positive groups respectively.

There was no difference in the use of adjuvant chemotherapy between patients who were biomarker negative and those with a single biomarker positive in all three cohorts. In the APGI cohort, patients with both biomarkers positive had lower adjuvant therapy use rate ($P = 0.025$). There were no significant differences in adjuvant therapy use amongst biomarker groups in the Glasgow and German cohorts. The reduced adjuvant therapy use in the APGI cohort for patients with both biomarkers positive may be due to an aggressive disease phenotype leading to more early recurrence and declining performance status and subsequently reduced adjuvant chemotherapy use.

Table 4-9 The association between S100A2 and S100A4 expression and adjuvant chemotherapy

	Adjuvant Chemotherapy	No Adjuvant Chemotherapy	*P*-value (logrank)
APGI Cohort			
S100A2 & A4 Negative	68 (46.9%)	77 (53.1%)	*P* = 0.025
S100A2 or A4 Positive	126 (47.9%)	137 (52.1%)	
Both Positive	60 (63.2%)	35 (36.8%)	
Glasgow Cohort			
S100A2 & A4 Negative	27 (47.4%)	30 (52.6%)	*P* = 0.065
S100A2 or A4 Positive	48 (58.5%)	34 (41.5%)	
Both Positive	38 (64.4%)	21 (35.6%)	
German Cohort			
S100A2 & A4 Negative	90 (70.9%)	37 (29.1%)	*P* = 0.851
S100A2 or A4 Positive	123 (62.4%)	74 (37.6%)	
Both Positive	67 (73.6%)	24 (26.4%)	

4.2.5 Expression of S100A2 and S100A4 co-segregates with the Squamous subtype of PC

In 96 patients that underwent RNA sequencing analysis as part of the APGI cohort, the squamous subtype was strongly associated with S100A2 ($P < 0.001$) and S100A4 ($P < 0.001$) mRNA expression (Figure 4-4, Table 4-10). This analysis was extended to include 235 patients that underwent micro-array mRNA analysis, as described by Bailey *et al.*(Bailey et al., 2016) Patients with high S100A2 ($P = 0.002$) and positive S100A4 ($P < 0.001$) expression were associated with the squamous subtype, with the strongest correlation seen in those with both biomarkers positive (Table 4-11). Later in this chapter a pre-operative nomogram that predicts recurrence following surgery is developed and tested. Consequently, tumours that were classified as squamous by Bailey *et al.* demonstrated a significantly higher mean nomogram score (associated with early recurrence) than other subtypes (140 vs 103; $P = 0.004$) (Table 4-11).

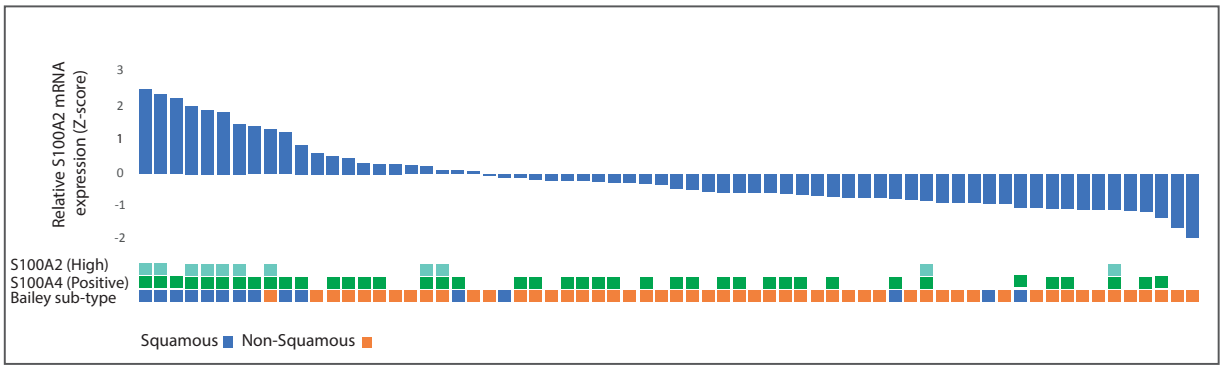

Figure 4-4 High S100A2 and positive S100A4 expression correlates with the squamous sub-type of PC. Patients are ranked according to S100A2 mRNA expression and the relative

expression *Z*-score is represented by a waterfall plot. High S100A2 and positive S100A4 IHC staining and Bailey sub-type is shown below.

Table 4-10 The association between Bailey sub-type and biomarker mRNA expression in APGI cohort [RNA sequencing] (*n* = 96)

	Non-Squamous	Squamous	*P*-value (logrank)
S100A2 mRNA expression			
Low	44 (62.0%)	4 (16.0%)	<0.001
High	27 (38.0%)	21 (84.0%)	
S100A4 mRNA expression			
Low	41 (57.7%)	7 (28.0%)	0.009
High	30 (42.3%)	18 (72.0%)	

Table 4-11 The association between Bailey sub-type, biomarker mRNA expression and biomarker immunohistochemistry in APGI cohort [micro-array analysis] (*n* = 235)

	Non-Squamous	Squamous	*P*-value (logrank)
mRNA Expression			
S100A2 Expression			
Low	123 (90.4%)	41 (71.9%)	0.002
High	13 (9.6%)	16 (28.1%)	
S100A4 Expression			
Negative	52 (38.2%)	7 (12.3%)	< 0.001
Positive	84 (61.8%)	50 (87.7%)	
Immunohistochemistry			
S100A2 & A4 Negative	49 (36.0%)	7 (12.3%)	
S100A2 or A4 Positive	77 (56.6%)	34 (59.6%)	< 0.001
Both Positive	10 (7.4%)	16 (28.1%)	
Pre-Operative Nomogram mean score (95% CI)	103	140	0.004

These results strongly suggest that S100A2 and S100A4 expression correlate with the squamous subtype of PDAC and provide a useful, cost-effective, method for detecting this pro-metastatic molecular subtype in clinical practice. To further investigate molecular features associated with early recurrence (< 12 months after surgery) a gene ontology (GO) enrichment analysis was performed comparing patients with early recurrence to the rest of the APGI cohort. GO enrichment analysis allows specific GO terms to be generated by associating differential gene expression across specific pathways to which they are functionally related (Balakrishnan et al., 2013). This allows an analysis of pathways that are differentially upregulated based upon mRNA expression (Balakrishnan et al., 2013) (Figure 4-5).

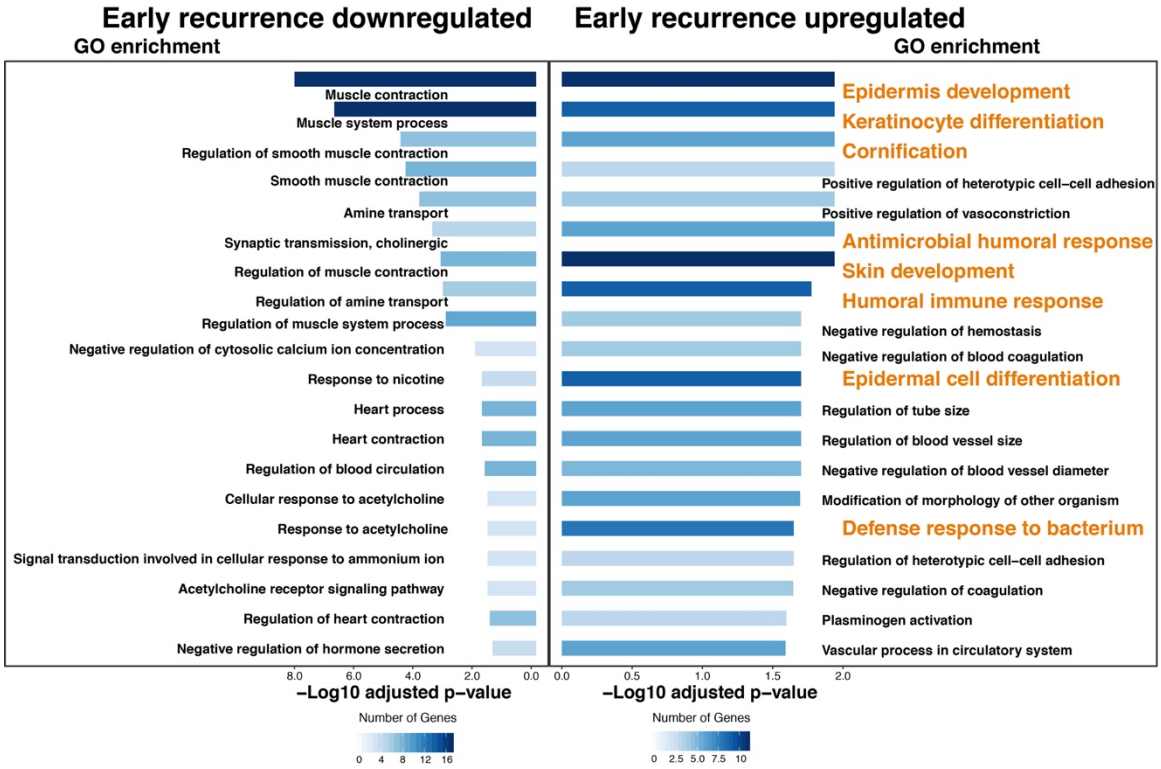

Figure 4-5 Gene ontology enrichment analysis in patients that developed early recurrence following pancreatectomy for PDAC

GO enrichment demonstrated that patients that developed early recurrence had significant enrichment of pathways associated with squamous differentiation of PDAC (*Epidermis development, Keratinocyte differentiation, Cornification, Skin development, Epidermal cell differentiation*). This correlates with and strengthens the results presented earlier, demonstrating a strong association between Squamous subtype, S100A2 and A4 expression and early recurrence after pancreatectomy for PDAC.

4.2.6 Expression of S100A2 and S100A4 is associated with body and tail PDAC

Following the findings presented in Chapter 3, an analysis of biomarker expression stratified by primary tumour location was performed. Body and tail PDAC was associated with high S100A2 ($P < 0.001$) and positive S100A4 ($P = 0.032$) expression (Table 4-12). Those with both biomarkers positive was roughly double in the body and tail group (33%) compared with the head tumours (15.9%) (Table 4-12). Subsequently, the body and tail group had a significantly higher mean nomogram score than those with head tumours (Table 4-12). This further complements the findings presented in Chapter 3 which demonstrates an association between increased tumour size and the squamous subtype (and

thus S100A2 / A4 expression) which contributes to a higher nomogram score, and subsequent poorer prognosis of body and tail PDAC.

Table 4-12 The association between tumour location and biomarker expression in APGI cohort

	Head	Body / Tail	*P*-value (logrank)
S100A2 Expression Low High	 338 (80.9%) 80 (19.1%)	 54 (60.7%) 35 (39.3%)	 < 0.001
S100A4 Expression Negative Positive	 147 (34.8%) 276 (65.2%)	 22 (24.2%) 69 (75.8%)	 0.032
S100A2 & A4 Negative S100A2 or A4 Positive Both Positive	130 (31.3%) 219 (52.8%) 66 (15.9%)	15 (17%) 44 (50%) 29 (33%)	 < 0.001
Pre-Operative Nomogram mean score (95% CI)	108.3	133.7	< 0.001

4.2.7 Prognostic Nomogram for Resectable PDAC

Up to 50% of unselected patients who undergo radical resection for PDAC will develop recurrent disease within a year of their operation. Predicting which patients are more likely to recur early would transform surgical approaches through avoiding primary surgery in biologically aggressive tumours, via a neoadjuvant approach, and justifying more aggressive surgery in better prognostic tumours. The biomarkers, S100A2 and S100A4, are demonstrated in this chapter to be associated with pro-metastatic molecular (squamous) subtype of PDAC and poor prognosis. Therefore, these biomarkers and clinicopathological variables associated with poor prognosis was used to develop a pre-operative nomogram to assist in these complex clinical decisions.

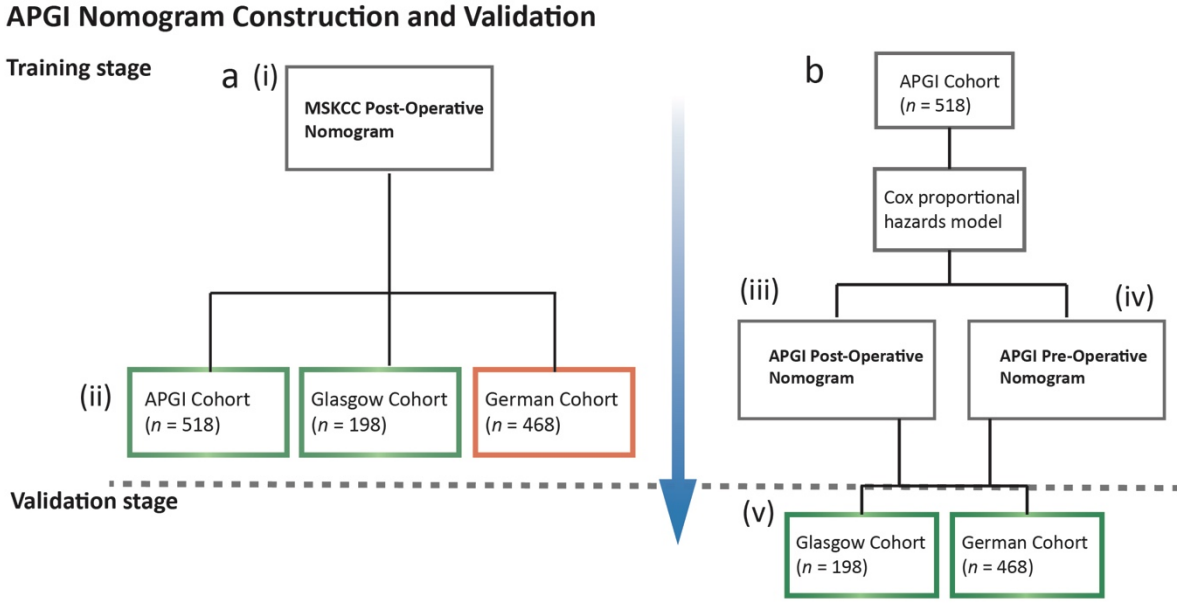

Figure 4-6 Methodology for nomogram construction and validation. a) Clinicopathological variables for all 3 cohorts were independently entered into the MSKCC post-operative nomogram to validate its performance in the patient cohorts. The MSKCC nomogram predicted survival in the APGI (P = 5.0 x 10^{-5}) and Glasgow cohorts (P = 0.025) (green), but not the German cohort (P = 0.31) (red). **b**) The APGI training cohort was used to construct two Cox proportional hazard models, one was termed the APGI post-operative prognostic nomogram, and one the APGI pre-operative prognostic nomogram. These were assessed and validated against the Glasgow (P = 1.7 x 10^{-3}) and German (P = 1.2 x 10^{-5}) validation cohorts with excellent fit in both cohorts.

First, the overall fit of the published MSKCC prognostic nomogram was assessed against all three cohorts by stratifying patients using predicted survival score and comparing observed and MSKCC predicted survival (Figure 4-6). Relative to the true clinical outcome, the MSKCC nomogram predictions were optimistic, particularly at later time points (Figure 4-7). The MSKCC nomogram risk score was prognostic in the APGI and Glasgow cohorts Cox regression coefficients 0.79 and 1.35, (likelihood ratio test for coefficient not zero, P = 5.0 x 10-5 and 0.025, respectively), but not the German cohort (coefficient 0.15, P = 0.31). The MSKCC risk score was well-calibrated against the APGI and Glasgow cohorts (Likelihood-ratio test for coefficient not unity, P = 0.28 and 0.56, respectively), but less well against the German cohort (P = 2.6 x 10-9) (Figure 4-6, Figure 4-7).

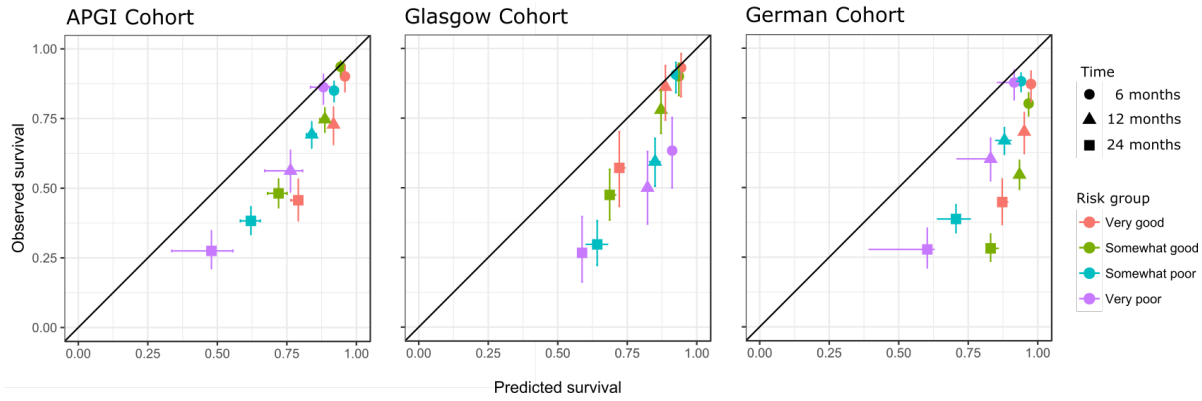

Figure 4-7 Comparison of observed and MSKCC-predicted survival in APGI, Glasgow and German cohorts. Overall fit is excellent for the APGI cohort, and poor for the German and Glasgow cohorts. Patients were divided into four risk groups by MSKCC risk score, and the observed and nomogram-predicted survival within each risk group was compared. Error bars denote the interdecile range (for predicted survival), or the 80% binomial confidence interval (observed survival). This suggests that the MSKCC nomogram does not accurately predict early recurrence in the Glasgow and German cohorts.

4.2.8 Pre-Operative Molecular Nomogram Predicts Survival after Pancreatectomy as accurately as Post-operative Clinicopathological Nomogram

The APGI cohort was used to construct two prognostic nomograms based on the Cox proportional hazards model: one employing traditional post-operatively available variables ("Post-operative Prognostic Nomogram") (Figure 4-6, Figure 4-8), and one employing only variables that can be measured pre-operatively ("Pre-operative Prognostic Nomogram") (Figure 4-6, Figure 4-9). To improve clinical utility and focus prediction on early recurrence and to incorporate the prognostic value of S100A4 into the nomogram over the initial 24 months following surgery, follow-up was truncated at 24 months. Both models included tumour location (pancreatic head vs body / tail), after exploratory analysis in the APGI cohort indicated differences in baseline hazard between these patient groups (Table 4-12).(Dreyer et al., 2018)

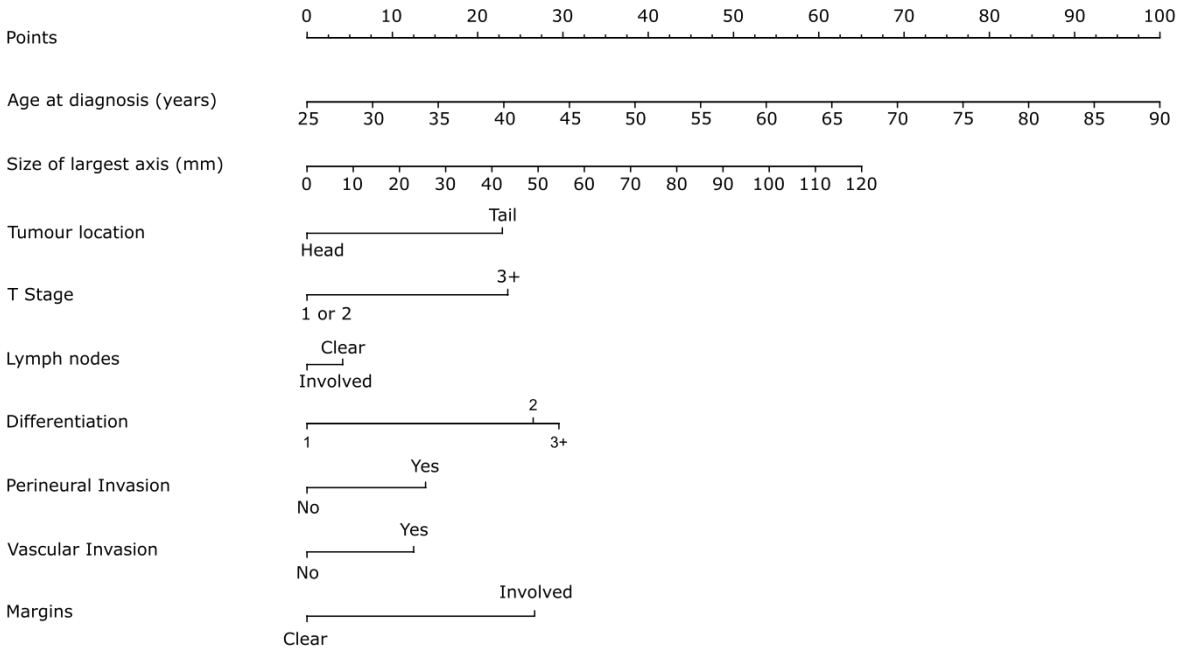

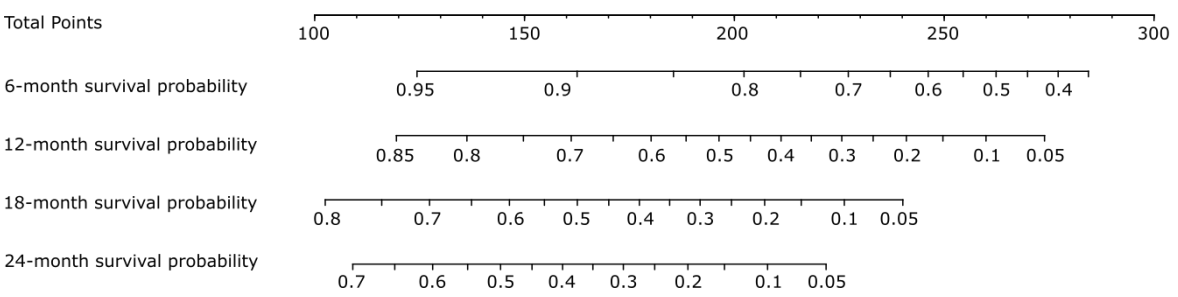

Figure 4-8 Post-operative molecular prognostic nomogram for resectable pancreatic cancer. Points are given for each risk factor and cumulatively gives a prognostic risk score. This can be correlated with survival probability on longitudinal scale at 6-monthly intervals.

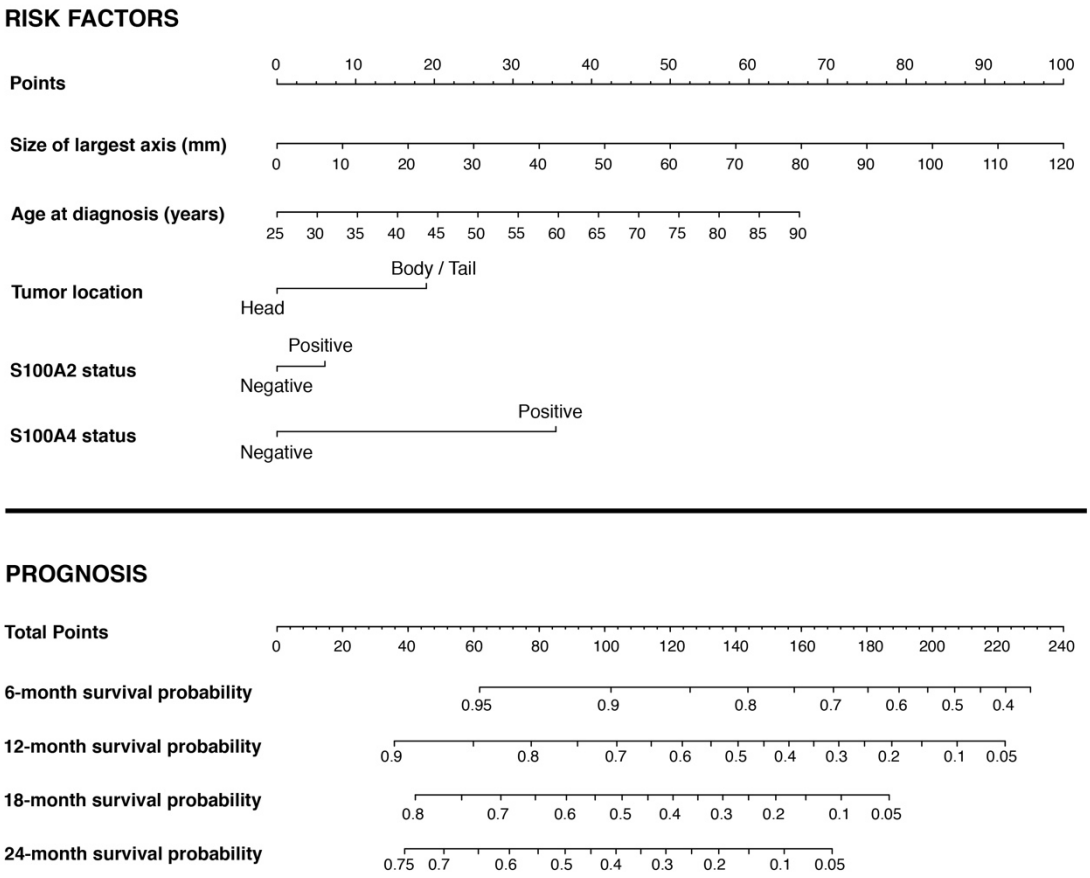

Figure 4-9 A pre-operative molecular prognostic nomogram. Points are given for each risk factor and cumulatively gives a prognostic risk score. This can be correlated with survival probability on longitudinal scale at 6-monthly intervals.

Risk stratification accuracy of the APGI pre-operative and APGI post-operative nomograms were assessed in the Glasgow and German validation cohorts. The pre-operative prognostic nomogram displayed good discrimination on both validation cohorts (risk score Cox coefficients 0.59 and 0.66, $P = 1.7 \times 10^{-3}$ and 1.2×10^{-5} for Glasgow and German respectively) (Figure 4-6, Figure 4-10). Notably, the APGI pre-operative nomogram was superior to the MSKCC post-operative prognostic nomogram in both its spread of risk scores, and the accuracy of its absolute survival estimates (Figure 4-7, Figure 4-10).

The overall accuracy of the APGI pre-operative nomogram in predicting patient survival was assessed and compared to the APGI post-operative nomogram. Although the pre-operative nomogram was slightly optimistic by predicting marginally better outcome probabilities than those observed in the Glasgow and German cohorts, it was more accurate than the MSKCC post-operative nomogram (Figure 4-7, Figure 4-10). Brier scores was

used to formally evaluate the relative performance of the APGI pre-operative and post-operative nomograms with over 5,000 bootstrap draws of each validation cohort. This demonstrated the APGI pre-operative nomogram was more accurate than the MSKCC post-operative nomogram, and as accurate as the APGI post-operative nomogram in outcome predictions (Figure 4-11, Figure 4-12).

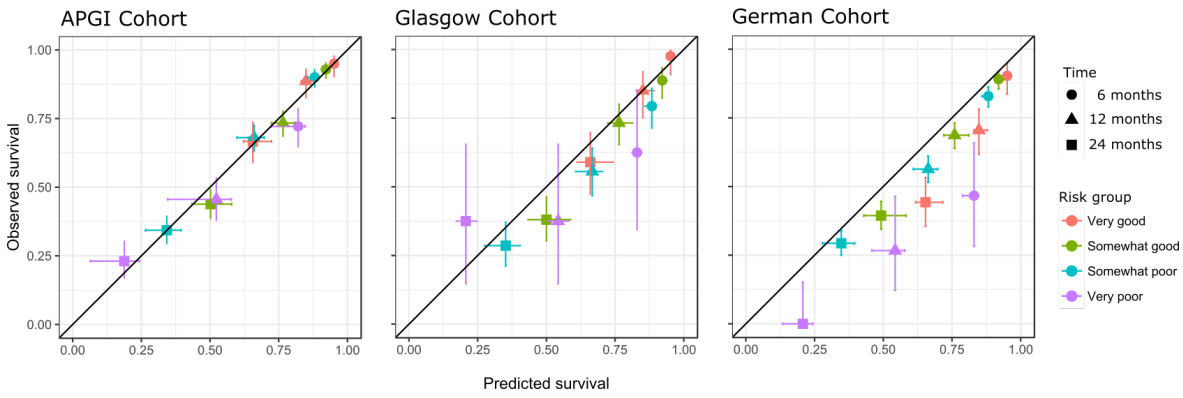

Figure 4-10 Comparison of observed and APGI preoperative nomogram predictions of survival in all cohorts. Patients were divided into four risk groups by APGI preoperative risk score, and the observed and nomogram-predicted survival within each risk group was compared. Error bars denote the interdecile range (for predicted survival), or the 80% binomial confidence interval (observed survival). Overall fit is acceptable in most cases, although the APGI nomogram is generally optimistic, predicting better survival than was observed in the validation cohorts. This is especially pronounced for the Glasgow very poor prognosis group, which displays far worse 6 - and 12 - month survival than was predicted by the APGI preoperative nomogram.

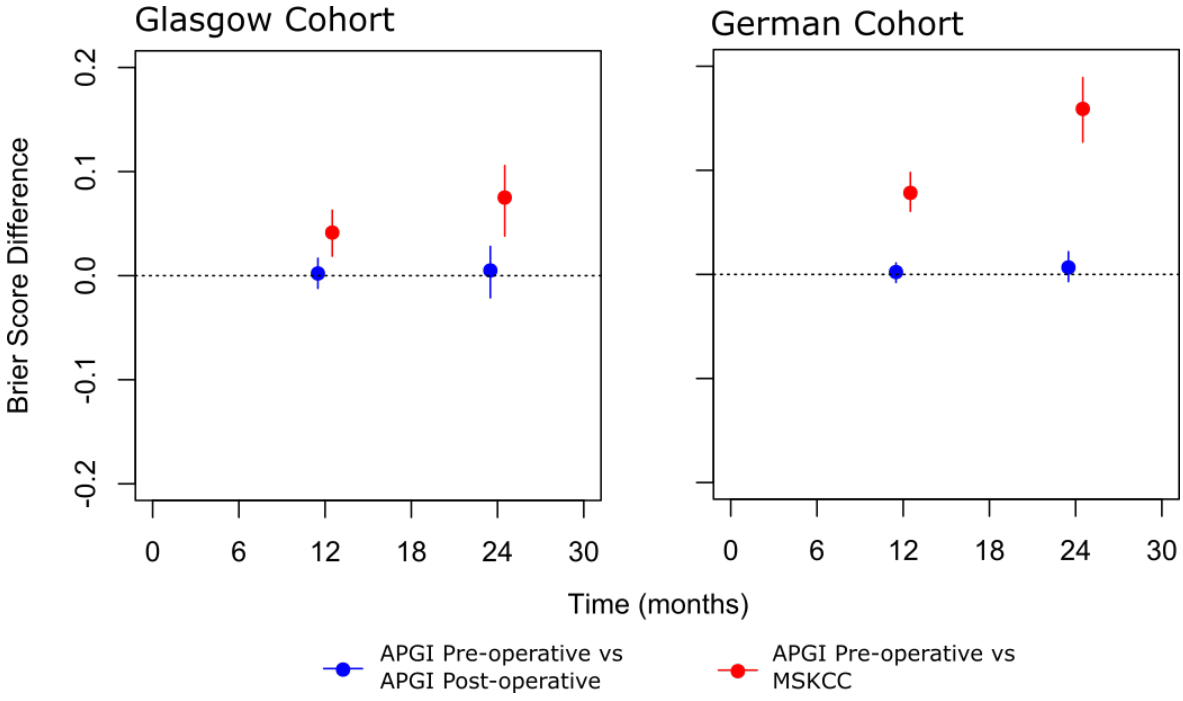

Figure 4-11 Comparison of the validation cohorts' overall prediction accuracy between APGI pre-operative, APGI post-operative, and MSKCC post-operative nomograms. Differences in Brier score between the APGI pre-operative, and either the APGI or MSKCC post-operative

nomograms, are shown at three time points (12, 24 & 36 months). Positive values indicate lower error in the pre-operative nomogram; negative values lower error in the post-operative nomogram. Points denote modal values, and bars denote 90% highest posterior density intervals, over 5,000 bootstrap resamples of each validation cohort.

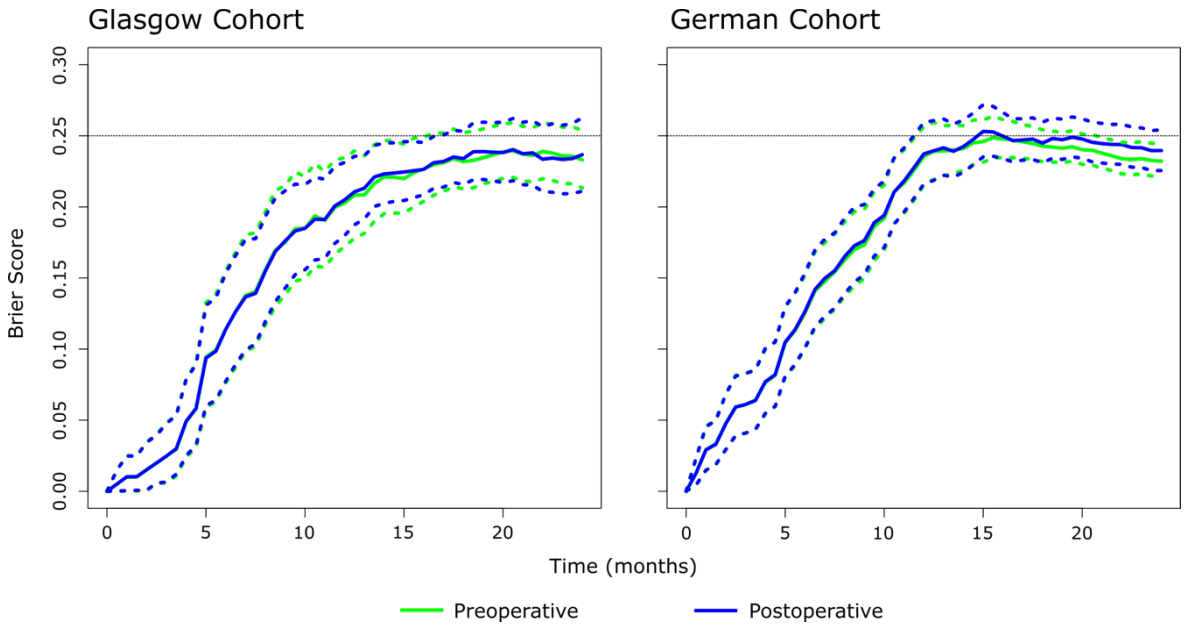

Figure 4-12 Brier score plots demonstrate the pre-operative nomogram predicts prognosis as accurately as the APGI post-operative nomogram in the Glasgow and German cohorts

4.2.8.1 Pre-operative Assessment of Biomarker Expression in EUS-FNA Samples

A pilot study was performed to compare biomarker expression status between pre-operative EUS-FNA cell blocks and the corresponding surgical resection specimen, to assess the feasibility of determining biomarker status pre-operatively.(Nguyen et al., 2014) Seventeen consecutive patients with both EUS-FNA cell blocks and resection specimen blocks were available (Table 4-13). S100A2 and S100A4 expression correlated in 15 (88%) and 14 (82%) out of 17 patients respectively, based on the EUS-FNA cell block and the surgical specimen for both biomarkers examined (Figure 4-13). This demonstrates that biomarker status can be measured pre-operatively using immunohistochemistry, and it is likely that EUS biopsy assessment will improve with the current development of more effective biopsy needles and standardization of processing techniques.

Table 4-13 S100A2 and A4 expression in paired EUS-FNA and resection specimens

	S100A2		S100A4	
Histological Diagnosis	EUS	Resection	EUS	Resection
PDAC	Low	Low	Negative	Positive
PDAC	High	High	Negative	Negative
PDAC (background of IPMN)	Low	Low	Positive	Positive
PDAC	Low	Low	Negative	Negative
PDAC	Low	Low	Positive	Positive
PDAC	High	Low	Positive	Positive
PDAC	Low	Low	Negative	Positive
PDAC	Low	Low	Negative	Negative
PDAC	Low	Low	Positive	Positive
PDAC	Low	Low	Positive	Positive
PDAC	High	Low	Negative	Negative
PDAC	Low	Low	Positive	Positive
PDAC	Low	Low	Positive	Positive
PDAC	Low	Low	Negative	Negative
PDAC	Low	Low	Negative	Positive
PDAC	Low	Low	Negative	Negative
PDAC	Low	Low	Negative	Negative

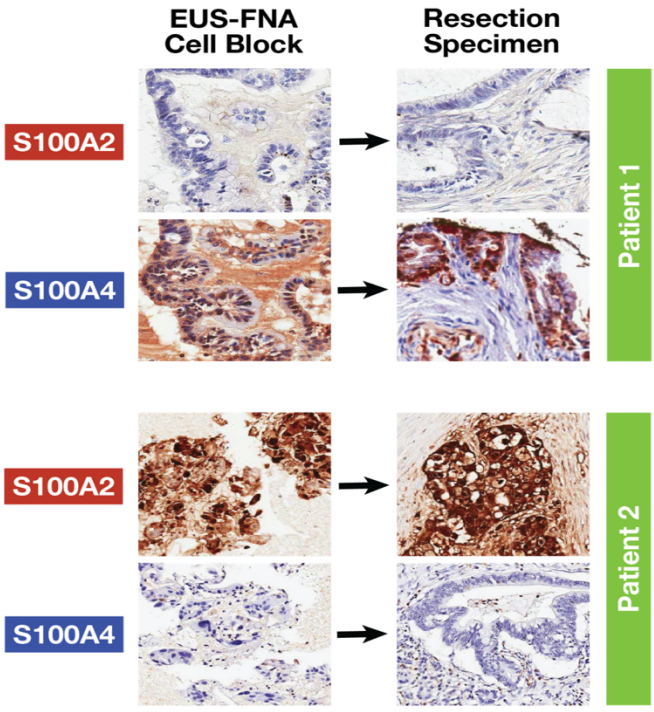

Figure 4-13 Immunohistochemistry of EUS-FNA vs resection specimen in 2 patients

4.3 Discussion

Despite our increasing understanding of the molecular heterogeneity in morphologically identical cancers, and the advances in molecularly guided targeted therapy selection, the impact of these findings in surgical decision-making has not been addressed. Perioperative mortality for pancreatectomy has improved dramatically over the last 30 years and the definition of "resectability" has been expanded over the last decade with increasingly aggressive surgery being performed (Isaji et al., 2018, Gemenetzis et al., 2018). However, early recurrence remains the Achilles' heel of surgical resection, making better patient selection for surgery a priority area of research.

The expression of two molecules, S100A2 and S100A4, which functionally promote carcinogenesis and metastasis, were validated as prognostic biomarkers in multiple independent cohorts of patients with resectable PDAC (n = 1184), in keeping with earlier studies (n = ~400) (Biankin et al., 2009). These two biomarkers were used to stratify patients with resectable PDAC into distinct prognostic phenotypes after pancreatectomy. Patients with both biomarkers positive are at significant risk of early recurrence, with almost half of these patients succumbing within 12 months after pancreatectomy (12-month survival rate = 54%). Suggesting that disease recurrence occur at around 6 months or earlier for the majority of this group. The risk and pattern of disease recurrence following pancreatectomy is not proportional and early recurrence has recently been defined as within 12 months following surgery (Groot et al., 2018, Groot et al., 2017). We focused the follow up in the first 24 months post-operative period for nomogram construction since the majority of patients that develop early recurrence will succumb to the disease by this point, and thus improve its clinical utility (Groot et al., 2018). A pre-operative prognostic nomogram incorporating these two biomarkers, and pre-operatively determined variables including age, tumour size and location was developed and independently validated. This pre-operative prognostic nomogram performed as well as the published MSKCC post-operative prognostic nomogram, which is the most widely used, and currently considered the gold standard. In the comparison presented above, a number of variables used in the MSKCC nomogram was missing and thus comparing the performance of both nomograms in these cohorts is not optimal. The APGI pre-operative nomogram, however, utilises less variables and all are obtainable prior to surgical resection to aid decision making.

As a proof-of-concept, biomarker expression status was assessed using immunohistochemical staining of the EUS-FNA cell blocks. A limitation of this study is that larger numbers of pre-operative EUS samples were not available for comparison with post-operative S100A2 and S100A4 immunostaining. The cohorts studied are mature with long term follow up, where EUS were not routinely used pre-operatively. In order to further validate the clinical utility of the pre-operative nomogram, its use should be tested in parallel with trials in PDAC comparing upfront resection and neoadjuvant therapy. This will further aid the study of EUS-FNA biomarker directed therapy and early recurrence, whilst avoiding false positive results from preventing patients undergoing potentially beneficial surgery. This study was limited by missing specific recurrence pattern data for a number of patients. Therefore, the association between recurrence patterns and biomarker expression was not assessed. Additionally, pre-operative CA19-9 measurements were not available for the majority of patients due to the nature of retrospective cohort studies. Increased serum levels of CA19-9 has been shown to be associated with early recurrence, and may improve the performance of a pre-operative nomogram (Groot et al., 2018). Finally, this study was not powered nor designed to assess S100A2 and S100A4 expression and response to adjuvant chemotherapy. Chemotherapy response in the adjuvant setting is difficult to reliably assess as survival difference is dependent on many factors including residual occult metastatic disease and performance status, requiring multi-centre personalised medicine trials (such as *PRECISION-Panc* in the UK and *Precision Promise* in the USA) to further delineate this relationship. Interestingly, in the APGI cohort, patients with both biomarkers positive were less likely to be administered adjuvant therapy, possibly due to an aggressive disease phenotype leading to more early recurrence and declining performance status and subsequently reduced adjuvant chemotherapy use.

Aberrant S100A2 and S100A4 expression correlated to the recently described poor prognostic ‘squamous’ (also termed QM or Basal) (Moffitt et al., 2015, Collisson et al., 2011) subtype of PDAC which is enriched by transcriptomic gene programs associated with proliferation, inflammation and metastasis (Bailey et al., 2016). S100A2 hypomethylation is a feature of the squamous subtype and this leads to overexpression in this subtype (Bailey et al., 2016). S100A4 expression is more complex as it is regulated by Wnt and TGF-beta signalling, and can also be expressed in the microenvironment by lymphocytes and fibroblasts, which may be secondary to differential gene expression in the squamous subtype but requires further investigation (Fei et al., 2017). The squamous subtype was associated with a higher mean nomogram score and demonstrates the potential

clinical utility of the currently presented molecular prognostic nomogram in identifying patients with aggressive tumour biology and a pro-metastatic phenotype. These patients are at high risk of early recurrence and are unlikely to benefit from pancreatectomy and are perhaps better treated with neoadjuvant therapy (an increasingly popular approach to PDAC in many centres internationally), as occult metastatic disease that is not detected by current staging modalities will likely manifest itself during this period. The use of neoadjuvant therapy, however, is not universal and a significant proportion of patients do not respond to this approach (Murphy et al., 2018). Thus, patients predicted to have a favourable prognosis, may be better served with upfront surgery and adjuvant therapy with median survival up to 54 months reported using adjuvant modified FOLFIRINOX in patient cohorts with favourable post-operative prognostic features (Conroy et al., 2018). Furthermore, the growing interest in more aggressive and extensive surgery in the setting of borderline resectable or locally advanced disease could be justified by prognostic indicators prior to initiating therapy (Isaji et al., 2018, Gemenetzis et al., 2018). Accurate prognostication can assist multidisciplinary and shared decision-making, especially in patients with borderline fitness for surgery, which is a significant proportion of patients with PDAC, delivering a more personalized treatment plan. This approach has the potential to improve the overall outcomes and quality of life for patients with PDAC.

5 Targeting DNA damage response deficiency and replication stress in PDAC

5.1 Introduction

There is growing interest in targeting DNA damage response (DDR) deficiency in many cancer types, particularly with an improved understanding of DNA damage repair mechanisms and therapeutic sensitivity (Lord and Ashworth, 2016). Yet, various aberrations in genes that impact on DDR mechanisms often lead to different phenotypes and therapeutic sensitivity. As agents targeting DDR mechanisms expand, it is crucial to identify patient subgroups that respond differentially to these and define robust therapeutic biomarkers of patient selection for clinical testing.

The platinum-based combination therapy FOLFIRINOX (folinic acid, fluorouracil, irinotecan and oxaliplatin) has demonstrated significant promise in clinical practice with objective response rates in the region of 30% (Conroy et al., 2011). This far exceeds previous rates using traditional cytotoxic regimens used in PDAC, however, this does not translate into improved long-term survival. Yet, it does lead to disease stabilisation in a large proportion of patients that can be built upon with novel agents in 2nd line. These (occasional exceptional) responders to platinum-based chemotherapy are associated with specific genomic aberrations, with the most widely accepted benefits occurring in patients with germline mutations in *BRCA 1 & 2* (Waddell et al., 2015, Lord and Ashworth, 2012). Yet, there is growing evidence that the prevalence of patients responding to platinum is much greater than the frequency of germline *BRCA 1 & 2* mutations alone and extends beyond point mutations in DDR pathway genes in PDAC (Waddell et al., 2015, Lord and Ashworth, 2016). Conversely, many mutations in these genes do not induce functional deficiencies in DNA repair and thus does not lead to therapeutic sensitivity (Lord and Ashworth, 2016). Platinum chemotherapy is associated with significant morbidity, occasional mortality, and prevents patients from receiving novel agents in clinical trials of 1st line therapy. FOLFIRINOX should ideally be utilised only when there is high confidence of clinical efficacy. In order to better stratify patients, biomarkers of platinum sensitivity are required that extend beyond germline *BRCA 1 & 2* mutations alone, as these may only capture around a quarter or less of potential responders.

The increasing evidence of DDR deficiency in cancer, including PDAC, have in recent years led to the development of numerous agents specifically targeting DNA damage

response and repair mechanisms. Moreover, our improved understanding of genomic instability in cancer cells as a result of replication stress has led to the development of numerous agents targeting cell cycle regulatory checkpoints, including inhibitors of CHEK1, ATR, WEE1 and CDK4/6 (Dobbelstein and Sorensen, 2015). These are showing promise in pre-clinical and phase I clinical trials in several cancer types, however responsive patient groups are largely undefined with many biomarkers proposed but not clinically validated (Lecona and Fernandez-Capetillo, 2018). It appears that replication stress in cancer cells can persist following the development of platinum resistance (Drean et al., 2017). Thus, these agents may also play a role in 2nd line once platinum resistance has developed. This is a substantial opportunity for PDAC, where no recognised 2nd line treatment is available for patients that progress on 1st line chemotherapy.

The relationship between DDR deficiency, replication stress and defined molecular subtypes of PDAC has not been delineated. The largest integrated molecular analysis of PDAC thus far, demonstrated no association between DDR deficiency and molecular subtypes of PDAC (Bailey et al., 2016). Yet, a key gene program defining the squamous subtype (Gene Program 4) is largely populated by genes controlling proliferation and cell cycle control (Bailey et al., 2016). This includes ATR signalling and cell cycle regulatory checkpoints suggesting that this subtype may be enriched for tumours with replication stress (Bailey et al., 2016). This may prove a therapeutic opportunity for targeting these poor prognosis patients and requires exploration.

This chapter addresses these questions by using an extensive array of fully characterised pre-clinical models of PDAC to define therapeutic responsive biomarkers for agents targeting DDR deficiency in PDAC. This was achieved using numerous approaches. First, biomarkers of DDR and HR deficiency are applied to patient derived cell lines (PDCL) and xenografts (PDX) to test platinum and PARP inhibitor responsiveness. Next, transcriptomic, proteomic and functional data from a large panel of PDCLs is interrogated to identify evidence of replication stress. The therapeutic response to cell cycle checkpoint inhibitors is next investigated in PDCLs and the relationship between DDR deficiency and replication stress delineated, with supportive in-vivo therapeutic testing data.

5.2 Targeting DDR deficiency

5.2.1 Defining DDR deficiency in Pancreatic Cancer

Numerous predictive biomarkers of DDR deficiency have been proposed, but not validated in PDAC. Genomic markers of DDR deficiency include genomic signatures described by Waddell *et al*. relating to structural variation patterns and the Cosmic BRCA mutational signature (Waddell et al., 2015). High ranking BRCA point mutational signature overlapped with high prevalence structural variations, termed the 'unstable' genome subtype, and point mutations in the HRD pathway such as *BRCA 1 & 2* and *PALB 2* (Waddell et al., 2015). In patients and pre-clinical models with evidence of these signatures there were significant responses to platinum chemotherapy, with occasional exceptional responses to therapy in the clinic (Waddell et al., 2015). However, these signatures have a number of limitations in clinical practice. First, these require whole genome sequencing which has significant implications for cost, data storage and also the practicalities of the patient sampling process and genomic sequencing, including tumour cellularity which is a major obstacle in PDAC. Second, the BRCA mutational signature score is defined as the frequency of BRCA related mutations per MB and whether an individual is perceived to have a low or high signature is determined by the ranking within a specified cohort and no recognised clinically relevant signature threshold exists (Alexandrov et al., 2013). Thus, making it challenging for a single patient being profiled to be categorised based on the point mutation signature alone.

To combat these limitations and the logistical issues surrounding whole genome sequencing for precision oncology (tissue fixation, high cost, not suitable for low cellularity tumours, data storage) a clinically applicable targeted capture sequencing panel has been developed. The PhD candidate is part of the team developing and validating what is called the ***Glasgow Precision Oncology Laboratory (GPOL) Clinical Cancer Genome™*** (Appendix II). The design of the assay is based on large scale sequencing studies of PDAC and other cancers, including the ongoing ICGC Pan-Cancer Analysis of Whole Genomes (PCAWG) project (Bailey et al., 2016, Waddell et al., 2015, Notta et al., 2016). This detects somatic mutations, but also structural variation patterns and can generate specific signatures for mismatch repair deficiency and homologous recombination deficiency (HRD). The latter has been designed, and is undergoing the validation stage at present, to be used as a biomarker for platinum response. The HRD signature is generated using genomic features such as structural variations, somatic mutations in DDR genes and

loss of the 2nd allele. The exact design and validation of this signature will not be presented in this PhD thesis, but the HRD signature included in the assay will be tested as a putative biomarker of therapeutic response for therapeutics targeting DDR pathways.

In order to further investigate the clinical utility of these biomarkers, a panel of patient derived cell lines (PDCL) and xenografts (PDX) selected to represent the spectrum of DDR proficiency and deficiency were identified for therapeutic testing with Platinum and PARP-inhibitors. PDCLs were defined as DDR deficient based on structural variation pattern (> 200 SVs), a high BRCA mutational signature (ranked within top 20% of PDAC genomes), a positive homologous recombination deficiency (HRD) signature and mutations in DDR genes (including *BRCA1, BRCA2, ATM, ATR, RPA1, RAD51, RAD54, FANCA*) (Figure 5-1, Table 5-1). BRCA mutational signature ranking was defined using the Cosmic mutational signature 3 and ranking is based on PDCLs (n = 48) that underwent WGS.

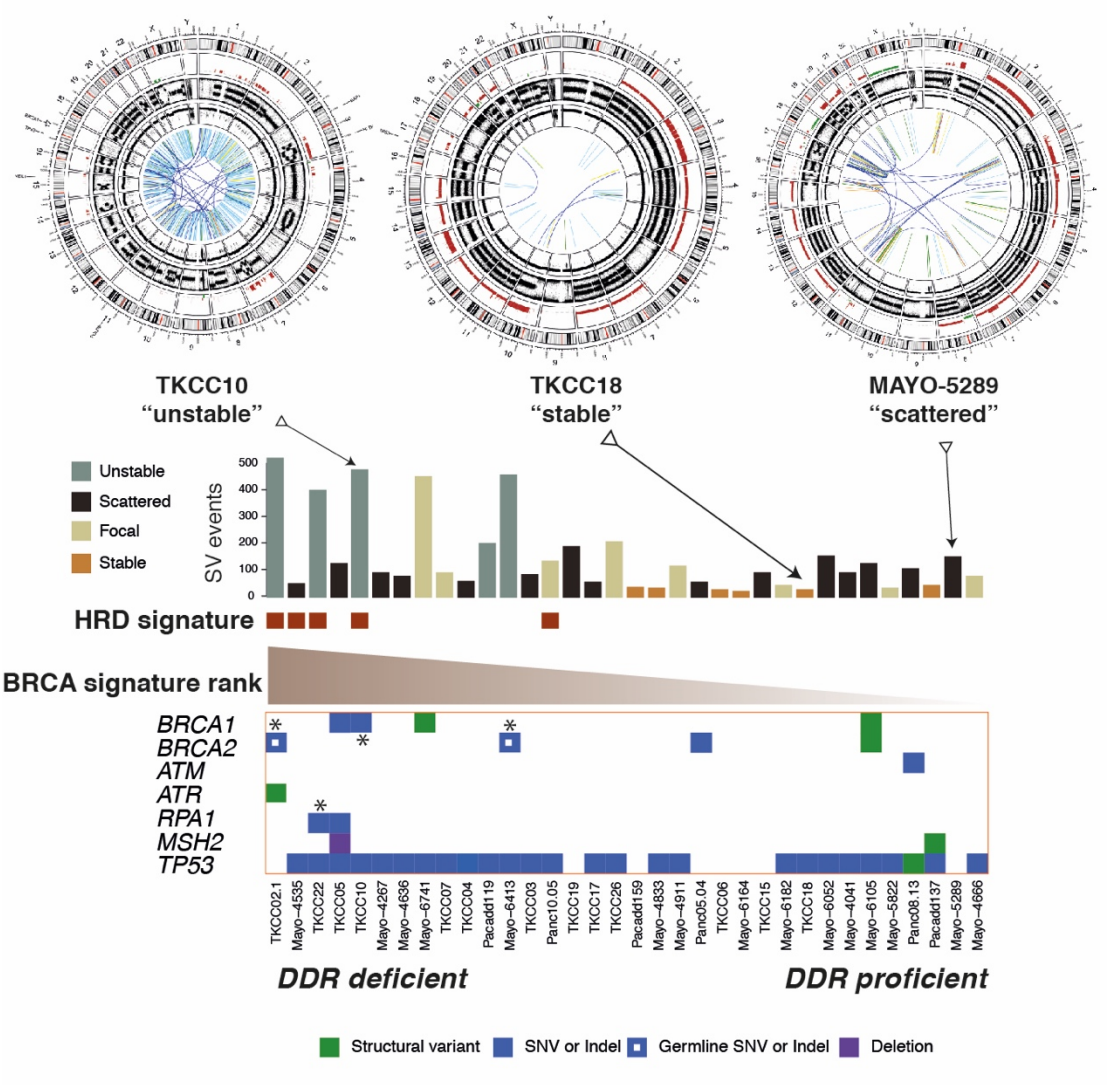

Figure 5-1 Defining DDR deficiency in patient derived cell lines of PDAC. Surrogate biomarkers of DDR deficiency, defined by large scale sequencing projects of PDAC, include the unstable genome (> 200SVs), the homologous recombination deficiency (HRD) signature, high ranking BRCA mutational signature and synonymous mutations in DDR pathway genes. These are associated with each other and can be used to classify PDCLs as DDR deficient or proficient for testing therapeutic hypothesis. PDCLs are ranked from left to right based upon the COSMIC BRCA mutational signature, with SV subtype, number of structural variations and HRD signature status symbolised on the top bar. Examples of Circos plots for 3 PDCLs are included, representing structural variations, copy number changes and point mutations in individual chromosomes. Loss of 2nd allele in DDR pathway gene (indicated by *) is associated with high number of SVs (> 200, termed the unstable genome).

PDAC, and tumour models such as cell lines, can be categorised based on DDR status. Broadly, this is defined as DDR deficient and DDR proficient. Furthermore, PDAC with genomic evidence of homologous recombination deficiency (HRD positive signature) is a sub-set of DDR deficient PDAC with specific genomic features indicating a deficiency in the homologous recombination pathway within the DDR machinery (Figure 5-2).

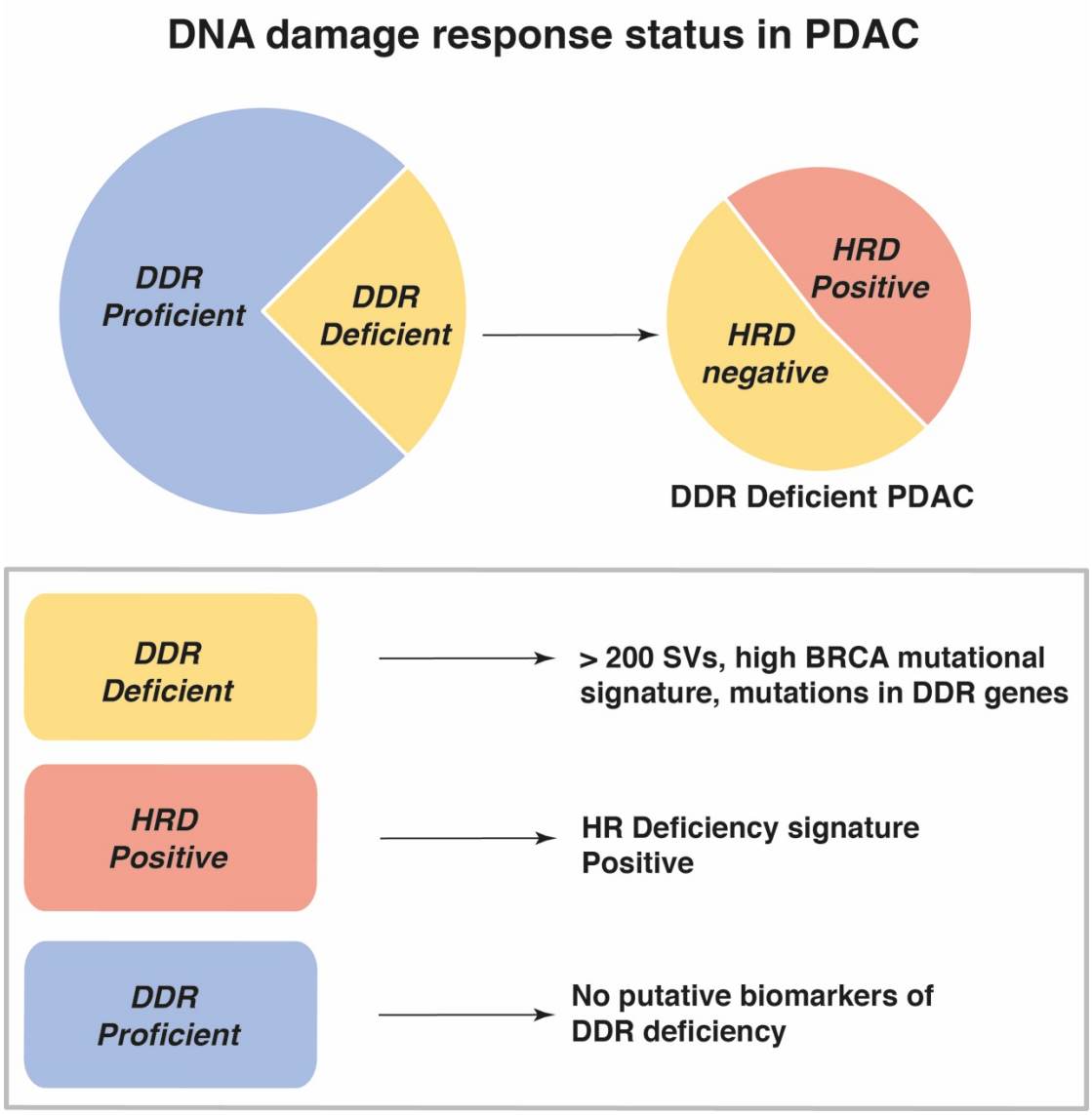

Figure 5-2 Categorising PDCLs based on putative biomarkers of DDR deficiency. PDCLs were defined as DDR deficient (putative biomarkers of DDR deficiency but not HR deficient) or DDR proficient (no markers of DDR deficiency). Within the DDR deficient group there were a subset that were defined as HRD positive (HRD signature positive), this is hypothesised to exist in around 12% of PDAC. This allows categorising of models into 3 groups DDR deficient (HRD signature negative, **orange**), HRD signature positive (HRD positive, **red**) and DDR proficient (**blue**).

For the purpose of therapeutic testing PDCLs were categorised as 1. DDR deficient (putative biomarkers of DDR deficiency but HRD signature negative) 2. HRD positive (putative biomarkers of DDR deficiency including HRD signature positive) and 3. DDR proficient PDAC (no putative biomarkers of DDR deficiency) (Figure 5-2). PDCLs were separated between HRD positive and DDR deficient to investigate the novel HRD signature in relation to previously defined putative biomarkers of DDR deficiency. In total, 3 PDCLs were selected as HRD signature positive:

- TKCC02.1 (*BRCA2* mutation, unstable, high ranking BRCA signature, HRD signature Positive);

- TKCC10 (*BRCA 1* mutation, unstable genome, high BRCA signature ranking, HRD signature positive);

- TKCC22 (*RPA* mutation, unstable genome, high ranking BRCA mutational signature, HRD signature positive) (Table 5-1).

The next set of PDCLs were defined as DDR deficient but HRD signature negative based on putative biomarkers of DDR deficiency (Table 5-1):

- TKCC05 (mutations in *BRCA1, RPA1, RAD54, FANCA, CK12*),

- TKCC26 (>200 structural variations), MAYO-4636 (high ranking BRCA mutational signature),

- PaCadd137 (*PPPR2R2B / D* mutations),

- Panc08.13 (*ATM* mutation)

The remaining PDCLs tested were defined as DDR proficient as these demonstrated no mutations or evidence of genomic changes that would suggest a defect in the DDR machinery.

Table 5-1 DDR status in panel of selected PDCLs for therapeutic testing. PDCLs are ranked by the COSMIC BRCA mutational signature. *indicates loss of 2nd allele in DDR gene.

	PDCL ID	Structural Variation Subtype	Number of Structural Variations	BRCA Signature Ranking	HR deficiency signature	*Mutations*	
						DDR Pathway	*TP53*
HRD Positive	**TKCC02.1**	Unstable	527	1	**Yes**	***BRCA2****	
	TKCC22	Unstable	408	5	**Yes**	***RPA1****	Mutant
	TKCC10	Unstable	484	7	**Yes**	***BRCA1****	Mutant
DDR Deficient	**TKCC05**	Scattered	131	6		***BRCA1, RPA1, RAD54, FANCA, CK12***	Mutant
	TKCC26	Focal	214	21			Mutant
	Panc08.13	Scattered	110	43		***ATM***	
	PaCadd137	Stable	49	44		***PPPR2R2B, PPPR2R2D***	Mutant
	MAYO-4636	Scattered	82	10			Mutant
DDR Proficient	**TKCC17**	Scattered	61	20			Mutant
	TKCC06	Stable	32	32			
	TKCC07	Focal	95	13			Mutant
	TKCC15	Stable	97	34			
	TKCC18	Stable	33	37			Mutant
	MAYO-4911	Focal	120	28			Mutant
	MAYO-5289	Scattered	155	46			

5.2.2 Targeting DDR deficient PDCLs with Platinum and PARP inhibitors

To investigate putative biomarkers of DDR deficiency and the relationship to Platinum and PARP inhibitor response, cell viability therapeutic sensitivity assays were performed. PDCLs were identified and selected for testing based on DDR status (Table 5-1). Cisplatin was used as the Platinum, whilst Rucaparib and BMN-673 (Talazoparib) were used as the PARP inhibitors. Cell viability experiments with Cisplatin therapy was performed in all PDCLs that were available and had comparable growth dynamics for testing (n = 15). Therapeutic testing using PARP inhibitors was more challenging and time-consuming.

Thus, proof-of-concept testing was performed in a selected subgroup of PDCLs (n = 4) and enhanced with in vivo testing that mirrors clinical PARP inhibitor regimes.

PDCLs defined as either HRD signature positive or DDR deficient (Table 5-1) were more sensitive to both Cisplatin therapy and PARP inhibition (Figure 5-3, Figure 5-4, Table 5-2). This reached statistical significance between HRD positive and DDR proficient PDCLs (P = 0.036) and between DDR deficient and DDR proficient (P = 0.016). There was no difference between HRD positive and DDR deficient PDCLs (P = 0.786). Of importance, is the fact that the DDR deficient PDCLs all had EC50s below 10μM. This is the sensitivity threshold set by large scale pan-cancer cell line drug screen (n = 880) using Cisplatin and indicates that these PDCLs are sensitive at clinically relevant doses (cancerrxgene.org (COSMIC)). These results suggest that DDR deficiency, as measured by putative biomarkers such as the HRD signature, has the potential to be used clinically to predict response to Platinum treatment. The only outlier to this was MAYO-4636, which was defined as DDR deficient due to a high ranking BRCA mutational signature yet was resistant to platinum (Figure 5-3). This is in contrast to Panc08.13 and PaCadd137, both of whom had low ranking BRCA mutational signatures but mutations in HR pathway genes, and were both sensitive to Platinum treatment (Table 5-2, Figure 5-3). This suggests that the BRCA mutational signature alone is not a robust biomarker of platinum response, likely because of the complexity of the signature, and requires further testing in clinical cohorts.

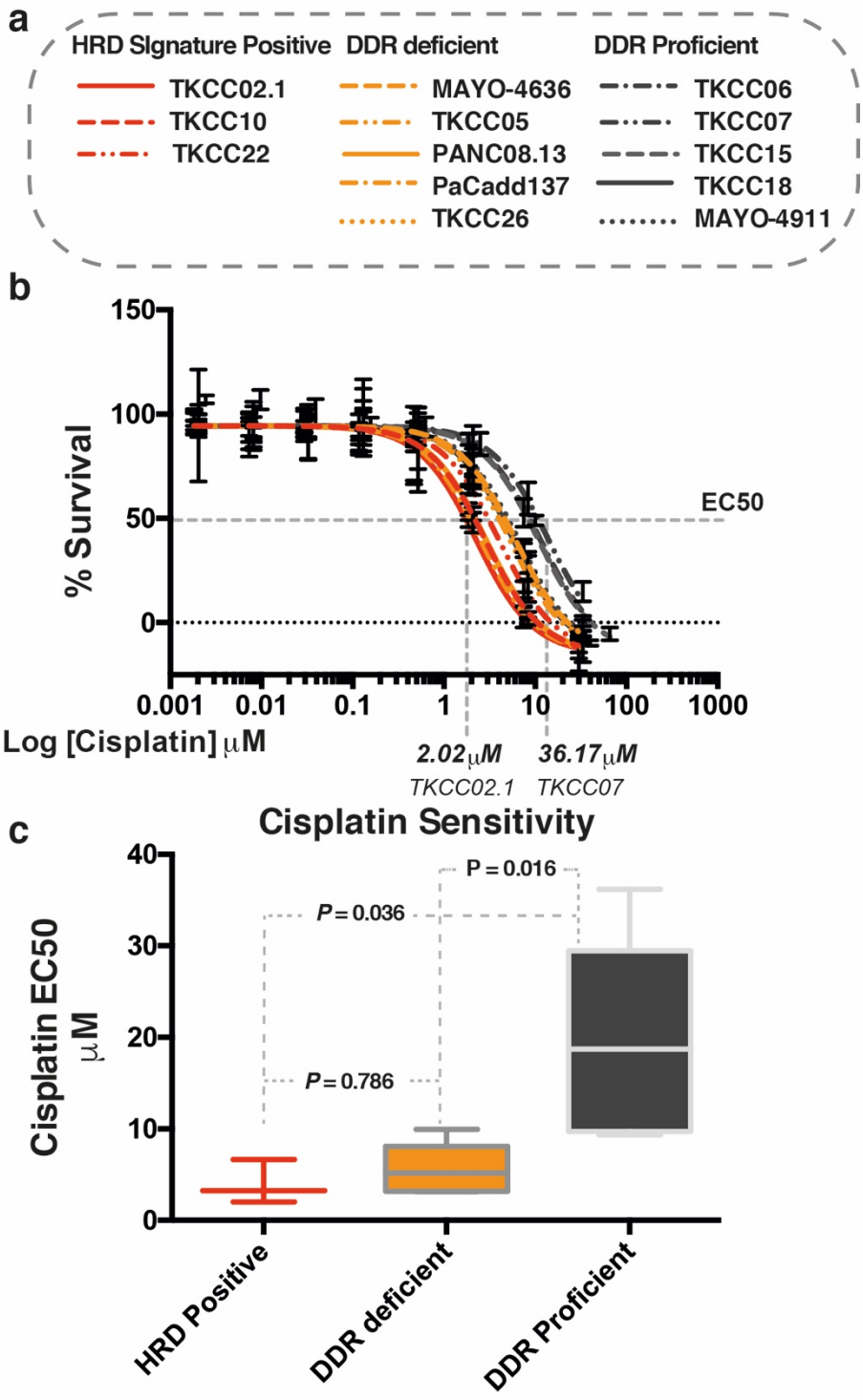

Figure 5-3 Platinum sensitivity and DDR status in PDCLs. PDCLs that were classified as HRD signature positive or DDR deficient was significantly more sensitive to Cisplatin than DDR proficient PDCLs. a) PDCLs were classified by DDR status as HRD signature positive (positive on HRD signature analysis), DDR deficient (HRD signature negative, but evidence of putative biomarkers of DDR deficiency including unstable genome, high ranking BRCA mutational signature and HR pathway gene mutations) and DDR proficient (no evidence of DDR deficiency on signature analysis or mutational profile). b) Cell viability after 72 hours of Cisplatin treatment in PDCLs. Dotted line indicates IC50 in most sensitive PDCL was around 15 times more sensitive than most resistant PDCls. c) Boxplot of mean Cisplatin EC50 in PDCLS stratified by DDR status. Box represents 95% confidence interval, and whiskers minimum and maximum range. *P* calculated using Mann Whitney test between mean EC50 in each group.

The PDCLs TKCC02.1 and TKCC10 were selected as examples of HRD positive cell lines to compare with DDR proficient PDCLs TKCC15 and TKCC18 for PARP inhibitor sensitivity testing. The HRD positive PDCLs were more sensitive to PARP inhibition than the DDR proficient PDCLs to both PARP inhibitors (Figure 5-4). This suggests that HR deficiency in PDAC, as seen in other cancer subtypes, can potentially be used as a biomarker of PARP inhibitor responsiveness.

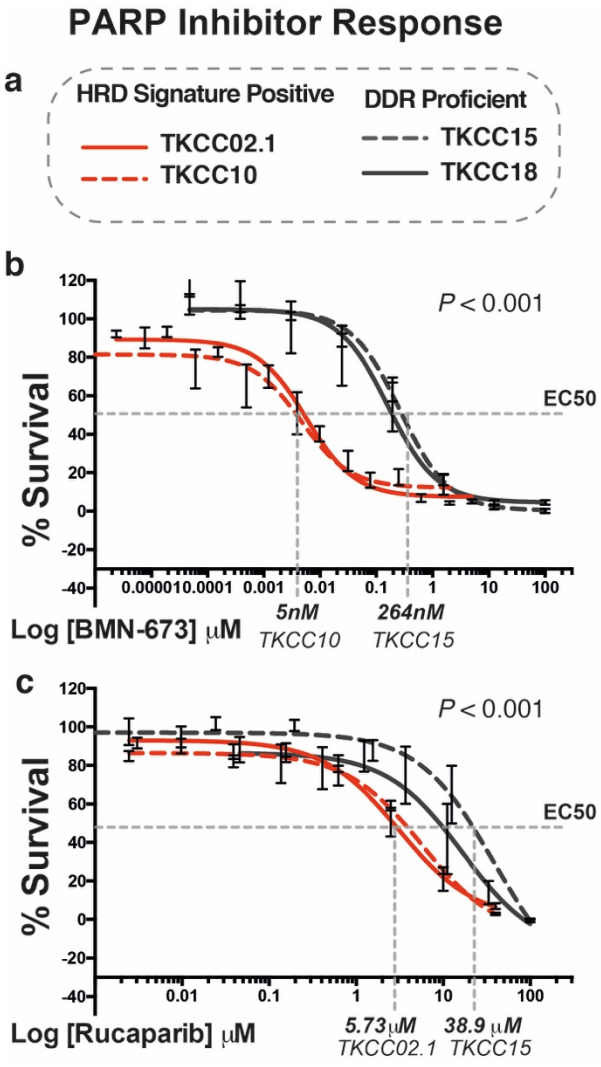

Figure 5-4 PARP-inhibitor sensitivity in PDCLs. DDR deficient PDCLs (HRD signature positive) were significantly more sensitive to PARP inhibition than DDR proficient PDCLs. a) PDCLs were classified as HRD signature positive (red) and DDR proficient (black) and treated with the PARP inhibitors b) BMN-637 and c) Rucaparib. Dotted lines indicate IC50 between most sensitive and most resistant PDCLs. *P* indicates statistical difference between TKCC 10 (HRD signature positive) and TKCC15 (DDR proficient) using non-linear regression analysis. Experiments performed by Eirini-Maria Lampraki.

Table 5-2 DDR status, Platinum and PARP inhibitor sensitivity in PDCLs. Therapeutic sensitivity is colour graded according to sensitivity indicated by green (sensitive) and red (resistant). Sensitivity was defined as < 7μM and resistance as > 10 μM based on pan-cancer Cisplatin drug screen involving 880 cell lines (cancerrxgene.org (COSMIC)).

PDCL ID	DDR Status	*Cisplatin* (Platinum) EC50 μM	*BMN-673* PARPi EC50 μM	*Rucaparib* PARPi EC50 μM
TKCC02.1	HRD Positive	2.019	0.006	3.111
TKCC10	HRD Positive	3.249	0.005	5.728
TKCC22	HRD Positive	6.659		
TKCC05	DDR Deficient	6.231		
TKCC26	DDR Deficient	5.183		
Panc08.13	DDR Deficient	3.14		
PaCadd137	DDR Deficient	3.234		
MAYO-4636	DDR Deficient	9.964		
TKCC07	DDR Proficient	36.17		
TKCC06	DDR Proficient	22.72		
TKCC15	DDR Proficient	18.72	0.264	38.9
TKCC18	DDR Proficient	10.09	0.16	16.68
MAYO-4911	DDR Proficient	9.353		

5.2.3 Targeting DDR deficiency in PDX models

Patient derived xenografts (PDXs) are generated by engrafting fresh tumour tissue directly into immunocompromised mice (e.g. balb/c nude mice). These have been shown to recapitulate the histological, genomic and transcriptomic features associated with the donor tumour, including PDAC (Aparicio et al., 2015). There is, however, evidence that some selection does occur, and it is likely that the less differentiated cells are most likely to survive the engraftment process (Aparicio et al., 2015). Furthermore, not all primary tumours successfully generate PDXs and thus selection does occur in generating these as PDAC models for translation research. Yet, therapeutic responses in PDXs represent those in the primary tumours and are thus considered an excellent resource for therapeutic testing especially if they are well characterised molecularly (Roife et al., 2016).

To investigate therapeutic response biomarkers of DDR deficiency *in vivo,* bulk tumour PDX models that represent both DDR proficient (PDX 2133) and deficient (PDX 2179)

PDAC were generated in balb/c nude mice. Therapeutic testing was performed using a range of agents including Cisplatin (Platinum salt), Olaparib (PARP inhibitor), AZD6738 (ATR inhibitor), Gemcitabine and combinations of these. PDXs were treated once tumour size reached 150mm^3 and treatment regimens were designed to reflect clinical dosing as closely as possible. An exception to this was AZD6738, which at the starting time of these experiments were still being tested in Phase I clinical trials with no defined clinical dosing schedule at the time of experiment initiation.

PDX 2133 was selected as a DDR proficient model for a number of reasons. Firstly, it demonstrated no functional evidence of HR deficiency. Based upon WGS, the tumour was defined as a scattered genome with a very low ranking BRCA point mutational signature. In addition, there were heterozygous mutations for *ARID1A* and *PALB2* of which the functional and therapeutic consequences are not known (sequenced data from each PDX can be found in Chapter 2 Materials and Methods). Targeting mutations only is unlikely to reflect true DDR deficiency in the absence of a genomic signature yet requires further testing. The lack of functional genomic evidence of DDR deficiency in this model reflects that these mutations do not impair the HR machinery. 40 Balb/C nude mice were implanted with PDX fragments in the right flank, of which 24 (60%) developed measurable tumours that were suitable for treatment.

PDX 2133 demonstrated no evidence of response to therapy using agents targeting DDR deficiency including combining Cisplatin with either Olaparib or AZD6738 (Figure 5-5a). At 60 days after the treatment initiation, the mean tumour volume for each of the treatment regimens (excluding Gemcitabine) was similar to the saline control (Figure 5-5a). At this point a decrease in tumour volume is observed in the Olaparib, Olaparib + Cisplatin and AZD6738 + Cisplatin groups. This observation is secondary to the majority of models reaching end-point in each group, with only singular models (n = 1) remaining for each of the Olaparib, Olaparib + Cisplatin and AZD6738 + Cisplatin groups (Figure 5-5a). From the outset, these appeared to be more indolent growing PDXs and likely reflects this observation rather than true drug response. Gemcitabine appeared to induce good responses in this PDX model with secondary responses after subsequent cycles of therapy. Whether this is due to true Gemcitabine sensitivity or whether this reflects the effect of

cytotoxic chemotherapy in rapidly dividing cells is not clear and not investigated in this study.

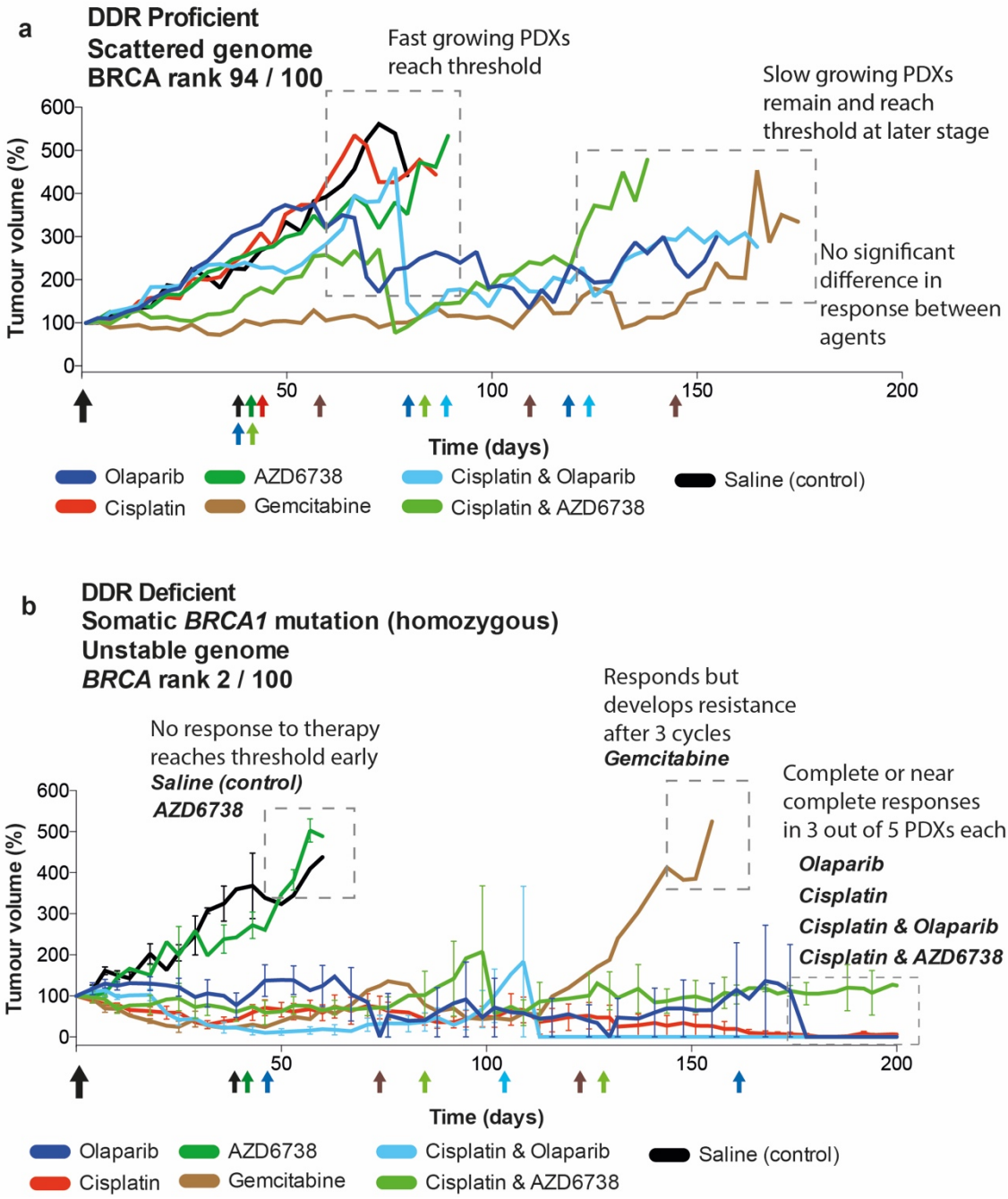

Figure 5-5 PDX response to agents targeting DNA damage repair repsonse. A DDR deficient PDX (2179), but not DDR proficient (2133), responds to PARPi and Platinum. **a**) PDX 2133 (no evidence of DDR deficiency) treated with a panel of agents targeting DDR deficiency and Gemcitabine. Models were treated for 28-day cycles with 2-week treatment breaks, up to 3 treatment cycles in those models that did not respond to therapy. **b**) PDX 2179 (DDR deficient) treated with a panel of agents targeting DDR deficiency and Gemcitabine. Models were treated for 28-day cycles with treatment restarting once PDX volume regrows and reaches treatment threshold (represented by coloured arrows). In models that did not respond, 2-week treatment breaks followed each cycle, with up to 3 treatment cycles in those that did not respond to therapy. Results shown are up to 200 days after start of treatment.

A DDR deficient PDX model (unstable genome, high ranking BRCA signature and *BRCA1* homozygous mutation) was selected for therapeutic testing (PDX 2179). In total, 33 nude mice were enrolled into treatment and treatment schedules were randomised after each round of allocation (see Chapter 2 Methods). In contrast to the DDR proficient model, the DDR deficient PDX model responded exceptionally to both Cisplatin and Olaparib monotherapy (Figure 5-5b). Of these, there were 2 out of 5 complete responders in the Olaparib monotherapy group after 1 cycle of therapy. There was no evidence of tumour regrowth at 300 days after treatment initiation in both of these tumours (Figure 5-5b). In the Cisplatin monotherapy group there were 3 out of 5 complete responders, 1 each after 1, 2 and 3 cycles respectively. In the Cisplatin & Olaparib combination group, there were 3 out of 5 complete responders after 1 cycle. Of these, 1 regrew and responded completely after a 2nd cycle, and the others were tumour free at 180 and 300 days after treatment initiation respectively. AZD6738 demonstrated no response as a mono therapy agent, however in combination with half dose Cisplatin induced long term responses similar to Cisplatin and Olaparib combination therapy (Figure 5-5b).

These results are extremely promising for the use of PARP inhibitors, such as Olaparib, in PDAC. This study suggests that PARP inhibition is as efficient as Platinum chemotherapy in DDR deficient PDAC and may spare patients significant side-effects of cytotoxic treatments. Furthermore, these results imply that combination therapies can be very effective even when reducing the dose of cytotoxic platinum. This in turn may reduce patient side-effects, whilst ensuring efficacy. Of interest, however, is the fact that only a proportion of the PDXs in each of the responding groups responded completely. In the Platinum only group, 2 out of 5 developed resistance after 2 cycles of therapy. This suggests that resistant clones within individual tumours either develop by secondary genomic evolution or are allowed to expand as sensitive clones are destroyed by treatment. There are reports of patients responding to PARP inhibitors after resistance to Platinum develops in the DDR deficient PC setting, similar to observations in Ovarian Cancer (Pishvaian et al., 2017, Mirza et al., 2016). Platinum resistance is complex and multi-factorial and to investigate this requires well designed clinical trials with sequential tumour sampling, as pre-clinical models may not reveal the complete picture of resistance mechanisms. This concept is addressed later in this chapter by implementing these strategies into novel clinical trials investigating drug response in parallel to platinum and PARP inhibitor resistance in the 2nd line PDAC setting.

These results further add to the growing evidence that targeting point mutations in coding genes alone, such as *ARID1A* and *PALB2* (PDX 2133), does not guarantee therapeutic response. In order to elucidate a high response rate in genotype subgroups, either a functional signature that is well defined is required to be present, or mutational assays that reflect changes in both alleles are well validated with functional and response data. Unfortunately, neither PDX had any clinical patient treatment response data available for either platinum or PARP inhibitor therapy and thus a comparison between patient and PDX response was not possible with these models.

Table 5-3 DDR status and response to DDR agents in PDX models.

PDX	DDR status	Biomarkers of DDR Deficiency	DDR agent Response
PDX2179	DDR Deficient HR Deficient	*BRCA1* mutation (bi-allelic) Unstable genome High Ranking BRCA mutational signature (2/100) HRD signature Positive	Cisplatin, Olaparib Cisplatin + Olaparib Cisplatin + AZD6738
PDX2133	DDR proficient	*ARID1A, PALB2* heterozygous mutations Low ranking BRCA mutational signature (94/100), scattered genome	None

5.3 Targeting Replication Stress in PDAC

Genomic instability is a hallmark of cancer, typically secondary to defects in DNA replication and repair during the cell cycle, usually resulting in replication stress (Lecona and Fernandez-Capetillo, 2018, Hanahan and Weinberg, 2011). Replication stress is defined as the stalling, or more simply the slowing down, of the DNA replication fork during replication (Zeman and Cimprich, 2014). The replication stress response is activated by persisting single stranded DNA (ssDNA) at stalled replication forks resulting in the activation of ATR and Chk1 and subsequent cell cycle checkpoints via WEE1 and CDK 1 / 2 (Figure 5-6) (Lecona and Fernandez-Capetillo, 2018). There is growing evidence demonstrating that oncogene activation drives replication stress, particularly through RAS and Myc signalling, both features of human PDAC (Lecona and Fernandez-Capetillo, 2018, Di Micco et al., 2006, Macheret and Halazonetis, 2018). Furthermore, the majority of PDAC, in the region of 70%, demonstrate loss of *TP53* which renders the cell reliant on the G2 / M checkpoint for DNA repair prior to cell division.

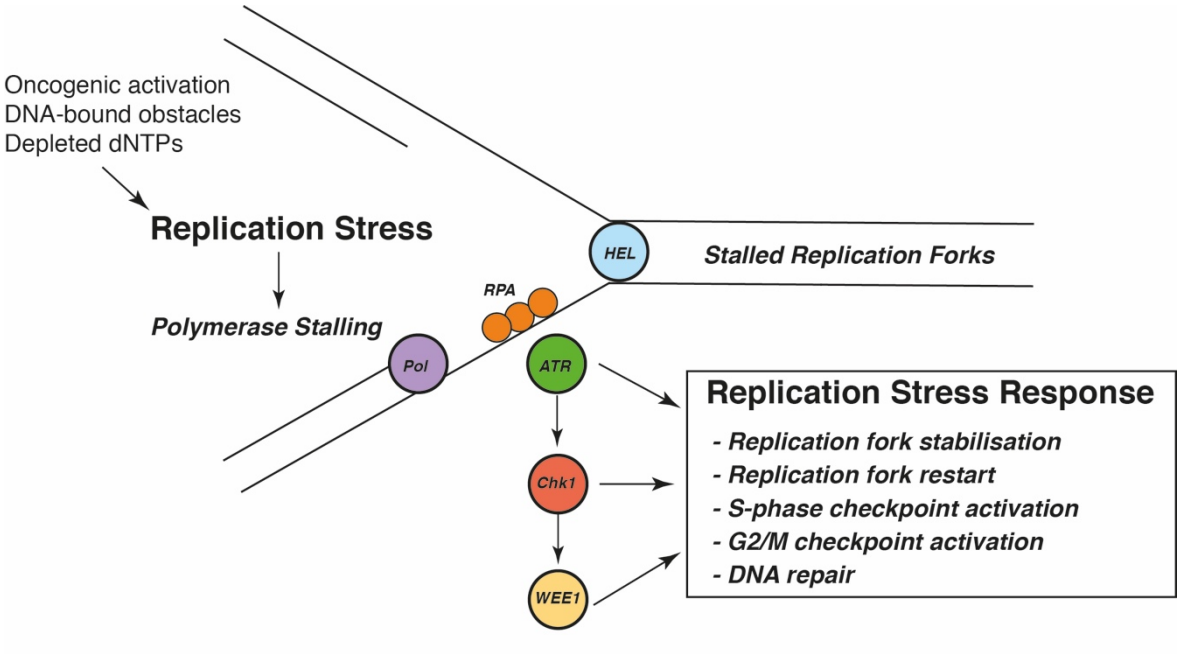

Figure 5-6 The Replication Stress response. Replication stress can be induced by multiple factors including oncogenic activation (KRAS, Myc) and chemotherapeutics (e.g. Platinum). This results in stalled replication forks when DNA polymerases (Pol) are separated from DNA helicase (HEL). This results in the coating of ssDNA by replication protein A (RPA) which results in ATR activation. This, in turn, generates the Replication Stress response via Chk1 and WEE1 resulting in checkpoint activation and DNA repair. This safeguards the integrity of the genome by preventing entry into mitosis with incompletely replicated genomes.

Initial transcriptomic analysis of PDAC demonstrates that subgroups of patients have enriched expression of genes and pathways involved in cell cycle control, suggesting activation of these in response to replication stress (Bailey et al., 2016). This, along with the enrichment of oncogene activation in PDAC suggests that replication stress may be a significant feature of the disease in a specific subgroup of patients. The development of inhibitors for proteins involved in the replication stress response, e.g. ATR, WEE1 and Chk1 may potentially exploit a therapeutic vulnerability in this subgroup of patients. This was explored using a large set of extensively characterised patient derived cell lines, to generate pre-clinical response data and a platform of evidence to define strategies for clinical testing in PDAC.

5.3.1 Transcriptomic evidence of Replication Stress

To assess the role of cell cycle control, activation of cell cycle checkpoints and induction of replication stress in PDAC, an integrated transcriptomic analysis was performed on a panel of 48 PDCLs, generated as part of the ICGC project. This enables gene expression originating from the tumour epithelium to be enriched and interpreted without stromal

influences. Hierarchical clustering, using gene classifiers defined in Bailey *et al.* (Bailey et al., 2016), allowed classification of PDCLs into 2 broad lineages: Squamous (58%) and Classical Pancreatic (42%). In addition to differences in gene expression which defines these classes, there were significant differences in many important mechanisms of carcinogenesis that included cell cycle control and DNA damage response (Figure 5-7).

There were significant differences in the expression of genes controlling cell cycle, in particular, the G2/M checkpoint (Figure 5-7). This included significant differential expression of *WEE1* ($P = 0.006$), *CDK6* ($P = 0.02$) and *CDK7* ($P < 0.001$) in the PDCLs and bulk tumour samples with high expression of these in the squamous subtype (Figure 5-7a). Furthermore, enriched expression in the squamous subtype was seen for *MYC* and *CCNE1* in both bulk tumour and PDCLs (Figure 5-7a). Activation of these oncogenes induces replication stress secondary to genomic instability and may reveal insights into the mechanisms underlying these changes (Macheret and Halazonetis, 2018). This suggests that there is differential activation of genes controlling the cell cycle, particularly the G2 / M checkpoint, as a result of replication stress within a subgroup of patients, and this is strongly correlated with the squamous subtype. Furthermore, it appears that oncogene activation is associated with the squamous subtype and may be driving replication stress in these tumours.

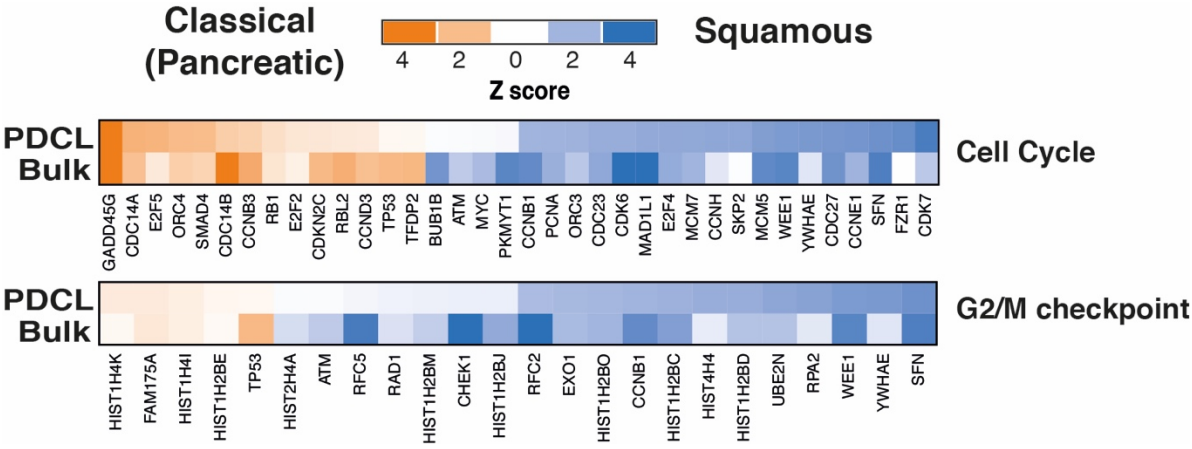

Figure 5-7 Gene expression profiles related to cell cycle control between molecular subtypes, bulk tumour and PDCLs of PDAC. This demonstrates that, in both the PDCLs and bulk tumours, the Squamous subtype is enriched for genes involved in cell cycle control and oncogenes that are associated with inducing replication stress. Heatmap constructed of cumulative gene expression scores for all samples in each subtype showing differential expression of genes important in cell cycle control and G2/M DNA damage checkpoint. The degree of colour saturation is proportional to the degree of enrichment in the Squamous (blue) and Classical Pancreatic (orange) subtypes for all samples within each subtype.

Differential gene expression associated with cell cycle control and replication was used to perform Gene Ontology (GO) and pathway enrichment analysis for individual PDCLs. This creates specific pathways of interactive sets of genes and allows quantification of potential differential activity of each pathway based on gene mRNA expression. This generated a number of differentially upregulated GO terms that apply to cell cycle control, DNA damage response and replication stress (Figure 5-8). Combining the differential expression score for each pathway, a composite score of replication stress can be generated (Figure 5-8). This demonstrated that the squamous subtype is enriched for upregulated expression of genes associated with replication stress and DNA damage response pathways (Figure 5-8). Furthermore, a composite score of these gene pathways, generates a transcriptomic signature (termed the Replication Stress signature) and can potentially be applied as a transcriptomic biomarker of replication stress, which was explored further.

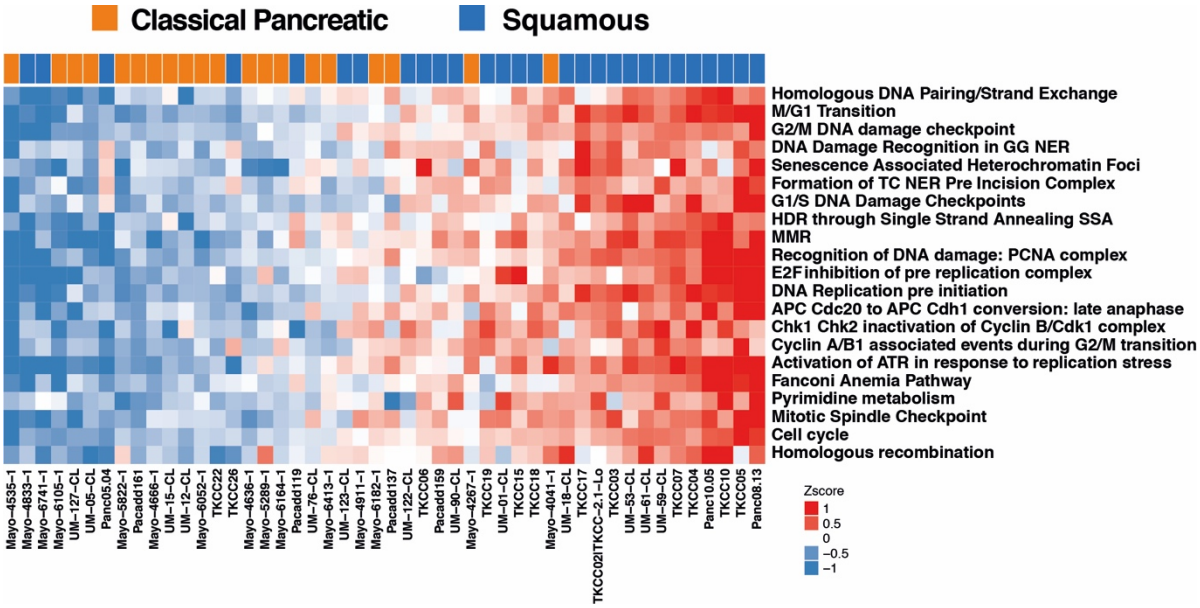

Figure 5-8 The association between the Replication Stress signature and the Squamous subtype. The replication stress signature is strongly associated with the squamous subtype (indicated by blue in the top row). Heatmap of pathways and molecular processes (GO terms) involved in DNA maintenance and cell cycle regulation activated in replication stress and DNA damage response. The Replication Stress transcriptomic signature is based on the replication stress response and generated as a cumulative score of gene expression secondary to replication stress. PDCLs are ranked from right to left based on the novel transcriptomic signature score of replication stress (a composite score of each individual GO term) and molecular subtype is indicated in the top bar showing the association between activation of replication stress and the squamous subtype.

These findings suggest that the Squamous subtype is enriched for pathways controlling cell cycle checkpoints associated with evidence of replication stress. A possible explanation for this association is the enrichment of activated oncogenes within this subtype (Macheret and

Halazonetis, 2018). In order to assess whether gene expression translates into a therapeutic vulnerability in tumours with a high replication stress signature score, the functional attributes of the replication stress signature were investigated.

5.3.2 Functional evidence of Replication stress in PDAC

To determine the functional relevance of the novel transcriptomic replication stress signature, a number of protein-based assays were performed. First, immunofluorescence was used to identify foci of DNA damage repair proteins in a panel of PDCLs with varying degrees of replication stress and DDR deficiency. The definition of replication stress is the persistence of single stranded DNA (ssDNA), also known as stalled replication forks, and this leads to phosphorylation of RPA (pRPA) (Zeman and Cimprich, 2014). pRPA binds to sites of ssDNA and activates the ATR mediated replication stress response (Zeman and Cimprich, 2014). H2AX is phosphorylated (γH2AX) in response to double stranded DNA breaks (DSBs), and thus demonstrates an inability of the cell to repair ssDNA breaks (Zeman and Cimprich, 2014). This may be due to defects in the homologous recombination pathway (DDR deficiency) or due to an overload of ssDNA secondary to excessive replication stress (Zeman and Cimprich, 2014, Dobbelstein and Sorensen, 2015). Thus, pRPA was used as a marker of ssDNA breaks (replication stress) and γH2AX as a marker of DSBs (failed repair of ssDNA leading to double stranded breaks) (Chanoux et al., 2009, Dobbelstein and Sorensen, 2015, Karnitz and Zou, 2015, Macheret and Halazonetis, 2018, Zhang et al., 2016b).

PDCLs selected from the squamous subtype were classified as high or moderate replication stress based on their signature, and the Classical Pancreatic PDCLs as low replication stress based upon the Replication Stress signature (Figure 5-9). Squamous PDCLs (high and moderate replication stress) had significantly higher levels of pRPA at rest ($P < 0.0001$) (Figure 5-9a). Analysing the total number of pRPA foci per cell demonstrated a pattern suggesting increased frequency of foci per cell in the squamous subtype (Figure 5-9a). By defining pRPA positive cells as those with ≥10 foci per cell, the number of positive cells is significantly higher in the squamous subtype ($P < 0.0001$), implying that there is significantly increased frequency of stalled replication forks and single stranded DNA in squamous PDCLs. These are hallmarks of replication stress and suggests that the replication stress signature is associated with functional replication stress in the PDCLs with a high or moderate signature score (Figure 5-9).

γH2AX positive cells were defined as those with ≥10 foci per cell, identifying cells with a high number of double stranded DNA breaks. PDCLs with high levels of replication stress had a higher proportion of γH2AX positive cells at rest (no exposure to DNA damaging agents or IR) ($P = 0.0086$) (Figure 5-9). This was evident in TKCC02.1 and TKCC10, PDCLs with high replication stress and concurrent homologous recombination deficiency (Figure 5-9, Table 5-1). In response to 4Gy ionising radiation (IR), all PDCLs had increased numbers of pRPA and γH2AX positive cells at 2 and 4 hours after exposure (Figure 5-9 d & e). This demonstrates the effects of IR on DNA damage in generating both single and double-stranded DNA breaks. However, PDCLs TKCC02.1, TKCC10 and TKCC15 had persistent levels of higher pRPA and γH2AX positive cells at 20hours, a time-point at which pRPA and γH2AX should return to normal level in cells with no replication defects that are able to repair this level of DNA damage (Figure 5-9). This suggest that these PDCLs, in contrast to low replication stress PDCLs, are unable to return to a baseline level of repair and may be reflective of the persistent levels of elevated replication stress.

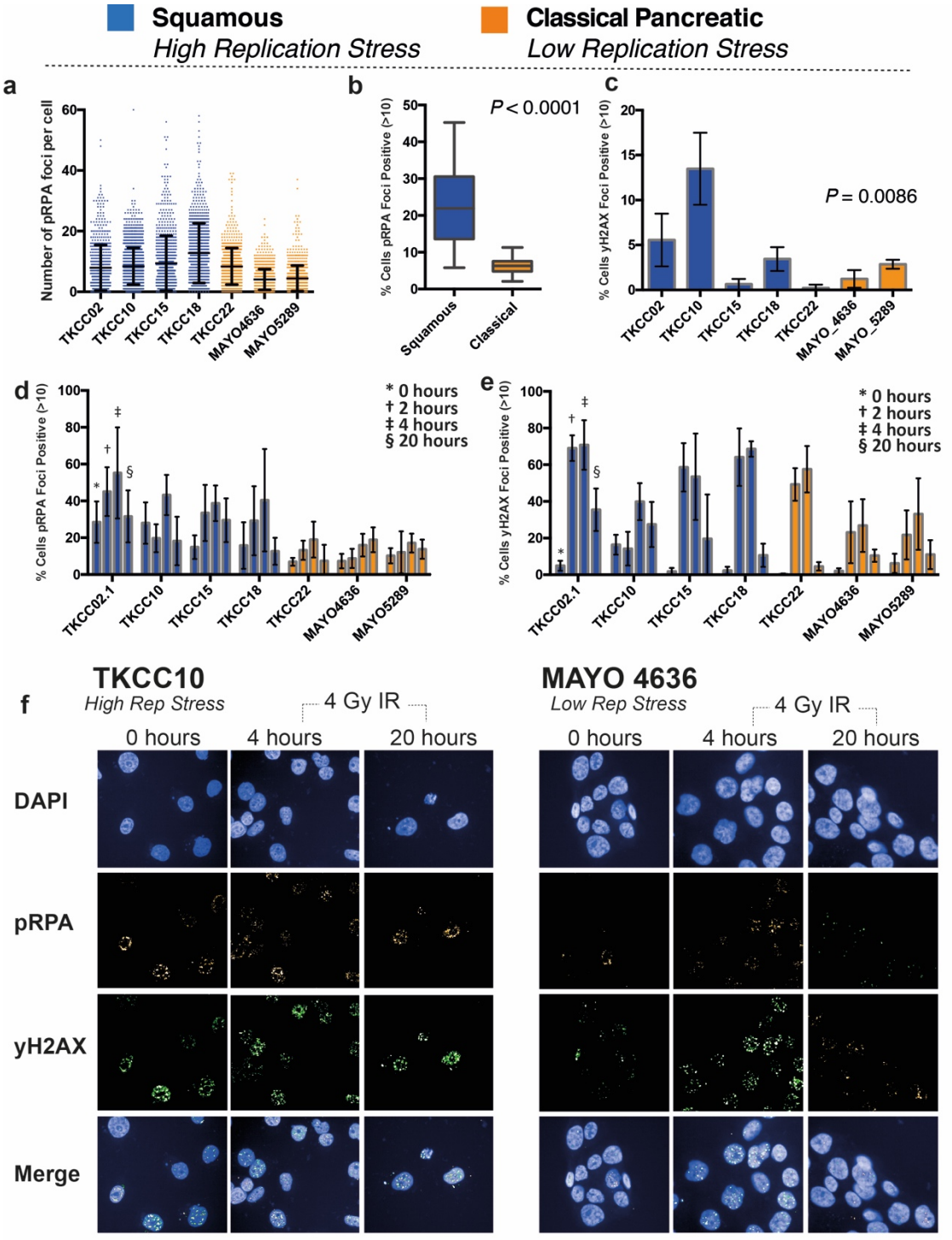

Figure 5-9 Immunofluorescent quantification of Replication Stress in PDCLs. The squamous (high replication stress signature), but not the Classical Pancreatic (low replication stress signature), PDCLS demonstrated functional evidence of activation of the replication stress response at normal conditions. The significant elevation of pRPA at normal conditions demonstrate an increased baseline replication stress response in the squamous (high replication stress signature) PDCLs. Immunofluorescent quantification of pRPA (a and b) and γH2AX (c) at normal conditions are elevated in the Squamous (blue), but not the Classical Pancreatic (orange) PDCLs. pRPA and γH2AX positive cells are defined as cells with > 10 foci of pRPA and γH2AX per cell. Immunofluorescent quantification of pRPA (d) and γH2AX (e) after 0 – 20 hours of 4Gy IR in PDCLs. f) Immunofluorescent images of TKCC10 (Squamous,) and Mayo-4636 (Classical Pancreatic) PDCLs at normal, and 4 and 20 hours post 4Gy IR.

Reverse phase protein arrays (RPPA) were performed as part of a broad proteomic analysis of squamous versus progenitor PDCLs to validate transcriptomic changes between molecular subtypes. Validated functional read-outs of DNA replication and repair were used to compare subgroups, including activation and phosphorylation of ATM and ATR substrates, γH2AX, ChK1 and ChK2. These are all activated in response to replication stress after activation of ATR and ATM by pRPA (Zeman and Cimprich, 2014). In the squamous PDCLs at rest, ATM and ATR substrates, γH2AX, Chk1 and Chk2 protein phosphorylation were significantly elevated in comparison with the Classical Pancreatic PDCLs (Figure 5-10). This correlates with the immunofluorescent findings suggesting a baseline level of elevated replication stress leading to single stranded DNA, and activation of DNA damage response checkpoints and pathways to repair these such as ATM, ATR, Chk1 and Chk2. γH2AX can be activated by numerous pathways, including but not exclusively, by ATR activation in response to replication stress. The RPPA analysis, thus, supports the transcriptomic data with increased activation of proteins involved in the replication stress response in those with a high replication stress signature (Figure 5-10).

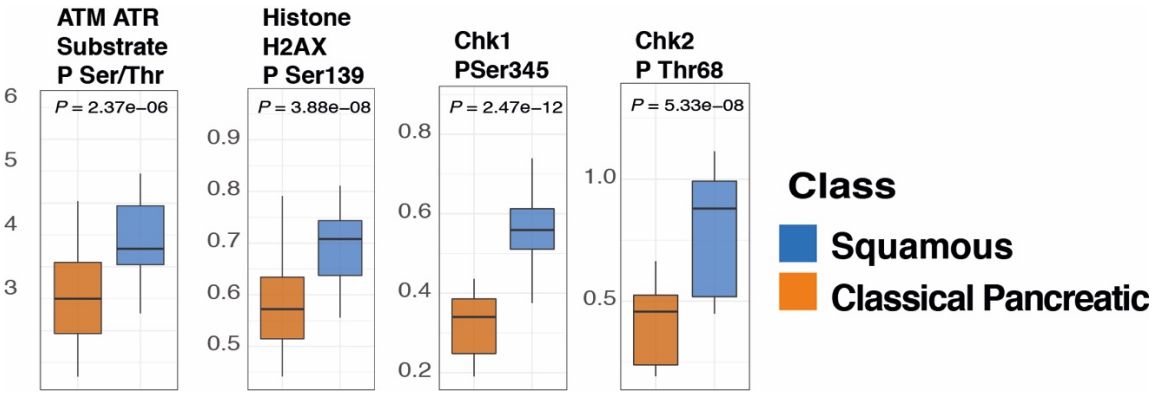

Figure 5-10 RPPA analysis of key proteins in the replication stress response. The squamous PDCLs (high replication stress) demonstrate proteomic evidence of increased activation of the replication stress response comparative to the Classical Pancreatic (low replication stress) subtype. Proteomic analysis using RPPA of a panel of PDCLs demonstrated that replication stress response proteins are differentially activated in the squamous subtype, including substrates of ATR and ATM signalling, yH2AX, Chk1 and Chk2. This supports the transcriptomic data that demonstrates enrichment of these in the squamous subtype.

In summary, these functional data validate the transcriptomic signature of replication stress, which is associated with the squamous subtype in PDCLs, and that these tumours demonstrate functional dependencies on cell cycle control and DNA damage response proteins. This implies a potential therapeutic vulnerability in these tumours and may offer a subtype specific target within the poor prognostic Squamous subtype of PDAC. This could

potentially be targeted with novel small molecule inhibitors of these pathways in this subgroup.

5.3.3 Replication stress signature in bulk tumour profile of PDAC

To extend the pre-clinical data further into larger sample sets, the relationship between the replication stress signature and molecular subtypes in bulk tumour samples was investigated using published transcriptomic data sets of PDAC (Bailey et al., 2016), (Cancer Genome Atlas Research Network. Electronic address and Cancer Genome Atlas Research, 2017). This included the RNA sequencing sets acquired via the International Cancer Genome Consortium (ICGC), totalling 94 patients with primary resectable PDAC (Figure 5-11). Since the immunogenic and ADEX subtypes were sub-classifications of the Classical Pancreatic subtype in this cohort, tumours were classified as either Classical Pancreatic or Squamous as was done with the PDCLs (Figure 5-11). This recapitulated, as seen in the PDCLs, a significant association between molecular subtype and the replication stress signature. The squamous subtype was significantly enriched for the Replication Stress signature ($P < 0.006$) (Figure 5-11). By classifying the top-ranking quartile of replication stress signature score as high demonstrated that 50% of squamous tumours were within this group, compared to only 21% of the Classical Pancreatic tumours (Figure 5-11).

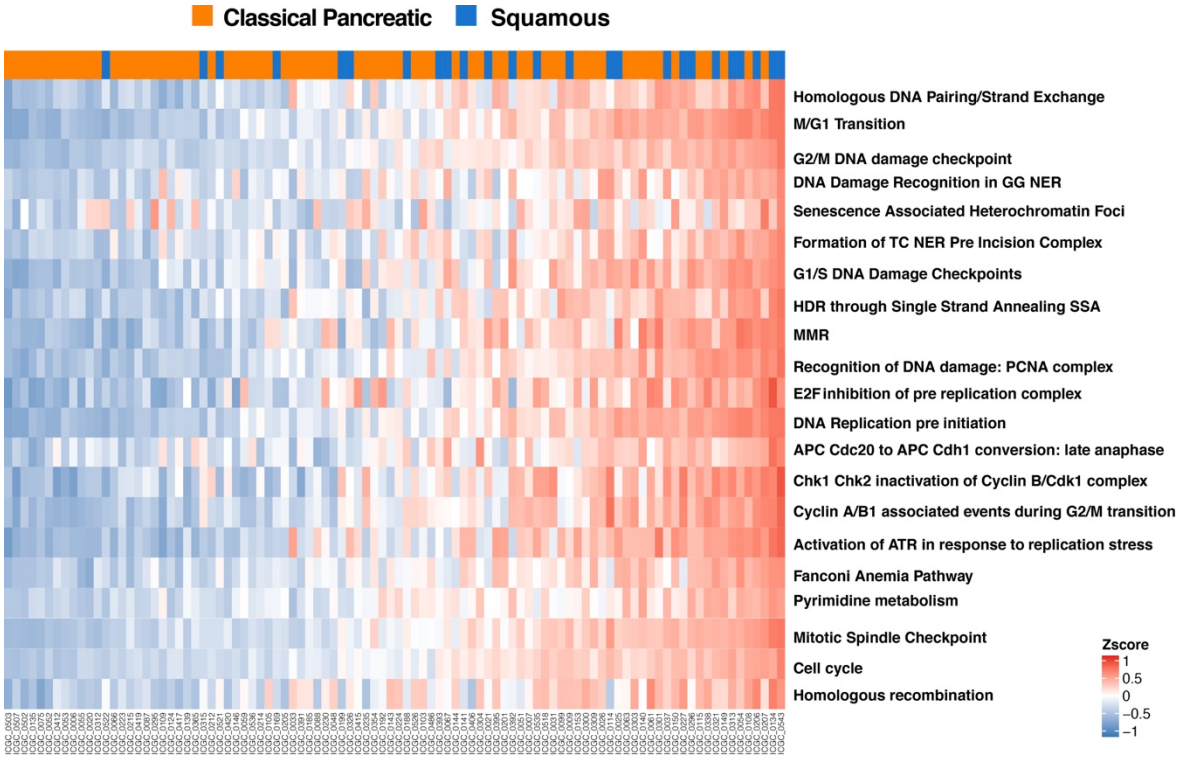

Figure 5-11 The association between molecular subtype and replication stress signature in the ICGC RNA sequenced set (*n* = 94). In this cohort, high replication stress was significantly enriched for the squamous subtype (*P* < 0.006). Heatmap of pathways and molecular processes (GO terms) involved in DNA maintenance and cell cycle regulation activated in replication stress and DNA damage response. The Replication Stress transcriptomic signature is based on the replication stress response and generated as a cumulative score of gene expression secondary to replication stress. Tumours are ranked from right to left based on the novel transcriptomic signature score of replication stress (a composite score of each individual GO term) and molecular subtype is indicated in the top bar showing the association between activation of replication stress and the squamous subtype. High replication stress was defined as the top ranking quartile in this cohort.

The replication stress signature was next applied to The Cancer Genome Atlas (TCGA) PDAC and the ICGC micro-array transcriptomic sets (Figure 5-12). Both sets were classified as either Classical Pancreatic or Squamous to match the analyses performed in the PDCLs and the ICGC RNAseq sets. The TCGA set was analysed to only include those with sufficient cellularity (ABSOLUTE purity ≥0.2) as the lower cellularity samples are unreliable when clustering into subtypes. In this set, the top ranking quartile of replication stress signature, as in the ICGC set, was associated with significant enrichment of the squamous subtype ($P = 0.009$) (Figure 5-12). This analysis was next applied to the ICGC micro-array set, which again was classified as either Classical Pancreatic or Squamous. As seen in the previous RNA sequenced cohorts, there was an association between high replication stress and the squamous subtype ($P = 0.037$) (Figure 5-12). However, this association was not as strong and may be due to the lower cellularity of the micro-array cohort and the implications of using a smaller gene set in order to classify tumours according to subtype.

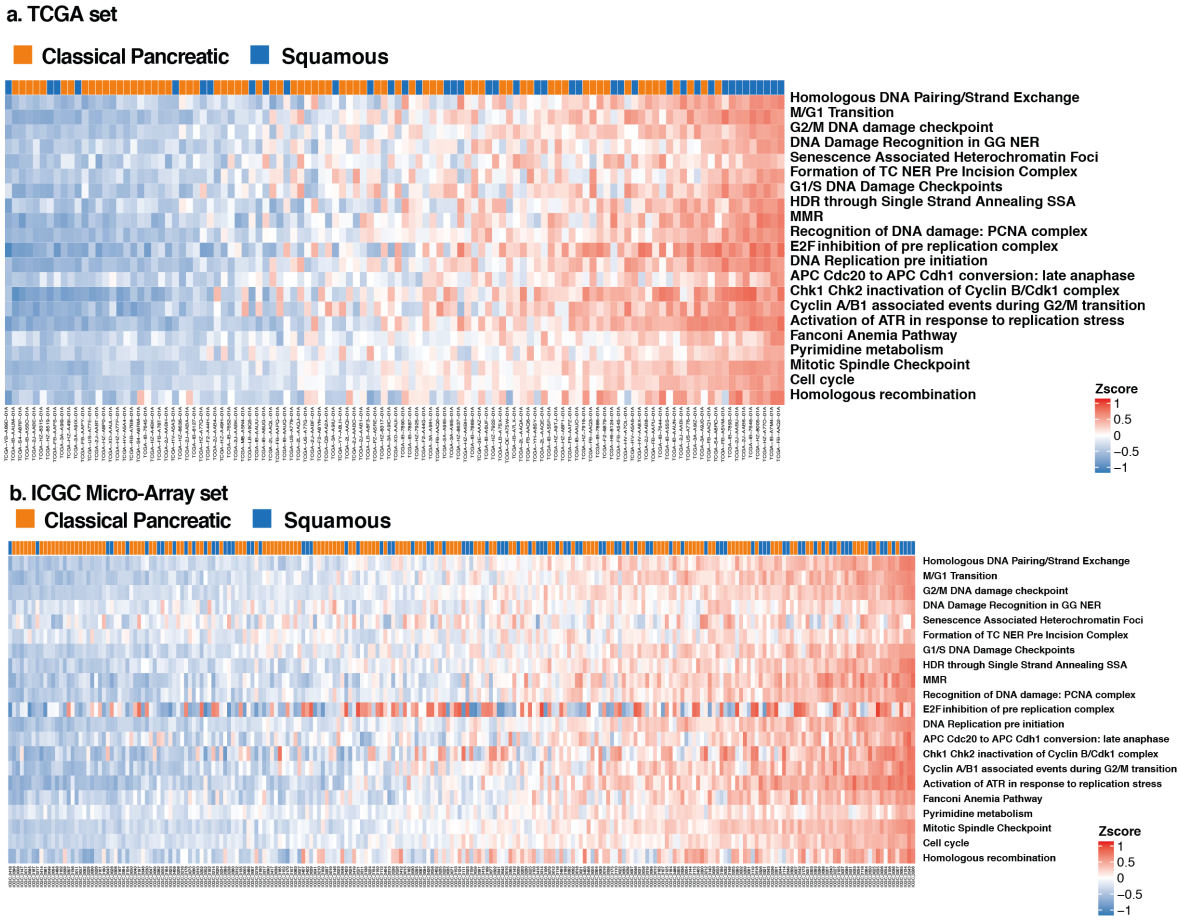

Figure 5-12 The association between molecular subtype and replication stress in the (a) TCGA (*n* = 112) and (b) ICGC micro-array (*n* = 232) cohorts. In both the TCGA (*P* = 0.009) and the ICGC micro-array cohort (*P* = 0.037), high replication stress was significantly enriched for the squamous subtype. Heatmap of pathways and molecular processes (GO terms) involved in DNA maintenance and cell cycle regulation activated in replication stress and DNA damage response. The Replication Stress transcriptomic signature is based on the replication stress response and generated as a cumulative score of gene expression secondary to replication stress. Tumours are ranked from right to left based on the novel transcriptomic signature score of replication stress (a composite score of each individual GO term) and molecular subtype is indicated in the top bar showing the association between activation of replication stress and the squamous subtype. High replication stress was defined as the top-ranking quartile in this cohort.

These results demonstrate that squamous PDAC is associated with high replication stress signature in bulk tumours. These findings support the PDCL data and suggests that the replication stress signature and its association with the squamous subtype is not an artefact of cell culture conditions. This further supports high replication stress as a potential therapeutic vulnerability that is enriched in this poor prognostic group of patients. Next, the therapeutic opportunities to target high replication stress was investigated using novel agents targeting DNA damage repair and the cell cycle.

5.3.4 Targeting Replication Stress in PDCLs

A therapeutic hypothesis for targeting tumours with high replication stress was developed by investigating early phase clinical trial and robust preclinical data (Karnitz and Zou, 2015, Zhang et al., 2016b, Zheng et al., 2017, Yap et al., Do et al., 2015). This was overlapped with the transcriptomic and proteomic analysis in the PDCLs described above. Several targets were identified based on these findings. The significant enrichment of genes expressed controlling the G2/M checkpoint in PDCLs and bulk tumours (such as *WEE1* and *CHEK1*) (Figure 5-7), and the dependence on ATR activation in response to replication stress (Figure 5-8) suggested that inhibitors of WEE1, CHEK1 and ATR would be high ranking targets to investigate. This is in keeping with early phase clinical trial results which have shown promise using these agents in numerous cancer types, including PDAC. The WEE1 inhibitor, AZD1775, has shown single agent activity in patients with advanced solid tumours with the best responses seen in those with evidence of DDR deficiency (Do et al., 2015). Pre-clinical and early clinical studies have shown great promise using ATR inhibitors in various tumour types, both as monotherapy or in combination (Kim et al., 2017, Yap et al.). Furthermore, the CDK4/6 inhibitor Palbociclib has recently been approved for use in combination in hormone -positive, HER2-negative breast cancer and shown promise in pre-clinical studies of PDAC (Chou et al., 2017, Turner et al., 2015). Based on this data, and the significant enrichment of the cell cycle checkpoints in a sub-group of patients, a therapeutic hypothesis to target these with novel agents targeting replication stress was generated.

As part of a high throughput discovery effort for of therapeutic targets in PDAC, an siRNA screen was performed in a subset of PDCLs. Targeting genes controlling DNA damage repair and replication was investigated in a sub-analysis and compared amongst molecular subtypes (Figure 5-13). Squamous subtype PDCLs demonstrated a functional dependency on DNA damage response proteins, including ATM, ATR and Chk1 (Figure 5-13). This is in keeping with the results from the immunofluorescent and RPPA analyses suggesting higher baseline levels of replication stress in the squamous PDCLs and a subsequent dependency on these proteins and checkpoints for maintaining genomic integrity and cell survival.

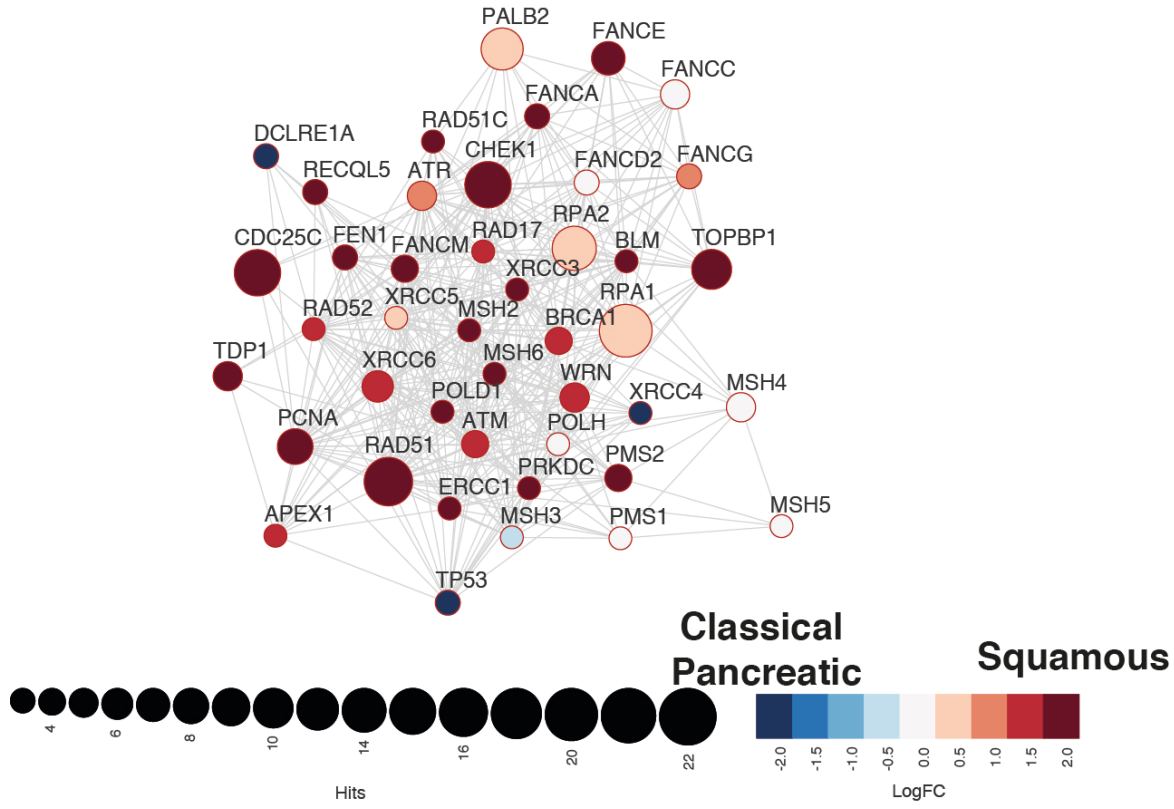

Figure 5-13 siRNA screen of PDCLs targeting DDR and cell cycle control. The squamous PDCLs demonstrate a functional dependency on genes involved in DDR and replication stress. siRNA screen demonstrating transcriptome functional interaction (FI) sub-network, and preferential dependencies of cell cycle control and DNA maintenance genes in the squamous subtype. Different node colours represent dependencies in different molecular subtypes, and the size of each node is relative to the number of siRNA hits.

Next, PDCLs were selected and classified based on the novel replication stress signature score (high, medium, low) irrespective of DDR status. This revealed multiple targets at different points during the cell cycle, which corresponds with the enriched expression of genes such as *WEE1* and *CHEK1* in squamous PDAC tumours (Figure 5-15a). Therapeutic agents were selected based on the mechanism of mechanism (cell cycle checkpoint inhibitor or targeting replication stress) and with evidence of pre-clinical or clinical effectiveness in other studies. Based on this an initial panel of 5 agents were selected targeting: CHK1, CDK4/6, PLK4, ATR and WEE1 (Table 5-4).

Table 5-4 Novel agents targeting replication stress and the cell cycle

Drug	Protein Target	Cell Cycle target	References
AZD6738	ATR	S-phase, G2 / M checkpoint	(Lecona and Fernandez-Capetillo, 2018, Yazinski et al., 2017, Williamson et al., 2016, Reaper et al., 2011, Yap et al.)
AZD1775	WEE1	G2 / M checkpoint	(Zheng et al., 2017, Geenen and Schellens, 2017, Leijen et al., 2016b, Leijen et al., 2016a, Do et al., 2015, Rajeshkumar et al., 2011)
AZD7762	CHK1	G2 / M checkpoint	(Zhang et al., 2016b, Al-Ejeh et al., 2014)
Palbociclib	CDK 4 / 6	G1 / S checkpoint	(Turner et al., 2015, Chou et al., 2017)
CFI-400945	Polo-like Kinase 4	Centrioles Duplication	(Lohse et al., 2017, Bedard et al., 2016)

Next a panel of PDCLs that reflected the range of replication stress scores and DDR status that has been previously defined in this chapter, and was suitable for therapeutic testing, was selected (Table 5-5). This generated a 2 x 2 grid of replication stress (high vs low) and DDR status (deficient vs proficient) and allowed testing of multiple potential biomarkers of therapeutic response (Figure 5-14).

Table 5-5 Replication Stress signature rank and DDR status in PDCLs available for therapeutic testing. Replication stress signature rank based on all 48 PDCLs that were sequenced.

	PDCL ID	Replication Stress Signature Rank	Structural Variation Subtype	Number of Structural Variations	BRCA Signature Rank	HR deficiency signature	*Mutations*	
							DDR Pathway	*TP53*
Replication Stress High DDR deficient	**Panc08.13**	1	Scattered	110	43		*ATM*	
	TKCC05	2	Scattered	131	6		*BRCA1, RPA1, RAD54, FANCA, CK12*	Mutant
	TKCC10	3	Unstable	484	7	Yes	*BRCA1**	Mutant
	TKCC02.1	11	Unstable	527	1	Yes	*BRCA2**	
	PaCadd137	24	Stable	49	44		*PPPR2R2B, PPPR2R2D*	Mutant
Replication Stress High DDR Proficient	**TKCC07**	6	Focal	95	13			Mutant
	TKCC17	12	Scattered	61	20			Mutant
	TKCC18	15	Stable	33	37			Mutant
	TKCC15	16	Stable	97	34			
	TKCC06	22	Stable	32	32			
Replication Stress Low DDR Deficient	**MAYO-4636**	33	Scattered	82	10			Mutant
	TKCC26	34	Focal	214	21			Mutant
	TKCC22	35	Unstable	408	5	Yes	*RPA1**	Mutant
Replication Stress Low DDR Proficient	**MAYO-4911**	26	Focal	120	28			Mutant
	MAYO-5289	32	Scattered	155	46			

*Demonstrates bi-allelic mutation in DDR gene

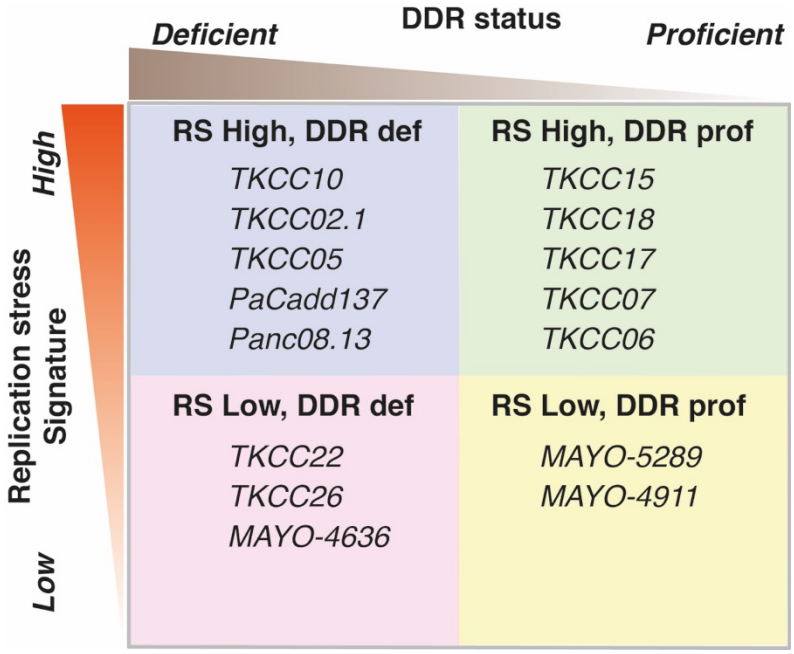

Figure 5-14 Replication stress and DDR status in PDCLs selected for therapeutic testing. Replication stress was defined by the transcriptomic signature of replication stress. DDR deficiency was defined using putative biomarkers including mutations in the homologous recombination pathway, number of structural variations (> 200), high ranking BRCA mutational signature and the novel HR deficiency signature. PDCLs can be classified as either high replication stress, DDR deficient (RS high, DDR def); high replication stress, DDR proficient (RS high, DDR def), low replication stress and DDR deficient (RS low, DDR def) or low replication stress and DDR proficient (RS low, DDR prof).

Therapeutic testing was performed initially on a panel of PDCLs that reflected the range of replication stress and DDR deficiency. More extensive testing was done using the WEE1 (AZD1775) and ATR (AZD6738) inhibitors as these were most promising based on pre-clinical evidence and early phase clinical therapeutic development, and most likely to target the replication stress identified in PDCLs (Figure 5-8).

Sensitivity to novel agents was assessed using cell viability response curves after PDCLs were treated with increasing doses of agents inhibiting CHK1 (AZD7762), CDK 4/6 (Palbociclib) and PLK 4 (CFI-400945). The replication stress signature predicted differential responses to CHK1 inhibition (Figure 5-15d). PDCLs with high replication stress (TKCC10, TKCC02.1) were 10-fold more sensitive to CHK1 inhibition when compared with those of low replication stress (Mayo-4636, TKCC22) (Figure 5-15 d). Similar findings were found using Palbociclib, however the DDR defective PDCL TKCC02.1 *(RS high, DDR def)* demonstrated resistance to CDK4/6 inhibition, likely secondary to low *RB1* expression(Chou et al., 2017) (Figure 5-15b). The PLK4 inhibitor

response need to be interpreted with some caution at this stage due to the marked differences seen in drug response amongst the PDCLs treated (Figure 5-15c).

In summary these results suggest that targeting the cell cycle checkpoints holds promise in PDAC with high replication stress. Due to the later stages of clinical development, with evidence of response and tolerability in PDAC and other cancer subtypes, the next stage of investigation was focused on the ATR and WEE1 inhibitors.

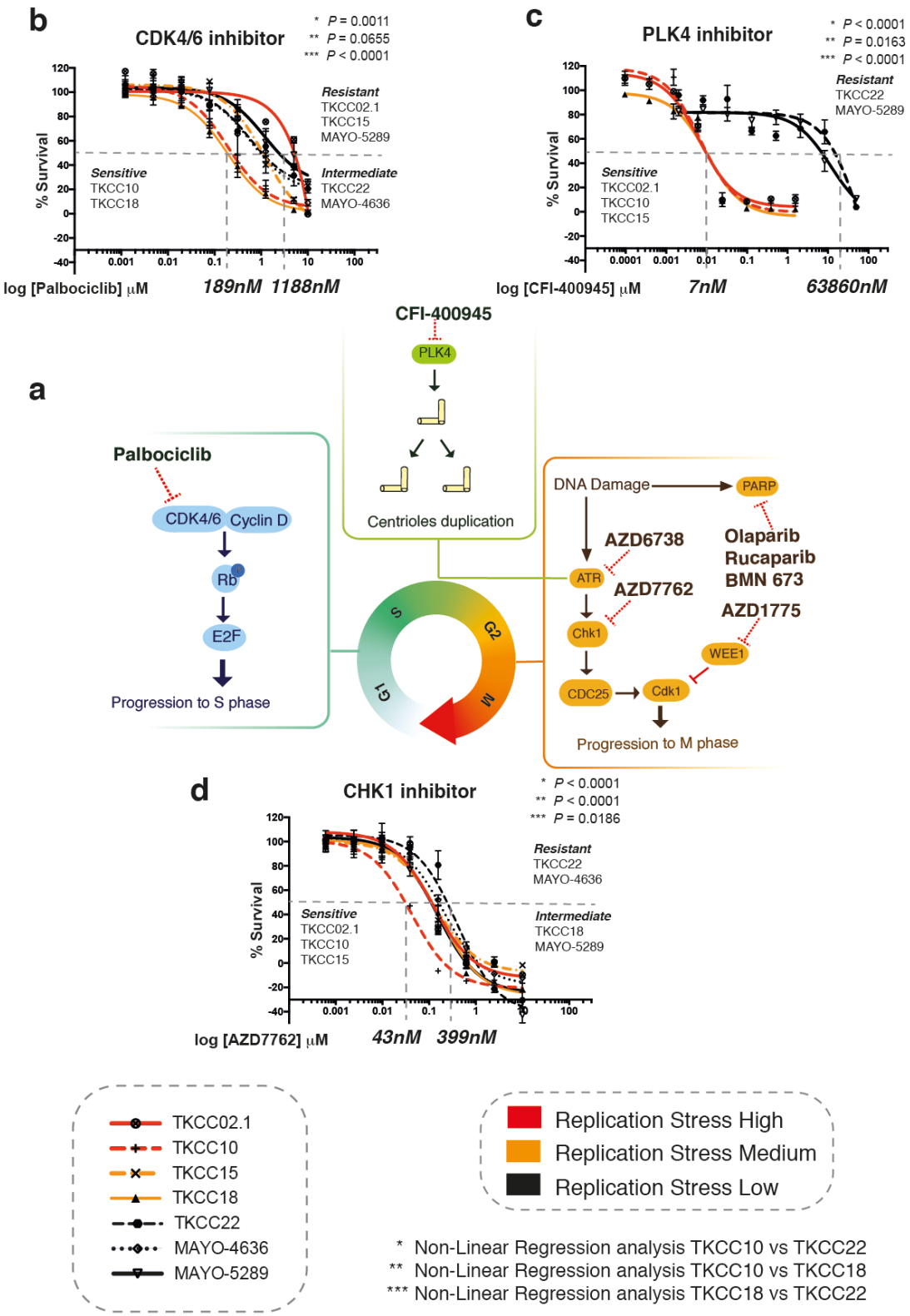

Figure 5-15 Targeting the cell cycle checkpoints and replication stress in PDAC. a) Agents currently in clinical trial or approved for use in other cancer types that target cell cycle checkpoints. Cell viability curves for agents inhibiting a) CDK4/6 (Palbociclib) b) PLK4 (CDI-400945) and c) Chk1 (AZD7762). PDCLs were classified by replication stress signature score as high (red), medium (orange) and low (black).

Due to earlier analysis (Figure 5-7) demonstrating significant enrichment of the G2/M cell cycle checkpoint and activation of ATR, and the promising early clinical trial results in other cancer types, more extensive testing was done using inhibitors of ATR (AZD6738) and WEE1 (AZD1775) (Figure 5-16). PDCLs were defined as high, low and medium replication stress based on the relative replication stress signature score (Figure 5-16a) and cell viability assessed after 72hrs of treatment of increasing doses of both agents. This demonstrated that there is a general trend of increased sensitivity to both ATR and WEE1 inhibition as the replication stress signature score increases (Figure 5-16). When comparing each subgroup with each other, this fails to reach statistical significance due to 1 or 2 outliers amongst each subgroup (n = 5) making this study underpowered to statistically confirm these differences. However, the general trend of increased sensitivity as replication stress increases suggests that this may predict response to ATR and WEE1 inhibition. Unfortunately, the current study is underpowered and not designed to investigate resistance mechanisms to these agents.

Remarkably and importantly these responses were independent of DDR status. The DDR defective PDCL TKCC22 *(RS low, DDR def)* (high ranking BRCA point mutational signature, unstable genome and SV signature positive) was highly resistant to WEE1 and ATR inhibition. In contrast TKCC 15 and TKCC18 (*RS high, DDR prof)* are both sensitive to ATR and WEE1 inhibition yet have no evidence of DDR deficiency and previously resistant to platinum and PARP inhibition (Figure 5-3, Figure 5-4). These data suggest that response to cell cycle checkpoint inhibitors is independent of DDR status, and the replication stress signature is a more reliable biomarker of therapeutic response. These results demonstrate a therapeutic vulnerability that can potentially be targeted in tumours with high replication stress and this novel transcriptomic biomarker can be tested and refined in clinical trials.

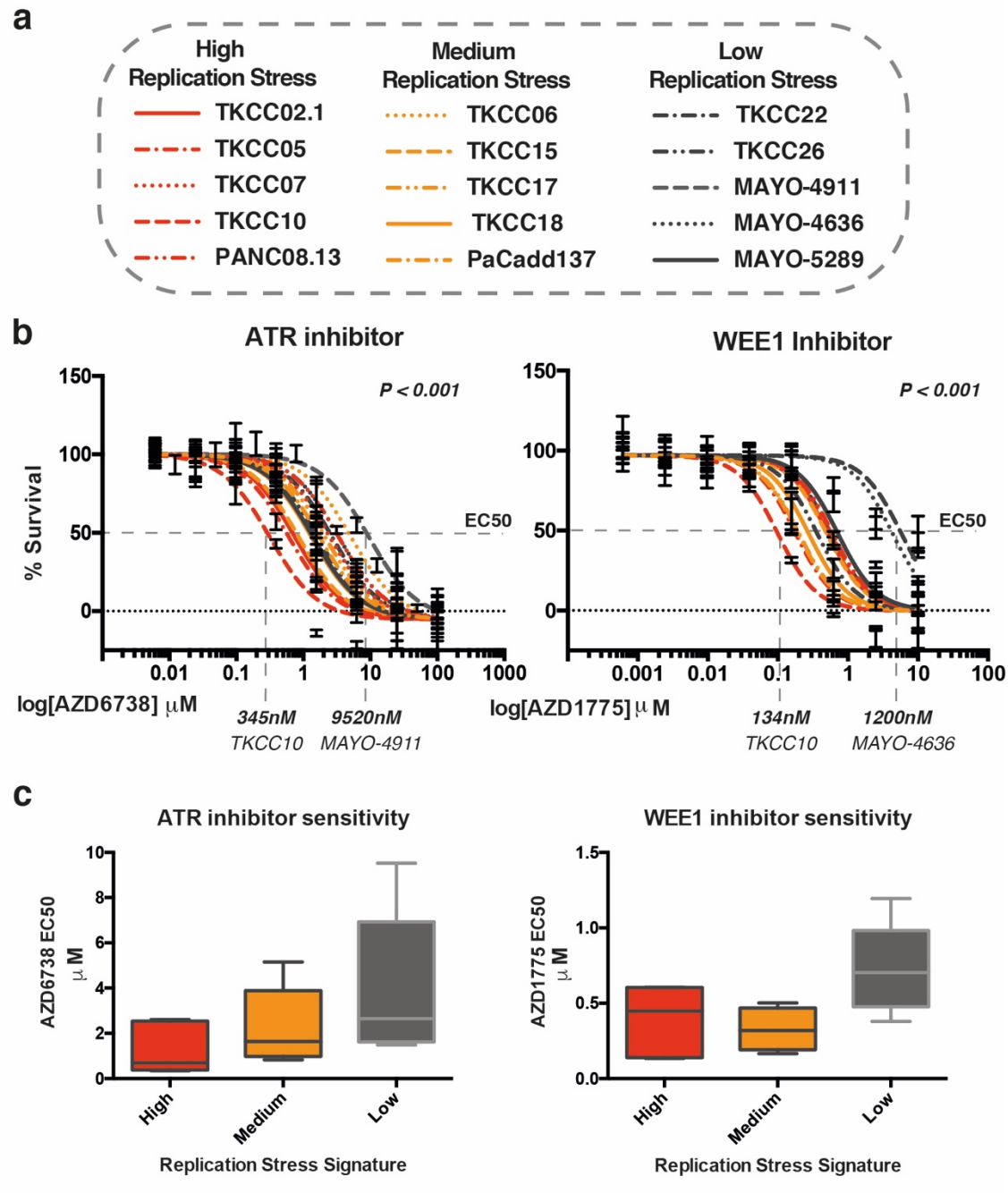

Figure 5-16 PDCLs with High Replication Stress is more sensitive to ATR and WEE1 inhibition. a) PDCLs were classified as either high (red), medium (orange) or low (tungsten) on the replication stress scale (based on the novel transcriptomic signature). b) Dose response curves (EC50 shift) for ATR and WEE1 inhibitors calculated using MTS assay after 72 hours of drug treatment. c) Mean relative EC50 for PDCLs stratified by replication stress score. Each boxplot represents mean EC50, box and whiskers represent minimum and maximum EC50 with 95% confidence interval. Relative EC50 significantly underestimates EC50 in very resistant cell lines (that does not reach 0% survival) and thus difference is likely to be much higher than represented. PDCLs with a high and medium replication stress signature scores were more sensitive to ATR or WEE1 inhibition than those with low replication stress scores.

5.3.5 Targeting Replication Stress *In Vivo*

In order to build on the preclinical results obtained in the PDCLs and generate a robust preclinical platform of evidence to take this strategy into clinical trials, the *in vivo* effects of targeting replication stress were investigated. 3 PDCLs were selected for implantations as xenografts into CD-1 nude mice. PDCLs were selected based on their transcriptomic and genomic signatures of replication stress and DDR deficiency, and previous evidence of satisfactory growth as xenografts when implanted. These were TKCC10 *(RS high, DDR def;* unstable genome, high ranking BRCA mutational signature, *BRCA1* mutation), TKCC18 *(RS high, DDR prof;* stable genome, low ranking BRCA mutational signature, *ARID1A* mutant) and TKCC22 *(RS low, DDR def;* unstable genome, high ranking BRCA mutational signature, *RPA1* mutation). Treatment schedules were selected to reflect proposed clinical trials targeting DDR deficiency and replication stress via the *PRECISION-Panc* platform (discussed in Chapter 6).

PDXs were allowed to grow following transplantation until established and were of sufficient size to be measured with a high level of accuracy (volume at least $50mm^3$). This is lower than used for bulk tumour PDXs, as preliminary experiments demonstrated rapid disease progression once a size of 150mm3 is reached that makes therapeutic evaluation not feasible. In each arm, 5 mice were implanted with 1 million cells after preliminary experiments demonstrated this produces satisfactory growth. This was followed by 4 weeks of treatment with either Olaparib monotherapy, AZD6738 monotherapy or a combination of Olaparib and AZD6738 (dosage schedules in Chapter 2 Methods). Saline administered by oral gavage was used as the control.

Treatment with AZD6738 as monotherapy, and in combination with Olaparib, induced excellent responses in the TKCC10 *(RS high, DDR def)* PDX (Figure 5-17). At the end of 37 days after treatment initiation, the saline control and Olaparib groups both reached tumour endpoints and were sacrificed, however, the AZD6738 containing groups demonstrated no evidence of tumour growth (Figure 5-17a). In the AZD6738 & Olaparib combination group there were 2 out of 5 tumours that demonstrated complete response to therapy with complete regression of the implanted tumour at autopsy.

In both the TKCC18 *(RS high, DDR prof)* and TKCC22 PDX *(RS low, DDR def)* groups there was no evidence of treatment benefit between any of the groups (Figure 5-17b & c). However, both models demonstrated growth rates between the 3 drug treatment arms that

were similar to that of the control treatment (Saline). In the TKCC18 *(RS high, DDR prof)* group, the saline control demonstrated no significant growth 48 days after treatment initiation (Figure 5-17b). Whereas, TKCC22 *(RS low, DDR def)* demonstrated a reduction in tumour size in all treatment arms, including the control, over this time period (Figure 5-17c). Due to these unexpected growth dynamics makes it impossible to draw any conclusions from these 2 xenograft models (TKCC18 and TKCC22) in terms of tumour response to therapy.

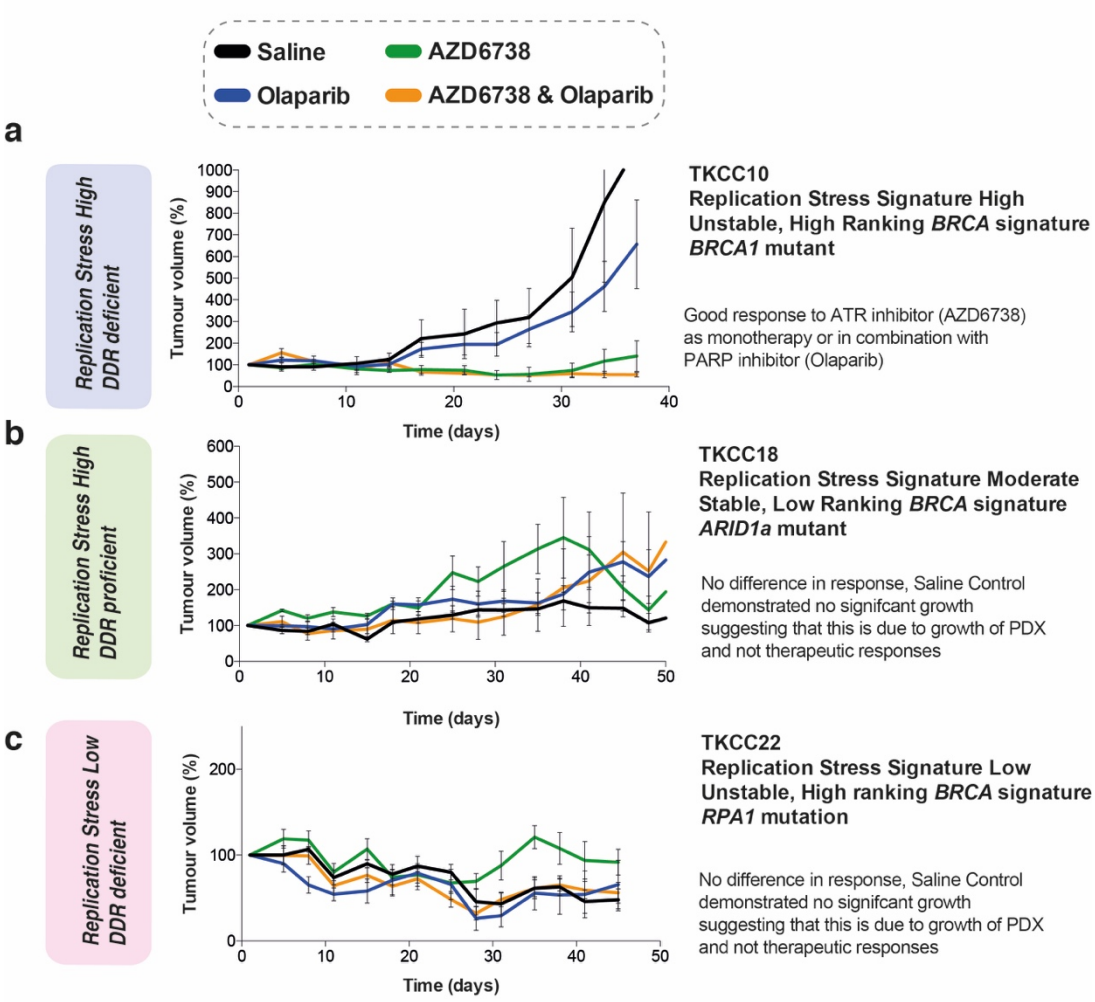

Figure 5-17 PDCL xenograft response to PARP and ATR inhibition. Clinical responses to ATR inhibition in combination and as single agent was seen in a high replication stress model (a). In Moderate (b) and low (c)replication stress models, there appeared to be inconsistent tumour growth within the model leading to results demonstrating no difference in the treatment regimes.

Xenograft growth depends on a number of factors (Aparicio et al., 2015, Hidalgo et al., 2014). In this case, the poor growth in both TKCC18 *(RS high, DDR prof)* and TKCC22 *(RS low, DDR def)* models suggest that even though there was significant expansion initially, certain factors prohibited further growth and establishment of the xenograft. These have previously demonstrated satisfactory growth on preliminary experiments and

was thus unexpected. On the other hand, TKCC10 *(RS high, DDR def)* demonstrated growth and establishment of tumours in both the Olaparib and Saline control groups (Figure 5-17a), but excellent disease control in the AZD6738 containing groups. In view of the findings in the other 2 models, these results should be interpreted with caution, but suggest that AZD6738 is an effective treatment in this model with high replication stress. The lack of response to Olaparib, however, is surprising as TKCC10 *(RS high, DDR def)* also demonstrates HR deficiency and a bi-allelic somatic *BRCA1* mutation.

The *in vivo* experiments presented here demonstrate some promise in the TKCC10 *(RS high, DDR def)* cell line PDX model but unfortunately the results from the other 2 models should be interpreted with caution. The results presented earlier in chapter generated from the PDCLs, however, are very promising for targeting replication stress in PDAC. This, along with results from other studies, suggest that this is a therapeutic strategy that warrants clinical testing in PDAC using precision oncology clinical trials. In order to design a suitable trial (discussed in Chapter 6), the relationship of replication stress with DDR deficiency was next investigated.

5.4 The relationship of DDR deficiency with Replication Stress in PDAC

In order to further investigate the relationship between DDR deficiency, replication stress, molecular subtype and therapeutic response an integrated analysis of RNAseq, WGS and therapeutic response data from PDCLs and the APGI cohort was performed. PDCL sensitivity data to ATR / WEE1 inhibition and Platinum was stratified based upon DDR status and the replication stress signature (Table 5-6). PDCLs were classified as high replication stress if ranked in the top 50% by the replication stress signature score. DDR deficiency was determined by either a high ranking (top 20%) BRCA mutational signature, unstable genome (or focal if > 200 SVs), HRD signature positive or mutations in the HR pathway (Table 5-1, Table 5-6).

PDCLs with high replication stress and DDR deficiency were sensitive to both ATR and WEE1 inhibition as well as Platinum (Table 5-6). PDCLs with high replication stress that were DDR proficient were more likely to be sensitive to ATR and WEE1 inhibition, but resistant to Platinum treatment (Table 5-6). The exceptions in this group included TKCC07 *(RS high, DDR prof)* and TKCC06 *(RS high, DDR prof)*, which was resistant to all treatments. PANC08.13 and TKCC17 *(RS High, DDR Prof)*, deemed high replication

stress by signature rank, were both more resistant to ATR inhibition than expected but remained sensitive to WEE1 inhibition (Table 5-6). Furthermore, Panc08.13 *(RS high, DDR def)* defined as DDR deficient because of *ATM* mutation in only one allele (but low BRCA mutational signature and HRD signature negative) was more sensitive to Platinum than expected. In the DDR deficient and low replication stress group, PDCLs were sensitive to platinum but more resistant to ATR and WEE1 inhibition (Table 5-6). In this group, MAYO-4636 *(RS low, DDR def)* was more resistant to platinum than predicted even though it was defined as DDR deficient based on high ranking BRCA mutational signature. PDCLs with low replication stress and DDR proficient were more resistant to all therapeutics (Table 5-6). The exception to this were MAYO-5289 *(RS low, DDR prof)*, which was more sensitive to ATR and WEE1 inhibition than predicted.

Table 5-6 PDCL sensitivity to ATR / WEE1 inhibition and Platinum stratified by DDR status and Replication Stress. Coloured heatmap reflects replication stress signature score (red = high) and drug sensitivity (green = most sensitive, red = resistant). In general, PDCLs with high replication stress are more sensitive to ATR and WEE1 inhibition, irrespective of DDR status. In general, platinum sensitivity is dependent of DDR status, irrespective of Replication Stress signature score.

PDCL DDR / Replication Status

- High Replication Stress / DDR Deficient
- Low Replication Stress / DDR Deficient
- High Replication Stress / DDR Proficient
- Low Replication Stress / DDR Proficient

Drug Response

- Sensitive
- Resistant

	Cell line	Replication Stress Signature Score	Replication Stress Signature Rank	SV subtype	HRD Signature Positive	BRCA signature rank	DDR Mutations	*TP53* status	*ATR Inhibitor* AZD6738 EC50 μM	*WEE1 Inhibitor* AZD1775 EC50 μM	*Platinum* Cisplatin EC50 μM
RS High DDR def	TKCC10	11.38	3	unstable	1	7	*BRCA1, ARID1A*	Mutant	0.345	0.134	3.249
	TKCC02.1	6.43	11	unstable	1	1	*BRCA2*		0.693	0.605	2.019
	TKCC05	11.43	2	scattered	0	6	*BRCA1, RPA1, RAD54L2, FANCA, CK12*	Mutant	0.410	0.145	6.231
	Pacadd137	0.93	24	stable	0	44	*PPPr2R2B, PPPR2R2D, ARID1A*	Mutant	1.635	0.164	3.234
	Panc08.13	14.07	1	scattered	0	43	*ATM*		2.606	0.449	3.140
RS High DDR prof	TKCC15	3.85	16	scattered	0	34			0.832	0.501	18.72
	TKCC18	4.08	15	stable	0	37	*ARID1a*	Mutant	1.12	0.364	10.09
	TKCC17	6.29	12	scattered	0	20		Mutant	2.617	0.272	-
	TKCC07	8.74	6	focal	0	13		Mutant	2.47	0.605	36.17
	TKCC06	1.96	22	stable	0	32			5.154	-	22.72
RS Lo DDR def	TKCC22	-5.54	35	unstable	1	5	*RPA1*	Mutant	4.332	0.77	6.659
	TKCC26	-5.43	34	focal (>200SVs)	0	21	*ARID1A*	Mutant	1.757	0.575	5.183
	Mayo-4636	-5.30	33	scattered	0	10		Mutant	2.644	1.195	9.964
RS Lo DDR Prof	Mayo-5289	-3.71	32	scattered	0	46			1.491	0.380	-
	Mayo-4911	0.39	26	focal	0	28		Mutant	9.52	0.703	9.353

Replication Stress Signature Score

- High Replication Stress
- Low Replication Stress

Several therapeutic response hypotheses for clinical testing can be generated from this pre-clinical platform of evidence. First, this suggests that a high-ranking replication stress signature, in general, predicts response to ATR and WEE1 inhibition. There are some outliers to this, such as the very resistant PDCLs TKCC06 *(RS high, DDR prof)* and TKCC07 *(RS high, DDR prof)*. Yet, this does generate a therapeutic biomarker question that requires clinical testing in PDAC.

MAYO-4636 *(RS low, DDR def)* was found to be resistant to Platinum treatment, despite a high ranking BRCA mutational signature. Interestingly, MAYO-4636 harbours no evidence of HR pathway mutations or any significant structural variation changes. This data, in conjunction with the significant sensitivity of PaCadd137 *(RS high, DDR def)* and Panc08.13 *(RS high, DDR def)* (low BRCA signature rank, but evidence of mutations in HR pathway), suggests that the BRCA mutational signature alone may not be a robust predictive biomarker of platinum response. From the data presented here, it suggests that mutations in the HR pathway, the HRD signature and structural variation changes (unstable or >200SVs if focal) is more predictive of Platinum response. This will require clinical testing using well validated mutational assays, such as in the PRIMUS-001 and -002 trials (see Chapter 6).

Based on this data, a therapeutic hypothesis was generated for testing in clinical trials. Tumours that are DDR deficient can be targeted with platinum therapy, or in the context of a patient with declining performance status, PARP inhibitors (Figure 5-18). Patients with high replication stress can be targeted with ATR or WEE1 inhibitors, and that these can be combined with PARP inhibitors or Platinum if concurrent DDR deficiency exist. This can be performed as a combination strategy such as Olaparib (PARP-inhibitor) with AZD6738 (ATR inhibitor) (explored in a novel trial design in Chapter 6). However, there is also growing pre-clinical evidence that sensitivity to ATR and WEE1 inhibitors persist after platinum resistance develops, thus providing a strategy for 2nd line therapy. This is further discussed in chapter 6 where a novel clinical trial targeting replication stress and DDR deficiency is designed. In cases of either of these present, novel agents such as immunotherapies are required to be developed with a valid hypothesis to be utilised in clinical trials.

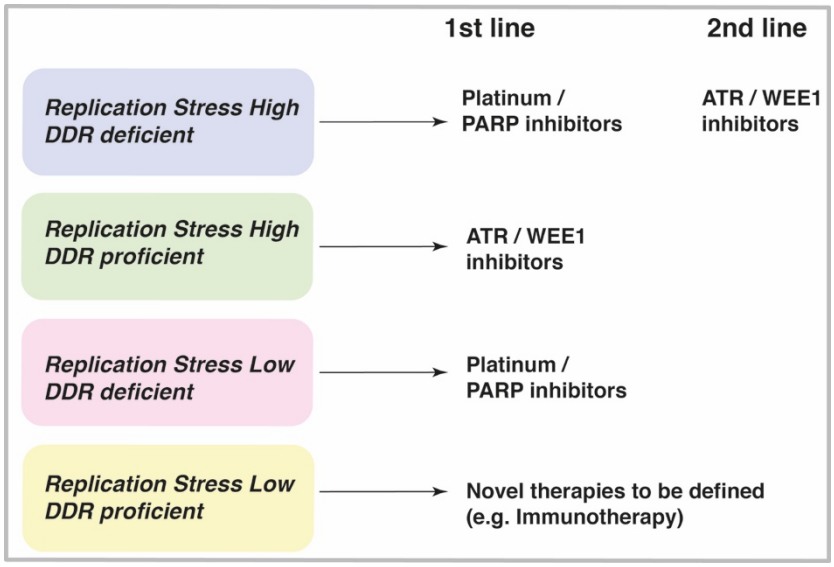

Figure 5-18 Therapeutic hypothesis targeting replications stress and DDR deficiency in PDAC. Patients that are DDR deficient can be targeted with Platinum based chemotherapy (good performance status) or PARP inhibitors (poor performance status). High replication stress can be targeted with either ATR or WEE1 inhibitors. In cases where both high replication stress and DDR deficiency co-exist, ATR / WEE1 inhibition can be used after platinum resistance develops.

In order to further investigate the relationship of replication and DDR deficiency and exactly how these therapeutic segments might align with one another, a comparison of replication stress and DDR deficiency was performed in the PDCLs. Using the PDCL sequencing data, a 2 by 2 grid was constructed to directly compare replication stress ranking and DDR deficiency (Figure 5-19). PDCLs were ranked on the Y-axis top to bottom from highest to lowest using the replication stress signature score. On the X-axis, PDCLs were ranked based on the Cosmic BRCA point mutational signature with corresponding HRD signature and SV subtypes annotated (Figure 5-19). This demonstrated that signatures of DDR deficiency and replication stress are independent of each other, yet high replication stress is enriched in the squamous subtype ($P = 0.007$, Chi-squared) (Figure 5-19). Therapeutic response data was overlapped based upon previously described experiments using ATR / WEE1 inhibitors and Platinum. This generates a 2 x 2 therapeutic box which can be utilised as a biomarker hypothesis for therapeutic responsiveness. PDCLs that are DDR deficient, high replication stress respond to both DDR agents and cell cycle checkpoint inhibitors; DDR deficient, low replication stress to DDR agents only; DDR proficient, high replication stress to cell cycle checkpoint inhibitors only; and DDR proficient, low replication stress to neither class of agent.

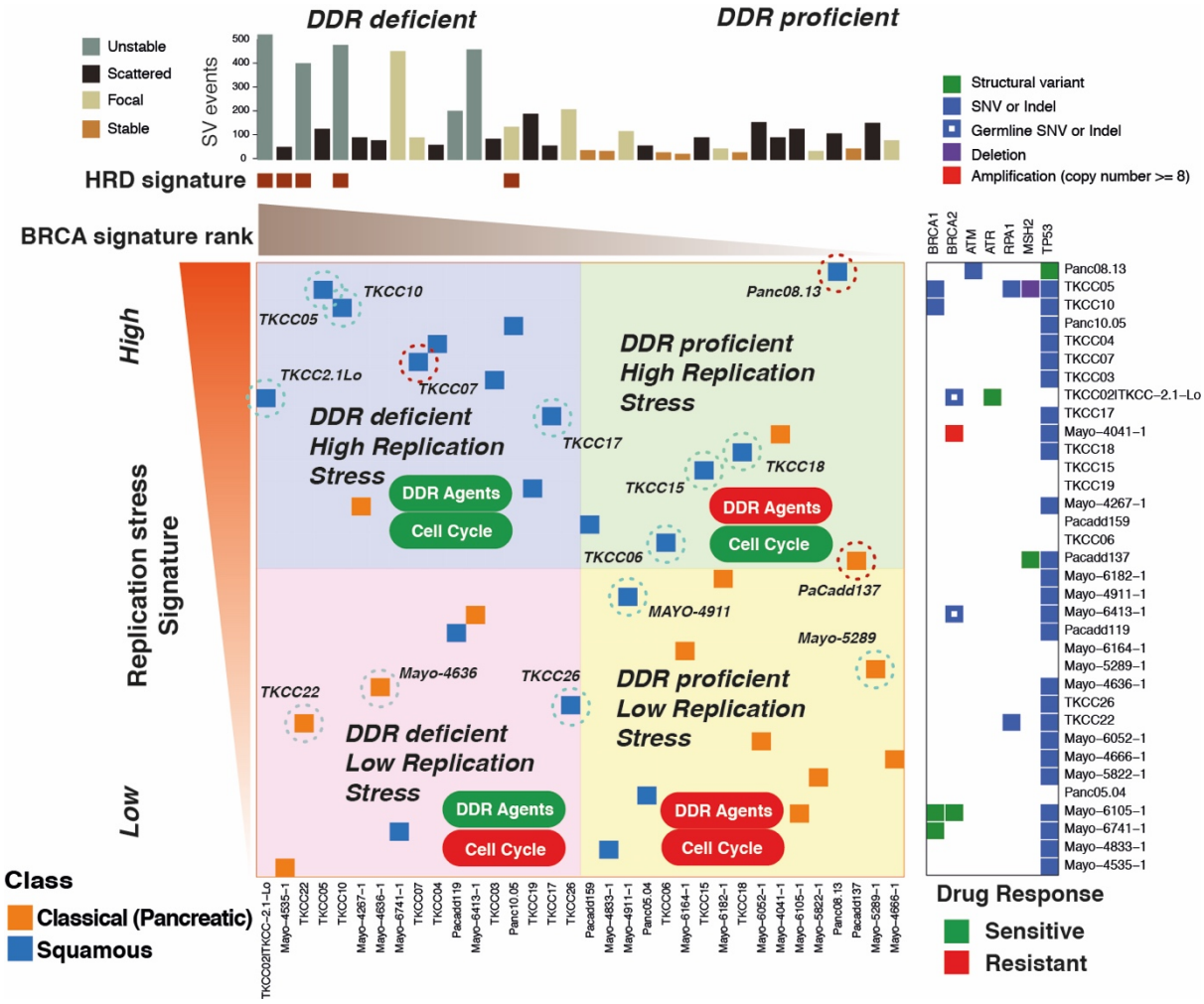

Figure 5-19 Relationship between DDR deficiency and Replication Stress in PDAC PDCLs. PDCLs are ranked based on a novel transcriptomic signature of replication stress (y-axis) and ranked based on a composite genomic readout of DDR deficiency (x-axis). DDR deficiency is a hierarchical score which incorporates the Cosmic BRCA mutational signature (signature 3), the number of structural variants distributed across the genome, and the HRD signature associated with BRCA deficiency. The combination of high/low states of each characteristic result in 4 groups. Squamous subtype PDCLs (blue squares) are associated with high replication stress (P = 0.007, Chi-squared). PDCLs tested are identified and encircled blue. PDCLs that were deemed DDR deficient (PaCadd137 and Panc08.13) despite a low ranking BRCA mutational signature, and DDR proficient (TKCC07) despite a high ranking BRCA mutational signature are encircled red.

In order to further examine the relationship between replication stress signature status and DDR deficiency, a 2 by 2 grid comparing these were constructed using the APGI whole genome and RNA sequenced data (Figure 5-20). The frequency of squamous tumours is much less in this cohort compared to the PDCLs (24%), but again demonstrates a strong association with high ranking replication stress (P = 0.009, Chi square test) (Figure 5-20). Clinical and PDX responses to platinum are overlaid in the figure and show an association between Platinum response and DDR deficiency (Figure 5-20).

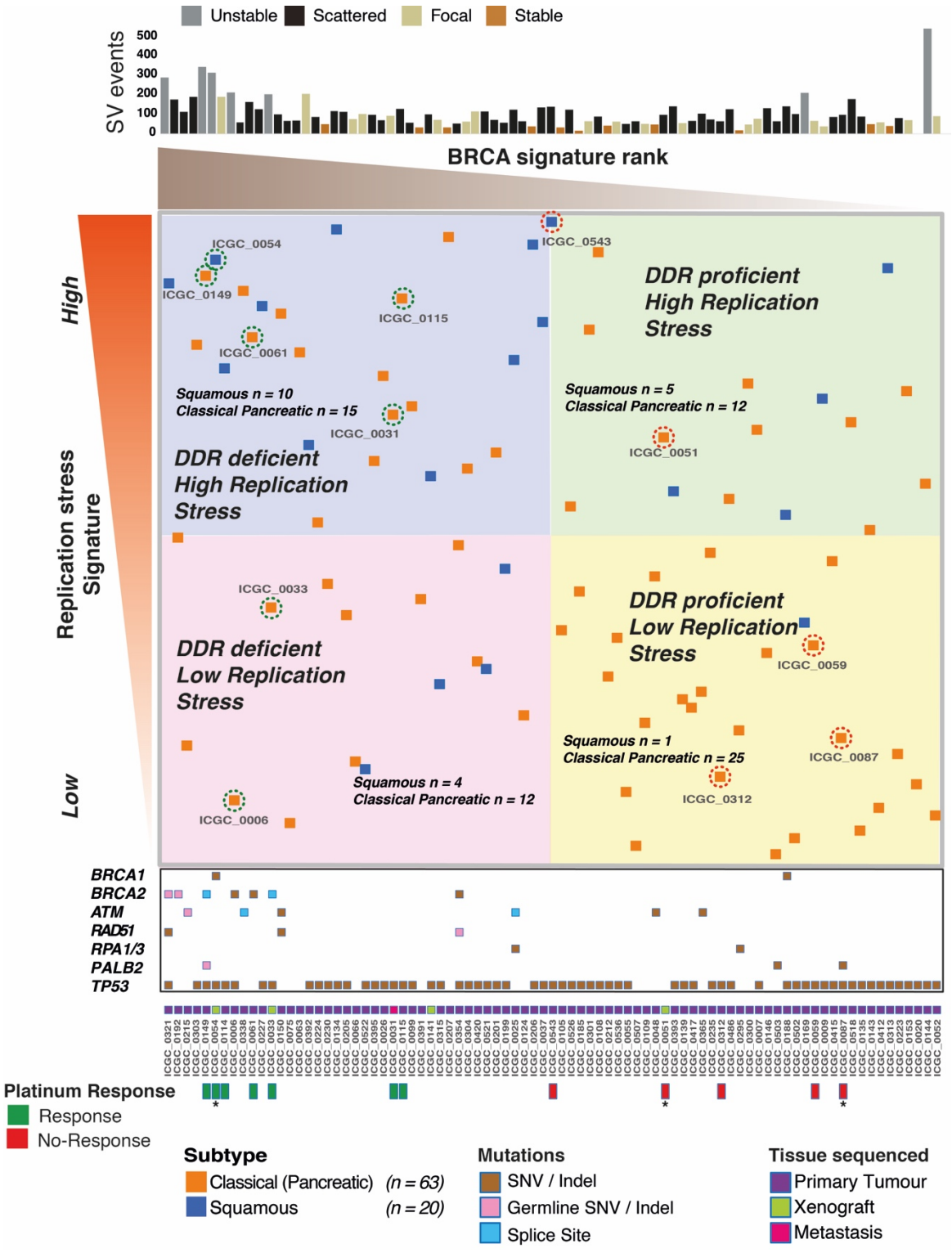

Figure 5-20 The relationship between DDR deficiency and Replication stress in the APGI clinical cohort. Patient samples that have undergone both WGS and RNAseq are ranked from left to right based on the BRCA mutational signature as a scale of DDR deficiency (x-axis) and top to bottom by the novel transcriptomic signature of replication stress (y-axis). HR pathway mutations and source of tissue sequenced is marked along the x-axis. Platinum response is marked along x-axis and related patient encircled at individual points where green represents response and red indicates resistance. * indicates PDX response data. Relevant molecular subtype frequency (squamous versus classical pancreatic) is indicated for each quadrant, demonstrating that Squamous PDAC was associated with high ranking replication stress score (15 out of 41 versus 5 out of 42) (P = 0.009; Chi-square test).

As in the PDCLs, the clinical set demonstrates that the transcriptomic signature of replication stress and putative biomarkers of DDR deficiency (unstable genome, COSMIC BRCA mutational signature) exist independent of each other. The pre-clinical therapeutic testing performed in this chapter show that high replication stress is a putative biomarker of therapeutic response to agents such as ATR inhibitors. Further refining replication stress response will require testing of larger cohorts of PDCLs and patient samples to define an optimal and practical biomarker that can predict and direct patient therapy. Using both replication stress and DDR biomarkers as separate entities can direct therapy in patients with PDAC either as combinations (e.g. PARP and ATR inhibitors) or as monotherapy. This strategy is further discussed in Chapter 6 which shows the design of a novel clinical trial to target replication stress and DDR deficiency in PDAC.

5.5 Discussion

Identifying therapeutic responsive subgroups in PDAC is crucial to improving survival in all stages of the disease. Only 15% of patients have localised surgically resectable disease of which 80% still succumb to recurrent disease within 5 years. This results in an overall 5-year survival in the region of only 5% for PDAC. Genomic sequencing studies and the development of novel agents has made DDR deficiency the most attractive therapeutic segment at present in PDAC (Waddell et al., 2015, Dreyer et al., 2017). Numerous clinical trials have identified clinically meaningful responses in unselected subgroups using Platinum in PDAC, and evidence of responses to PARP, ATR and WEE1 inhibitors is ever expanding in undefined subgroups of patient populations in other cancer types. The results presented in this chapter builds on the growing pre-clinical evidence that aims to define and refine biomarkers of response to Platinum and novel agents targeting DDR deficiency and replication stress, with sufficient evidence to support a clinical trial which has subsequently been endorsed by Cancer Research UK (see next chapter).

Using surrogate markers of DDR deficiency (HRD signature, structural variation pattern, BRCA mutational signature, mutations in HR pathway) the results in this chapter demonstrate that DDR deficient PDAC respond preferentially to platinum and PARP inhibitors. Extensive low throughput testing (n = 15 cell lines) demonstrated DDR deficient PDCLs are preferentially sensitive to platinum when compared to DDR proficient PDCLs. A DDR proficient PDX model demonstrated no significant responses to platinum, PARP-, ATR-inhibition or combinations of these. On the other hand, long lasting complete and near complete responses were obtained in a DDR deficient PDX model using single agent Olaparib therapy (PARP-inhibitor). This proved to be as effective as Cisplatin monotherapy, or combination treatment using Cisplatin and Olaparib. Suggesting, that in appropriate patients this can potentially induce clinically relevant responses similar to platinum, but with a reduction in toxicity and thus improved patient quality of life. This potentially provides clinically effective therapeutics that can be utilised in patients with poor performance status, which unfortunately are the vast majority in PDAC. Clinical assessment of pre-clinical data supporting Platinum and PARP-inhibition in DDR deficient PDAC requires well designed precision oncology trials addressing the molecular pathology which is related to clinical response such as PRIMUS-001 and 002 under the *PRECISION-Panc* platform (Appendix I). Furthermore, refining a robust and reproducible therapeutic biomarker using a validated molecular assay is required to enable future stratification of platinum therapy to appropriate patients.

The data presented thus far suggest that predicting platinum response is more complex than using point mutations in DDR genes and the COSMIC BRCA mutational signature alone. Structural variation signatures, including > 200 SVs (Waddell et al., 2015) and the homologous recombination deficiency (HRD) signature appear robust but requires testing in well-designed clinical trials, powered to detect clinically relevant responses in specific biomarker subgroups. The data obtained from the APGI cohort is underpowered to assess the comparative platinum response between patient and the associated PDCL. It is difficult to predict how well PDCL sensitivity translates to clinical response. However, the pre-clinical data presented in this chapter, using multiple biomarkers of DDR deficiency and replication stress, suggest that there is significant potential in PDAC. Furthermore, the exact relationship of platinum and ATR / WEE1 inhibitor response requires investigation as this may prove an important therapeutic strategy once platinum resistance develops. This is a major area of interest of the *PRECISION-Panc* platform and its *PRIMUS* clinical trials designed to investigate this is discussed in Chapter 6.

The data presented here demonstrate that the replication stress signature, generated from PDCL data, is associated with the squamous subtype in both bulk tumour and PDCLs in multiple PDAC cohorts. Elevated replication stress, as defined by this signature, is associated with functional deficiencies in DNA replication, leading to a potential therapeutic vulnerability. These results suggest that PDAC with high replication stress can be targeted with agents inhibiting cell cycle control checkpoints. By inhibiting cell cycle checkpoints, the in-built ‘stop and repair’ system within the cell is lost. This leads to an accumulation of single stranded DNA, and subsequently double stranded DNA breaks, which can lead to cell death if not repaired.

PDCLs with high replication stress were more sensitive to treatment with agents inhibiting cell cycle checkpoints, particularly targeting the G2/M checkpoint such as ATR and WEE1. According to the data in this chapter, replication stress is a molecular feature that is independent of DDR deficiency and Platinum response and can offer patients that have ‘DNA replication defects’ therapeutic options outside of standard Platinum chemotherapy. These results are beginning to define sub-groups in PDAC that respond to novel agents and requires clinical testing to define the relationship between replication stress, DDR deficiency, platinum response, molecular subtype and clinically relevant responses in the clinic. This will allow refinement of the responsive biomarkers predicting meaningful responses and clinical translation is further discussed in Chapter 6.

A weakness of the data presented here is that the relative number of DDR proficient and low replication stress PDCLs tested were low in comparison to those with high replication stress. This is unfortunately due to the lack of availability of some PDCLs that underwent genomic and transcriptomic analysis for therapeutic testing at the time. More extensive testing using a wider range of low replication stress and DDR proficient PDCLs would help inform human clinical trial data, to further refine clinically relevant predictive biomarkers of response to these therapies.

This chapter aimed to identify biomarkers of response to agents targeting DNA damage repair deficiency and replication stress. Evidence supporting surrogate markers of DDR deficiency as predictors of platinum response are presented. Furthermore, the association between response to cell cycle checkpoint inhibitors and a novel replication stress signature is presented. These results demonstrate significant clinical potential of inducing clinically relevant responses in patient subgroups. Subsequently, these results have informed multi-centre personalised medicine clinical trial designs investigating both platinum containing regimens, as well as the novel Olaparib and AZD6738 combination in PDAC, which are presented in the next chapter.

6 Developing precision oncology clinical trials to target molecular subgroups of PDAC

6.1 Introduction

With the increased understanding of the molecular pathology of PDAC, it is becoming clear that the disease can no longer be considered a single, homogenous entity. Instead, it should be viewed as a collection of individually rare, heterogeneous tumours that cannot be distinguished histologically (Dreyer et al., 2017). It makes sense, that PDAC should not be treated the same in all patients. Current therapeutics for the disease, especially in the advanced setting, offers very little improvement in survival in the overall patient population, yet subgroups of responders exist that gain significant benefit from these therapies (Chang et al., 2014b). Currently, large groups of patients are treated to provide benefit to small, undefined patient subgroups. Similarly, not all patients with what is described as early-stage 'resectable' disease benefit from surgery, and many patients with locally advanced PDAC are denied surgical intervention due to radiological appearances without accounting for the underlying biological properties of each individual tumour. This leads to significant treatment related morbidity, and mortality, in a large proportion of patients who gain little benefit from these therapies.

Developing new therapies that target molecular aberrations of low prevalence is challenging. In order to demonstrate a clinical benefit in a small proportion of patients, requires hundreds or even thousands of patients, at great cost, and leads to high clinical trial failure rates (Biankin et al., 2015). Thus, it makes sense and may seem obvious to some, to adapt clinical trials to enrich for molecular subgroups that are likely to respond. However, identifying and characterising individual molecular subgroups in a clinically relevant time-frame is extremely challenging.

In this chapter, the challenge of targeting low prevalence molecular sub-groups is addressed using real-world health system patient flow calculations to understand the clinical trial opportunities that exist in PDAC. This demonstrates that small subgroups with potentially beneficial treatments used in other cancers, e.g. PD-1 / PD-L1 blockade in MMR deficient tumours, offer very attractive targets to study. Yet, the low prevalence leads to significant challenges in study design in order to reach a clinically meaningful endpoint. Understanding this landscape is crucial to designing contemporary, personalised clinical trials in PDAC. Using this information, a 2nd line study targeting DNA damage

repair deficiency and Replication Stress is designed to enrich for potential responders. This is based directly on the results presented in Chapter 5 of this PhD thesis and has received financial support from the pharmaceutical industry and is currently awaiting endorsement by Cancer Research UK. In conclusion to this PhD thesis, this chapter demonstrates the practicalities and successes of understanding clinical and logistical challenges to personalised medicine. By addressing these, the applicant demonstrates the real-world feasibility of rapidly translating pre-clinical research into the clinic.

In order to fully utilise the potential of molecular profiling PDAC using the variety of assays described in this thesis and apply it to patient care, the molecular landscape of PDAC and how it applies to clinical trials require to be defined. This allows the generation of clinical trial opportunity space in PDAC. Thereby, identifying feasible sub-groups of patients that can enrich molecular guided trials and providing patients and trials with the greatest chance of success. The recent advances in the molecular landscape of PDAC, including the work presented in this PhD thesis, was applied to the clinical landscape of the disease. This was used to generate a clinical trial opportunity map for both localised and metastatic disease.

6.2 The *PRECISION-Panc* Therapeutic development platform

PRECISION-Panc is a therapeutic development platform that aims to integrate pre-clinical discovery with clinical trials in order to facilitate precision oncology in PDAC. This is based on a philosophy of forward and backward translation, utilising pre-clinical advances to inform clinical trials with robust hypotheses, which in turn allow further discovery through the means of studying therapeutic response and resistance along with patients' molecular profile.

Using large integrative datasets and robust pre-clinical data, such as that presented in Chapter 5 of this PhD thesis, will inform clinical trial design within a platform that provides rapid translation from the lab to the clinic. All patients undergo molecular profiling, which in turn generates a knowledge bank of molecular and clinical data to further refine biomarkers of response. The ability to perform longitudinal molecular profiling, before and after treatment using a variety of assays, will allow unique insights into treatment resistance which can inform future therapeutic development and clinical testing.

The clinical development pillar of *PRECISION-Panc* is *PRIMUS* (Pancreatic Cancer individualised Multi-arm Umbrella Study), a clinical trial platform that is aimed at finding the right trial for the patient. (Appendix I) By providing a portfolio of clinical trials, targeting different molecular sub-groups, in different disease stages, will allow multiple novel therapeutic opportunities for patients. This will allow clinical testing in individually small, yet cumulatively large patient groups which is aimed both at early stage drug development and larger scale Phase II / III studies.

In order to complete such an ambitious project, 3 main areas required to be addressed. First, a robust tissue acquisition and sequencing protocol is required to enable molecular profiling in almost all patients, irrespective of disease stage (discussed in Chapter 7). Second, a master protocol that enrols patients into molecular profiling and identifies valid clinical trial options is required (discussed in next section). Lastly, the clinical trial landscape of PDAC needs to be defined to identify clinical and molecular subgroups that need clinical trial options. This is required to be matched up with robust pre-clinical data, or clinical evidence from other cancer subtypes, in order to translate into options for patients with PDAC. These issues are addressed during this chapter as the PhD candidate played a vital role in addressing these during the development of the *PRECISION-Panc* platform.

6.2.1 The *PRECISION-Panc* Master Protocol

In order to enrol patients into clinical trials which allow molecular profiling not to delay or disrupt clinical care, a standardised master protocol was designed. The PhD candidate was a member of the Master Protocol design team and forms part of the Master Protocol trial management group.

The *PRECISION-Panc* master protocol approaches patients at the first point of referral to the tertiary pancreatic cancer service, even prior to histological diagnosis is made. Thus, patients are consented for additional biopsies which will allow them access and opportunity for personalised medicine trials. Patients with suspected (or confirmed) PDAC are consented for extra biopsies, and once diagnosis confirmed, consented for molecular profiling. This process occurs in parallel to the standard diagnostic procedure thus leading to a rapid molecular assay report in the region of 2 weeks after index biopsy. This allows patients to attend their oncology appointment with a diagnosis, and clinical trial option at the point of first treatment discussion. This will hopefully lead to a higher proportion of

patients enrolling into personalised trials, whilst not delaying their standard treatment pathway.

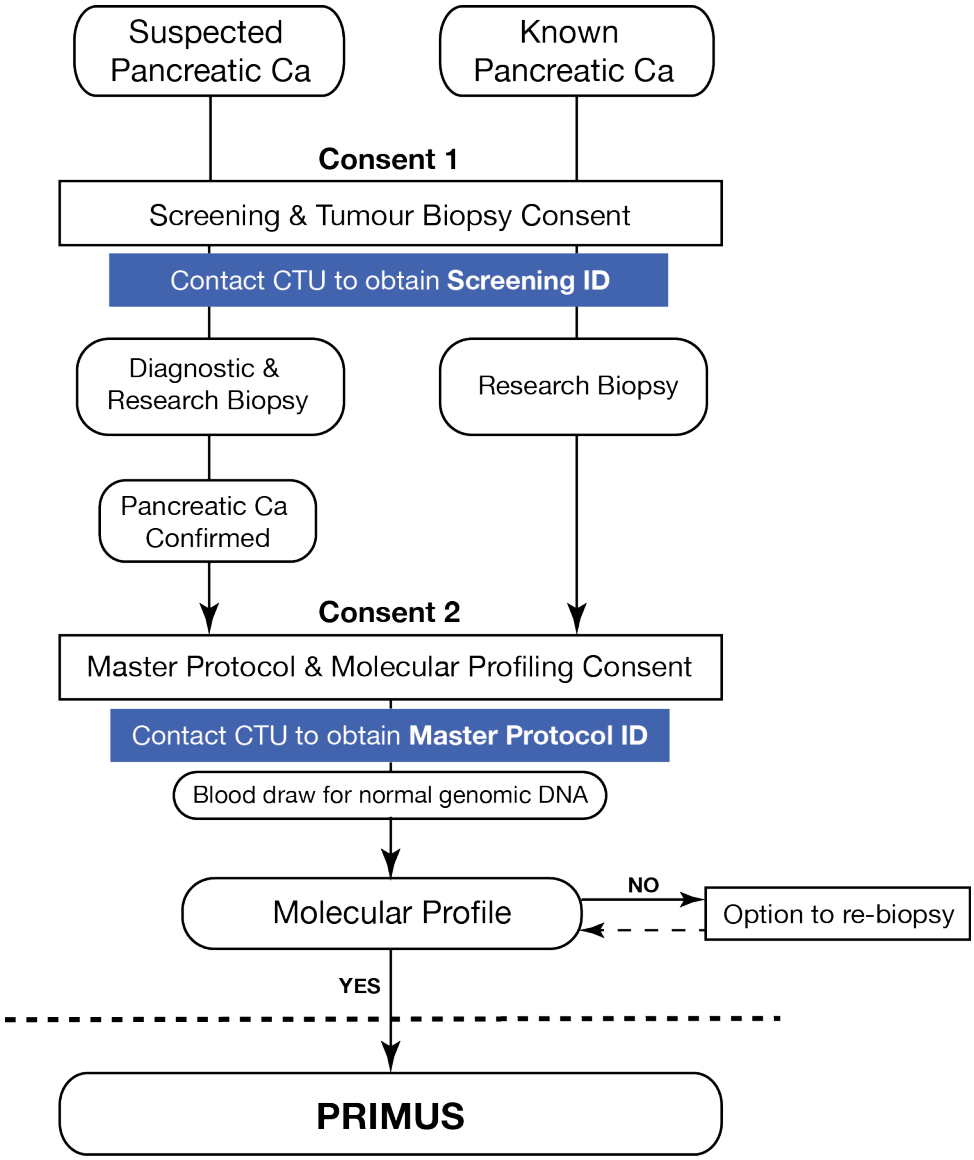

Figure 6-1 The *PRECISION-Panc* master protocol. Patients can enter the master protocol even prior to a high diagnosis of PDAC, provided they have a suspicious lesion and potentially suitable for any of the clinical trials that are open. Molecular profiling is done using the diagnostic biopsy, and thus leads to rapid diagnosis and proceed to DNA extraction and sequencing. Patients can re-enter the master protocol pathway at any stage of their treatment journey, provided there is a suitable trial option available.

A major challenge of this approach will be the high dropout rate due to disease progression and deterioration of performance status, a major challenge in the management of advanced PDAC. To combat this, appropriate support structures and trials for performance status 1 – 2 should be put in place for all patients that enter the master protocol. This is currently

being developed and is discussed later in this chapter. Detailed *PRECISION-Panc* trial protocols are included as Appendices at the end of this thesis.

6.3 Defining personalised clinical trial opportunities in molecular sub-groups of PDAC

The clinical trial opportunity space that exists for PDAC is complex. The majority of patients present with advanced disease and can deteriorate rapidly in terms of performance status. This results in only around 50% of patients with metastatic PDAC receiving any form of systemic treatment. Furthermore, the nihilism that surrounds treating PDAC significantly reduces the opportunities patients are offered in the advanced disease setting. Thus, as part of the *PRECISION-Panc* clinical trial platform, a detailed trial opportunity map was generated for patients with metastatic PDAC to identify and define the clinical trial opportunities that exist. Currently around 9000 patients are diagnosed with Pancreatic Cancer annually, of these, the majority (in the region of 50%) present with metastatic disease (CRUK, 2018).

Translating pre-clinical advances into clinical trials requires allocating the right patient to right trial that allows both patients and the trial the optimal chance at success. This PhD thesis infers that clinically significant molecular sub-groups exist in PDAC with predictive biomarkers that predict response to established and novel therapies, as well as surgical intervention. Enriching each clinical trial with the target patient population will allow accurate testing of precision oncology therapies. For example, PD-1 inhibitors (e.g. Pembroluzimab) has recently been approved for use in Mismatch Repair deficiency (MMRd) tumours regardless of which cancer type (Boyiadzis et al., 2018). However, only 1-2% of PDAC has been found to be MMRd (Humphris et al., 2017) and thus any trials investigating this agent in PDAC requires enrichment for MMRd patients, otherwise the trial is destined to fail and potentially prevent a number of patients from benefiting from this potential therapy.

6.3.1 Molecular landscape and trial opportunities

The recent advances in the molecular landscape of PDAC has revealed 2 major subtypes of the disease (Classical Pancreatic and Squamous) that within each exist clinically actionable molecular phenotypes. These include DNA damage repair and cell cycle control deficiencies, of which Homologous Recombination deficient and High Replication Stress are associated sub-groups with novel therapeutic biomarkers, which has been shown in this

PhD thesis to be preferentially responsive to Platinum and novel DDR inhibitors (e.g. PARP and ATR inhibitors) (see Chapter 5). However, there exists further actionable sub-groups which are gradually being identified and requires clinical testing. This includes those responsive to Gemcitabine and Abraxane of which the molecular signature still needs to be defined. Furthermore, MMRd (PD-1 inhibitor), *KRAS* wild-type (targeted with Erlotinib) and HER2+ amplified (targeted by Herceptin) PDAC provide clinical trial opportunities in selected, yet small, sub-groups of patients that may lead to clinically relevant therapeutic responses (Table 6-1).

Table 6-1 Clinically actionable molecular landscape of PDAC. Advances in the molecular landscape have identified clinically relevant molecular sub-groups of PDAC that are demonstrating potential for clinical testing. The overlap of these with one another is yet to be defined, but may be significant, thus providing patients with multiple options as resistance develops.

Molecular Sub-Groups of PDAC	Proportion of Patients	Therapeutics	Clinical Trial Option
Squamous	50%	*Myeloid depleting (e.g. CXCR2)*	*PRIMUS-003*
Classical Pancreatic	50%		
DNA Damage Repair deficient	20 – 25%	*Platinum, PARP inhibitors*	*PRIMUS-001, PRIMUS-002, PRIMUS-004*
Homologous Recombination Deficient	10-15%	*Platinum, PARP inhibitors*	*PRIMUS-001, PRIMUS-002, PRIMUS-004*
High Replication Stress	15-20%	*ATR inhibitors, PARP inhibitors, WEE1 inhibitors*	*PRIMUS-004*
***KRAS* wild-type**	7%	*ERLOTINIB*	
HER2+ Amplified	1%	*HERCEPTIN*	
MMR deficient	2%	*PD-L1 inhibitor*	

In order to design clinically feasible trials with achievable end-points and allow sufficient patients of each molecular phenotype to enter, it is crucial to understand the opportunities that exist for targetable sub-groups within the current clinical environment for PDAC.

6.3.2 Clinical Trial Opportunities for patients with Metastatic PDAC

Many patients with metastatic PDAC never receive any treatment for their disease due to a number of reasons. This includes the rapid deterioration of patients' performance status, the nihilism surrounding the prognosis of metastatic PDAC as well as the lack of therapeutic options for patients outside of cytotoxic chemotherapy regimens. Identifying the reasons why patients do not receive treatment, and the subsequent journey of those that do, is crucial to designing umbrella studies in the metastatic setting of PDAC. This provides an understanding of the opportunities for clinical trials and for patients that target molecular subgroups. Furthermore, novel targeted therapies may have less side effects than standard cytotoxic regimens and may provide options for patients with ECOG performance status 1-2.

The launch of PRIMUS-001 (a randomised adaptive Phase II study comparing FOLFOX-A (combination of 5-fluorouracil, Oxaliplatin, Leucoverin and Nab-Paclitaxel) with Gemcitabine-Abraxane (nab-Paclitaxel) in the metastatic setting), as part of *PRECISION-Panc* platform, is currently the leading late stage therapeutic trial for metastatic PDAC available in the UK. Patients are randomised to each treatment arm in the initial stages, with an interim analysis at 15 months determining whether recruitment should continue in all-comers or in biomarker specific sub-groups. Thereby, assessing the therapeutic response biomarker for Platinum (FOLFOX-A arm) in comparison with Gemcitabine-Abraxane (Figure 6-2).

Following 1st line chemotherapy for metastatic PDAC, only around half of patients will be fit for 2nd line therapy upon disease progression. This significantly reduces the options for 2nd line metastatic trials, as patients are usually unable to tolerate further treatment. However, a significant proportion of patients respond to platinum-based regimes and Gemcitabine-Abraxane combinations (Conroy et al., 2011, Von Hoff et al., 2013). Thus, it is anticipated that a number of patients annually will be able to tolerate 2nd line therapy after completing PRIMUS-001. In order to offer patients an efficient strategy to enter 2nd line trials immediately at the point of disease progression (at which time patients are withdrawn from the PRIMUS-001 trial regime), an understanding of further trial opportunities for each patient is required well in advance of this inevitability. Upfront molecular profiling, as part of the *PRECISION-Panc* Master Protocol will allow patients to be identified for molecularly stratified 2nd line trials in advance of completing the 1st line

PRIMUS-001 trial. Thus, when patients progress they can immediately start on 2nd line therapy that offers novel, stratified treatments to patients. This allows rapid change of treatment to allow patients best chance of response as well as enriching each trial with the right patient population.

The first of the 2nd line trials within the *PRECISION-Panc* 2nd line metastatic umbrella is directly based on work from this PhD thesis (of which the PhD applicant is the primary investigator) which investigates novel DNA damage repair strategies in patients following development of platinum resistance. This is discussed in greater detail later in this chapter, but this is an example of utilising patients' molecular profile prior to 1st line therapy to identify 2nd line trial opportunities and therefore efficiently transferring patients from one trial to the other. This strategy can offer patients the greatest opportunity for benefit from treatment in this poor prognostic setting.

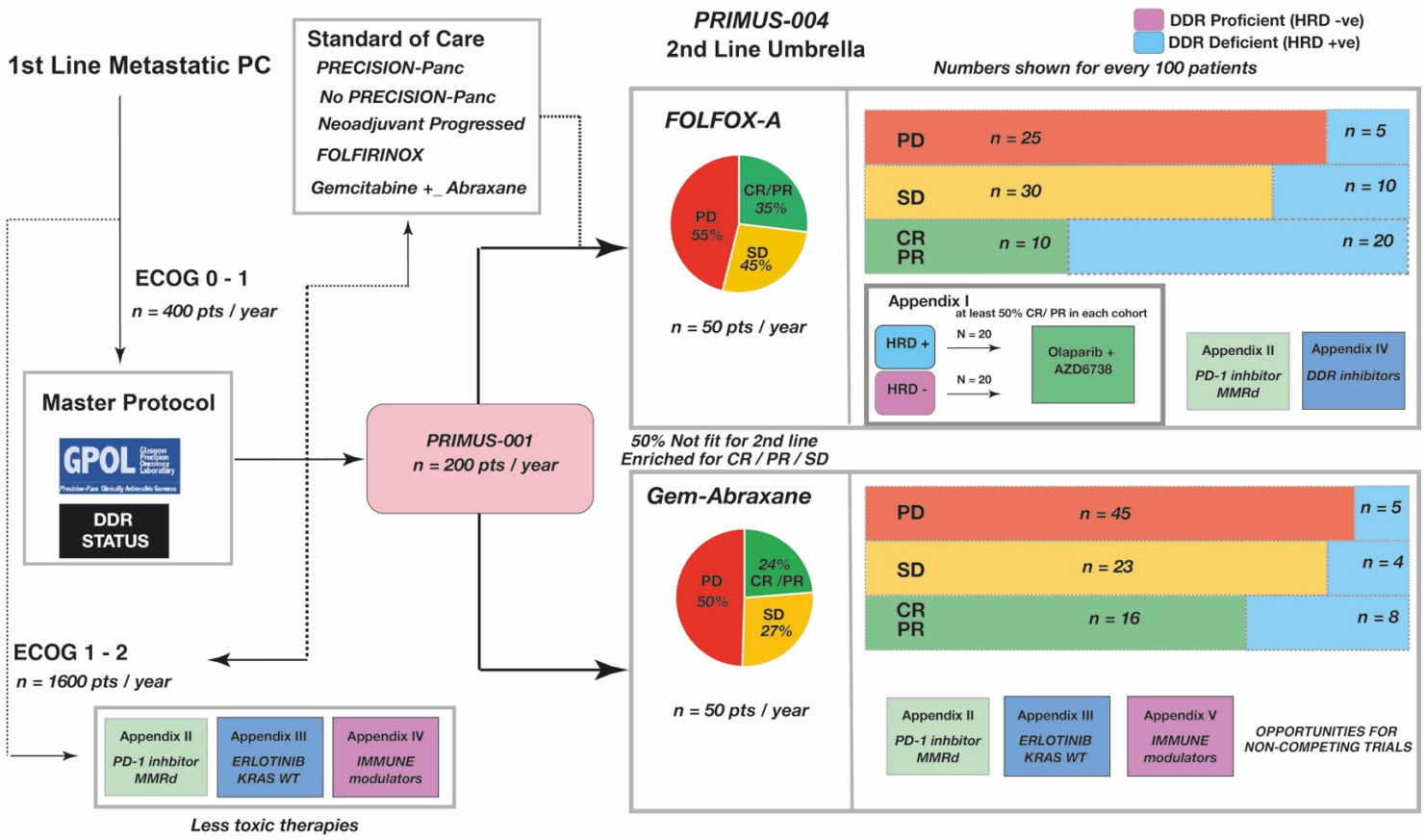

Figure 6-2 Clinical trial opportunity space in Metastatic PDAC. Patients enter the *PRECISION-Panc* master protocol and if performance status (ECOG) 0 or 1 can enter PRIMUS-001 to be randomised to FOLFOX-A or Gemcitabine-Abraxane arm. Following progression, around 50% of patients will be fit to tolerate 2nd line therapy and be able to be enrolled into 2nd line trials. Depending on the homologous recombination deficiency and response to each arm will generate multiple small patient cohorts that can be stratified based on 1st line response, DNA damage repair status and novel molecular biomarkers. This generates multiple small cohorts (in the region of n = 20) that can be tested using novel therapies. Identifying which novel trial option (e.g. PD-1 inhibitor in MMRd PDAC) upfront can allow early stratification to 2nd line trial options. The majority of patients will be ECOG status 1 or 2 and targeted treatment options are attractive in this large patient cohort that do not tolerate systemic chemotherapy regimens.

6.3.3 Clinical trial opportunities for patients with non-metastatic PDAC

The non-metastatic setting offers patients and researchers an exceptional opportunity for studying PDAC whilst making significant improvements in disease outcomes, with the aim of cure in a significant proportion of patients. The boundaries between locally advanced and 'resectable' PDAC is becoming less and less defined, with novel treatment strategies leading to long term survival in both groups (Gemenetzis et al., 2018, Murphy et al., 2018). Data presented in this thesis demonstrates that there appear to be molecular differences between pro-metastatic and non-metastatic PDAC that underlie the disease patterns observed. Molecularly targeted therapies can lead to complete or near complete tumour responses, which if resected, leads to excellent survival benefit at 5 years and may significantly improve the long-term survival of patients with non-metastatic PDAC (Murphy et al., 2018).

The neoadjuvant setting offers an excellent opportunity to study disease response to therapy alongside clonal evolution, tumour heterogeneity and the development of treatment resistance (Figure 6-3). Surgical resection offers the opportunity to pathologically assess response to therapy which can demonstrate, in a relatively short space of time, a reliable indicator of treatment response. Thus, this provides a very attractive opportunity to study molecular profiles and treatment response in PDAC, as novel drug combinations or with the addition of radiotherapy.

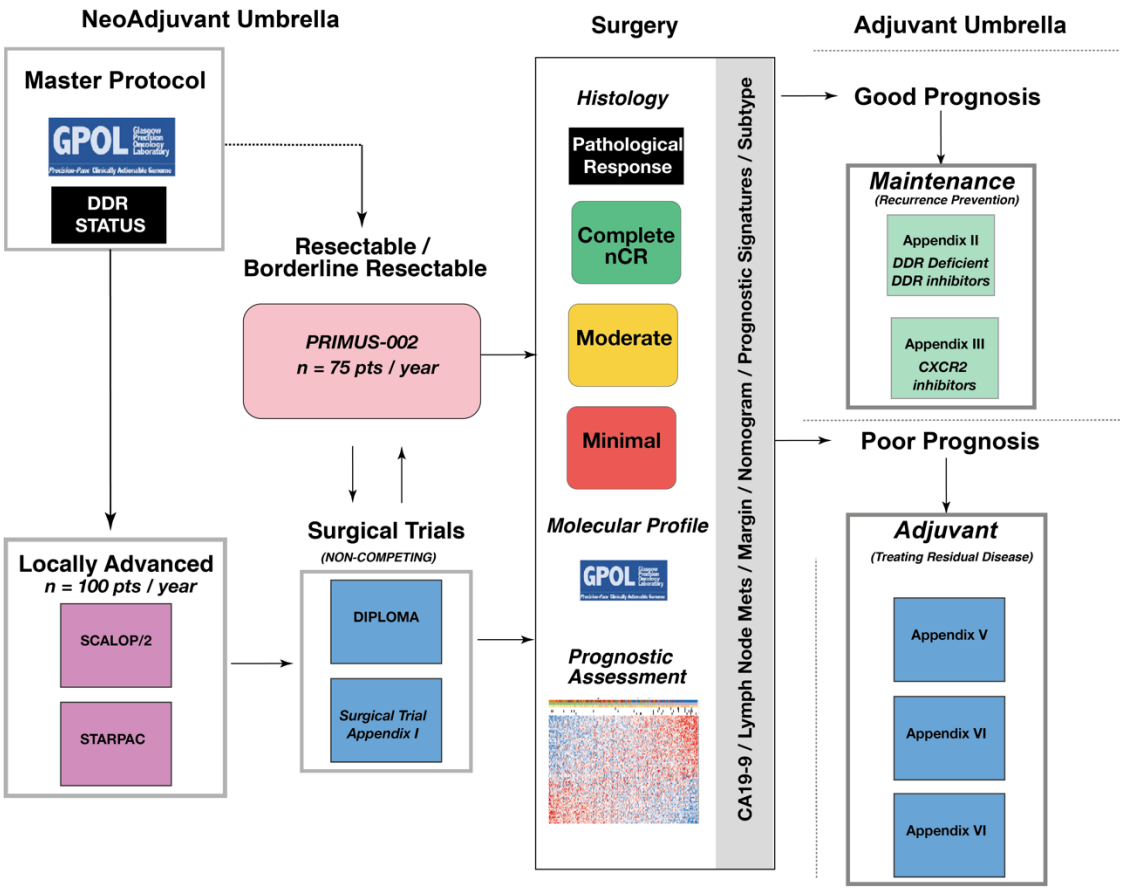

Figure 6-3 Clinical trial opportunity space in non-Metastatic PDAC. Patients with non-metastatic PDAC (locally advanced and resectable / borderline resectable (BR-R)) can enter the *PRECISION-Panc* master protocol. Patients with BR-R disease can enter PRIMUS-002 and if suitable undergo surgical resection. Locally advanced patients can be offered novel trial options, including radiotherapy trials (e.g. SCALOP/2). Parallel to this, surgical studies such as DIPLOMA (minimally invasive versus open distal pancreatectomy) can recruit patients provided that these do not compete directly with the outcomes and treatments assessed in PRIMUS trials. Following resection, patients are assessed to determine their prognostic outcomes and stratified to either maintenance or adjuvant trials. This allows patients multiple opportunities to be involved in novel, cutting-edge treatments – so called 'multiple shots at goal'. Furthermore, this strategy allows trials further down the treatment pathway to be tailored to suit patients that have already been on trials earlier in their disease course. Thus, preventing neoadjuvant trials from excluding patients in the post-operative setting.

6.3.3.1 Summary

These figures demonstrate significant opportunities for novel trial design that will allow testing of novel and repurposed therapeutic strategies in molecular sub-groups of PDAC. An attractive clinical area to target is the 2nd line metastatic setting, where there are currently no therapeutic options available for patients with any proven efficacy. Utilising pre-clinical data presented in this PhD thesis, this strategy is used to design a 2nd line Phase 1b / II clinical trial investigating the combination of ATR and PARP inhibitors to target DNA damage repair deficiency and replication stress in PDAC. The PhD candidate is the primary investigator for this trial which is currently awaiting formal endorsement from Cancer Research UK after being supported by the National Cancer Research Institute Upper GI subgroup committee. This serves as an example on utilising the clinical trial opportunity space to identify a target patient population and translating pre-clinical evidence into trial.

6.4 Developing a 2nd line clinical trial to target DNA damage response deficiency and replication stress in PDAC

6.4.1 PRIMUS-004: 2nd line umbrella study in PDAC

The *PRECISION-Panc* 2nd line umbrella (PRIMUS-004) is a clinical proposal aimed at offering a range of small signal seeking studies in biomarker enriched subgroups of patients with advanced PDAC. The PhD candidate is a principal investigator of this umbrella study and has been a member of the trial design team from the outset. The aim of which is two-fold, to offer patients better selected 2nd line clinical trial options, and to evaluate clinical biomarkers and novel therapies in well-designed Phase Ib / II signal seeking studies that can inform late stage therapeutic testing in larger studies.

The current prognosis for patients with advanced PDAC is dismal. The current best options for metastatic disease are FOLFIRINOX or Gemcitabine-Abraxane combinations with no proven effective 2nd line therapy after disease progression. However, The MPACT trial demonstrated that 2nd line therapy can be of benefit to patients with metastatic PDAC (Von Hoff et al., 2013, Conroy et al., 2011). Patients who received FOLFIRINOX as 2nd line therapy after progressing on Gemcitabine-Abraxane demonstrated a median OS of 15.7 months (Chiorean et al., 2016). However, the majority of patients will be unable to tolerate two intensive cytotoxic chemotherapy regimens, particularly with the rapid decline of performance status in metastatic PDAC. No targeted therapies have been proven efficacious as 2nd line therapy in PDAC. However, numerous responders to agents targeting DDR and Replication stress have been reported (Kaufman et al., 2015, Do et al., 2015).

The PRIMUS-004 umbrella will offer patients a portfolio of 2nd line, early phase, clinical trials with clear biomarker-based hypotheses using well tolerated targeted therapies. This will aim to offer patients a range of options targeting many different disease mechanisms and provide therapies for those unfit for further cytotoxic chemotherapy. The promising results seen targeting DDR and replication stress in the 2nd line setting in other cancer subtypes, primarily breast and ovarian, suggests that this is a promising area to investigate (Do et al., 2015, Leijen et al., 2016a, Leijen et al., 2016b, Domchek et al., 2016, Fong et al., 2010, Matulonis et al., 2016, Swisher et al., 2016). The pre-clinical results presented in Chapter 5 of this PhD thesis define predictive biomarkers for therapies targeting these mechanisms and provide a clear biomarker rationale for clinical testing. Thus, the first

wave of PRIMUS-004 studies is aimed at targeting DDR and replication stress with the Olaparib (PARP-inhibitor) and AZD6738 (ATR inhibitor) combination being the first tested regimen (**named PRIMUS-004: Appendix I**).

6.4.2 Background and Therapeutic Rationale

The pre-clinical findings described in Chapter 5 suggests that a sub-group of patients with PDAC will respond to agents targeting the G2/M checkpoint, such as ATR and WEE1 inhibitors. Transcriptomic signatures of replication stress are predictive of response in PDCLs to ATR and WEE1 inhibition, however, requires well designed clinical testing to investigate whether this translates into meaningful responses for patients.

Increasing case reports and pre-clinical evidence are demonstrating acquired resistance to platinum therapy in *BRCA* mutant tumours (Lord and Ashworth, 2013, Lord and Ashworth, 2016, Pishvaian et al., 2017, Lheureux et al., 2017). Evidence from other cancer types, e.g. ovarian (Fong et al., 2010, Mirza et al., 2016) and breast cancer (Robson et al., 2017), reveal responses to PARP-inhibitors (PARPi) after previous treatment with platinum chemotherapy, and responses can occur in both primary platinum sensitive and resistant disease.

Clinical resistance to PARP inhibition can occur after restoration of *BRCA1/2* function due to secondary mutations in these genes (Lheureux et al., 2017, Pishvaian et al., 2017). There is growing pre-clinical evidence suggesting that adding ATR inhibitors in combination delays the acquisition of resistance to PARP inhibitors (Kim et al., 2017, Yazinski et al., 2017). ATR inhibition appears to sensitise DDR deficient cancer cells to PARPi *in vitro* and *in vivo*, and combination treatment delays resistant clone emergence (Kim et al., 2017). Furthermore, combination treatment re-sensitises cancer cells following acquisition of PARPi resistance (Yazinski et al., 2017). Pre-clinical tumour models, including pancreatic tumour models with *BRCA* reversions and resistance to platinum and PARP inhibitors, appear to maintain sensitivity to cell checkpoint inhibitors such as ATR and WEE1 inhibition, potentially due to retained levels of genomic instability and high replication stress (Drean et al., 2017, Kim et al., 2017). In addition, PARP inhibition increases replication stress and can in turn sensitise cells with replication defects to ATR inhibition, irrespective of DDR status (Yazinski et al., 2017). This suggests that combined inhibition of PARP and ATR (e.g. Olaparib and AZD6738) can target both HR deficient PDAC, even after Platinum resistance develops, whilst acting synergistically to enhance

response in those with high replication stress by 1) enhancing replication stress and thus ATR inhibitor responsiveness, 2) delaying formation of resistant clones to PARP inhibition and 3) bypassing resistance mechanisms in acquired PARPi resistance.

In order to address these questions, a signal seeking Phase 1b/II clinical trial that will run through the *PRECISION-Panc* platform was designed. Suitable patients would be those with metastatic PDAC, previously treated with Platinum based chemotherapy. This does not exclude patients who had 1st line Platinum chemotherapy outside of the *PRECISION-Panc* framework or progressed to metastatic disease on Platinum during neoadjuvant treatment, provided there is appropriate pre-Platinum tissue available for genomic analysis (biopsy or resection specimen).

Patients will enter the trial cohort based on initial response to platinum therapy in 1st line and homologous recombination repair gene mutation (HRRm) status defined using the ***GPOL PRECISION-Panc clinical cancer genome*™** (Appendix II).

6.4.3 Description of therapeutic cohort

6.4.3.1 Trial Design

The aim of PRIMUS-004 Appendix I will be to investigate 2nd line treatment with the combination of Olaparib and AZD6738 in patients stratified by HRRm status completing first line Platinum based chemotherapy for PDAC. Patients will be selected based on their initial pre-treatment biopsy and response to Platinum (Figure 6-4). Patients with partial or complete response or stable disease will enter the study cohort under the same trial protocol. However, patients will then be primarily stratified by HRRm status to allow comparison between these groups (HRRm +ve and -ve). Each cohort will be controlled to ensure at least 50% of patients included had a complete (CR) or partial response (PR) to platinum therapy to prevent over recruitment of patients with stable disease (SD) to each cohort (Figure 6-4). This will allow early stopping in futile patient cohorts, whilst continuing recruitment in cohorts in which responses are demonstrated. In parallel with response to platinum, we will test biomarkers of responsiveness based on pre- and post-platinum treatment biopsies. Hypothesised biomarkers include the GPOL HR deficiency signature, transcriptomic replication stress signature, PDAC molecular subtype (squamous vs classical pancreatic) and DDR pathway mutations (HRRm). Initial enrolment will involve 20 patients with expansion if required to further refine the initial clinical response signal.

6.4.3.2 Cohort Definition

Early drug development trials, such as these, are designed and powered to detect early response signals in patient subgroups to justify clinical testing in larger patient cohorts (Biankin et al., 2015). To translate this form of trial design into molecular era, the optimal patient population should be predetermined, to allow patients and the trial the best opportunity for success. In order to successfully target these subgroups, it is crucial to define patient populations and how they will be identified from the 1st line setting.

Patients entering PRIMUS 001 (metastatic PDAC comparing FOLFOX-A vs Gemcitabine-Abraxane) will undergo tumour biopsy and molecular profiling using the ***GPOL PRECISION-Panc clinical cancer genome™.*** This will determine each patient's HRRm status prior to platinum therapy (Figure 6-4). Patients treated with FOLFOX-A (a platinum-based triplet chemotherapy regimen) will be eligible for the studies described here. Patients from out with PRIMUS 001, that have been treated with platinum-based chemotherapy, can also be enrolled provided there is a pre-platinum tumour sample available for sequencing and molecular analysis. This includes patients that are receiving platinum as neoadjuvant therapy that progress to metastatic disease, e.g. in PRIMUS-002: neoadjuvant biomarker-based trial investigating FOLFOX-A versus Gemcitabine-Abraxane, as this is defined as progression on 1st line platinum chemotherapy.

Patients will be selected and stratified based on their initial pre-treatment HRRm status and response to first-line Platinum (Figure 6-4). HRRm status will be defined based upon the pre-Platinum (first-line) treatment biopsy using the GPOL clinically actionable genome 25mb panel assay©. HRRm +ve patients are defined as having at least one mutation in the following genes *ATM, BARD1, BRCA1, BRCA2, BRIP1, CDK12, CHEK1, CHEK2, FANCL, PALB2, PPP2R2A, RAD51B, RAD51C, RAD51D* and *RAD54L*. All patients will undergo biopsy prior to second-line treatment to allow exploration of resistance mechanisms and other biomarkers of therapeutic responsiveness (e.g. GPOL HR deficiency signature, replication stress signature, molecular subtype).

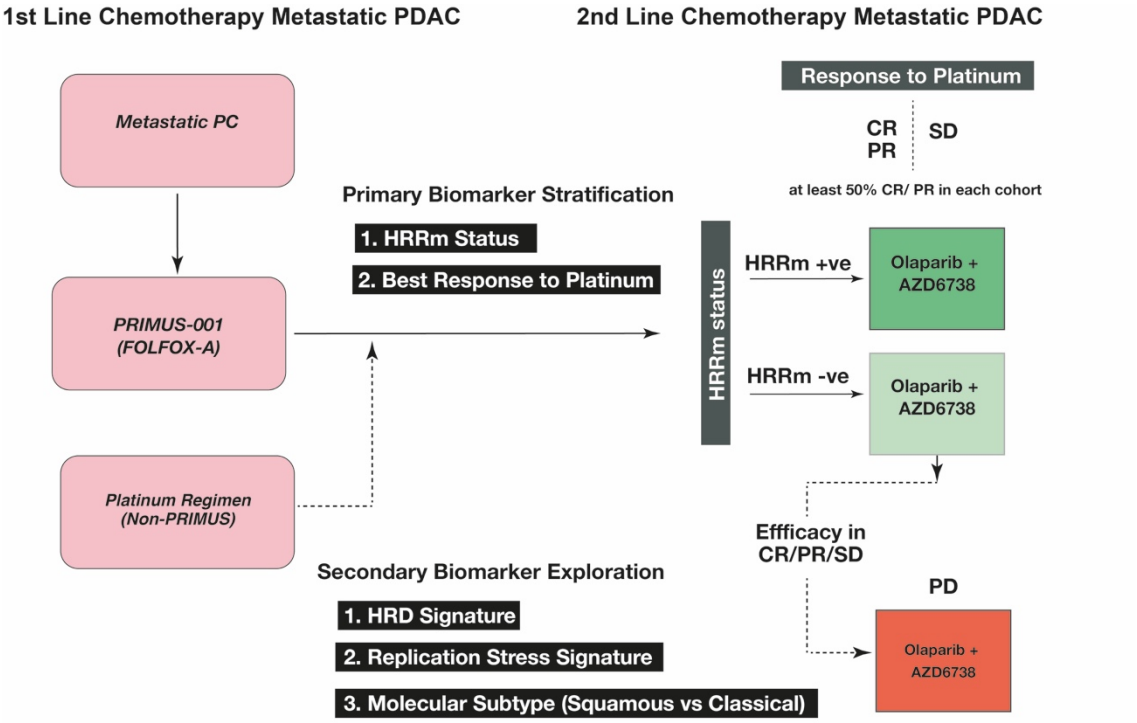

Figure 6-4 Primus-004 Appendix I trial schema. The *PRECISION-Panc* Master Protocol will screen patients with advanced, metastatic PDAC that have been previously treated with Platinum based chemotherapy as 1st line. This is envisaged to be mostly patients from PRIMUS-001, however, patients treated with 1st line platinum chemotherapy outside of the *PRECISION-Panc* framework can also be included. A tumour sample (biopsy or resection specimen) prior to 1st line platinum therapy is a prerequisite for inclusion. Patients will then be primarily stratified based on HRRm status and best response to 1st line chemotherapy, and each cohort will be controlled to ensure at least 50% of patients included had a CR or PR to platinum therapy. Retrospective analysis of exploratory biomarkers will include the GPOL HRD signature, Replication Stress transcriptomic signature and Molecular subtype (squamous vs rest). If efficacy is determined in platinum responders (CR/PR/SD) then enrolment will expand to include those that progress primarily on platinum 1st line therapy (PD).

6.4.3.3 Outcomes and statistical calculation

The primary outcome of PRIMUS-004 Appendix I is the objective response rate in patients with advanced PDAC to combined treatment with Olaparib and AZD6738 in the second-line, post-platinum setting. The secondary outcomes are aimed at assessing efficacy in terms of progression free survival (PFS) and overall survival (OS) and biomarkers of response assessed. Response rates will be determined using the internationally established Response Evaluation Criteria in Solid Tumours (RECIST) (Schwartz et al., 2016). Target lesions will be defined as measurable lesions on cross-sectional imaging (in this case CT imaging) with up to 2 lesions per organ and 5 lesions in total (Schwartz et al., 2016). Response will be defined as complete response (CR; disappearance of all target lesions), Partial Response (PR; at least a 30% decrease in the sum of longest diameter of all the target lesions, Stable Disease (SD; insufficient shrinkage to qualify for PR but not enough

growth to qualify as PD) and Progressive Disease (PD; 20% increase in the sum of the LD of target lesions) (Schwartz et al., 2016). All response data will be recorded by a qualified consultant radiologist with an interest in clinical research and pancreatic cancer. The treatment duration will be until disease progression or lack of tolerability.

The overall design for the PRIMUS 004 studies under this second-line umbrella uses a single arm phase IB/II four-stage approach that has good power (>87%) to detect response rates of >25% but allows early stopping if response rates are low (<10%). The response rates required to prevent early stopping are presented for decision making after 10/20/30 and 40 patients have been recruited (Lee and Liu, 2008) (Figure 6-5, Table 6-2). Each cohort of patients will follow the representative schema (Figure 6-5), within a statistical framework (Table 6-2) where studies can adapt, expand, open and close based on accumulating data. This study design allow recruitment to be focussed on or stopped in particular subgroups depending on the observed results and provide flexibility to identify responsive biomarker subgroups within a structured statistical design. For example, in this case, if the HRRm -ve patients fail to meet the response criteria to the Olaparib & AZD6738 combination, then a secondary analysis stratified by platinum response in the HRRm -ve (CR/PR versus SD) can be performed to determine whether the response criteria are met in each of these subgroups. Recruitment can then open and close, as appropriate, and a decision made whether to expand to include patients with PD to platinum (Figure 6-5). If the combination is deemed effective, then this will inform and direct late therapeutic development by determining whether Phase III trials should be pursued in a 'all-comer' or biomarker specified sub-group only (Biankin et al., 2015) (Figure 6-5).

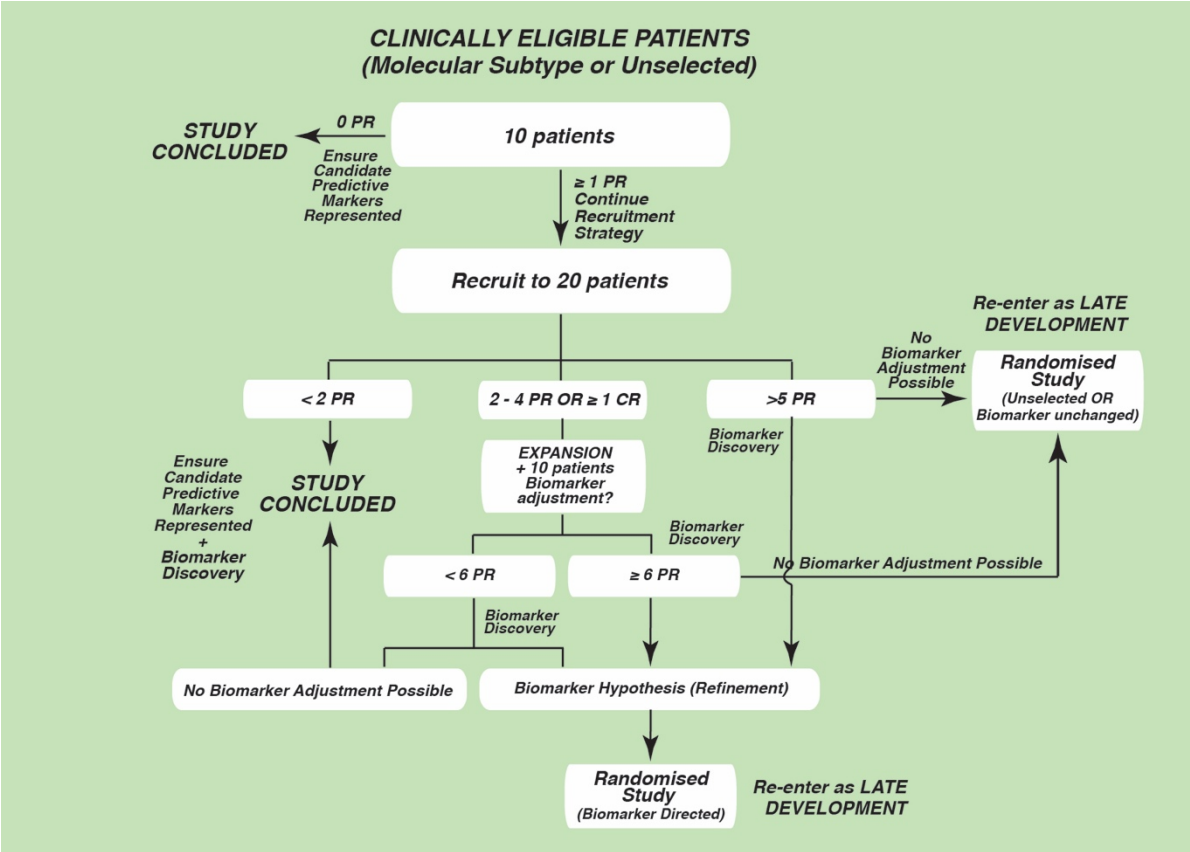

Figure 6-5 The PRIMUS-004 early therapeutic development schema. The 2nd line umbrella is aimed at small signal seeking trials that are supported by an understanding of tumour molecular pathology with a clear biomarker-based hypothesis. This will follow a stepwise approach, with each step supported by clear statistical calculations for efficacy and futility. The results of these will determine the design of Phase II/III trials (late therapeutic development) and whether these are to be tested in all-comers or biomarker specific sub-groups.

Table 6-2 Power calculations and Stopping Boundaries and Probability of Declaring Futility/Efficacy for Different Response Rates for second-line PRIMUS-004 studies.

True response rate	Number of patients recruited	Number of responses to declare futility	Cumulative probability of stopping for futility	Number of responses to declare efficacy	Cumulative probability of stopping for efficacy
10%	10	0	.35	≥4	.01
	20	≤1	.48	≥5	.05
	30	≤3	.70	≥7	.05
	40	≤6	.90	≥7	.10
25%	10	0	.06	≥4	.22
	20	≤1	.07	≥5	.59
	30	≤3	.09	≥7	.70
	40	≤6	.13	≥7	.87
40%	10	0	.01	≥4	.62
	20	≤1	.01	≥5	.95
	30	≤3	.01	≥7	.98
	40	≤6	.01	≥7	.99

6.5 Discussion

Translating the rapid progress in pre-clinical advances in PDAC into meaningful clinical treatments for patients requires well designed clinical trials that considers the molecular heterogeneity of the disease. Identifying clinical and molecular sub-groups that do not have clinical trial options is key to finding the right trial for the patient and translating pre-clinical findings as expeditiously as possible. This PhD thesis demonstrates the development of a novel therapeutic strategy and clinical trial to target replication stress and DNA damage repair deficiency in PDAC. By developing a pre-clinical hypothesis and utilising the results to design a therapeutic strategy for clinical testing, this PhD candidate demonstrates the opportunities for translation in 2nd line PDAC.

Sequencing studies and the development of novel agents has made DDR deficiency the most attractive therapeutic segment at present in PDAC. Results in Chapter 5 demonstrates that replication stress presents a therapeutic vulnerability in a sub-set of patients that deserves further investigation. A clinical trial (PRIMUS-004: Appendix I) was designed and submitted for endorsement that aims to investigate the clinical responses to the Olaparib (PARP inhibitor) and AZD6738 (ATR inhibitor) combination in PDAC. This will investigate the 2nd line response to these agents and whether the pre-clinical data described in this chapter translates into clinically meaningful responses for patients. Performing molecular assays before and after platinum therapy, will investigate the role of therapeutic biomarkers in parallel to targeting these mechanisms after platinum resistance develops. This will then inform late stage therapeutic testing, if the treatment is non-futile, by directing biomarker specific clinical trials.

7 Feasibility and clinical utility of Endoscopic Ultrasound guided biopsies of PDAC for next-generation molecular profiling

7.1 Introduction

A major challenge of translating recent genomic and pre-clinical discoveries in PDAC into clinical practice for precision medicine has been implementing real time molecular profiling of patients to inform clinical decision making. NGS from core biopsies of metastatic lesions can be done with high success rates in PDAC (Aguirre et al., 2018, Aung et al., 2018). However, most patients present with lesions that are not accessible percutaneously and only 15 - 20% of patients present with resectable disease. This provides a significant challenge to obtaining tissue for molecular phenotyping in PDAC, particularly in localised or locally advanced disease. Thus, there is an urgent need to develop strategies to safely acquire good quality tissue suitable for NGS for every patient with PDAC.

There has been significant progress in the use of endoscopic ultrasound (EUS) in the diagnosis and management of PDAC in the last decade (Bang et al., 2017, Catenacci et al., 2015, Chang et al., 2009b, Gleeson et al., 2016). The development of new fine needle core biopsy needles have increased the quality and quantity of tissue samples that can be obtained even from low cellularity tumours that are typical of PDAC (Artifon et al., 2017, Valero et al., 2016). Utilising diagnostic samples for molecular analysis, however, is associated with high failure rates in many cancer types including PDAC (Hagemann et al., 2015, Thompson et al., 2016, Meric-Bernstam et al., 2015, Zill et al., 2015). Utilising percutaneous biopsies only for personalised medicine trials in PDAC will result in a large proportion of patients being excluded from these trials.

Many studies describing the use of tumour biopsies, including EUS guided, for therapeutic stratification in PDAC have failed to describe the patient denominator included in the studies from the outset (Valero et al., 2016, Gleeson et al., 2016, Aguirre et al., 2018). Thus, the failure rate of utilising EUS guided biopsies for NGS have never been reported and described in detail. The low epithelial tumour cellularity of PDAC makes sequencing studies challenging, particularly in the setting of low tissue volume when using biopsy material. This makes it challenging to predict the accuracy and success rates of these

strategies to realistically define patient numbers that will be able to enrol into molecularly guided personalised trials in PDAC.

The rapid disease progression seen in metastatic patients with advanced disease results in major challenges to demonstrate meaningful treatment benefits in clinical trials in this setting. In addition, the rapid disease progression suggest that many patients only have a single opportunity at effective treatment and limits the timeline between molecular profiling and definitive stratified treatment in PDAC. This provides significant challenges to introducing a precision medicine approach in this disease. As a result, the rapid accumulation of molecular data in PDAC and preclinical evidence for stratified therapy has not yet translated into major clinical success in the disease (Aguirre et al., 2018, Aung et al., 2018). To overcome these challenges and facilitate realistic personalised clinical trials in all stages of PDAC, a clinically integrated patient pathway that allows molecular phenotyping using EUS guided biopsies in parallel to the standard diagnostic process was developed.

In this chapter, the sample processing and next generation sequencing techniques that allow fully integrated genomic and transcriptomic profiling of PDAC using EUS guided biopsies is developed and described. This study, led by the PhD applicant, has been translated into clinical practice with more than 50 subsequent patients undergoing tumour sampling under this protocol to allow entry into the *PRECISION-Panc* clinical trial umbrella.

7.2 Results

7.2.1 Clinical implications of utilising EUS biopsies for next generation sequencing

To date over 140 patients have undergone EUS guided biopsy for molecular profiling using the protocol described in Material and Methods section (Chapter 2) of this PhD thesis. Of these, 90 were used as a training set to identify and develop key steps in the molecular profiling pathway that requires to be optimised in order to enable clinical feasibility. Briefly, patients with a pancreatic mass suspicious of Pancreatic Cancer were consented for extra EUS biopsies for research at the time of presentation to the local Pancreaticobiliary surgical unit. Patients underwent a mean number of 3-5 biopsies using 3 different EUS core biopsy needles (Table 7-1). Extra biopsies were preserved and processed either as fresh frozen, or in standard methanol or formalin fixative.

In the 90 patient EUS training set, the majority of patients (n = 82, 91%) had a pathological diagnosis obtained from the initial EUS biopsy. The remaining patients' diagnosis was confirmed on repeat EUS (n = 6) or laparoscopy (n = 2) and 1 patient failed to obtain histological diagnosis using multiple attempts. There were no false positives or negatives after a final diagnosis was decided upon by the Pancreatic Cancer Multi-disciplinary meeting. The majority of patients were diagnosed with PDAC (n = 65), followed by Pancreatic Neuroendocrine Tumour (n =8), Cholangiocarcinoma (n = 1), IPMN (n = 2), Benign lesions (n = 8) and the remaining 5 were a mix of different pathologies including metastases to the pancreas (n = 2). Of these patients, only 2 patients suffered morbidity during the time period of their diagnostic EUS. Both developed acute pancreatitis and subsequent acute renal failure. This was felt by the treating clinical teams to be associated with ERCP, rather than EUS, and both made a complete recovery.

These findings demonstrate that using a protocol aimed at molecular profiling of EUS biopsies lead to excellent diagnostic rates (> 90% on initial EUS) with very low associated morbidity. This suggest that this protocol is safe and clinically acceptable to be utilised in parallel with molecular profiling and the standard diagnostic pathway. The next question that required to be addressed was whether the tissue sampled using this technique provided sufficient DNA and RNA for next generation sequencing.

7.2.2 Fresh Frozen EUS guided biopsies provide sufficient DNA and RNA yields for next generation sequencing

A major challenge to utilising EUS biopsies for molecular profiling is the perceived low DNA yields obtained from traditional fine needle aspirates. The advent of EUS core biopsy needles allow micro-biopsies with significantly more tissue to be sampled (Bang et al., 2017). In order to assess the feasibility of utilising EUS samples for NGS, fresh frozen and standard diagnostic FFPE samples were collected and DNA extracted for sequencing. After histological confirmation, fresh frozen samples were macro-dissected, and DNA extracted as described in Materials and Methods. The DNA yield obtained was sufficient using a variety of needles for targeted NGS, as well as whole genome sequencing in the majority (73%) of patients with fresh frozen biopsy (Table 7-1). Furthermore, fresh frozen biopsies allow sufficient RNA for whole transcriptome RNA sequencing in the majority of specimens (Table 7-1). Only 1 of the fresh frozen EUS guided biopsies provided insufficient DNA for sequencing, whilst all samples were used for RNA sequencing using a low input library preparation protocol (see chapter 2 Methods and Materials).

Table 7-1 DNA and RNA yield from EUS core biopsy needles

		Fresh Frozen	
	Size	**DNA Yield (mean, range (ng))**	**RNA Yield (mean, range (ng))**
Boston Acquire®	22G	1819 (133 – 7350)	191 (30 – 1187)
Sharkcore®	19G	2170 (11.4 – 6000)	N/A
Sharkcore®	22G	2939 (1134 – 7595)	481 (40 – 1790)
Cook Procore®	20G	1745 (290 – 4750)	18 (3.6 – 44)

As seen above, fresh frozen samples provide excellent quality and quantity of DNA. However, the feasibility and technicalities of cryopreserving biopsies in the standard diagnostic process is a significant logistical challenge and will lead to poor uptake from the majority of clinical units due to local expertise and resources available. Thus, a protocol was developed to allow diagnostic, formalin fixed paraffin embedded (FFPE), samples to be utilised for NGS. In parallel, a targeted sequencing and analysis platform has been developed, the ***GPOL PRECISION-Panc clinical cancer genome™*** panel (Appendix II). Which is a custom build PDAC specific multiplex assay. By targeting specific genomic regions and performing a collection of sub-assays; point mutations, copy number and structural changes and mutational signatures can be determined. Importantly, the

PRECISION-Panc panel is specifically designed to overcome the sequencing challenges of low cellularity samples, a hallmark of PDAC. This is ideal for utilising FFPE preserved biopsy samples, providing that enough DNA can be obtained from each set of biopsies.

7.2.3 FFPE preserved EUS biopsies provide sufficient DNA for next generation sequencing

A training set of 14 diagnostic FFPE samples were used for DNA extraction and targeted panel sequencing. Of these, all 14 cases produced sufficient DNA (> 100ng) for the *PRECISION-Panc* NGS diagnostic™ panel. Of these, 9 had matched fresh frozen biopsies that were processed and sequenced in parallel (results are discussed later in this chapter). To date, 45 *PRECISION-Panc* patients' samples have been extracted with excellent results demonstrating only 1 DNA extraction failures (Table 7-2). Of these, 27 were EUS biopsies and 19 percutaneous core biopsies of various metastatic lesions (Table 7-2). Interestingly, the only extraction failure was from a core biopsy from a liver metastasis.

Table 7-2 DNA and RNA yields from EUS guided FFPE biopsies

		FFPE	
	Needle Size	**DNA Yield (mean, range (ng))**	**RNA Yield (mean, range (ng))**
Training set (n = 14)	22G	1819 (133 – 7350)	191 (30 – 1187)
PRECISION-Panc EUS set (n = 27)	22G	2694 (102 – 28600)	n/a
PRECISION-Panc Core set (n = 19)	Various	550 (0 – 1730)	

These results demonstrate that diagnostic FFPE EUS guided biopsy specimens, provided they are processed according to a standardised protocol, provide sufficient DNA for targeted NGS sequencing. Of note, in the *PRECISION-Panc* set to date, EUS biopsies provided significantly more DNA on average than percutaneous core biopsies, although this has not reached statistical significance (2694ng vs 550ng, $P = 0.062$) (Table 7-2). This demonstrates that EUS biopsies can be utilised with good success to provide sufficient DNA for NGS in the personalised trial protocol. This has a huge impact on the translational potential of personalised therapy in PDAC and enrolment into personalised PDAC clinical trials. In order to further investigate the feasibility of molecularly guided therapy, and the value of EUS biopsies for NGS in translational research, a number of molecular assays were performed using both fresh frozen and FFPE samples.

7.2.4 EUS guided biopsies can be utilised for targeted panel sequencing

A cohort of consecutive patients undergoing EUS biopsy were selected for molecular profiling using targeted panel, RNA (RNAseq) and Whole Genome Sequencing (WGS). The majority of patients had a diagnosis of PDAC (*n* = 36, 88%) followed by pNET (n=3, 7%), Cholangiocarcinoma (*n* = 1, 1%) and 1 patient with a pancreatic metastasis from a primary lung cancer (Table 7-3). The profiled cohort was enriched for borderline resectable / resectable patients (*n* = 13, 36%), and further consisted of locally advanced (*n* = 11, 30%) and metastatic (*n* = 12, 33%) patients (Table 7-3).

Table 7-3 Histological and clinical features of the EUS training cohort that underwent NGS

EUS Sequenced Training Cohort	
Variables	**n = 41 No. (%)**
Histological Subtype	
PDAC	36 (87.8)
PNET	3 (7.3)
Cholangiocarcinoma	1 (2.4)
Pancreas Metastasis	1 (2.4)
Stage (PDAC only)	
Resectable / Borderline Resectable	13 (36.1)
Locally Advanced	11 (30.6)
Metastatic	12 (33.3)

Targeted panel sequencing was performed following extraction of sufficient DNA (> 50ng). This demonstrated evidence of *KRAS* mutations in 39 out of 42 samples (92%) (25 out of 26 patients). Only 1 sample was deemed to be a sequencing failure (EUS 16) based on quality control metrics but demonstrated a mutational profile consistent with PDAC (Figure 7-1). In 1 patient with no detectable *KRAS* mutation (EUS 22), there was a *BRAF* mutation suggesting that this was a true *KRAS* wild-type tumour and not due to a sequencing failure (Figure 7-1). Furthermore, the mean allelic frequency of mutated KRAS appeared to correlate with histological tissue cellularity, with very low KRAS frequency (< 10%) being associated with histological cellularity < 10% (Figure 7-1). Well known PDAC mutations in *TP53* (78%), *CDKN2A* (34%) and *SMAD4* (32%) were identified in sub-groups of patients in keeping with previously described PDAC cohorts (Figure 7-1) (Bailey et al., 2016, Biankin et al., 2012, Waddell et al., 2015). Potentially

actionable mutations were identified in a small sub-group of patients, including *ATM* (12%) and *BRCA1* (6%) (Figure 7-1).

These results are encouraging for clinical implementation EUS biopsies for targeted capture sequencing and demonstrates a high level of sequencing success. Only 3 samples demonstrated no evidence of a *KRAS* mutation, of which 2 are potentially true *KRAS* wild-type. Furthermore, in all the other samples with low *KRAS* allelic frequency, this is secondary to low cellularity rather than sequencing failures or DNA quality. These findings strongly support the use of EUS biopsies for targeted profiling in the clinical setting and makes it an ideal tool for personalised trials in the locally advanced, neoadjuvant and metastatic settings.

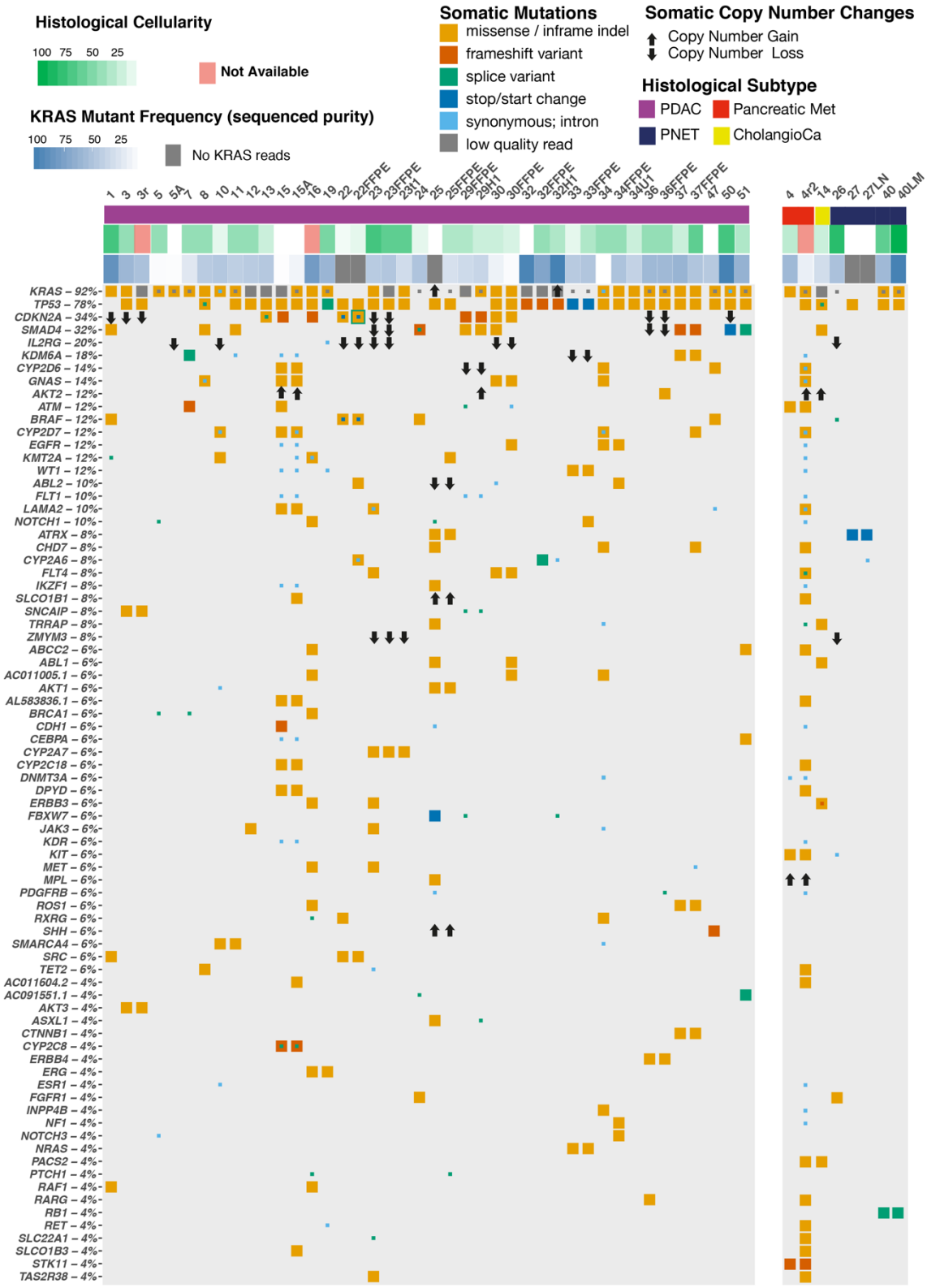

Figure 7-1 Point mutations and copy number variations in the EUS biopsy cohort. Oncoplot demonstrating somatic mutations (coloured boxes) and copy number changes (arrows) are indicated for the EUS biopsy training cohort. Pathology, histological cellularity and *KRAS* mutant allele frequency are on the top x-axis. The majority of PDAC specimens identified well known mutations including *KRAS, TP53, SMAD4* and *CDKN2A*.

Utilising FFPE biopsies would significantly improve the translational potential of using EUS for sampling patients and improve the general uptake of collaborating centres to the *PRECISION-Panc* protocol. FFPE preserved biopsies performed satisfactorily and provided sufficient DNA of sufficient quality for panel sequencing. Based upon quality control analysis, these were above the thresholds required to call observed mutations (Appendix III). Furthermore, the mutational profile obtained from FFPE samples were almost identical to that of the paired fresh frozen sample in both point mutation and copy number analyses (Figure 7-2).

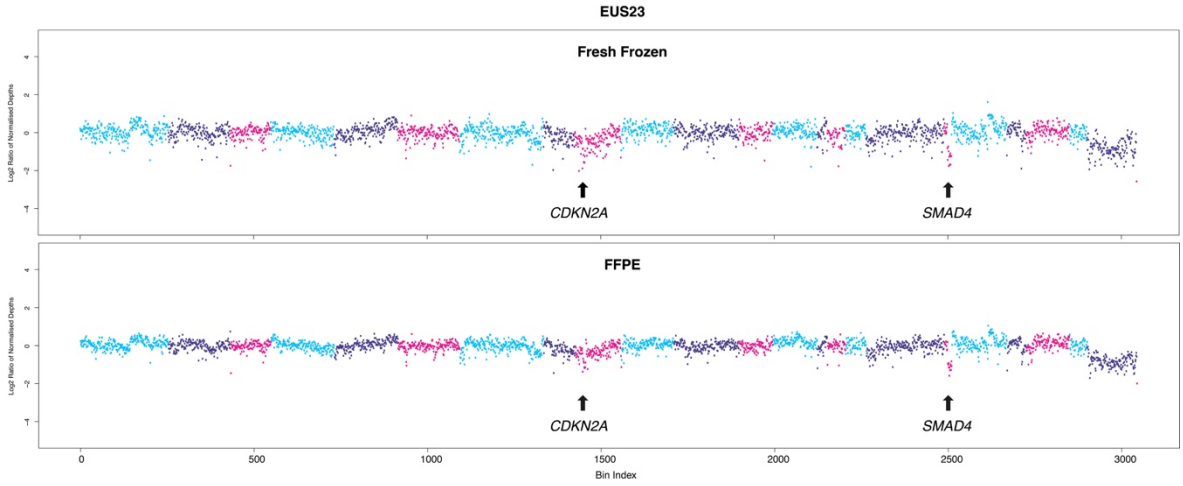

Figure 7-2 Copy number alterations in fresh frozen and FFPE samples from the same primary tumour (EUS22). Example of copy number plot comparison between fresh frozen and FFPE biopsies. Significant copy number variations were equal in both samples. Well documented PDAC copy number loss in *SMAD4* and *CDKN2A* are shown in both samples. The similarities seen between fresh frozen and FFPE samples were consistent in the FFPE versus frozen comparison set (n = 9) and further demonstrates the utility of FFPE diagnostic EUS biopsies for targeted genomic profiling.

These results strongly support the clinical role of EUS guided biopsies samples for targeted panel profiling in PDAC to enable personalised medicine trials. Utilising diagnostic FFPE samples for profiling allows targeted sequencing to the same standard as frozen samples and can be performed in a clinically relevant time-frame that will allow molecularly guided clinical trials with no delay in current treatment pathways. This is crucial in PDAC, a disease with rapid progression and deterioration of performance status and is key to the clinical implementation of molecularly guided therapy.

A major advantage of utilising EUS guided biopsies for molecular profiling is the ability to investigate temporal and spatial heterogeneity in patients undergoing neoadjuvant therapy prior to surgical resection. Furthermore, subtyping of PDAC has been a major endeavour

in the lab but has not yet made a clinical difference for patients. The results in this PhD thesis suggest that molecular subtyping may well play a significant role in the future management of PDAC. Thus, in order to further investigate the translational potential of EUS biopsies in molecularly guided clinical trials, whole genome sequencing (to investigate evolution and heterogeneity) and RNA sequencing (subtyping and transcriptomic signature analysis) was performed in a subset of samples.

7.2.4.1 EUS guided biopsies can be utilised for whole genome sequencing of PDAC

The often-rapid emergence of resistance and parallel genomic evolution of PDAC in response to chemotherapy has led to an urgent need to be able to measure the evolution of tumours in response to therapeutics (Burrell and Swanton, 2014). In order to investigate this by considering genomic rearrangements and somatic mutations, whole genome sequencing (WGS) is required. The feasibility of WGS using pre-treatment EUS biopsies was investigated using a pilot study of 5 samples that were selected for WGS. Frozen samples were selected based on cellularity on panel sequencing (> 25%) and DNA quantity available (> 500ng). This is greater than the minimum thresholds required but was selected in order to increase the likelihood of sequencing success. In total, 31 out of 43 patients (72%) had samples with sufficient quantity DNA for WGS, and 5 were selected as a proof of principle study with no sequencing failures. WGS revealed mutational signatures described in PDAC including the COSMIC BRCA mutational signature (Figure 7-3). Circos plots allow visualisation of genomic re-arrangements and can demonstrate the high number of structural variations, as seen in EUS4 (Figure 7-3). This was later confirmed as a primary bronchial carcinoma that has metastasised to the pancreas. This data suggests that fresh frozen EUS samples can be utilised for WGS to enable novel investigative techniques into the clonal evolution of PDAC, particularly in the neoadjuvant and advanced disease settings.

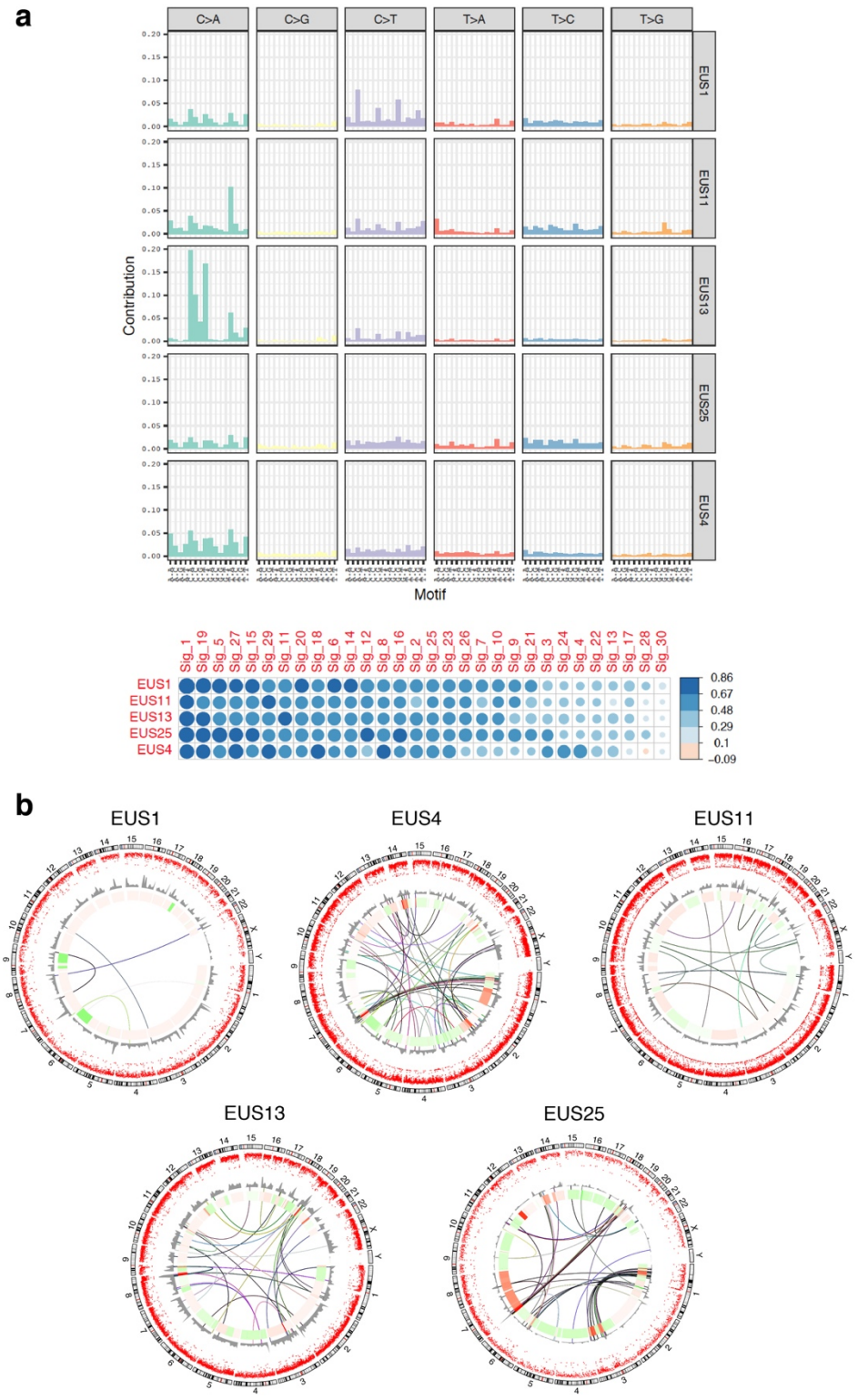

Figure 7-3 Whole genome sequencing of EUS guided biopsies is feasible for translational research in PDAC. a) Mutational signature contribution in 5 EUS samples that underwent WGS. b) Circos plots demonstrating structural variations and copy number changes in EUS samples. EUS 4 reveals a high number of structural variations suggesting a high level of genomic instability. WGS allows in-depth study of tumour evolution and heterogeneity, whilst having the potential to reveal novel resistance mechanisms in the neoadjuvant and advanced disease settings.

7.2.5 RNA sequencing allows transcriptomic sub-typing of PDAC

Molecular subtyping of tumours is becoming clinically relevant as therapeutic targets within subtypes are being identified and clinically tested. In order to allow treatment stratification based on molecular subtyping, the utility of RNAseq using EUS guided biopsies was investigated. Gene expression was normalised, and consensus clustering performed based upon the gene programs described by Bailey *et al*.(Bailey et al., 2016). Due to the relatively small cohort (n = 35), and the strong overlap between Pancreatic Progenitor, ADEX and Immunogenic subtypes, patients were subtyped as either Classical Pancreatic and Squamous (Figure 7-4). Since this cohort contained patients presenting with all stages of PDAC, molecular subtypes were correlated with stage of presentation (Figure 7-4). Out of 35 patients, 16 (46%) were classified as Classical Pancreatic and 19 (54%) Squamous (Figure 7-4). The squamous subtype was significantly associated with *de novo* metastatic disease (n = 10, 53%) compared to the Classical Pancreatic subtype (n = 3, 19%) (P = 0.042, Chi square-test). In contrast, the Classical Pancreatic group was associated with locally advanced disease (50% vs 21%, P = 0.075, Chi square-test), however, this failed to reach significance due to low patient numbers. To further investigate the association of a metastatic phenotype and the squamous subtype, gene expression analysis was performed by clustering gene programs based upon disease stage at presentation. Patients presenting with *de novo* metastatic disease, had significant enrichment of GP2 expression in comparison with locally advanced (P = 0.006) and resectable (P = 0.0058) PDAC (Figure 7-4). GP2 is the strongest classifying gene program defining the squamous subtype, and thus further strengthens the association of the squamous subtype with metastatic PDAC. In 2 patients, both the PDAC primary and liver metastasis was biopsied and underwent RNAseq (Figure 7-4). This demonstrated that primary and metastasis cluster to the same subtype, but some differences exist in gene programs (Figure 7-4). Determining the significance of this is not possible in such a small sample size, but this demonstrates that transcriptomic profiling of both primary and metastatic lesion is possible using this technique. The exact implications of these in terms of therapeutic response and the transcriptomic evolution of PDAC metastases, require further investigation.

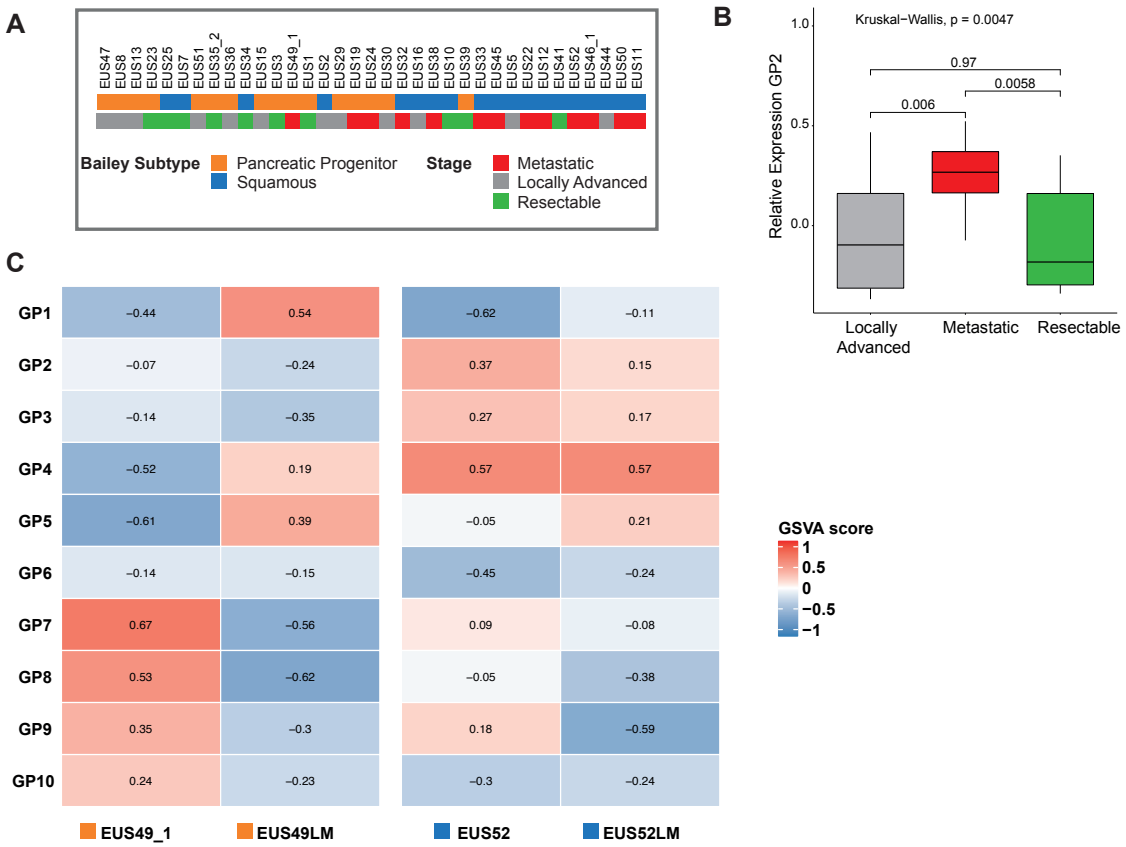

Figure 7-4 Transcriptomic profiling of PDAC using EUS guided biopsies. RNA sequencing of 35 patients across all clinical stages of presentation of PDAC is feasible and clinically relevant. A) Molecular subtype can be identified using EUS guided biopsies and demonstrate that the squamous subtype is associated with metastatic disease at presentation. B) Metastatic PDAC at the time of presentation is enriched for gene program 2, which defines the squamous subtype. C) Comparison between metastatic and primary PDAC demonstrate differences in gene programs 7 – 10 with loss of gene expression associated with the microenvironment (immune) and normal pancreatic signalling.

7.3 Discussion

The results presented here demonstrate that EUS guided biopsies can be utilised with high success rates in a patient centred pathway for next generation molecular analysis to facilitate precision medicine in PDAC. Importantly, acquiring extra biopsies at the time of EUS is not associated with increased morbidity and is associated with high diagnostic rates without significantly increasing the morbidity associated with the procedure. These results suggest that integrating sequencing into the clinical pathway is not detrimental to the current level of patient care and may only add to it.

Panel sequencing from diagnostic EUS FNAs has previously been shown to be feasible and can identify mutations could potentially select for therapy (Gleeson et al., 2016). However, failure rates in diagnostic samples remain high and can result in a large proportion of patients requiring repeat procedures or missing out on personalised clinical trials. The results presented here demonstrate if sample acquisition is performed using a protocol tailored towards both diagnosis and NGS, panel-based sequencing can be performed with excellent success rates. Both fresh frozen and FFPE tissue provide sufficient DNA yields in almost all patients with high sequencing success rates (> 90%). Using a number of paired fresh frozen and FFPE samples, our results demonstrate high concordance between both tissue acquisition and processing strategies. As a result, for ease of use and greater applicability to all clinical units performing EUS, FFPE embedded biopsy tissue will be utilised for the *PRECISION-Panc* trial Master Protocol.

Targeting point mutations only as yet to demonstrate significant clinical impact in the majority of cancer subtypes and this is particularly so in PDAC. Developing a clinically integrated pathway that allows sequencing assays that identify molecular subtypes and signatures will allow greater therapeutic options for patients with PDAC. Our results demonstrate that these can be performed using fresh frozen EUS tissues for WGS and RNAseq. Developing a pancreatic cancer specific panel based molecular assay that identifies signatures of therapeutic vulnerabilities such as DDR and MMR deficiency is a priority. WGS is significantly more expensive and requires much larger storage capacity, and as of yet has not been shown to be superior in therapeutic selection. This is the aim of the ***GPOL PRECISION-Panc clinical cancer genome*** **™** panel (Appendix II) and is currently being validated as a molecular profiling tool. On the other hand, in well-designed studies aimed at studying the clonal evolution of PDAC during neoadjuvant therapy for example, WGS of EUS biopsies and subsequent resection specimen will allow unique

insights into the development of therapeutic resistance. RNAseq and molecular subtyping of EUS guided biopsies can provide unique insights into the underlying biology of advanced disease, as well as potentially direct therapy in future clinical trials.

This chapter demonstrates the safety and feasibility of implementing a molecular profiling protocol into clinical practice for enabling precision oncology in almost all patients with PDAC. This is crucial to the philosophy of *PRECISION-Panc* which aims to provide clinical trial options for all patients with PDAC. The protocol developed here has been used successfully in > 50 patients demonstrating the widespread implementation within the *PRECISION-Panc* framework. Ongoing evolution of this protocol and strategy is crucial as biomarkers of therapeutic response and molecular assays develop, to enable optimal patient selection for precision oncology in PDAC.

8 Conclusions and Future Directions

Pancreatic Cancer is due to become the 2nd leading cause of cancer death in western societies within the next decade. The major advances in our understanding of the molecular diversity of this disease has not yet improved patient outcomes. This PhD thesis builds upon these advances and the clinical responses observed in subgroups of patients to surgical resection and platinum-based chemotherapy in order to develop personalised medicine strategies for patients with pancreatic cancer.

Large scale molecular subtyping studies have defined 2 subtypes of PDAC, termed Squamous and Classical Pancreatic. Data from this PhD thesis demonstrates the clinical and pathological disease patterns associated with these subtypes and how this impact on prognosis and outcome following surgical resection. The Squamous subtype is associated with early recurrence following surgery and liver metastases. Whereas, the Classical Pancreatic subtype appears associated with lung metastases and improved outcome. PDAC that occurs in the body and tail of pancreas is more likely to be Squamous subtype and these findings may be secondary to the late clinical presentation associated with these tumours. These findings, for the first time, has mapped out different disease patterns seen in clinical practice with large scale next generation sequencing studies. This is clinically significant for a number of reasons. The phenotypic differences between the Squamous and Classical Pancreatic subtypes highlights the importance of molecular subtyping to sub-classify cancers of a single organ. These differences have been suspected for a long time, but only recently has the technology developed to detect differences in individual tumours at a molecular level. In fact, the physician Sir William Osler (1849 – 1919) described this concept more than a century ago by saying:

"Variability is the law of life, and as no two faces are the same, so no two bodies are alike, and no two individuals react alike and behave alike under abnormal conditions we know as disease"

Building on these findings, the concept of personalised treatment for patients with PDAC was further explored. This was firstly approached by developing an accurate predictor of patients that respond to surgery. The expression of 2 biomarkers that are associated with squamous PDAC, S100A2 and S100A4, predicted early recurrence following pancreatectomy. This was used to develop a novel biomarker based pre-operative nomogram that can inform surgical decision making. Current surgical decision making is

almost exclusively based upon cross sectional imaging with no consideration of the underlying biology of each individual tumour. Thus, a large number of patients with 'resectable' PDAC develop early recurrence and do not benefit from surgical resection. The findings presented in this thesis can help inform these decisions to select patients with good prognosis for an aggressive surgical approach, even in the setting of locally advanced or borderline resectable tumours. In cases where prognosis is poor, patients can be stratified to neoadjuvant therapy even with resectable disease, in order to give these patients a period of biological selection prior to undergoing potentially morbid surgery such as pancreatectomy. This has the potential to transform surgical decision making from using imaging only, to a biological assessment that can improve survival and quality of life for patients with PDAC.

The concept of precision medicine for PDAC was further explored by building upon the clinical responses seen with platinum-based chemotherapy regimens and the recent finding that deficiency in DNA damage repair mechanisms exist in up to 24% of patients (Waddell et al., 2015). Genomic features of DDR deficiency (unstable genome, BRCA mutational signature, homologous recombination deficiency signature, mutations in DDR pathways) were utilised as biomarkers that predicted sensitivity to both platinum and PARP inhibitors in cell lines and xenograft models. Numerous studies have shown that a subgroup of patients can have durable, clinically relevant responses to platinum (Waddell et al., 2015, Conroy et al., 2011, Conroy et al., 2018, He et al., 2018). However, there is little benefit for patients that do not respond, and platinum chemotherapy is associated with both morbidity and mortality. Thus, utilising biomarkers to predict response is of utmost importance. This is currently being tested in clinical trials in the metastatic (*PRIMUS-001, PRECISION-Panc*) and neoadjuvant (*PRIMUS-002, PRECISION-Panc*) settings.

Defects in DNA damage repair mechanisms extend beyond homologous recombination deficiency (associated with platinum response) in PDAC and can offer a therapeutic vulnerability that can be targeted with novel agents targeting these mechanisms. This was explored by demonstrating the transcriptomic enrichment of replication stress pathways in a subgroup of patients and its association with the squamous subtype of PDAC. This was found to be functionally relevant and associated with sensitivity to agents inhibiting cell checkpoint and DNA damage repair proteins such as ATR and WEE1. The sensitivity to these agents only partially overlaps with platinum response and thus offers an extended therapeutic strategy targeting DDR in PDAC. Furthermore, acquired resistance to platinum therapy is common even in *BRCA* mutant tumours (Lord and Ashworth, 2013, Lord and

Ashworth, 2016, Pishvaian et al., 2017, Lheureux et al., 2017). Evidence from other cancer subtypes, e.g. ovarian (Fong et al., 2010, Mirza et al., 2016) and breast cancer (Robson et al., 2017), reveal responses to PARP inhibitors even after previous treatment with platinum chemotherapy, and responses can occur in both primary platinum sensitive and resistant disease. However, clinical resistance to PARP inhibition can develop due to *BRCA 1 / 2* reversion (Lheureux et al., 2017). There is growing pre-clinical evidence that demonstrates delayed resistance to PARP inhibition, when combined with ATR inhibition (Kim et al., 2017, Yazinski et al., 2017). In addition, PARP inhibition increases replication stress and can in turn sensitise cells with replication defects to ATR inhibition, irrespective of DDR status (Yazinski et al., 2017). Suggesting that combined inhibition of PARP and ATR (e.g. Olaparib and AZD6738) can target both DDR deficient PDAC, whilst acting synergistically to enhance response in those with high replication stress by 1) enhancing replication stress and thus ATR inhibitor responsiveness, 2) delaying formation of resistant clones to PARP inhibition and 3) bypassing resistance mechanisms in acquired PARPi resistance.

In order to clinically target DDR and replication stress in PDAC, a clinical trial in the 2nd line metastatic setting was designed and has been endorsed by Cancer Research UK and the National Cancer Research Institute (NCRI) pancreatic subgroup. The combination of ATR and PARP inhibitors will aim to target both DDR deficient and high replication stress PDAC, even in the presence of acquired platinum resistance, based on the mechanisms described above. This will be investigated in patients that have responded or achieved stable disease on platinum in the first line setting, and in both DDR deficient (n = 20) and proficient (n = 20) patients with an adaptive design that allows early stopping in futile patient cohorts. As the translational primary investigator (PI) for this trial, the PhD candidate will develop this concept by further investigating biomarkers of response to this combination in the pre-clinical setting. The results of which will be combined with the clinical and molecular data obtained from the trial, if successful, to develop a therapeutic biomarker hypothesis for further testing in a randomised Phase III trial.

A major challenge for implementing personalised medicine for pancreatic cancer is acquiring tissue for molecular profiling to inform clinical trial and treatment stratification. PDAC offers unique challenges due to rapid disease progression, low epithelial cellularity, the low (around 10%) resectability rate and relative inaccessibility of the pancreas for percutaneous biopsy. In order to overcome these and to allow personalised medicine trials for all patients, irrespective of the disease stage, a protocol for utilising EUS guided

biopsies was developed. The results in this PhD thesis demonstrates the utility of fresh frozen biopsies for targeted, whole genome and RNA sequencing. This facilitates molecularly stratified trial allocation as well as enabling novel translational research using clinical samples. Importantly, the data presented here demonstrates that formalin fixed biopsies, utilised in the standard diagnostic pathway, can provide targeted sequencing results as accurate as fresh frozen tissue. This has major impact on the transferability of this protocol to other centres and enabling a greater number of patients to enter the *PRECISION-Panc* master protocol. Crucially, this does not delay the diagnostic or treatment decision process and using this protocol patients will be able to enrol in molecularly stratified trials in a timeframe similar to standard treatment pathway.

The major advances in the molecular diversity of pancreatic cancer is opening the door to making massive improvements in the outcome of this truly devastating disease. In order to translate the potential of these advances, we need to understand the clinical and therapeutic implications of the molecular pathology of individual tumours. By correlating the growing 'knowledge bank' of molecular data with clinical and therapeutic response, we can generate and test pre-clinical hypotheses that can inform future clinical trials. This, in turn, will further add to 'knowledge banks' and inform further pre-clinical studies to refine therapeutic strategies for PDAC. By harmonising this forward and backward translation we, as a pancreatic cancer research community, can finally begin to improve survival and the quality of life for patients. This requires global collaboration to study a cancer with low incidence but high mortality. The data presented in this thesis has provided a small, but significant, contribution to this cause. The impact of which can be demonstrated by several high impact peer-reviewed publications, the translation of pre-clinical findings into a novel 2nd line metastatic trial for which there is currently no therapeutic options for patients, and the adoption of a tissue acquisition protocol for EUS biopsies across multiple centres in both the United Kingdom and Europe to facilitate personalised medicine trials. It is crucial, however, that these findings and strategies are further refined to optimise the care and treatment of patients with Pancreatic Cancer.

9 Appendices

9.1 Appendix I

PRECISION-Panc Clinical Trial Portfolio

9.1.1 PRIMUS-001

Adaptive Phase II study in Metastatic PDAC:

FOLFOX-A (FOLFOX and nab-Paclitaxel) versus Gem-Abraxane (Gemcitabine and nab-Paclitaxel) in patients with metastatic pancreatic cancer, with integrated biomarker evaluation and progression-free survival as primary endpoint.

9.1.2 PRIMUS-002

An umbrella phase II study in the neoadjuvant setting (resectable / borderline resectable PDAC):

Examining two -neoadjuvant regimens (FOLFOX-A and Gem-Abraxane) focusing on biomarker and liquid biopsy development. The primary aim here is to define the biomarkers of therapeutic responsiveness of both regimens by comparing pre- and post-treatment biopsies and resection specimens.

9.1.3 PRIMUS-003

An initial open-label, non-randomised, single arm, phase 2 study combining myeloid depletion by CXCR2 inhibition in combinations with immune checkpoint inhibition (PDL-1). This will be offered as second line therapy in patients with metastatic PDAC. Patient samples will be taken pre-treatment and post treatment, but the primary objective here is to test the efficacy of the drug combination.

9.2 Appendix II

9.2.1 GPOL PRECISION-Panc clinical cancer genome™

The ***GPOL PRECISION-Panc clinical cancer genome™*** is a multiplex assay specifically designed to overcome the technical limitations of WGS in fixed and low cellularity samples, whilst still capturing an equivalent range of genomic features. The table below illustrates the technical, time and cost advantages of the *Precision-Panc* NGS Diagnostic sequencing over WGS.

Table 9-1 Comparison between GPOL clinical cancer genome and whole genome sequencing. As well as being faster, cheaper and higher throughput, the higher depth of panel sequencing makes it more suitable for low cellularity samples than whole genome sequencing, which does not sample each position deeply enough to reliably detect mutations that are at low frequency due to an excess of germ line sequence from contaminating stromal cells. DNA ideally provided as 25µl at 10ng/µl for panel sequencing.

	GPOL clinical cancer genome	**Whole genome**
Starting material	Fixed/unfixed	Unfixed
Amount DNA needed	50-200ng	100ng-2µg
Depth generated	200-400x	60-75x
Library prep time	2.5 days	1.5 days
Time on sequencer	15-18 hrs	~3 days
Compute time	< 10 hrs	~24 hrs
Throughput	14 samples/HiSeq4000 run	2.5 samples/HiSeqX run
Sequencing cost	++	++
Data storage cost p.a.	+	+++

Most available cancer panels contain the coding exons of known cancer genes, allowing only point mutation and small indel detection. However, a much larger range of events are of importance in cancer diagnosis, prognosis and therapeutic response. These include copy number changes such as amplification of oncogenes, homozygous deletion of tumour suppressor genes; large-scale structural alterations, giving rise to gene fusion or disrupting tumour suppressor genes; non-coding events such as *TERT* promoter mutations and genome-wide signatures, including defects in DNA damage response deficiency such as microsatellite instability and overall levels of genomic disruption. The ***GPOL PRECISION-Panc clinical cancer genome™*** is a collection of sub-assays, each of which targets a different type of genomic event.

The features, genes and regions of interest for each sub-assay have been identified through integrated data analysis of whole genome data from the International Cancer Genome Consortium (ICGC), The Cancer Genome Atlas (TCGA) and other large databases of

genomic data such as the ICGC PCAWG (PanCancer Analysis of Whole Genomes; https://dcc.icgc.org/pcawg), including extensive literature curation[1-10]. By distilling all known interpretable events from these sources into these assays we obtain a similar quantity of information about each sample as would be obtained from a deep whole genome but with the technical advantages of a selected genomic region approach.

Sub- assays include:

1. Mutations in 164 genes known to be important in pancreatic cancer, including point mutations, small indels, copy number changes (amplification, deletion), gene fusion and other large-scale structural variants.

2. Key non-coding driver events

3. Microsatellite instability status

4. Genome-wide CNV

5. Signatures of DNA Damage Response deficiency (in development), including overall levels of sequence-level and structural genomic alteration

6. Retrotransposon activity levels

7. Embedded quality control features, such as sample swap and contamination level measures

8. Cellularity assessment (in development)

The base content is designed to encompass relevant events for most common solid tumour types, but is ***extended to pancreatic cancer-specific genomic features***, specialising in support for biomarker discovery[9,11-24]. It includes all events that are clinically relevant and potentially actionable, including those linked to therapeutic response. To analyse and interpret the complex data generated by the assay we have developed ***HOLMES***, a bespoke pipeline combining best-of-breed third-party software with custom algorithms to deliver the required analytics.

Gene List:

ACVR1B
ACVR2A
AJUBA
AKT1
AKT2
AKT3
ALK
ALOX12B
ALOX15B
APC
ARAF
ARID1A
ARID1B
ARID2
ATM
ATR
ATRX
AXIN1
B2M
BLM
BRAF
BRCA1
BRCA2
C11orf30
CCND1
CCND2
CCND3
CCNE1
CD274
CDH1
CDK4
CDK6
CDKN1B
CDKN2A
CDKN2B
CHEK2
CIITA
CTNNB1
DAXX
DNMT3A
EGFR
ERBB2
ERBB3
ERBB4
EZH2
FAM135B
FANCA
FANCC
FANCD2
FANCF
FANCG
FANCM
FBXW7
FGFR1
FGFR2
FGFR3
FGFR4
FLT3
FOXL2
GATA3
GATA6
GNA11
GNAQ
GNAS
HIF1A
HLA-A
HLA-B
HLA-C
HRAS
IDH1
IDH2
IDO1
IDO2
IRS2
JAK1
JAK2
KDM6A
KDR
KIT
KMT2A
KMT2C
KMT2D
KRAS
MAP2K1
MAP2K2
MAP2K4
MAP3K1
MAPK1
MDM2
MDM4
MEN1
MET
MLH1
MSH2
MSH6
MTOR
MUTYH
MYC
MYCL
MYCN
NF1
NF2
NOTCH1
NOTCH2
NOTCH3
NOV
NRAS
NTRK1
NTRK2
NTRK3
PALB2
PBRM1
PDCD1LG2
PDGFRA
PIK3CA
PIK3CB
PIK3R1
PIK3R2
PIK3R3
POLE
PPP2R1A
PPP6R3
PREX2
PTCH1
PTEN
PTK2
PTPN11
RAD21
RAD50
RAF1
RB1
RBM10
RET
REV3L
RFX5
RFXAP
RHOA
RNF43
ROBO1
ROBO2
RPA1
RUNX1
SETD2
SF3B1
SLIT2
SMAD4
SMARCA2
SMARCA4
SMO
SOX9
STAG2
STK11
TAP1
TAP2
TERT
TET2
TGFBR1
TGFBR2
TP53
TSC1
TSC2
U2AF1
VEGFA
VH

9.3 Appendix III

9.3.1 Quality control metrics EUS guided biopsy 151 gene panel

Table 9-2 Quality control metrics of EUS guided biopsies in paired fresh frozen and FFPE samples.

ID	DISCORDANT_PCT	UNMAPPED_PCT	ON_TARGET_MB	AVG_DEPTH	DUPLICATES_PCT
EUS22FFPE	1.878660931	1.648449209	188.381775	239.1499643	0.414222
EUS23FFPE	1.160586505	1.119745314	481.09095	610.7431758	0.162273
EUS25FFPE	1.090161738	0.851240867	357.447	453.7776401	0.160076
EUS29FFPE	1.307303101	0.987152781	470.521725	597.3255839	0.170565
EUS30FFPE	1.867584474	1.451020795	151.4472	192.2616584	0.293025
EUS32FFPE	1.186870502	1.191414899	408.728625	518.8794728	0.194453
EUS33FFPE	1.294069766	0.956311442	395.7807	502.44213	0.151165
EUS34FFPE	2.900727343	1.885807067	151.306875	192.0835164	0.463899
EUS36FFPE	1.619420087	1.279839973	216.128025	274.3737257	0.25693
EUS37FFPE	2.223729901	2.044954602	192.47835	244.3505511	0.396797
EUS38FFPE	2.160360251	2.874692229	139.130925	176.626193	0.455647
EUS39FFPE	1.553120221	1.360973616	289.620075	367.6716105	0.219366
EUS43FFPE	2.402593409	1.985618201	183.7905	233.3213578	0.458582
EUS44FFPE	1.769249912	1.207252611	272.587275	346.0485341	0.250356
EUS22	1.170933926	0.532084394	145.600425	184.8391993	0.0204255
EUS23	1.037663964	0.507760828	235.5693	299.0543522	0.0237046
EUS23t1	1.163312143	0.505483901	176.148225	223.619518	0.0192176
EUS25	2.055981718	0.198158392	79.054875	100.3598705	0.0242651
EUS29H1	0.935246327	0.075824018	125.460975	159.2722422	0.0280716
EUS30	2.564997083	0.195347506	91.1667	115.7357874	0.0384105
EUS32H1	2.557635438	0.080665822	107.074575	135.9307756	0.0301099
EUS32	1.59910975	0.069204439	89.133975	113.1552505	0.0294499
EUS33	2.283051686	0.56700697	547.1592	694.616574	0.191091
EUS34	1.905538897	0.553729691	638.324025	810.3499811	0.275744
EUS34U1	1.804071111	0.597677584	543.131625	689.5035825	0.232679
EUS36	1.763108158	0.601256045	611.464875	776.2523898	0.172882
EUS37	2.628380109	0.084280942	113.703825	144.3465839	0.0400983

List of References

AGUIRRE, A. J., NOWAK, J. A., CAMARDA, N. D., MOFFITT, R. A., GHAZANI, A. A., HAZAR-RETHINAM, M., RAGHAVAN, S., KIM, J., BRAIS, L. K., RAGON, D., WELCH, M. W., REILLY, E., MCCABE, D., MARINI, L., ANDERKA, K., HELVIE, K., OLIVER, N., BABIC, A., DA SILVA, A., NADRES, B., VAN SEVENTER, E. E., SHAHZADE, H. A., ST PIERRE, J. P., BURKE, K. P., CLANCY, T. E., CLEARY, J. M., DOYLE, L. A., JAJOO, K., MCCLEARY, N. J., MEYERHARDT, J. A., MURPHY, J. E., NG, K., PATEL, A. K., PEREZ, K., ROSENTHAL, M. H., RUBINSON, D. A., RYOU, M., SHAPIRO, G. I., SICINSKA, E., SILVERMAN, S. G., NAGY, R. J., LANMAN, R. B., KNOERZER, D., WELSCH, D. J., YURGELUN, M. B., FUCHS, C. S., GARRAWAY, L. A., GETZ, G., HORNICK, J. L., JOHNSON, B. E., KULKE, M. H., MAYER, R. J., MILLER, J. W., SHYN, P. B., TUVESON, D. A., WAGLE, N., YEH, J. J., HAHN, W. C., CORCORAN, R. B., CARTER, S. L. & WOLPIN, B. M. 2018. Real-time genomic characterization of advanced pancreatic cancer to enable precision medicine. *Cancer Discov*.

AI, K. X., LU, L. Y., HUANG, X. Y., CHEN, W. & ZHANG, H. Z. 2008. Prognostic significance of S100A4 and vascular endothelial growth factor expression in pancreatic cancer. *World J Gastroenterol,* 14**,** 1931-5.

AL-EJEH, F., PAJIC, M., SHI, W., KALIMUTHO, M., MIRANDA, M., NAGRIAL, A. M., CHOU, A., BIANKIN, A. V., GRIMMOND, S. M., BROWN, M. P. & KHANNA, K. K. 2014. Gemcitabine and CHK1 inhibition potentiate EGFR-directed radioimmunotherapy against pancreatic ductal adenocarcinoma. *Clin Cancer Res,* 20**,** 3187-97.

ALEXANDROV, L. B., NIK-ZAINAL, S., WEDGE, D. C., APARICIO, S. A., BEHJATI, S., BIANKIN, A. V., BIGNELL, G. R., BOLLI, N., BORG, A., BORRESEN-DALE, A. L., BOYAULT, S., BURKHARDT, B., BUTLER, A. P., CALDAS, C., DAVIES, H. R., DESMEDT, C., EILS, R., EYFJORD, J. E., FOEKENS, J. A., GREAVES, M., HOSODA, F., HUTTER, B., ILICIC, T., IMBEAUD, S., IMIELINSKI, M., JAGER, N., JONES, D. T., JONES, D., KNAPPSKOG, S., KOOL, M., LAKHANI, S. R., LOPEZ-OTIN, C., MARTIN, S., MUNSHI, N. C., NAKAMURA, H., NORTHCOTT, P. A., PAJIC, M., PAPAEMMANUIL, E., PARADISO, A., PEARSON, J. V., PUENTE, X. S., RAINE, K., RAMAKRISHNA, M., RICHARDSON, A. L., RICHTER, J., ROSENSTIEL, P., SCHLESNER, M., SCHUMACHER, T. N., SPAN, P. N., TEAGUE, J. W., TOTOKI, Y., TUTT, A. N., VALDES-MAS, R., VAN BUUREN, M. M., VAN 'T VEER, L., VINCENT-SALOMON, A., WADDELL, N., YATES, L. R., ZUCMAN-ROSSI, J., FUTREAL, P. A., MCDERMOTT, U., LICHTER, P., MEYERSON, M., GRIMMOND, S. M., SIEBERT, R., CAMPO, E., SHIBATA, T., PFISTER, S. M., CAMPBELL, P. J. & STRATTON, M. R. 2013. Signatures of mutational processes in human cancer. *Nature,* 500**,** 415-21.

ALLEN, P. J., KUK, D., CASTILLO, C. F., BASTURK, O., WOLFGANG, C. L., CAMERON, J. L., LILLEMOE, K. D., FERRONE, C. R., MORALES-OYARVIDE, V., HE, J., WEISS, M. J., HRUBAN, R. H., GONEN, M., KLIMSTRA, D. S. & MINO-KENUDSON, M. 2017. Multi-institutional Validation Study of the American Joint Commission on Cancer (8th Edition) Changes for T and N Staging in Patients With Pancreatic Adenocarcinoma. *Ann Surg,* 265**,** 185-191.

ALTMAN, D. G. & ROYSTON, P. 2000. What do we mean by validating a prognostic model? *Stat Med,* 19**,** 453-73.

ANDOR, N. & GRAHAM, T. A. 2016. Pan-cancer analysis of the extent and consequences of intratumor heterogeneity. 22**,** 105-13.

ANSARI, D., ROSENDAHL, A., ELEBRO, J. & ANDERSSON, R. 2011. Systematic review of immunohistochemical biomarkers to identify prognostic subgroups of patients with pancreatic cancer. *Br J Surg*.

APARICIO, S., HIDALGO, M. & KUNG, A. L. 2015. Examining the utility of patient-derived xenograft mouse models. *Nat Rev Cancer,* 15**,** 311-6.

ARTIFON, E. L. A., GUEDES, H. G. & CHENG, S. 2017. Maximizing the Diagnostic Yield of Endoscopic Ultrasound-Guided Fine-Needle Aspiration Biopsy. *Gastroenterology,* 153**,** 881-885.

ARTINYAN, A., SORIANO, P. A., PRENDERGAST, C., LOW, T., ELLENHORN, J. D. & KIM, J. 2008. The anatomic location of pancreatic cancer is a prognostic factor for survival. *HPB (Oxford),* 10**,** 371-6.

AUNG, K. L., FISCHER, S. E., DENROCHE, R. E., JANG, G. H., DODD, A., CREIGHTON, S., SOUTHWOOD, B., LIANG, S. B., CHADWICK, D., ZHANG, A., O'KANE, G. M., ALBABA, H., MOURA, S., GRANT, R. C., MILLER, J. K., MBABAALI, F., PASTERNACK, D., LUNGU, I. M., BARTLETT, J. M. S., GHAI, S., LEMIRE, M., HOLTER, S., CONNOR, A. A., MOFFITT, R. A., YEH, J. J., TIMMS, L., KRZYZANOWSKI, P. M., DHANI, N., HEDLEY, D., NOTTA, F., WILSON, J. M., MOORE, M. J., GALLINGER, S. & KNOX, J. J. 2018. Genomics-Driven Precision Medicine for Advanced Pancreatic Cancer: Early Results from the COMPASS Trial. *Clin Cancer Res,* 24**,** 1344-1354.

BAILEY, P., CHANG, D. K., NONES, K., JOHNS, A. L., PATCH, A. M., GINGRAS, M. C., MILLER, D. K., CHRIST, A. N., BRUXNER, T. J., QUINN, M. C., NOURSE, C., MURTAUGH, L. C., HARLIWONG, I., IDRISOGLU, S., MANNING, S., NOURBAKHSH, E., WANI, S., FINK, L., HOLMES, O., CHIN, V., ANDERSON, M. J., KAZAKOFF, S., LEONARD, C., NEWELL, F., WADDELL, N., WOOD, S., XU, Q., WILSON, P. J., CLOONAN, N., KASSAHN, K. S., TAYLOR, D., QUEK, K., ROBERTSON, A., PANTANO, L., MINCARELLI, L., SANCHEZ, L. N., EVERS, L., WU, J., PINESE, M., COWLEY, M. J., JONES, M. D., COLVIN, E. K., NAGRIAL, A. M., HUMPHREY, E. S., CHANTRILL, L. A., MAWSON, A., HUMPHRIS, J., CHOU, A., PAJIC, M., SCARLETT, C. J., PINHO, A. V., GIRY-LATERRIERE, M., ROOMAN, I., SAMRA, J. S., KENCH, J. G., LOVELL, J. A., MERRETT, N. D., TOON, C. W., EPARI, K., NGUYEN, N. Q., BARBOUR, A., ZEPS, N., MORAN-JONES, K., JAMIESON, N. B., GRAHAM, J. S., DUTHIE, F., OIEN, K., HAIR, J., GRUTZMANN, R., MAITRA, A., IACOBUZIO-DONAHUE, C. A., WOLFGANG, C. L., MORGAN, R. A., LAWLOR, R. T., CORBO, V., BASSI, C., RUSEV, B., CAPELLI, P., SALVIA, R., TORTORA, G., MUKHOPADHYAY, D., PETERSEN, G. M., AUSTRALIAN PANCREATIC CANCER GENOME, I., MUNZY, D. M., FISHER, W. E., KARIM, S. A., ESHLEMAN, J. R., HRUBAN, R. H., PILARSKY, C., MORTON, J. P., SANSOM, O. J., SCARPA, A., MUSGROVE, E. A., BAILEY, U. M., HOFMANN, O., SUTHERLAND, R. L., WHEELER, D. A., GILL, A. J., GIBBS, R. A., PEARSON, J. V., et al. 2016. Genomic analyses identify molecular subtypes of pancreatic cancer. *Nature,* 531**,** 47-52.

BALABAN, E. P., MANGU, P. B., KHORANA, A. A., SHAH, M. A., MUKHERJEE, S., CRANE, C. H., JAVLE, M. M., EADS, J. R., ALLEN, P., KO, A. H., ENGEBRETSON, A., HERMAN, J. M., STRICKLER, J. H., BENSON, A. B., 3RD, URBA, S. & YEE, N. S. 2016. Locally Advanced, Unresectable Pancreatic Cancer: American Society of Clinical Oncology Clinical Practice Guideline. *J Clin Oncol,* 34**,** 2654-68.

BALACHANDRAN, V. P., LUKSZA, M., ZHAO, J. N., MAKAROV, V., MORAL, J. A., REMARK, R., HERBST, B., ASKAN, G., BHANOT, U., SENBABAOGLU, Y., WELLS, D. K., CARY, C. I. O., GRBOVIC-HUEZO, O., ATTIYEH, M., MEDINA, B., ZHANG, J., LOO, J., SAGLIMBENI, J., ABU-AKEEL, M., ZAPPASODI, R., RIAZ, N., SMORAGIEWICZ, M., KELLEY, Z. L., BASTURK, O., AUSTRALIAN PANCREATIC CANCER GENOME, I., GARVAN INSTITUTE OF MEDICAL, R., PRINCE OF WALES, H., ROYAL NORTH SHORE, H., UNIVERSITY OF, G., ST VINCENT'S, H., INSTITUTE, Q. B. M. R., UNIVERSITY OF MELBOURNE, C. F. C. R., UNIVERSITY OF QUEENSLAND, I. F. M. B., BANKSTOWN, H., LIVERPOOL, H., ROYAL PRINCE ALFRED HOSPITAL, C. O. B. L., WESTMEAD, H., FREMANTLE, H., ST JOHN OF GOD, H., ROYAL ADELAIDE, H., FLINDERS MEDICAL, C., ENVOI, P., PRINCESS ALEXANDRIA, H., AUSTIN, H., JOHNS HOPKINS MEDICAL, I., CANCER, A. R.-N. C. F. A. R. O., GONEN, M., LEVINE, A. J., ALLEN, P. J., FEARON, D. T., MERAD, M., GNJATIC, S., IACOBUZIO-DONAHUE, C. A., WOLCHOK, J. D., DEMATTEO, R. P., CHAN, T. A., GREENBAUM, B. D., MERGHOUB, T. & LEACH, S. D. 2017. Identification of unique neoantigen qualities in long-term survivors of pancreatic cancer. *Nature,* 551**,** 512-516.

BALAKRISHNAN, R., HARRIS, M. A., HUNTLEY, R., VAN AUKEN, K. & CHERRY, J. M. 2013. A guide to best practices for Gene Ontology (GO) manual annotation. *Database: The Journal of Biological Databases and Curation,* 2013**,** bat054.

BANG, J. Y., HEBERT-MAGEE, S., NAVANEETHAN, U., HASAN, M. K., HAWES, R. & VARADARAJULU, S. 2017. EUS-guided fine needle biopsy of pancreatic masses can yield true histology: results of a randomised trial. *Gut*.

BANG, Y. J., IM, S. A., LEE, K. W., CHO, J. Y., SONG, E. K., LEE, K. H., KIM, Y. H., PARK, J. O., CHUN, H. G., ZANG, D. Y., FIELDING, A., ROWBOTTOM, J., HODGSON, D., O'CONNOR, M. J., YIN, X. & KIM, W. H. 2015. Randomized, Double-Blind Phase II Trial With Prospective Classification by ATM Protein Level to Evaluate the Efficacy and Tolerability of Olaparib Plus Paclitaxel in Patients With Recurrent or Metastatic Gastric Cancer. *J Clin Oncol,* 33**,** 3858-65.

BARBER, L. J., SANDHU, S., CHEN, L., CAMPBELL, J., KOZAREWA, I., FENWICK, K., ASSIOTIS, I., RODRIGUES, D. N., REIS FILHO, J. S., MORENO, V., MATEO, J., MOLIFE, L. R., DE BONO, J., KAYE, S., LORD, C. J. & ASHWORTH, A. 2013. Secondary mutations in BRCA2 associated with clinical resistance to a PARP inhibitor. *J Pathol,* 229**,** 422-9.

BARUGOLA, G., FALCONI, M., BETTINI, R., BONINSEGNA, L., CASAROTTO, A., SALVIA, R., BASSI, C. & PEDERZOLI, P. 2007. The determinant factors of recurrence following resection for ductal pancreatic cancer. *JOP,* 8**,** 132-40.

BEDARD, P. L., CESCON, D. W., FLETCHER, G., DENNY, T., BROKX, R., SAMPSON, P., BRAY, M. R., SLAMON, D. J., MAK, T. W. & WAINBERG, Z. A. 2016. First-in-human phase I trial of the oral PLK4 inhibitor CFI-400945 in patients with advanced solid tumors. *AACR 107th Annual Meeting.* New Orleans, USA: Cancer Research.

BIANKIN, A. V., KENCH, J. G., COLVIN, E. K., SEGARA, D., SCARLETT, C. J., NGUYEN, N. Q., CHANG, D. K., MOREY, A. L., LEE, C. S., PINESE, M., KUO, S. C., SUSANTO, J. M., COSMAN, P. H., LINDEMAN, G. J., VISVADER, J. E., NGUYEN, T. V., MERRETT, N. D., WARUSAVITARNE, J., MUSGROVE, E. A., HENSHALL, S. M. & SUTHERLAND, R. L. 2009. Expression of S100A2 calcium-binding protein predicts response to pancreatectomy for pancreatic cancer. *Gastroenterology,* 137**,** 558-68, 568.e1-11.

BIANKIN, A. V., PIANTADOSI, S. & HOLLINGSWORTH, S. J. 2015. Patient-centric trials for therapeutic development in precision oncology. *Nature,* 526**,** 361-70.

BIANKIN, A. V., WADDELL, N., KASSAHN, K. S., GINGRAS, M. C., MUTHUSWAMY, L. B., JOHNS, A. L., MILLER, D. K., WILSON, P. J., PATCH, A. M., WU, J., CHANG, D. K., COWLEY, M. J., GARDINER, B. B., SONG, S., HARLIWONG, I., IDRISOGLU, S., NOURSE, C., NOURBAKHSH, E., MANNING, S., WANI, S., GONGORA, M., PAJIC, M., SCARLETT, C. J., GILL, A. J., PINHO, A. V., ROOMAN, I., ANDERSON, M., HOLMES, O., LEONARD, C., TAYLOR, D., WOOD, S., XU, Q., NONES, K., FINK, J. L., CHRIST, A., BRUXNER, T., CLOONAN, N., KOLLE, G., NEWELL, F., PINESE, M., MEAD, R. S., HUMPHRIS, J. L., KAPLAN, W., JONES, M. D., COLVIN, E. K., NAGRIAL, A. M., HUMPHREY, E. S., CHOU, A., CHIN, V. T., CHANTRILL, L. A., MAWSON, A., SAMRA, J. S., KENCH, J. G., LOVELL, J. A., DALY, R. J., MERRETT, N. D., TOON, C., EPARI, K., NGUYEN, N. Q., BARBOUR, A., ZEPS, N., KAKKAR, N., ZHAO, F., WU, Y. Q., WANG, M., MUZNY, D. M., FISHER, W. E., BRUNICARDI, F. C., HODGES, S. E., REID, J. G., DRUMMOND, J., CHANG, K., HAN, Y., LEWIS, L. R., DINH, H., BUHAY, C. J., BECK, T., TIMMS, L., SAM, M., BEGLEY, K., BROWN, A., PAI, D., PANCHAL, A., BUCHNER, N., DE BORJA, R., DENROCHE, R. E., YUNG, C. K., SERRA, S., ONETTO, N., MUKHOPADHYAY, D., TSAO, M. S., SHAW, P. A., PETERSEN, G. M., GALLINGER, S., HRUBAN, R. H., MAITRA, A., IACOBUZIO-DONAHUE, C. A., SCHULICK, R. D., WOLFGANG, C. L., MORGAN, R. A., et al. 2012. Pancreatic cancer genomes reveal aberrations in axon guidance pathway genes. *Nature,* 491**,** 399-405.

BINDEA, G., GALON, J. & MLECNIK, B. 2013. CluePedia Cytoscape plugin: pathway insights using integrated experimental and in silico data. *Bioinformatics,* 29**,** 661-3.

BINDEA, G., MLECNIK, B., HACKL, H., CHAROENTONG, P., TOSOLINI, M., KIRILOVSKY, A., FRIDMAN, W. H., PAGES, F., TRAJANOSKI, Z. & GALON, J. 2009. ClueGO: a Cytoscape plug-in to decipher functionally grouped gene ontology and pathway annotation networks. *Bioinformatics,* 25**,** 1091-3.

BLAND, J. M. & ALTMAN, D. G. 2004. The logrank test. *BMJ,* 328**,** 1073.

BOUTROS, M., BRAS, L. P. & HUBER, W. 2006. Analysis of cell-based RNAi screens. *Genome Biol,* 7**,** R66.

BOYIADZIS, M. M., KIRKWOOD, J. M., MARSHALL, J. L., PRITCHARD, C. C., AZAD, N. S. & GULLEY, J. L. 2018. Significance and implications of FDA approval of pembrolizumab for biomarker-defined disease. *J Immunother Cancer,* 6**,** 35.

BRENNAN, M. F., KATTAN, M. W., KLIMSTRA, D. & CONLON, K. 2004. Prognostic nomogram for patients undergoing resection for adenocarcinoma of the pancreas. *Ann Surg,* 240**,** 293-8.

BRENNAN, M. F., MOCCIA, R. D. & KLIMSTRA, D. 1996. Management of adenocarcinoma of the body and tail of the pancreas. *Ann Surg,* 223**,** 506-11; discussion 511-2.

BRYANT, H. E., SCHULTZ, N., THOMAS, H. D., PARKER, K. M., FLOWER, D., LOPEZ, E., KYLE, S., MEUTH, M., CURTIN, N. J. & HELLEDAY, T. 2005. Specific killing of BRCA2-deficient tumours with inhibitors of poly(ADP-ribose) polymerase. *Nature,* 434**,** 913-7.

BURRELL, R. A. & SWANTON, C. 2014. Tumour heterogeneity and the evolution of polyclonal drug resistance. *Mol Oncol,* 8**,** 1095-111.

CAMERON, J. L., RIALL, T. S., COLEMAN, J. & BELCHER, K. A. 2006. One thousand consecutive pancreaticoduodenectomies. *Ann Surg,* 244**,** 10-5.

CAMPBELL, P. J., PLEASANCE, E. D., STEPHENS, P. J., DICKS, E., RANCE, R., GOODHEAD, I., FOLLOWS, G. A., GREEN, A. R., FUTREAL, P. A. & STRATTON, M. R. 2008. Subclonal phylogenetic structures in cancer revealed by ultra-deep sequencing. *Proc Natl Acad Sci U S A,* 105**,** 13081-6.

CAMPBELL, P. J., YACHIDA, S., MUDIE, L. J., STEPHENS, P. J., PLEASANCE, E. D., STEBBINGS, L. A., MORSBERGER, L. A., LATIMER, C., MCLAREN, S., LIN, M. L., MCBRIDE, D. J., VARELA, I., NIK-ZAINAL, S. A., LEROY, C., JIA, M., MENZIES, A., BUTLER, A. P., TEAGUE, J. W., GRIFFIN, C. A., BURTON, J., SWERDLOW, H., QUAIL, M. A., STRATTON, M. R., IACOBUZIO-DONAHUE, C. & FUTREAL, P. A. 2010. The patterns and dynamics of genomic instability in metastatic pancreatic cancer. *Nature,* 467**,** 1109-13.

CANCER GENOME ATLAS RESEARCH NETWORK. ELECTRONIC ADDRESS, A. A. D. H. E. & CANCER GENOME ATLAS RESEARCH, N. 2017. Integrated Genomic Characterization of Pancreatic Ductal Adenocarcinoma. *Cancer Cell,* 32**,** 185-203 e13.

CANDIDO, J. B., MORTON, J. P., BAILEY, P., CAMPBELL, A. D., KARIM, S. A., JAMIESON, T., LAPIENYTE, L., GOPINATHAN, A., CLARK, W., MCGHEE, E. J., WANG, J., ESCORCIO-CORREIA, M., ZOLLINGER, R., ROSHANI, R., DREW, L., RISHI, L., ARKELL, R., EVANS, T. R. J., NIXON, C., JODRELL, D. I., WILKINSON, R. W., BIANKIN, A. V., BARRY, S. T., BALKWILL, F. R. & SANSOM, O. J. 2018. CSF1R(+) Macrophages Sustain Pancreatic Tumor Growth through T Cell Suppression and Maintenance of Key Gene Programs that Define the Squamous Subtype. *Cell Rep,* 23**,** 1448-1460.

CASTRO, M. A., WANG, X., FLETCHER, M. N., MEYER, K. B. & MARKOWETZ, F. 2012. RedeR: R/Bioconductor package for representing modular structures, nested networks and multiple levels of hierarchical associations. *Genome Biol,* 13**,** R29.

CATALANO, C., LAGHI, A., FRAIOLI, F., PEDICONI, F., NAPOLI, A., DANTI, M., REITANO, I. & PASSARIELLO, R. 2003. Pancreatic carcinoma: the role of high-resolution multislice spiral CT in the diagnosis and assessment of resectability. *Eur Radiol,* 13**,** 149-56.

CATENACCI, D. V., CHAPMAN, C. G., XU, P., KOONS, A., KONDA, V. J., SIDDIQUI, U. D. & WAXMAN, I. 2015. Acquisition of Portal Venous Circulating Tumor Cells From Patients With Pancreaticobiliary Cancers by Endoscopic Ultrasound. *Gastroenterology,* 149**,** 1794-1803 e4.

CHANG, D. K., GRIMMOND, S. M. & BIANKIN, A. V. 2014a. Pancreatic cancer genomics. *Curr Opin Genet Dev,* 24**,** 74-81.

CHANG, D. K., GRIMMOND, S. M., EVANS, T. R. & BIANKIN, A. V. 2014b. Mining the genomes of exceptional responders. *Nat Rev Cancer,* 14**,** 291-2.

CHANG, D. K., JOHNS, A. L., MERRETT, N. D., GILL, A. J., COLVIN, E. K., SCARLETT, C. J., NGUYEN, N. Q., LEONG, R. W., COSMAN, P. H., KELLY, M. I., SUTHERLAND, R. L., HENSHALL, S. M., KENCH, J. G. & BIANKIN, A. V. 2009a. Margin clearance and outcome in resected pancreatic cancer. *J Clin Oncol,* 27**,** 2855-62.

CHANG, D. K., NGUYEN, N. Q., MERRETT, N. D., DIXSON, H., LEONG, R. W. & BIANKIN, A. V. 2009b. Role of endoscopic ultrasound in pancreatic cancer. *Expert Rev Gastroenterol Hepatol,* 3**,** 293-303.

CHANOUX, R. A., YIN, B., URTISHAK, K. A., ASARE, A., BASSING, C. H. & BROWN, E. J. 2009. ATR and H2AX cooperate in maintaining genome stability under replication stress. *J Biol Chem,* 284**,** 5994-6003.

CHANTRILL, L. A., NAGRIAL, A. M., WATSON, C., JOHNS, A. L., MARTYN-SMITH, M., SIMPSON, S., MEAD, S., JONES, M. D., SAMRA, J. S., GILL, A. J., WATSON, N., CHIN, V. T., HUMPHRIS, J. L., CHOU, A., BROWN, B., MOREY, A., PAJIC, M., GRIMMOND, S. M., CHANG, D. K., THOMAS, D., SEBASTIAN, L., SJOQUIST, K., YIP, S., PAVLAKIS, N., ASGHARI, R., HARVEY, S., GRIMISON, P., SIMES, J. & BIANKIN, A. V. 2015. Precision Medicine for Advanced Pancreas Cancer: The Individualized Molecular Pancreatic Cancer Therapy (IMPaCT) Trial. *Clin Cancer Res,* 21**,** 2029-37.

CHATTERJEE, D., KATZ, M. H., RASHID, A., VARADHACHARY, G. R., WOLFF, R. A., WANG, H., LEE, J. E., PISTERS, P. W., VAUTHEY, J. N., CRANE, C., GOMEZ, H. F., ABBRUZZESE, J. L., FLEMING, J. B. & WANG, H. 2012. Histologic grading of the extent of residual carcinoma following neoadjuvant chemoradiation in pancreatic ductal adenocarcinoma: a predictor for patient outcome. *Cancer,* 118**,** 3182-90.

CHIOREAN, E. G., VON HOFF, D. D., TABERNERO, J., EL-MARAGHI, R., WEE MA, W., RENI, M., HARRIS, M., WHORF, R., LIU, H., SHIANSONG LI, J., MANAX, V., ROMANO, A., LU, B. & GOLDSTEIN, D. 2016. Second-line therapy after nab-paclitaxel plus gemcitabine or after gemcitabine for patients with metastatic pancreatic cancer. *Br J Cancer,* 115**,** e13.

CHOU, A., FROIO, D., NAGRIAL, A., PARKIN, A., MURPHY, K. J., CHIN, V., WOHL, D., STEINMANN, A. M., STARK, R., DRURY, A., WALTERS, S. N., VENNIN, C., BURGESS, A., PINESE, M., CHANTRILL, L., COWLEY, M., MOLLOY, T., APGI, WADDELL, N., JOHNS, A., GRIMMOND, S. M., CHANG, D., BIANKIN, A. V., SAMSON, O. J., MORTON, J. P., GREY, S. T., COX, T., TURCHINI, J., SAMRA, J. S., CLARKE, S. J., TIMPSON, P., GILL, A. J. & PAJIC, M. 2017. Tailored first-line and second-line CDK4-targeting treatment combinations in mouse models of pancreatic cancer. *Gut*.

CHUN, Y. S., COOPER, H. S., COHEN, S. J., KONSKI, A., BURTNESS, B., DENLINGER, C. S., ASTSATUROV, I., HALL, M. J. & HOFFMAN, J. P. 2011. Significance of pathologic response to preoperative therapy in pancreatic cancer. *Ann Surg Oncol,* 18**,** 3601-7.

CICCIA, A. & ELLEDGE, S. J. 2010. The DNA Damage Response: Making it safe to play with knives. *Mol Cell,* 40**,** 179 - 204.

CILIBERTO, D., BOTTA, C., CORREALE, P., ROSSI, M., CARAGLIA, M., TASSONE, P. & TAGLIAFERRI, P. 2013. Role of gemcitabine-based combination therapy in the management of advanced pancreatic cancer: a meta-analysis of randomised trials. *Eur J Cancer,* 49**,** 593-603.

COHEN, S. J., PUNT, C. J., IANNOTTI, N., SAIDMAN, B. H., SABBATH, K. D., GABRAIL, N. Y., PICUS, J., MORSE, M., MITCHELL, E., MILLER, M. C., DOYLE, G. V., TISSING, H., TERSTAPPEN, L. W. & MEROPOL, N. J. 2008. Relationship of circulating tumor cells to tumor response, progression-free survival, and overall survival in patients with metastatic colorectal cancer. *J Clin Oncol,* 26**,** 3213-21.

COLLINS, G. S., REITSMA, J. B., ALTMAN, D. G. & MOONS, K. G. 2015. Transparent Reporting of a multivariable prediction model for Individual Prognosis Or Diagnosis (TRIPOD). *Ann Intern Med,* 162**,** 735-6.

COLLISSON, E. A., BAILEY, P., CHANG, D. K. & BIANKIN, A. V. 2019. Molecular subtypes of pancreatic cancer. *Nature Reviews Gastroenterology & Hepatology*.

COLLISSON, E. A., SADANANDAM, A., OLSON, P., GIBB, W. J., TRUITT, M., GU, S., COOC, J., WEINKLE, J., KIM, G. E., JAKKULA, L., FEILER, H. S., KO, A. H., OLSHEN, A. B., DANENBERG, K. L., TEMPERO, M. A., SPELLMAN, P. T., HANAHAN, D. & GRAY, J. W. 2011. Subtypes of pancreatic ductal adenocarcinoma and their differing responses to therapy. *Nat Med,* 17**,** 500-3.

CONNOR, A. A., DENROCHE, R. E., JANG, G. H., TIMMS, L., KALIMUTHU, S. N., SELANDER, I., MCPHERSON, T., WILSON, G. W., CHAN-SENG-YUE, M. A., BOROZAN, I., FERRETTI, V., GRANT, R. C., LUNGU, I. M., COSTELLO, E., GREENHALF, W., PALMER, D., GHANEH, P., NEOPTOLEMOS, J. P., BUCHLER, M., PETERSEN, G., THAYER, S., HOLLINGSWORTH, M. A., SHERKER, A., DUROCHER, D., DHANI, N., HEDLEY, D., SERRA, S., POLLETT, A., ROEHRL, M. H., BAVI, P., BARTLETT, J. M., CLEARY, S., WILSON, J. M., ALEXANDROV, L. B., MOORE, M., WOUTERS, B. G., MCPHERSON, J. D., NOTTA, F., STEIN, L. D. & GALLINGER, S. 2016. Association of Distinct Mutational Signatures With Correlates of Increased Immune Activity in Pancreatic Ductal Adenocarcinoma. *JAMA Oncol*.

CONROY, T., DESSEIGNE, F., YCHOU, M., BOUCHE, O., GUIMBAUD, R., BECOUARN, Y., ADENIS, A., RAOUL, J. L., GOURGOU-BOURGADE, S., DE LA FOUCHARDIERE, C., BENNOUNA, J., BACHET, J. B., KHEMISSA-AKOUZ, F., PERE-VERGE, D., DELBALDO, C., ASSENAT, E., CHAUFFERT, B., MICHEL, P., MONTOTO-GRILLOT, C. & DUCREUX, M. 2011. FOLFIRINOX versus gemcitabine for metastatic pancreatic cancer. *N Engl J Med,* 364**,** 1817-25.

CONROY, T., HAMMEL, P., HEBBAR, M., ABDELGHANI, M. B., WEI, A. C.-C., RAOUL, J.-L., CHONE, L., FRANCOIS, E., ARTRU, P., BIAGI, J. J., LECOMTE, T., ASSENAT, E., FAROUX, R., YCHOU, M., VOLET, J., SAUVANET, A., JOUFFROY-ZELLER, C., RAT, P., CASTAN, F. & BACHET, J.-B. 2018. Unicancer GI PRODIGE 24/CCTG PA.6 trial: A multicenter international randomized phase III trial of adjuvant mFOLFIRINOX versus gemcitabine (gem) in patients with resected pancreatic ductal adenocarcinomas. *Journal of Clinical Oncology,* 36**,** LBA4001-LBA4001.

CRISTOFANILLI, M., HAYES, D. F., BUDD, G. T., ELLIS, M. J., STOPECK, A., REUBEN, J. M., DOYLE, G. V., MATERA, J., ALLARD, W. J., MILLER, M. C., FRITSCHE, H. A., HORTOBAGYI, G. N. & TERSTAPPEN, L. W. 2005. Circulating tumor cells: a novel prognostic factor for newly diagnosed metastatic breast cancer. *J Clin Oncol,* 23**,** 1420-30.

CRUK. 2018. *Pancreatic Cancer Statistics* [Online]. Available: http://www.cancerresearchuk.org [Accessed].

DAVIES, H., GLODZIK, D., MORGANELLA, S., YATES, L. R., STAAF, J., ZOU, X., RAMAKRISHNA, M., MARTIN, S., BOYAULT, S., SIEUWERTS, A. M., SIMPSON, P. T., KING, T. A., RAINE, K., EYFJORD, J. E., KONG, G., BORG, A., BIRNEY, E., STUNNENBERG, H. G., VAN DE VIJVER, M. J., BORRESEN-DALE, A. L., MARTENS, J. W., SPAN, P. N., LAKHANI, S. R., VINCENT-SALOMON, A., SOTIRIOU, C., TUTT, A., THOMPSON, A. M., VAN LAERE, S., RICHARDSON, A. L., VIARI, A., CAMPBELL, P. J., STRATTON, M. R. & NIK-ZAINAL, S. 2017. HRDetect is a predictor of BRCA1 and BRCA2 deficiency based on mutational signatures. *Nat Med,* 23**,** 517-525.

DE BONO, J. S., SCHER, H. I., MONTGOMERY, R. B., PARKER, C., MILLER, M. C., TISSING, H., DOYLE, G. V., TERSTAPPEN, L. W., PIENTA, K. J. & RAGHAVAN, D. 2008. Circulating tumor cells predict survival benefit from treatment in metastatic castration-resistant prostate cancer. *Clin Cancer Res,* 14**,** 6302-9.

DE CASTRO, S. M., BIERE, S. S., LAGARDE, S. M., BUSCH, O. R., VAN GULIK, T. M. & GOUMA, D. J. 2009. Validation of a nomogram for predicting survival after resection for adenocarcinoma of the pancreas. *Br J Surg,* 96**,** 417-23.

DE ROOIJ, T., TOL, J. A., VAN EIJCK, C. H., BOERMA, D., BONSING, B. A., BOSSCHA, K., VAN DAM, R. M., DIJKGRAAF, M. G., GERHARDS, M. F., VAN GOOR, H., VAN DER HARST, E., DE HINGH, I. H., KAZEMIER, G., KLAASE, J. M., MOLENAAR, I. Q., PATIJN, G. A., VAN SANTVOORT, H. C., SCHEEPERS, J. J., VAN DER SCHELLING, G. P., SIEDERS, E., BUSCH, O. R., BESSELINK, M. G. & DUTCH PANCREATIC CANCER, G. 2016. Outcomes of Distal Pancreatectomy for Pancreatic Ductal Adenocarcinoma in the Netherlands: A Nationwide Retrospective Analysis. *Ann Surg Oncol,* 23**,** 585-91.

DI MICCO, R., FUMAGALLI, M., CICALESE, A., PICCININ, S., GASPARINI, P., LUISE, C., SCHURRA, C., GARRE, M., NUCIFORO, P. G., BENSIMON, A., MAESTRO, R., PELICCI, P. G. & D'ADDA DI FAGAGNA, F. 2006. Oncogene-induced senescence is a DNA damage response triggered by DNA hyper-replication. *Nature,* 444**,** 638-42.

DO, K., WILSKER, D., JI, J., ZLOTT, J., FRESHWATER, T., KINDERS, R. J., COLLINS, J., CHEN, A. P., DOROSHOW, J. H. & KUMMAR, S. 2015. Phase I Study of Single-Agent AZD1775 (MK-1775), a Wee1 Kinase Inhibitor, in Patients With Refractory Solid Tumors. *J Clin Oncol,* 33**,** 3409-15.

DOBBELSTEIN, M. & SORENSEN, C. S. 2015. Exploiting replicative stress to treat cancer. *Nat Rev Drug Discov,* 14**,** 405-23.

DOBIN, A., DAVIS, C. A., SCHLESINGER, F., DRENKOW, J., ZALESKI, C., JHA, S., BATUT, P., CHAISSON, M. & GINGERAS, T. R. 2013. STAR: ultrafast universal RNA-seq aligner. *Bioinformatics,* 29**,** 15-21.

DOMCHEK, S. M., AGHAJANIAN, C., SHAPIRA-FROMMER, R., SCHMUTZLER, R. K., AUDEH, M. W., FRIEDLANDER, M., BALMANA, J., MITCHELL, G., FRIED, G., STEMMER, S. M., HUBERT, A., ROSENGARTEN, O., LOMAN, N., ROBERTSON, J. D., MANN, H. & KAUFMAN, B. 2016. Efficacy and safety of olaparib monotherapy in germline BRCA1/2 mutation carriers with advanced ovarian cancer and three or more lines of prior therapy. *Gynecol Oncol,* 140**,** 199-203.

DREAN, A., WILLIAMSON, C. T., BROUGH, R., BRANDSMA, I., MENON, M., KONDE, A., GARCIA-MURILLAS, I., PEMBERTON, H. N., FRANKUM, J., RAFIQ, R., BADHAM, N., CAMPBELL, J., GULATI, A., TURNER, N. C., PETTITT, S. J., ASHWORTH, A. & LORD, C. J. 2017. Modeling Therapy Resistance in BRCA1/2-Mutant Cancers. *Mol Cancer Ther,* 16**,** 2022-2034.

DREYER, S. B., CHANG, D. K., BAILEY, P. & BIANKIN, A. V. 2017. Pancreatic Cancer Genomes: Implications for Clinical Management and Therapeutic Development. *Clin Cancer Res,* 23**,** 1638-1646.

DREYER, S. B., JAMIESON, N. B., UPSTILL-GODDARD, R., BAILEY, P. J., MCKAY, C. J., BIANKIN, A. V. & CHANG, D. K. 2018. Defining the molecular pathology of pancreatic body and tail adenocarcinoma. *Br J Surg,* 105**,** e183-e191.

EDWARDS, S. L., BROUGH, R., LORD, C. J., NATRAJAN, R., VATCHEVA, R., LEVINE, D. A., BOYD, J., REIS-FILHO, J. S. & ASHWORTH, A. 2008. Resistance to therapy caused by intragenic deletion in BRCA2. *Nature,* 451**,** 1111-5.

ENGELMANN, D. & PUTZER, B. M. 2014. Emerging from the shade of p53 mutants: N-terminally truncated variants of the p53 family in EMT signaling and cancer progression. *Sci Signal,* 7**,** re9.

FANG, H. & GOUGH, J. 2014. The 'dnet' approach promotes emerging research on cancer patient survival. *Genome Med,* 6**,** 64.

FANG, Y., SU, Z., XIE, J., XUE, R., MA, Q., LI, Y., ZHAO, Y., SONG, Z., LU, X., LI, H., PENG, C., BAI, F. & SHEN, B. 2017. Genomic signatures of pancreatic adenosquamous carcinoma (PASC). *J Pathol,* 243**,** 155-159.

FEI, F., QU, J., ZHANG, M., LI, Y. & ZHANG, S. 2017. S100A4 in cancer progression and metastasis: A systematic review. *Oncotarget,* 8**,** 73219-73239.

FELSENSTEIN, M., NOE, M., MASICA, D. L., HOSODA, W., CHIANCHIANO, P., FISCHER, C. G., LIONHEART, G., BROSENS, L. A. A., PEA, A., YU, J., GEMENETZIS, G., GROOT, V. P., MAKARY, M. A., HE, J., WEISS, M. J., CAMERON, J. L., WOLFGANG, C. L., HRUBAN, R. H., ROBERTS, N. J., KARCHIN, R., GOGGINS, M. G. & WOOD, L. D. 2018. IPMNs with co-occurring invasive cancers: neighbours but not always relatives. *Gut*.

FERRONE, C. R., KATTAN, M. W., TOMLINSON, J. S., THAYER, S. P., BRENNAN, M. F. & WARSHAW, A. L. 2005. Validation of a postresection pancreatic adenocarcinoma nomogram for disease-specific survival. *J Clin Oncol,* 23**,** 7529-35.

FISCHER, K. R., DURRANS, A., LEE, S., SHENG, J., LI, F., WONG, S. T., CHOI, H., EL RAYES, T., RYU, S., TROEGER, J., SCHWABE, R. F., VAHDAT, L. T., ALTORKI, N. K., MITTAL, V. & GAO, D. 2015. Epithelial-to-mesenchymal transition is not required for lung metastasis but contributes to chemoresistance. *Nature,* 527**,** 472-6.

FISHER, R., PUSZTAI, L. & SWANTON, C. 2013. Cancer heterogeneity: implications for targeted therapeutics. *Br J Cancer,* 108**,** 479-85.

FOKAS, E., PREVO, R., HAMMOND, E. M., BRUNNER, T. B., MCKENNA, W. G. & MUSCHEL, R. J. 2014. Targeting ATR in DNA damage response and cancer therapeutics. *Cancer Treat Rev,* 40**,** 109-17.

FOKAS, E., PREVO, R., POLLARD, J. R., REAPER, P. M., CHARLTON, P. A., CORNELISSEN, B., VALLIS, K. A., HAMMOND, E. M., OLCINA, M. M., GILLIES MCKENNA, W., MUSCHEL, R. J. & BRUNNER, T. B. 2012. Targeting ATR in vivo using the novel inhibitor VE-822 results in selective sensitization of pancreatic tumors to radiation. *Cell Death Dis,* 3**,** e441.

FOLEY, K., KIM, V., JAFFEE, E. & ZHENG, L. 2015. Current progress in immunotherapy for pancreatic cancer. *Cancer Lett*.

FONG, P. C., YAP, T. A., BOSS, D. S., CARDEN, C. P., MERGUI-ROELVINK, M., GOURLEY, C., DE GREVE, J., LUBINSKI, J., SHANLEY, S., MESSIOU, C., A'HERN, R., TUTT, A., ASHWORTH, A., STONE, J., CARMICHAEL, J., SCHELLENS, J. H., DE BONO, J. S. & KAYE, S. B. 2010. Poly(ADP)-ribose polymerase inhibition: frequent durable responses in BRCA carrier ovarian cancer correlating with platinum-free interval. *J Clin Oncol,* 28**,** 2512-9.

GARCEA, G., NEAL, C. P., PATTENDEN, C. J., STEWARD, W. P. & BERRY, D. P. 2005. Molecular prognostic markers in pancreatic cancer: a systematic review. *Eur J Cancer,* 41**,** 2213-36.

GARRIDO-LAGUNA, I. & HIDALGO, M. 2015. Pancreatic cancer: from state-of-the-art treatments to promising novel therapies. *Nat Rev Clin Oncol,* 12**,** 319-34.

GEENEN, J. J. J. & SCHELLENS, J. H. M. 2017. Molecular Pathways: Targeting the Protein Kinase Wee1 in Cancer. *Clin Cancer Res,* 23**,** 4540-4544.

GEMENETZIS, G., GROOT, V. P., BLAIR, A. B., LAHERU, D. A., ZHENG, L., NARANG, A. K., FISHMAN, E. K., HRUBAN, R. H., YU, J., BURKHART, R. A., CAMERON, J. L., WEISS, M. J., WOLFGANG, C. L. & HE, J. 2018. Survival in Locally Advanced Pancreatic Cancer After Neoadjuvant Therapy and Surgical Resection. *Ann Surg*.

GERDS, T. A. & SCHUMACHER, M. 2006. Consistent estimation of the expected Brier score in general survival models with right-censored event times. *Biom J,* 48**,** 1029-40.

GERLINGER, M., ROWAN, A. J., HORSWELL, S., LARKIN, J., ENDESFELDER, D., GRONROOS, E., MARTINEZ, P., MATTHEWS, N., STEWART, A., TARPEY, P., VARELA, I., PHILLIMORE, B., BEGUM, S., MCDONALD, N. Q., BUTLER, A., JONES, D., RAINE, K., LATIMER, C., SANTOS, C. R., NOHADANI, M., EKLUND, A. C., SPENCER-DENE, B., CLARK, G., PICKERING, L., STAMP, G., GORE, M., SZALLASI, Z., DOWNWARD, J., FUTREAL, P. A. & SWANTON, C. 2012. Intratumor heterogeneity and branched evolution revealed by multiregion sequencing. *N Engl J Med,* 366**,** 883-92.

GILLEN, S., SCHUSTER, T., MEYER ZUM BUSCHENFELDE, C., FRIESS, H. & KLEEFF, J. 2010. Preoperative/neoadjuvant therapy in pancreatic cancer: a systematic review and meta-analysis of response and resection percentages. *PLoS Med,* 7**,** e1000267.

GLEESON, F. C., KERR, S. E., KIPP, B. R., VOSS, J. S., MINOT, D. M., TU, Z. J., HENRY, M. R., GRAHAM, R. P., VASMATZIS, G., CHEVILLE, J. C., LAZARIDIS, K. N. & LEVY, M. J. 2016. Targeted next generation sequencing of endoscopic ultrasound acquired cytology from ampullary and pancreatic adenocarcinoma has the potential to aid patient stratification for optimal therapy selection. *Oncotarget,* 7**,** 54526-54536.

GREAVES, M. & MALEY, C. C. 2012. Clonal evolution in cancer. *Nature,* 481**,** 306-13.

GROOT, V. P., GEMENETZIS, G., BLAIR, A. B., RIVERO-SOTO, R. J., YU, J., JAVED, A. A., BURKHART, R. A., RINKES, I., MOLENAAR, I. Q., CAMERON, J. L., WEISS, M. J., WOLFGANG, C. L. & HE, J. 2018. Defining and Predicting Early Recurrence in 957 Patients With Resected Pancreatic Ductal Adenocarcinoma. *Ann Surg*.

GROOT, V. P., REZAEE, N., WU, W., CAMERON, J. L., FISHMAN, E. K., HRUBAN, R. H., WEISS, M. J., ZHENG, L., WOLFGANG, C. L. & HE, J. 2017. Patterns, Timing, and Predictors of Recurrence Following Pancreatectomy for Pancreatic Ductal Adenocarcinoma. *Ann Surg*.

GU, Z., EILS, R. & SCHLESNER, M. 2016. Complex heatmaps reveal patterns and correlations in multidimensional genomic data. *Bioinformatics,* 32**,** 2847-9.

HACKERT, T., SACHSENMAIER, M., HINZ, U., SCHNEIDER, L., MICHALSKI, C. W., SPRINGFELD, C., STROBEL, O., JAGER, D., ULRICH, A. & BUCHLER, M. W. 2016. Locally Advanced Pancreatic Cancer: Neoadjuvant Therapy With Folfirinox Results in Resectability in 60% of the Patients. *Ann Surg,* 264**,** 457-63.

HAGEMANN, I. S., DEVARAKONDA, S., LOCKWOOD, C. M., SPENCER, D. H., GUEBERT, K., BREDEMEYER, A. J., AL-KATEB, H., NGUYEN, T. T., DUNCAVAGE, E. J., COTTRELL, C. E., KULKARNI, S., NAGARAJAN, R., SEIBERT, K., BAGGSTROM, M., WAQAR, S. N., PFEIFER, J. D., MORGENSZTERN, D. & GOVINDAN, R. 2015. Clinical next-generation sequencing in patients with non-small cell lung cancer. *Cancer,* 121**,** 631-9.

HAIBE-KAINS, B., DESMEDT, C., LOI, S., CULHANE, A. C., BONTEMPI, G., QUACKENBUSH, J. & SOTIRIOU, C. 2012. A three-gene model to robustly identify breast cancer molecular subtypes. *J Natl Cancer Inst,* 104**,** 311-25.

HAMID, O., ROBERT, C., DAUD, A., HODI, F. S., HWU, W. J., KEFFORD, R., WOLCHOK, J. D., HERSEY, P., JOSEPH, R. W., WEBER, J. S., DRONCA, R., GANGADHAR, T. C., PATNAIK, A., ZAROUR, H., JOSHUA, A. M., GERGICH, K., ELASSAISS-SCHAAP, J., ALGAZI, A., MATEUS, C., BOASBERG, P., TUMEH, P. C., CHMIELOWSKI, B., EBBINGHAUS, S. W., LI, X. N., KANG, S. P. & RIBAS, A. 2013. Safety and tumor responses with lambrolizumab (anti-PD-1) in melanoma. *N Engl J Med,* 369**,** 134-44.

HANAHAN, D. & WEINBERG, R. A. 2011. Hallmarks of cancer: the next generation. *Cell,* 144**,** 646-74.

HANNINEN, E. L., RICKE, J., AMTHAUER, H., ROTTGEN, R., BOHMIG, M., LANGREHR, J., PECH, M., DENECKE, T., ROSEWICZ, S. & FELIX, R. 2005. Magnetic resonance cholangiopancreatography: image quality, ductal morphology, and value of additional T2- and T1-weighted sequences for the assessment of suspected pancreatic cancer. *Acta Radiol,* 46**,** 117-25.

HARTWIG, W., GLUTH, A., HINZ, U., KOLIOGIANNIS, D., STROBEL, O., HACKERT, T., WERNER, J. & BUCHLER, M. W. 2016. Outcomes after extended pancreatectomy in patients with borderline resectable and locally advanced pancreatic cancer. *Br J Surg,* 103**,** 1683-1694.

HE, J., BLAIR, A. B., GROOT, V. P., JAVED, A. A., BURKHART, R. A., GEMENETZIS, G., HRUBAN, R. H., WATERS, K. M., POLING, J., ZHENG, L., LAHERU, D., HERMAN, J. M., MAKARY, M. A., WEISS, M. J., CAMERON, J. L. & WOLFGANG, C. L. 2018. Is a Pathological Complete Response Following Neoadjuvant Chemoradiation Associated With Prolonged Survival in Patients With Pancreatic Cancer? *Ann Surg*.

HE, J., PAGE, A. J., WEISS, M., WOLFGANG, C. L., HERMAN, J. M. & PAWLIK, T. M. 2014. Management of borderline and locally advanced pancreatic cancer: where do we stand? *World J Gastroenterol,* 20**,** 2255-66.

HEERKENS, H. D., VAN BERKEL, L., TSENG, D. S. J., MONNINKHOF, E. M., VAN SANTVOORT, H. C., HAGENDOORN, J., BOREL RINKES, I. H. M., LIPS, I. M., INTVEN, M. & MOLENAAR, I. Q. 2018. Long-term health-related quality of life after pancreatic resection for malignancy in patients with and without severe postoperative complications. *HPB (Oxford),* 20**,** 188-195.

HIDALGO, M. 2010. Pancreatic cancer. *N Engl J Med,* 362**,** 1605-17.

HIDALGO, M., AMANT, F., BIANKIN, A. V., BUDINSKA, E., BYRNE, A. T., CALDAS, C., CLARKE, R. B., DE JONG, S., JONKERS, J., MAELANDSMO, G. M., ROMAN-ROMAN, S., SEOANE, J., TRUSOLINO, L. & VILLANUEVA, A. 2014. Patient-derived xenograft models: an emerging platform for translational cancer research. *Cancer Discov,* 4**,** 998-1013.

HINGORANI, S. R., PETRICOIN, E. F., MAITRA, A., RAJAPAKSE, V., KING, C., JACOBETZ, M. A., ROSS, S., CONRADS, T. P., VEENSTRA, T. D., HITT, B. A., KAWAGUCHI, Y., JOHANN, D., LIOTTA, L. A., CRAWFORD, H. C., PUTT, M. E., JACKS, T., WRIGHT, C. V., HRUBAN, R. H., LOWY, A. M. & TUVESON, D. A. 2003. Preinvasive and invasive ductal pancreatic cancer and its early detection in the mouse. *Cancer Cell,* 4**,** 437-50.

HOADLEY, K. A., YAU, C., WOLF, D. M., CHERNIACK, A. D., TAMBORERO, D., NG, S., LEISERSON, M. D., NIU, B., MCLELLAN, M. D., UZUNANGELOV, V., ZHANG, J., KANDOTH, C., AKBANI, R., SHEN, H., OMBERG, L., CHU, A., MARGOLIN, A. A., VAN'T VEER, L. J., LOPEZ-BIGAS, N., LAIRD, P. W., RAPHAEL, B. J., DING, L., ROBERTSON, A. G., BYERS, L. A., MILLS, G. B., WEINSTEIN, J. N., VAN WAES, C., CHEN, Z., COLLISSON, E. A., CANCER GENOME ATLAS RESEARCH, N., BENZ, C. C., PEROU, C. M. & STUART, J. M. 2014. Multiplatform analysis of 12 cancer types reveals molecular classification within and across tissues of origin. *Cell,* 158**,** 929-44.

HRUBAN, R. H., GOGGINS, M., PARSONS, J. & KERN, S. E. 2000. Progression model for pancreatic cancer. *Clin Cancer Res,* 6**,** 2969-72.

HRUBAN, R. H., WILENTZ, R. E. & MAITRA, A. 2005. Identification and analysis of precursors to invasive pancreatic cancer. *Methods Mol Med,* 103**,** 1-13.

HUANG, S., ZHENG, J., HUANG, Y., SONG, L., YIN, Y., OU, D., HE, S., CHEN, X. & OUYANG, X. 2016. Impact of S100A4 Expression on Clinicopathological Characteristics and Prognosis in Pancreatic Cancer: A Meta-Analysis. *Dis Markers,* 2016**,** 8137378.

HUDSON, T. J., ANDERSON, W., ARTEZ, A., BARKER, A. D., BELL, C., BERNABE, R. R., BHAN, M. K., CALVO, F., EEROLA, I., GERHARD, D. S., GUTTMACHER, A., GUYER, M., HEMSLEY, F. M., JENNINGS, J. L., KERR, D., KLATT, P., KOLAR, P., KUSADA, J., LANE, D. P., LAPLACE, F., YOUYONG, L., NETTEKOVEN, G., OZENBERGER, B., PETERSON, J., RAO, T. S., REMACLE, J., SCHAFER, A. J., SHIBATA, T., STRATTON, M. R., VOCKLEY, J. G., WATANABE, K., YANG, H., YUEN, M. M., KNOPPERS, B. M., BOBROW, M., CAMBON-THOMSEN, A., DRESSLER, L. G., DYKE, S. O., JOLY, Y., KATO, K., KENNEDY, K. L., NICOLAS, P., PARKER, M. J., RIAL-SEBBAG, E., ROMEO-CASABONA, C. M., SHAW, K. M., WALLACE, S., WIESNER, G. L., ZEPS, N., LICHTER, P., BIANKIN, A. V., CHABANNON, C., CHIN, L., CLEMENT, B., DE ALAVA, E., DEGOS, F., FERGUSON, M. L., GEARY, P., HAYES, D. N., JOHNS, A. L., KASPRZYK, A., NAKAGAWA, H., PENNY, R., PIRIS, M. A., SARIN, R., SCARPA, A., VAN DE VIJVER, M., FUTREAL, P. A., ABURATANI, H., BAYES, M., BOTWELL, D. D., CAMPBELL, P. J., ESTIVILL, X., GRIMMOND, S. M., GUT, I., HIRST, M., LOPEZ-OTIN, C., MAJUMDER, P., MARRA, M., MCPHERSON, J. D., NING, Z., PUENTE, X. S., RUAN, Y., STUNNENBERG, H. G., SWERDLOW, H., VELCULESCU, V. E., WILSON, R. K., XUE, H. H., YANG, L., SPELLMAN, P. T., BADER, G. D., BOUTROS, P. C., FLICEK, P., GETZ, G., GUIGO, R., GUO, G., HAUSSLER, D., HEATH, S., HUBBARD, T. J., JIANG, T., et al. 2010. International network of cancer genome projects. *Nature,* 464**,** 993-8.

HUMPHRIS, J. L., PATCH, A. M., NONES, K., BAILEY, P. J., JOHNS, A. L., MCKAY, S., CHANG, D. K., MILLER, D. K., PAJIC, M., KASSAHN, K. S., QUINN, M. C., BRUXNER, T. J., CHRIST, A. N., HARLIWONG, I., IDRISOGLU, S., MANNING, S., NOURSE, C., NOURBAKHSH, E., STONE, A., WILSON, P. J., ANDERSON, M., FINK, J. L., HOLMES, O., KAZAKOFF, S., LEONARD, C., NEWELL, F., WADDELL, N., WOOD, S., MEAD, R. S., XU, Q., WU, J., PINESE, M., COWLEY, M. J., JONES, M. D., NAGRIAL, A. M., CHIN, V. T., CHANTRILL, L. A., MAWSON, A., CHOU, A., SCARLETT, C. J., PINHO, A. V., ROOMAN, I., GIRY-LATERRIERE, M., SAMRA, J. S., KENCH, J. G., MERRETT, N. D., TOON, C. W., EPARI, K., NGUYEN, N. Q., BARBOUR, A., ZEPS, N., JAMIESON, N. B., MCKAY, C. J., CARTER, C. R., DICKSON, E. J., GRAHAM, J. S., DUTHIE, F., OIEN, K., HAIR, J., MORTON, J. P., SANSOM, O. J., GRUTZMANN, R., HRUBAN, R. H., MAITRA, A., IACOBUZIO-DONAHUE, C. A., SCHULICK, R. D., WOLFGANG, C. L., MORGAN, R. A., LAWLOR, R. T., RUSEV, B., CORBO, V., SALVIA, R., CATALDO, I., TORTORA, G., TEMPERO, M. A., AUSTRALIAN PANCREATIC CANCER GENOME, I., HOFMANN, O., ESHLEMAN, J. R., PILARSKY, C., SCARPA, A., MUSGROVE, E. A., GILL, A. J., PEARSON, J.

V., GRIMMOND, S. M., WADDELL, N. & BIANKIN, A. V. 2016. Hypermutation In Pancreatic Cancer. *Gastroenterology*.

HUMPHRIS, J. L., PATCH, A. M., NONES, K., BAILEY, P. J., JOHNS, A. L., MCKAY, S., CHANG, D. K., MILLER, D. K., PAJIC, M., KASSAHN, K. S., QUINN, M. C., BRUXNER, T. J., CHRIST, A. N., HARLIWONG, I., IDRISOGLU, S., MANNING, S., NOURSE, C., NOURBAKHSH, E., STONE, A., WILSON, P. J., ANDERSON, M., FINK, J. L., HOLMES, O., KAZAKOFF, S., LEONARD, C., NEWELL, F., WADDELL, N., WOOD, S., MEAD, R. S., XU, Q., WU, J., PINESE, M., COWLEY, M. J., JONES, M. D., NAGRIAL, A. M., CHIN, V. T., CHANTRILL, L. A., MAWSON, A., CHOU, A., SCARLETT, C. J., PINHO, A. V., ROOMAN, I., GIRY-LATERRIERE, M., SAMRA, J. S., KENCH, J. G., MERRETT, N. D., TOON, C. W., EPARI, K., NGUYEN, N. Q., BARBOUR, A., ZEPS, N., JAMIESON, N. B., MCKAY, C. J., CARTER, C. R., DICKSON, E. J., GRAHAM, J. S., DUTHIE, F., OIEN, K., HAIR, J., MORTON, J. P., SANSOM, O. J., GRUTZMANN, R., HRUBAN, R. H., MAITRA, A., IACOBUZIO-DONAHUE, C. A., SCHULICK, R. D., WOLFGANG, C. L., MORGAN, R. A., LAWLOR, R. T., RUSEV, B., CORBO, V., SALVIA, R., CATALDO, I., TORTORA, G., TEMPERO, M. A., AUSTRALIAN PANCREATIC CANCER GENOME, I., HOFMANN, O., ESHLEMAN, J. R., PILARSKY, C., SCARPA, A., MUSGROVE, E. A., GILL, A. J., PEARSON, J. V., GRIMMOND, S. M., WADDELL, N. & BIANKIN, A. V. 2017. Hypermutation In Pancreatic Cancer. *Gastroenterology,* 152**,** 68-74 e2.

HUNTOON, C. J., FLATTEN, K. S., WAHNER HENDRICKSON, A. E., HUEHLS, A. M., SUTOR, S. L., KAUFMANN, S. H. & KARNITZ, L. M. 2013. ATR inhibition broadly sensitizes ovarian cancer cells to chemotherapy independent of BRCA status. *Cancer Res,* 73**,** 3683-91.

IACOBUZIO-DONAHUE, C. A., FU, B., YACHIDA, S., LUO, M., ABE, H., HENDERSON, C. M., VILARDELL, F., WANG, Z., KELLER, J. W., BANERJEE, P., HERMAN, J. M., CAMERON, J. L., YEO, C. J., HALUSHKA, M. K., ESHLEMAN, J. R., RABEN, M., KLEIN, A. P., HRUBAN, R. H., HIDALGO, M. & LAHERU, D. 2009. DPC4 gene status of the primary carcinoma correlates with patterns of failure in patients with pancreatic cancer. *J Clin Oncol,* 27**,** 1806-13.

ISAJI, S., MIZUNO, S., WINDSOR, J. A., BASSI, C., FERNANDEZ-DEL CASTILLO, C., HACKERT, T., HAYASAKI, A., KATZ, M. H. G., KIM, S. W., KISHIWADA, M., KITAGAWA, H., MICHALSKI, C. W. & WOLFGANG, C. L. 2018. International consensus on definition and criteria of borderline resectable pancreatic ductal adenocarcinoma 2017. *Pancreatology,* 18**,** 2-11.

JAMAL-HANJANI, M., WILSON, G. A., MCGRANAHAN, N., BIRKBAK, N. J., WATKINS, T. B. K., VEERIAH, S., SHAFI, S., JOHNSON, D. H., MITTER, R., ROSENTHAL, R., SALM, M., HORSWELL, S., ESCUDERO, M., MATTHEWS, N., ROWAN, A., CHAMBERS, T., MOORE, D. A., TURAJLIC, S., XU, H., LEE, S. M., FORSTER, M. D., AHMAD, T., HILEY, C. T., ABBOSH, C., FALZON, M., BORG, E., MARAFIOTI, T., LAWRENCE, D., HAYWARD, M., KOLVEKAR, S., PANAGIOTOPOULOS, N., JANES, S. M., THAKRAR, R., AHMED, A., BLACKHALL, F., SUMMERS, Y., SHAH, R., JOSEPH, L., QUINN, A. M., CROSBIE, P. A., NAIDU, B., MIDDLETON, G., LANGMAN, G., TROTTER, S., NICOLSON, M., REMMEN, H., KERR, K., CHETTY, M., GOMERSALL, L., FENNELL, D. A., NAKAS, A., RATHINAM, S., ANAND, G., KHAN, S., RUSSELL, P., EZHIL, V., ISMAIL, B., IRVIN-SELLERS, M., PRAKASH, V., LESTER, J. F., KORNASZEWSKA, M., ATTANOOS, R., ADAMS, H., DAVIES, H., DENTRO, S., TANIERE, P., O'SULLIVAN, B., LOWE, H. L., HARTLEY, J. A., ILES, N., BELL, H., NGAI, Y., SHAW, J. A., HERRERO, J., SZALLASI, Z., SCHWARZ, R. F., STEWART, A., QUEZADA, S. A., LE QUESNE, J., VAN LOO, P., DIVE, C., HACKSHAW, A., SWANTON, C. & CONSORTIUM, T. R. 2017. Tracking the Evolution of Non-Small-Cell Lung Cancer. *N Engl J Med,* 376**,** 2109-2121.

JAMIESON, N. B., CARTER, C. R., MCKAY, C. J. & OIEN, K. A. 2011. Tissue biomarkers for prognosis in pancreatic ductal adenocarcinoma: a systematic review and meta-analysis. *Clin Cancer Res,* 17**,** 3316-31.

JAMIESON, N. B., CHAN, N. I., FOULIS, A. K., DICKSON, E. J., MCKAY, C. J. & CARTER, C. R. 2013. The prognostic influence of resection margin clearance following pancreaticoduodenectomy for pancreatic ductal adenocarcinoma. *J Gastrointest Surg,* 17**,** 511-21.

JAMIESON, N. B., FOULIS, A. K., OIEN, K. A., GOING, J. J., GLEN, P., DICKSON, E. J., IMRIE, C. W., MCKAY, C. J. & CARTER, R. 2010. Positive mobilization margins alone do not influence survival following pancreatico-duodenectomy for pancreatic ductal adenocarcinoma. *Ann Surg,* 251**,** 1003-10.

JAMIESON, N. B., MOHAMED, M., OIEN, K. A., FOULIS, A. K., DICKSON, E. J., IMRIE, C. W., CARTER, C. R., MCKAY, C. J. & MCMILLAN, D. C. 2012. The relationship between tumor inflammatory cell infiltrate and outcome in patients with pancreatic ductal adenocarcinoma. *Ann Surg Oncol,* 19**,** 3581-90.

JIANG, H., HEGDE, S., KNOLHOFF, B. L., ZHU, Y., HERNDON, J. M., MEYER, M. A., NYWENING, T. M., HAWKINS, W. G., SHAPIRO, I. M., WEAVER, D. T., PACHTER, J. A., WANG-GILLAM, A. & DENARDO, D. G. 2016. Targeting focal adhesion kinase renders pancreatic cancers responsive to checkpoint immunotherapy. *Nat Med,* 22**,** 851-60.

JIANG, X., HAO, H. X., GROWNEY, J. D., WOOLFENDEN, S., BOTTIGLIO, C., NG, N., LU, B., HSIEH, M. H., BAGDASARIAN, L., MEYER, R., SMITH, T. R., AVELLO, M., CHARLAT, O., XIE, Y., PORTER, J. A., PAN, S., LIU, J., MCLAUGHLIN, M. E. & CONG, F. 2013. Inactivating mutations of RNF43 confer Wnt dependency in pancreatic ductal adenocarcinoma. *Proc Natl Acad Sci U S A,* 110**,** 12649-54.

JONES, S., ZHANG, X., PARSONS, D. W., LIN, J. C., LEARY, R. J., ANGENENDT, P., MANKOO, P., CARTER, H., KAMIYAMA, H., JIMENO, A., HONG, S. M., FU, B., LIN, M. T., CALHOUN, E. S., KAMIYAMA, M., WALTER, K., NIKOLSKAYA, T., NIKOLSKY, Y., HARTIGAN, J., SMITH, D. R., HIDALGO, M., LEACH, S. D., KLEIN, A. P., JAFFEE, E. M., GOGGINS, M., MAITRA, A., IACOBUZIO-DONAHUE, C., ESHLEMAN, J. R., KERN, S. E., HRUBAN, R. H., KARCHIN, R., PAPADOPOULOS, N., PARMIGIANI, G., VOGELSTEIN, B., VELCULESCU, V. E. & KINZLER, K. W. 2008. Core signaling pathways in human pancreatic cancers revealed by global genomic analyses. *Science,* 321**,** 1801-6.

KAELIN, W. G., JR. 2005. The concept of synthetic lethality in the context of anticancer therapy. *Nat Rev Cancer,* 5**,** 689-98.

KARNITZ, L. M. & ZOU, L. 2015. Molecular Pathways: Targeting ATR in Cancer Therapy. *Clin Cancer Res,* 21**,** 4780-5.

KAUFMAN, B., SHAPIRA-FROMMER, R., SCHMUTZLER, R. K., AUDEH, M. W., FRIEDLANDER, M., BALMANA, J., MITCHELL, G., FRIED, G., STEMMER, S. M., HUBERT, A., ROSENGARTEN, O., STEINER, M., LOMAN, N., BOWEN, K., FIELDING, A. & DOMCHEK, S. M. 2015. Olaparib monotherapy in patients with advanced cancer and a germline BRCA1/2 mutation. *J Clin Oncol,* 33**,** 244-50.

KENNEDY, R. D. & D'ANDREA, A. D. 2006. DNA repair pathways in clinical practice: lessons from pediatric cancer susceptibility syndromes. *J Clin Oncol,* 24**,** 3799-808.

KHOJA, L., BACKEN, A., SLOANE, R., MENASCE, L., RYDER, D., KREBS, M., BOARD, R., CLACK, G., HUGHES, A., BLACKHALL, F., VALLE, J. W. & DIVE, C. 2012. A pilot study to explore circulating tumour cells in pancreatic cancer as a novel biomarker. *Br J Cancer,* 106**,** 508-16.

KIM, H., GEORGE, E., RAGLAND, R., RAFIAL, S., ZHANG, R., KREPLER, C., MORGAN, M., HERLYN, M., BROWN, E. & SIMPKINS, F. 2017. Targeting the ATR/CHK1 Axis with PARP Inhibition Results in Tumor Regression in BRCA-Mutant Ovarian Cancer Models. *Clin Cancer Res,* 23**,** 3097-3108.

KIM, H., SAKA, B., KNIGHT, S., BORGES, M., CHILDS, E., KLEIN, A., WOLFGANG, C., HERMAN, J., ADSAY, V. N., HRUBAN, R. H. & GOGGINS, M. 2014. Having pancreatic cancer with tumoral loss of ATM and normal TP53 protein expression is associated with a poorer prognosis. *Clin Cancer Res,* 20**,** 1865-72.

KLEIN, A. P. 2013. Identifying people at a high risk of developing pancreatic cancer. *Nat Rev Cancer,* 13**,** 66-74.

KRAJEWSKA, M., FEHRMANN, R. S., SCHOONEN, P. M., LABIB, S., DE VRIES, E. G., FRANKE, L. & VAN VUGT, M. A. 2015. ATR inhibition preferentially targets homologous recombination-deficient tumor cells. *Oncogene,* 34**,** 3474-81.

KULU, Y., SCHMIED, B. M., WERNER, J., MUSELLI, P., BUCHLER, M. W. & SCHMIDT, J. 2009. Total pancreatectomy for pancreatic cancer: indications and operative technique. *HPB (Oxford),* 11**,** 469-75.

KURIHARA, T., ITOI, T., SOFUNI, A., ITOKAWA, F., TSUCHIYA, T., TSUJI, S., ISHII, K., IKEUCHI, N., TSUCHIDA, A., KASUYA, K., KAWAI, T., SAKAI, Y. & MORIYASU, F. 2008. Detection of circulating tumor cells in patients with pancreatic cancer: a preliminary result. *J Hepatobiliary Pancreat Surg,* 15**,** 189-95.

LAU, M. K., DAVILA, J. A. & SHAIB, Y. H. 2010. Incidence and survival of pancreatic head and body and tail cancers: a population-based study in the United States. *Pancreas,* 39**,** 458-62.

LE, D. T., URAM, J. N., WANG, H., BARTLETT, B. R., KEMBERLING, H., EYRING, A. D., SKORA, A. D., LUBER, B. S., AZAD, N. S., LAHERU, D., BIEDRZYCKI, B., DONEHOWER, R. C., ZAHEER, A., FISHER, G. A., CROCENZI, T. S., LEE, J. J., DUFFY, S. M., GOLDBERG, R. M., DE LA CHAPELLE, A., KOSHIJI, M., BHAIJEE, F., HUEBNER, T., HRUBAN, R. H., WOOD, L. D., CUKA, N., PARDOLL, D. M., PAPADOPOULOS, N., KINZLER, K. W., ZHOU, S., CORNISH, T. C., TAUBE, J. M., ANDERS, R. A., ESHLEMAN, J. R., VOGELSTEIN, B. & DIAZ, L. A., JR. 2015. PD-1 Blockade in Tumors with Mismatch-Repair Deficiency. *N Engl J Med,* 372**,** 2509-20.

LECONA, E. & FERNANDEZ-CAPETILLO, O. 2018. Targeting ATR in cancer. *Nat Rev Cancer*.

LEE, J. J. & LIU, D. D. 2008. A predictive probability design for phase II cancer clinical trials. *Clin Trials,* 5**,** 93-106.

LEIJEN, S., VAN GEEL, R. M., PAVLICK, A. C., TIBES, R., ROSEN, L., RAZAK, A. R., LAM, R., DEMUTH, T., ROSE, S., LEE, M. A., FRESHWATER, T., SHUMWAY, S., LIANG, L. W., OZA, A. M., SCHELLENS, J. H. & SHAPIRO, G. I. 2016a. Phase I Study Evaluating WEE1 Inhibitor AZD1775 As Monotherapy and in Combination With Gemcitabine, Cisplatin, or Carboplatin in Patients With Advanced Solid Tumors. *J Clin Oncol,* 34**,** 4371-4380.

LEIJEN, S., VAN GEEL, R. M., SONKE, G. S., DE JONG, D., ROSENBERG, E. H., MARCHETTI, S., PLUIM, D., VAN WERKHOVEN, E., ROSE, S., LEE, M. A., FRESHWATER, T., BEIJNEN, J. H. & SCHELLENS, J. H. 2016b. Phase II Study of WEE1 Inhibitor AZD1775 Plus Carboplatin in Patients With TP53-Mutated Ovarian Cancer Refractory or Resistant to First-Line Therapy Within 3 Months. *J Clin Oncol,* 34**,** 4354-4361.

LHEUREUX, S., BRUCE, J. P., BURNIER, J. V., KARAKASIS, K., SHAW, P. A., CLARKE, B. A., YANG, S. Y., QUEVEDO, R., LI, T., DOWAR, M., BOWERING, V., PUGH, T. J. & OZA, A. M. 2017. Somatic BRCA1/2 Recovery as a Resistance Mechanism After Exceptional Response to Poly (ADP-ribose) Polymerase Inhibition. *J Clin Oncol,* 35**,** 1240-1249.

LIAO, Y., SMYTH, G. K. & SHI, W. 2014. featureCounts: an efficient general purpose program for assigning sequence reads to genomic features. *Bioinformatics,* 30**,** 923-30.

LOHSE, I., MASON, J., CAO, P. M., PINTILIE, M., BRAY, M. & HEDLEY, D. W. 2017. Activity of the novel polo-like kinase 4 inhibitor CFI-400945 in pancreatic cancer patient-derived xenografts. *Oncotarget,* 8**,** 3064-3071.

LORD, C. J. & ASHWORTH, A. 2012. The DNA damage response and cancer therapy. *Nature,* 481**,** 287-94.

LORD, C. J. & ASHWORTH, A. 2013. Mechanisms of resistance to therapies targeting BRCA-mutant cancers. *Nat Med,* 19**,** 1381-8.

LORD, C. J. & ASHWORTH, A. 2016. BRCAness revisited. *Nat Rev Cancer,* 16**,** 110-20.

LORD, C. J., TUTT, A. N. & ASHWORTH, A. 2015. Synthetic lethality and cancer therapy: lessons learned from the development of PARP inhibitors. *Annu Rev Med,* 66**,** 455-70.

LOVE, M. I., HUBER, W. & ANDERS, S. 2014. Moderated estimation of fold change and dispersion for RNA-seq data with DESeq2. *Genome Biol,* 15**,** 550.

MACHERET, M. & HALAZONETIS, T. D. 2018. Intragenic origins due to short G1 phases underlie oncogene-induced DNA replication stress. *Nature,* 555**,** 112-116.

MACKAY, T. M., VAN ERNING, F. N., VAN DER GEEST, L. G. M., DE GROOT, J. W. B., HAJ MOHAMMAD, N., LEMMENS, V. E., VAN LAARHOVEN, H. W., BESSELINK, M. G. & WILMINK, J. W. 2018. Association between primary origin (head, body and tail) of metastasised pancreatic ductal adenocarcinoma and oncologic outcome: A population-based analysis. *Eur J Cancer,* 106**,** 99-105.

MAITRA, A., FUKUSHIMA, N., TAKAORI, K. & HRUBAN, R. H. 2005. Precursors to invasive pancreatic cancer. *Adv Anat Pathol,* 12**,** 81-91.

MAKOHON-MOORE, A. P., ZHANG, M., REITER, J. G., BOZIC, I., ALLEN, B., KUNDU, D., CHATTERJEE, K., WONG, F., JIAO, Y., KOHUTEK, Z. A., HONG, J., ATTIYEH, M., JAVIER, B., WOOD, L. D., HRUBAN, R. H., NOWAK, M. A., PAPADOPOULOS, N., KINZLER, K. W., VOGELSTEIN, B. & IACOBUZIO-DONAHUE, C. A. 2017. Limited heterogeneity of known driver gene mutations among the metastases of individual patients with pancreatic cancer. *Nat Genet*.

MANN, K. M., WARD, J. M., YEW, C. C., KOVOCHICH, A., DAWSON, D. W., BLACK, M. A., BRETT, B. T., SHEETZ, T. E., DUPUY, A. J., CHANG, D. K., BIANKIN, A. V., WADDELL, N., KASSAHN, K. S., GRIMMOND, S. M., RUST, A. G., ADAMS, D. J., JENKINS, N. A. & COPELAND, N. G. 2012. Sleeping Beauty mutagenesis reveals cooperating mutations and pathways in pancreatic adenocarcinoma. *Proc Natl Acad Sci U S A,* 109**,** 5934-41.

MARTINI, P., SALES, G., MASSA, M. S., CHIOGNA, M. & ROMUALDI, C. 2013. Along signal paths: an empirical gene set approach exploiting pathway topology. *Nucleic Acids Res,* 41**,** e19.

MATULONIS, U. A., PENSON, R. T., DOMCHEK, S. M., KAUFMAN, B., SHAPIRA-FROMMER, R., AUDEH, M. W., KAYE, S., MOLIFE, L. R., GELMON, K. A., ROBERTSON, J. D., MANN, H., HO, T. W. & COLEMAN, R. L. 2016. Olaparib monotherapy in patients with advanced relapsed ovarian cancer and a germline BRCA1/2 mutation: a multistudy analysis of response rates and safety. *Ann Oncol,* 27**,** 1013-9.

MCCABE, N., TURNER, N. C., LORD, C. J., KLUZEK, K., BIALKOWSKA, A., SWIFT, S., GIAVARA, S., O'CONNOR, M. J., TUTT, A. N., ZDZIENICKA, M. Z., SMITH, G. C. & ASHWORTH, A. 2006. Deficiency in the repair of DNA damage by homologous recombination and sensitivity to poly(ADP-ribose) polymerase inhibition. *Cancer Res,* 66**,** 8109-15.

MCGRANAHAN, N. & SWANTON, C. 2015. Biological and therapeutic impact of intratumor heterogeneity in cancer evolution. *Cancer Cell,* 27**,** 15-26.

MERIC-BERNSTAM, F., BRUSCO, L., SHAW, K., HOROMBE, C., KOPETZ, S., DAVIES, M. A., ROUTBORT, M., PIHA-PAUL, S. A., JANKU, F., UENO, N., HONG, D., DE GROOT, J., RAVI, V., LI, Y., LUTHRA, R., PATEL, K., BROADDUS, R., MENDELSOHN, J. & MILLS, G. B. 2015. Feasibility of Large-Scale Genomic Testing to Facilitate Enrollment Onto Genomically Matched Clinical Trials. *J Clin Oncol,* 33**,** 2753-62.

MIRZA, M. R., MONK, B. J., HERRSTEDT, J., OZA, A. M., MAHNER, S., REDONDO, A., FABBRO, M., LEDERMANN, J. A., LORUSSO, D., VERGOTE, I., BEN-BARUCH, N. E., MARTH, C., MADRY, R., CHRISTENSEN, R. D., BEREK, J. S., DORUM, A., TINKER, A. V., DU BOIS, A., GONZALEZ-MARTIN, A., FOLLANA, P., BENIGNO, B., ROSENBERG, P., GILBERT, L., RIMEL, B. J., BUSCEMA, J., BALSER, J. P., AGARWAL, S., MATULONIS, U. A. & INVESTIGATORS, E.-O. N. 2016. Niraparib Maintenance Therapy in Platinum-Sensitive, Recurrent Ovarian Cancer. *N Engl J Med,* 375**,** 2154-2164.

MOFFITT, R. A., MARAYATI, R., FLATE, E. L., VOLMAR, K. E., LOEZA, S. G., HOADLEY, K. A., RASHID, N. U., WILLIAMS, L. A., EATON, S. C., CHUNG, A. H., SMYLA, J. K., ANDERSON, J. M., KIM, H. J., BENTREM, D. J., TALAMONTI, M. S., IACOBUZIO-DONAHUE, C. A., HOLLINGSWORTH, M. A. & YEH, J. J. 2015. Virtual microdissection identifies distinct tumor- and stroma-specific subtypes of pancreatic ductal adenocarcinoma. *Nat Genet,* 47**,** 1168-78.

MOHNI, K. N., THOMPSON, P. S., LUZWICK, J. W., GLICK, G. G., PENDLETON, C. S., LEHMANN, B. D., PIETENPOL, J. A. & CORTEZ, D. 2015. A Synthetic Lethal Screen Identifies

DNA Repair Pathways that Sensitize Cancer Cells to Combined ATR Inhibition and Cisplatin Treatments. *PLoS One,* 10**,** e0125482.

MOKDAD, A. A., MINTER, R. M., ZHU, H., AUGUSTINE, M. M., POREMBKA, M. R., WANG, S. C., YOPP, A. C., MANSOUR, J. C., CHOTI, M. A. & POLANCO, P. M. 2017. Neoadjuvant Therapy Followed by Resection Versus Upfront Resection for Resectable Pancreatic Cancer: A Propensity Score Matched Analysis. *J Clin Oncol,* 35**,** 515-522.

MURPHY, J. E., WO, J. Y., RYAN, D. P., JIANG, W., YEAP, B. Y., DRAPEK, L. C., BLASZKOWSKY, L. S., KWAK, E. L., ALLEN, J. N., CLARK, J. W., FARIS, J. E., ZHU, A. X., GOYAL, L., LILLEMOE, K. D., DELANEY, T. F., FERNANDEZ-DEL CASTILLO, C., FERRONE, C. R. & HONG, T. S. 2018. Total Neoadjuvant Therapy With FOLFIRINOX Followed by Individualized Chemoradiotherapy for Borderline Resectable Pancreatic Adenocarcinoma: A Phase 2 Clinical Trial. *JAMA Oncol,* 4**,** 963-969.

MURPHY, N. C., SCARLETT, C. J., KENCH, J. G., SUM, E. Y., SEGARA, D., COLVIN, E. K., SUSANTO, J., COSMAN, P. H., LEE, C. S., MUSGROVE, E. A., SUTHERLAND, R. L., LINDEMAN, G. J., HENSHALL, S. M., VISVADER, J. E. & BIANKIN, A. V. 2008. Expression of LMO4 and outcome in pancreatic ductal adenocarcinoma. *Br J Cancer,* 98**,** 537-41.

NAVIN, N., KENDALL, J., TROGE, J., ANDREWS, P., RODGERS, L., MCINDOO, J., COOK, K., STEPANSKY, A., LEVY, D., ESPOSITO, D., MUTHUSWAMY, L., KRASNITZ, A., MCCOMBIE, W. R., HICKS, J. & WIGLER, M. 2011. Tumour evolution inferred by single-cell sequencing. *Nature,* 472**,** 90-4.

NEOPTOLEMOS, J. P., PALMER, D. H., GHANEH, P., PSARELLI, E. E., VALLE, J. W., HALLORAN, C. M., FALUYI, O., O'REILLY, D. A., CUNNINGHAM, D., WADSLEY, J., DARBY, S., MEYER, T., GILLMORE, R., ANTHONEY, A., LIND, P., GLIMELIUS, B., FALK, S., IZBICKI, J. R., MIDDLETON, G. W., CUMMINS, S., ROSS, P. J., WASAN, H., MCDONALD, A., CROSBY, T., MA, Y. T., PATEL, K., SHERRIFF, D., SOOMAL, R., BORG, D., SOTHI, S., HAMMEL, P., HACKERT, T., JACKSON, R., BUCHLER, M. W. & EUROPEAN STUDY GROUP FOR PANCREATIC, C. 2017. Comparison of adjuvant gemcitabine and capecitabine with gemcitabine monotherapy in patients with resected pancreatic cancer (ESPAC-4): a multicentre, open-label, randomised, phase 3 trial. *Lancet,* 389**,** 1011-1024.

NEOPTOLEMOS, J. P., STOCKEN, D. D., BASSI, C., GHANEH, P., CUNNINGHAM, D., GOLDSTEIN, D., PADBURY, R., MOORE, M. J., GALLINGER, S., MARIETTE, C., WENTE, M. N., IZBICKI, J. R., FRIESS, H., LERCH, M. M., DERVENIS, C., OLAH, A., BUTTURINI, G., DOI, R., LIND, P. A., SMITH, D., VALLE, J. W., PALMER, D. H., BUCKELS, J. A., THOMPSON, J., MCKAY, C. J., RAWCLIFFE, C. L., BUCHLER, M. W. & EUROPEAN STUDY GROUP FOR PANCREATIC, C. 2010. Adjuvant chemotherapy with fluorouracil plus folinic acid vs gemcitabine following pancreatic cancer resection: a randomized controlled trial. *JAMA,* 304**,** 1073-81.

NEOPTOLEMOS, J. P., STOCKEN, D. D., FRIESS, H., BASSI, C., DUNN, J. A., HICKEY, H., BEGER, H., FERNANDEZ-CRUZ, L., DERVENIS, C., LACAINE, F., FALCONI, M., PEDERZOLI, P., PAP, A., SPOONER, D., KERR, D. J., BUCHLER, M. W. & EUROPEAN STUDY GROUP FOR PANCREATIC, C. 2004. A randomized trial of chemoradiotherapy and chemotherapy after resection of pancreatic cancer. *N Engl J Med,* 350**,** 1200-10.

NGUYEN, N. Q., RUSZKIEWICZ, A., CHANG, D., BAMBRICK, J. & A.V., B. 2014. Biomarker assessment from EUS-guided biopsy to predict outcomes and treatment in pancreatic cancer. *J Clin Oncol,* 32**,** 182-182.

NIELSEN, S. R., QUARANTA, V., LINFORD, A., EMEAGI, P., RAINER, C., SANTOS, A., IRELAND, L., SAKAI, T., SAKAI, K., KIM, Y. S., ENGLE, D., CAMPBELL, F., PALMER, D., KO, J. H., TUVESON, D. A., HIRSCH, E., MIELGO, A. & SCHMID, M. C. 2016. Macrophage-secreted granulin supports pancreatic cancer metastasis by inducing liver fibrosis. *Nat Cell Biol,* 18**,** 549-60.

NONES, K., WADDELL, N., WAYTE, N., PATCH, A. M., BAILEY, P., NEWELL, F., HOLMES, O., FINK, J. L., QUINN, M. C. J., TANG, Y. H., LAMPE, G., QUEK, K., LOFFLER, K. A., MANNING, S., IDRISOGLU, S., MILLER, D., XU, Q., WADDELL, N., WILSON, P. J., BRUXNER, T. J. C., CHRIST, A. N., HARLIWONG, I., NOURSE, C., NOURBAKHSH, E., ANDERSON, M., KAZAKOFF, S., LEONARD, C., WOOD, S., SIMPSON, P. T., REID, L. E., KRAUSE, L., HUSSEY, D. J.,

WATSON, D. I., LORD, R. V., NANCARROW, D., PHILLIPS, W. A., GOTLEY, D., SMITHERS, B. M., WHITEMAN, D. C., HAYWARD, N. K., CAMPBELL, P. J., PEARSON, J. V., GRIMMOND, S. M. & BARBOUR, A. P. 2014. Genomic catastrophes frequently arise in esophageal adenocarcinoma and drive tumorigenesis. *Nat Commun,* 5**,** 5224.

NORQUIST, B., WURZ, K. A., PENNIL, C. C., GARCIA, R., GROSS, J., SAKAI, W., KARLAN, B. Y., TANIGUCHI, T. & SWISHER, E. M. 2011. Secondary somatic mutations restoring BRCA1/2 predict chemotherapy resistance in hereditary ovarian carcinomas. *J Clin Oncol,* 29**,** 3008-15.

NOTTA, F., CHAN-SENG-YUE, M., LEMIRE, M., LI, Y., WILSON, G. W., CONNOR, A. A., DENROCHE, R. E., LIANG, S. B., BROWN, A. M., KIM, J. C., WANG, T., SIMPSON, J. T., BECK, T., BORGIDA, A., BUCHNER, N., CHADWICK, D., HAFEZI-BAKHTIARI, S., DICK, J. E., HEISLER, L., HOLLINGSWORTH, M. A., IBRAHIMOV, E., JANG, G. H., JOHNS, J., JORGENSEN, L. G., LAW, C., LUDKOVSKI, O., LUNGU, I., NG, K., PASTERNACK, D., PETERSEN, G. M., SHLUSH, L. I., TIMMS, L., TSAO, M. S., WILSON, J. M., YUNG, C. K., ZOGOPOULOS, G., BARTLETT, J. M., ALEXANDROV, L. B., REAL, F. X., CLEARY, S. P., ROEHRL, M. H., MCPHERSON, J. D., STEIN, L. D., HUDSON, T. J., CAMPBELL, P. J. & GALLINGER, S. 2016. A renewed model of pancreatic cancer evolution based on genomic rearrangement patterns. *Nature,* 538**,** 378-382.

NYWENING, T. M., WANG-GILLAM, A., SANFORD, D. E., BELT, B. A., PANNI, R. Z., CUSWORTH, B. M., TORIOLA, A. T., NIEMAN, R. K., WORLEY, L. A., YANO, M., FOWLER, K. J., LOCKHART, A. C., SURESH, R., TAN, B. R., LIM, K. H., FIELDS, R. C., STRASBERG, S. M., HAWKINS, W. G., DENARDO, D. G., GOEDEGEBUURE, S. P. & LINEHAN, D. C. 2016. Targeting tumour-associated macrophages with CCR2 inhibition in combination with FOLFIRINOX in patients with borderline resectable and locally advanced pancreatic cancer: a single-centre, open-label, dose-finding, non-randomised, phase 1b trial. *Lancet Oncol,* 17**,** 651-62.

O'CONNOR, M. J. 2015. Targeting the DNA Damage Response in Cancer. *Mol Cell,* 60**,** 547-60.

OETTLE, H., NEUHAUS, P., HOCHHAUS, A., HARTMANN, J. T., GELLERT, K., RIDWELSKI, K., NIEDERGETHMANN, M., ZULKE, C., FAHLKE, J., ARNING, M. B., SINN, M., HINKE, A. & RIESS, H. 2013. Adjuvant chemotherapy with gemcitabine and long-term outcomes among patients with resected pancreatic cancer: the CONKO-001 randomized trial. *JAMA,* 310**,** 1473-81.

OETTLE, H., POST, S., NEUHAUS, P., GELLERT, K., LANGREHR, J., RIDWELSKI, K., SCHRAMM, H., FAHLKE, J., ZUELKE, C., BURKART, C., GUTBERLET, K., KETTNER, E., SCHMALENBERG, H., WEIGANG-KOEHLER, K., BECHSTEIN, W. O., NIEDERGETHMANN, M., SCHMIDT-WOLF, I., ROLL, L., DOERKEN, B. & RIESS, H. 2007. Adjuvant chemotherapy with gemcitabine vs observation in patients undergoing curative-intent resection of pancreatic cancer: a randomized controlled trial. *JAMA,* 297**,** 267-77.

PARRISH, R. S. & SPENCER, H. J., 3RD 2004. Effect of normalization on significance testing for oligonucleotide microarrays. *J Biopharm Stat,* 14**,** 575-89.

PATCH, A. M., CHRISTIE, E. L., ETEMADMOGHADAM, D., GARSED, D. W., GEORGE, J., FEREDAY, S., NONES, K., COWIN, P., ALSOP, K., BAILEY, P. J., KASSAHN, K. S., NEWELL, F., QUINN, M. C., KAZAKOFF, S., QUEK, K., WILHELM-BENARTZI, C., CURRY, E., LEONG, H. S., HAMILTON, A., MILESHKIN, L., AU-YEUNG, G., KENNEDY, C., HUNG, J., CHIEW, Y. E., HARNETT, P., FRIEDLANDER, M., QUINN, M., PYMAN, J., CORDNER, S., O'BRIEN, P., LEDITSCHKE, J., YOUNG, G., STRACHAN, K., WARING, P., AZAR, W., MITCHELL, C., TRAFICANTE, N., HENDLEY, J., THORNE, H., SHACKLETON, M., MILLER, D. K., ARNAU, G. M., TOTHILL, R. W., HOLLOWAY, T. P., SEMPLE, T., HARLIWONG, I., NOURSE, C., NOURBAKHSH, E., MANNING, S., IDRISOGLU, S., BRUXNER, T. J., CHRIST, A. N., POUDEL, B., HOLMES, O., ANDERSON, M., LEONARD, C., LONIE, A., HALL, N., WOOD, S., TAYLOR, D. F., XU, Q., FINK, J. L., WADDELL, N., DRAPKIN, R., STRONACH, E., GABRA, H., BROWN, R., JEWELL, A., NAGARAJ, S. H., MARKHAM, E., WILSON, P. J., ELLUL, J., MCNALLY, O., DOYLE, M. A., VEDURURU, R., STEWART, C., LENGYEL, E., PEARSON, J. V., WADDELL, N., DEFAZIO, A., GRIMMOND, S. M. & BOWTELL, D. D. 2015. Whole-genome characterization of chemoresistant ovarian cancer. *Nature,* 521**,** 489-94.

PAULL, T. T., ROGAKOU, E. P., YAMAZAKI, V., KIRCHGESSNER, C. U., GELLERT, M. & BONNER, W. M. 2000. A critical role for histone H2AX in recruitment of repair factors to nuclear foci after DNA damage. *Curr Biol,* 10**,** 886-95.

PISHVAIAN, M. J., BIANKIN, A. V., BAILEY, P., CHANG, D. K., LAHERU, D., WOLFGANG, C. L. & BRODY, J. R. 2017. BRCA2 secondary mutation-mediated resistance to platinum and PARP inhibitor-based therapy in pancreatic cancer. *Br J Cancer,* 116**,** 1021-1026.

POPLIN, E., WASAN, H., ROLFE, L., RAPONI, M., IKDAHL, T., BONDARENKO, I., DAVIDENKO, I., BONDAR, V., GARIN, A., BOECK, S., ORMANNS, S., HEINEMANN, V., BASSI, C., EVANS, T. R., ANDERSSON, R., HAHN, H., PICOZZI, V., DICKER, A., MANN, E., VOONG, C., KAUR, P., ISAACSON, J. & ALLEN, A. 2013. Randomized, multicenter, phase II study of CO-101 versus gemcitabine in patients with metastatic pancreatic ductal adenocarcinoma: including a prospective evaluation of the role of hENT1 in gemcitabine or CO-101 sensitivity. *J Clin Oncol,* 31**,** 4453-61.

PREVO, R., FOKAS, E., REAPER, P. M., CHARLTON, P. A., POLLARD, J. R., MCKENNA, W. G., MUSCHEL, R. J. & BRUNNER, T. B. 2012. The novel ATR inhibitor VE-821 increases sensitivity of pancreatic cancer cells to radiation and chemotherapy. *Cancer Biol Ther,* 13**,** 1072-81.

PULEO, F., NICOLLE, R., BLUM, Y., CROS, J., MARISA, L., DEMETTER, P., QUERTINMONT, E., SVRCEK, M., ELAROUCI, N., IOVANNA, J., FRANCHIMONT, D., VERSET, L., GALDON, M. G., DEVIERE, J., DE REYNIES, A., LAURENT-PUIG, P., VAN LAETHEM, J. L., BACHET, J. B. & MARECHAL, R. 2018. Stratification of Pancreatic Ductal Adenocarcinomas Based on Tumor and Microenvironment Features. *Gastroenterology*.

RAJESHKUMAR, N. V., DE OLIVEIRA, E., OTTENHOF, N., WATTERS, J., BROOKS, D., DEMUTH, T., SHUMWAY, S. D., MIZUARAI, S., HIRAI, H., MAITRA, A. & HIDALGO, M. 2011. MK-1775, a potent Wee1 inhibitor, synergizes with gemcitabine to achieve tumor regressions, selectively in p53-deficient pancreatic cancer xenografts. *Clin Cancer Res,* 17**,** 2799-806.

REAPER, P. M., GRIFFITHS, M. R., LONG, J. M., CHARRIER, J. D., MACCORMICK, S., CHARLTON, P. A., GOLEC, J. M. & POLLARD, J. R. 2011. Selective killing of ATM- or p53-deficient cancer cells through inhibition of ATR. *Nat Chem Biol,* 7**,** 428-30.

REGINE, W. F., WINTER, K. A., ABRAMS, R. A., SAFRAN, H., HOFFMAN, J. P., KONSKI, A., BENSON, A. B., MACDONALD, J. S., KUDRIMOTI, M. R., FROMM, M. L., HADDOCK, M. G., SCHAEFER, P., WILLETT, C. G. & RICH, T. A. 2008. Fluorouracil vs gemcitabine chemotherapy before and after fluorouracil-based chemoradiation following resection of pancreatic adenocarcinoma: a randomized controlled trial. *JAMA,* 299**,** 1019-26.

RIETHDORF, S., FRITSCHE, H., MULLER, V., RAU, T., SCHINDLBECK, C., RACK, B., JANNI, W., COITH, C., BECK, K., JANICKE, F., JACKSON, S., GORNET, T., CRISTOFANILLI, M. & PANTEL, K. 2007. Detection of circulating tumor cells in peripheral blood of patients with metastatic breast cancer: a validation study of the CellSearch system. *Clin Cancer Res,* 13**,** 920-8.

RIZVI, N. A., MAZIERES, J., PLANCHARD, D., STINCHCOMBE, T. E., DY, G. K., ANTONIA, S. J., HORN, L., LENA, H., MINENZA, E., MENNECIER, B., OTTERSON, G. A., CAMPOS, L. T., GANDARA, D. R., LEVY, B. P., NAIR, S. G., ZALCMAN, G., WOLF, J., SOUQUET, P. J., BALDINI, E., CAPPUZZO, F., CHOUAID, C., DOWLATI, A., SANBORN, R., LOPEZ-CHAVEZ, A., GROHE, C., HUBER, R. M., HARBISON, C. T., BAUDELET, C., LESTINI, B. J. & RAMALINGAM, S. S. 2015. Activity and safety of nivolumab, an anti-PD-1 immune checkpoint inhibitor, for patients with advanced, refractory squamous non-small-cell lung cancer (CheckMate 063): a phase 2, single-arm trial. *Lancet Oncol,* 16**,** 257-65.

ROBERTS, N. J., NORRIS, A. L., PETERSEN, G. M., BONDY, M. L., BRAND, R., GALLINGER, S., KURTZ, R. C., OLSON, S. H., RUSTGI, A. K., SCHWARTZ, A. G., STOFFEL, E., SYNGAL, S., ZOGOPOULOS, G., ALI, S. Z., AXILBUND, J., CHAFFEE, K. G., CHEN, Y. C., COTE, M. L., CHILDS, E. J., DOUVILLE, C., GOES, F. S., HERMAN, J. M., IACOBUZIO-DONAHUE, C., KRAMER, M., MAKOHON-MOORE, A., MCCOMBIE, R. W., MCMAHON, K. W., NIKNAFS, N., PARLA, J., PIROOZNIA, M., POTASH, J. B., RHIM, A. D., SMITH, A. L., WANG, Y., WOLFGANG, C. L., WOOD, L. D., ZANDI, P. P., GOGGINS, M., KARCHIN, R., ESHLEMAN, J. R., PAPADOPOULOS, N., KINZLER, K. W., VOGELSTEIN, B., HRUBAN, R. H. & KLEIN, A. P. 2016.

Whole Genome Sequencing Defines the Genetic Heterogeneity of Familial Pancreatic Cancer. *Cancer Discov,* 6**,** 166-75.

ROBSON, M., IM, S. A., SENKUS, E., XU, B., DOMCHEK, S. M., MASUDA, N., DELALOGE, S., LI, W., TUNG, N., ARMSTRONG, A., WU, W., GOESSL, C., RUNSWICK, S. & CONTE, P. 2017. Olaparib for Metastatic Breast Cancer in Patients with a Germline BRCA Mutation. *N Engl J Med,* 377**,** 523-533.

RODRIGUEZ, S. A., IMPEY, S. D., PELZ, C., ENESTVEDT, B., BAKIS, G., OWENS, M. & MORGAN, T. K. 2016. RNA sequencing distinguishes benign from malignant pancreatic lesions sampled by EUS-guided FNA. *Gastrointest Endosc,* 84**,** 252-8.

ROIFE, D., DAI, B., KANG, Y., PEREZ, M. V. R., PRATT, M., LI, X. & FLEMING, J. B. 2016. Ex Vivo Testing of Patient-Derived Xenografts Mirrors the Clinical Outcome of Patients with Pancreatic Ductal Adenocarcinoma. *Clin Cancer Res,* 22**,** 6021-6030.

ROMBOUTS, S. J., WALMA, M. S., VOGEL, J. A., VAN RIJSSEN, L. B., WILMINK, J. W., MOHAMMAD, N. H., VAN SANTVOORT, H. C., MOLENAAR, I. Q. & BESSELINK, M. G. 2016. Systematic Review of Resection Rates and Clinical Outcomes After FOLFIRINOX-Based Treatment in Patients with Locally Advanced Pancreatic Cancer. *Ann Surg Oncol,* 23**,** 4352-4360.

ROONEY, M. S., SHUKLA, S. A., WU, C. J., GETZ, G. & HACOHEN, N. 2015. Molecular and genetic properties of tumors associated with local immune cytolytic activity. *Cell,* 160**,** 48-61.

ROTH, B. J., KRILOV, L., ADAMS, S., AGHAJANIAN, C. A., BACH, P., BRAITEH, F., BROSE, M. S., ELLIS, L. M., ERBA, H., GEORGE, D. J., GILBERT, M. R., JACOBSON, J. O., LARSEN, E. C., LICHTMAN, S. M., PARTRIDGE, A. H., PATEL, J. D., QUINN, D. I., ROBISON, L. L., VON ROENN, J. H., SAMLOWSKI, W., SCHWARTZ, G. K. & VOGELZANG, N. J. 2013. Clinical cancer advances 2012: annual report on progress against cancer from the american society of clinical oncology. *J Clin Oncol,* 31**,** 131-61.

ROTTENBERG, S., NYGREN, A. O., PAJIC, M., VAN LEEUWEN, F. W., VAN DER HEIJDEN, I., VAN DE WETERING, K., LIU, X., DE VISSER, K. E., GILHUIJS, K. G., VAN TELLINGEN, O., SCHOUTEN, J. P., JONKERS, J. & BORST, P. 2007. Selective induction of chemotherapy resistance of mammary tumors in a conditional mouse model for hereditary breast cancer. *Proc Natl Acad Sci U S A,* 104**,** 12117-22.

ROY, N., MALIK, S., VILLANUEVA, K. E., URANO, A., LU, X., VON FIGURA, G., SEELEY, E. S., DAWSON, D. W., COLLISSON, E. A. & HEBROK, M. 2015. Brg1 promotes both tumor-suppressive and oncogenic activities at distinct stages of pancreatic cancer formation. *Genes Dev,* 29**,** 658-71.

SAKAI, W., SWISHER, E. M., KARLAN, B. Y., AGARWAL, M. K., HIGGINS, J., FRIEDMAN, C., VILLEGAS, E., JACQUEMONT, C., FARRUGIA, D. J., COUCH, F. J., URBAN, N. & TANIGUCHI, T. 2008. Secondary mutations as a mechanism of cisplatin resistance in BRCA2-mutated cancers. *Nature,* 451**,** 1116-20.

SCHNELLDORFER, T., WARE, A. L., SARR, M. G., SMYRK, T. C., ZHANG, L., QIN, R., GULLERUD, R. E., DONOHUE, J. H., NAGORNEY, D. M. & FARNELL, M. B. 2008. Long-term survival after pancreatoduodenectomy for pancreatic adenocarcinoma: is cure possible? *Ann Surg,* 247**,** 456-62.

SCHNIEWIND, B., BESTMANN, B., HENNE-BRUNS, D., FAENDRICH, F., KREMER, B. & KUECHLER, T. 2006. Quality of life after pancreaticoduodenectomy for ductal adenocarcinoma of the pancreatic head. *Br J Surg,* 93**,** 1099-107.

SCHWARTZ, L. H., SEYMOUR, L., LITIERE, S., FORD, R., GWYTHER, S., MANDREKAR, S., SHANKAR, L., BOGAERTS, J., CHEN, A., DANCEY, J., HAYES, W., HODI, F. S., HOEKSTRA, O. S., HUANG, E. P., LIN, N., LIU, Y., THERASSE, P., WOLCHOK, J. D. & DE VRIES, E. 2016. RECIST 1.1 - Standardisation and disease-specific adaptations: Perspectives from the RECIST Working Group. *Eur J Cancer,* 62**,** 138-45.

SENER, S. F., FREMGEN, A., MENCK, H. R. & WINCHESTER, D. P. 1999. Pancreatic cancer: a report of treatment and survival trends for 100,313 patients diagnosed from 1985-1995, using the National Cancer Database. *J Am Coll Surg,* 189**,** 1-7.

SHEN, J., PENG, Y., WEI, L., ZHANG, W., YANG, L., LAN, L., KAPOOR, P., JU, Z., MO, Q., SHIH IE, M., URAY, I. P., WU, X., BROWN, P. H., SHEN, X., MILLS, G. B. & PENG, G. 2015. ARID1A Deficiency Impairs the DNA Damage Checkpoint and Sensitizes Cells to PARP Inhibitors. *Cancer Discov,* 5**,** 752-67.

SIEGEL, R. L., MILLER, K. D. & JEMAL, A. 2018. Cancer statistics, 2018. *CA Cancer J Clin,* 68**,** 7-30.

SJOQUIST, K. M., CHIN, V. T., CHANTRILL, L. A., O'CONNOR, C., HEMMINGS, C., CHANG, D. K., CHOU, A., PAJIC, M., JOHNS, A. L., NAGRIAL, A. M., BIANKIN, A. V. & YIP, D. 2014. Personalising pancreas cancer treatment: When tissue is the issue. *World J Gastroenterol,* 20**,** 7849-63.

SOHN, T. A., YEO, C. J., CAMERON, J. L., KONIARIS, L., KAUSHAL, S., ABRAMS, R. A., SAUTER, P. K., COLEMAN, J., HRUBAN, R. H. & LILLEMOE, K. D. 2000. Resected adenocarcinoma of the pancreas-616 patients: results, outcomes, and prognostic indicators. *J Gastrointest Surg,* 4**,** 567-79.

SPERTI, C., PASQUALI, C., PICCOLI, A. & PEDRAZZOLI, S. 1997. Recurrence after resection for ductal adenocarcinoma of the pancreas. *World J Surg,* 21**,** 195-200.

STEELE, C. W., KARIM, S. A., LEACH, J. D., BAILEY, P., UPSTILL-GODDARD, R., RISHI, L., FOTH, M., BRYSON, S., MCDAID, K., WILSON, Z., EBERLEIN, C., CANDIDO, J. B., CLARKE, M., NIXON, C., CONNELLY, J., JAMIESON, N., CARTER, C. R., BALKWILL, F., CHANG, D. K., EVANS, T. R., STRATHDEE, D., BIANKIN, A. V., NIBBS, R. J., BARRY, S. T., SANSOM, O. J. & MORTON, J. P. 2016. CXCR2 Inhibition Profoundly Suppresses Metastases and Augments Immunotherapy in Pancreatic Ductal Adenocarcinoma. *Cancer Cell,* 29**,** 832-45.

STROBEL, O. & BUCHLER, M. W. 2016. [Therapy of locally advanced pancreatic cancer with FOLFIRINOX]. *Chirurg,* 87**,** 699.

STROBEL, O., HINZ, U., GLUTH, A., HANK, T., HACKERT, T., BERGMANN, F., WERNER, J. & BUCHLER, M. W. 2015. Pancreatic adenocarcinoma: number of positive nodes allows to distinguish several N categories. *Ann Surg,* 261**,** 961-9.

SUENAGA, M., FUJII, T., KANDA, M., TAKAMI, H., OKUMURA, N., INOKAWA, Y., KOBAYASHI, D., TANAKA, C., YAMADA, S., SUGIMOTO, H., NOMOTO, S., FUJIWARA, M. & KODERA, Y. 2014. Pattern of first recurrent lesions in pancreatic cancer: hepatic relapse is associated with dismal prognosis and portal vein invasion. *Hepatogastroenterology,* 61**,** 1756-61.

SUGIURA, T., UESAKA, K., MIHARA, K., SASAKI, K., KANEMOTO, H., MIZUNO, T. & OKAMURA, Y. 2013. Margin status, recurrence pattern, and prognosis after resection of pancreatic cancer. *Surgery,* 154**,** 1078-86.

SWANTON, C. 2012. Intratumor heterogeneity: evolution through space and time. *Cancer Res,* 72**,** 4875-82.

SWISHER, E. M., LIN, K. K., OZA, A. M., SCOTT, C. L., GIORDANO, H., SUN, J., KONECNY, G. E., COLEMAN, R. L., TINKER, A. V., O'MALLEY, D. M., KRISTELEIT, R. S., MA, L., BELL-MCGUINN, K. M., BRENTON, J. D., CRAGUN, J. M., OAKNIN, A., RAY-COQUARD, I., HARRELL, M. I., MANN, E., KAUFMANN, S. H., FLOQUET, A., LEARY, A., HARDING, T. C., GOBLE, S., MALONEY, L., ISAACSON, J., ALLEN, A. R., ROLFE, L., YELENSKY, R., RAPONI, M. & MCNEISH, I. A. 2016. Rucaparib in relapsed, platinum-sensitive high-grade ovarian carcinoma (ARIEL2 Part 1): an international, multicentre, open-label, phase 2 trial. *Lancet Oncol*.

SZKLARCZYK, D., FRANCESCHINI, A., WYDER, S., FORSLUND, K., HELLER, D., HUERTA-CEPAS, J., SIMONOVIC, M., ROTH, A., SANTOS, A., TSAFOU, K. P., KUHN, M., BORK, P., JENSEN, L. J. & VON MERING, C. 2015. STRING v10: protein-protein interaction networks, integrated over the tree of life. *Nucleic Acids Res,* 43**,** D447-52.

TANG, K., LU, W., QIN, W. & WU, Y. 2016. Neoadjuvant therapy for patients with borderline resectable pancreatic cancer: A systematic review and meta-analysis of response and resection percentages. *Pancreatology,* 16**,** 28-37.

TARANTINO, I., WARSCHKOW, R., HACKERT, T., SCHMIED, B. M., BUCHLER, M. W., STROBEL, O. & ULRICH, A. 2017. Staging of pancreatic cancer based on the number of positive lymph nodes. *Br J Surg,* 104**,** 608-618.

THOMPSON, J. C., YEE, S. S., TROXEL, A. B., SAVITCH, S. L., FAN, R., BALLI, D., LIEBERMAN, D. B., MORRISSETTE, J. D., EVANS, T. L., BAUML, J., AGGARWAL, C., KOSTEVA, J. A., ALLEY, E., CIUNCI, C., COHEN, R. B., BAGLEY, S., STONEHOUSE-LEE, S., SHERRY, V. E., GILBERT, E., LANGER, C., VACHANI, A. & CARPENTER, E. L. 2016. Detection of Therapeutically Targetable Driver and Resistance Mutations in Lung Cancer Patients by Next-Generation Sequencing of Cell-Free Circulating Tumor DNA. *Clin Cancer Res,* 22**,** 5772-5782.

TOL, J. A., GOUMA, D. J., BASSI, C., DERVENIS, C., MONTORSI, M., ADHAM, M., ANDREN-SANDBERG, A., ASBUN, H. J., BOCKHORN, M., BUCHLER, M. W., CONLON, K. C., FERNANDEZ-CRUZ, L., FINGERHUT, A., FRIESS, H., HARTWIG, W., IZBICKI, J. R., LILLEMOE, K. D., MILICEVIC, M. N., NEOPTOLEMOS, J. P., SHRIKHANDE, S. V., VOLLMER, C. M., YEO, C. J. & CHARNLEY, R. M. 2014. Definition of a standard lymphadenectomy in surgery for pancreatic ductal adenocarcinoma: a consensus statement by the International Study Group on Pancreatic Surgery (ISGPS). *Surgery,* 156**,** 591-600.

TSENG, J. F., TAMM, E. P., LEE, J. E., PISTERS, P. W. & EVANS, D. B. 2006. Venous resection in pancreatic cancer surgery. *Best Pract Res Clin Gastroenterol,* 20**,** 349-64.

TURNER, N. C., RO, J., ANDRE, F., LOI, S., VERMA, S., IWATA, H., HARBECK, N., LOIBL, S., HUANG BARTLETT, C., ZHANG, K., GIORGETTI, C., RANDOLPH, S., KOEHLER, M. & CRISTOFANILLI, M. 2015. Palbociclib in Hormone-Receptor-Positive Advanced Breast Cancer. *N Engl J Med,* 373**,** 209-19.

TUTT, A., GABRIEL, A., BERTWISTLE, D., CONNOR, F., PATERSON, H., PEACOCK, J., ROSS, G. & ASHWORTH, A. 1999. Absence of Brca2 causes genome instability by chromosome breakage and loss associated with centrosome amplification. *Curr Biol,* 9**,** 1107-10.

VALERO, V., 3RD, SAUNDERS, T. J., HE, J., WEISS, M. J., CAMERON, J. L., DHOLAKIA, A., WILD, A. T., SHIN, E. J., KHASHAB, M. A., O'BROIN-LENNON, A. M., ALI, S. Z., LAHERU, D., HRUBAN, R. H., IACOBUZIO-DONAHUE, C. A., HERMAN, J. M. & WOLFGANG, C. L. 2015. Reliable Detection of Somatic Mutations in Fine Needle Aspirates of Pancreatic Cancer With Next-generation Sequencing: Implications for Surgical Management. *Ann Surg*.

VALERO, V., 3RD, SAUNDERS, T. J., HE, J., WEISS, M. J., CAMERON, J. L., DHOLAKIA, A., WILD, A. T., SHIN, E. J., KHASHAB, M. A., O'BROIN-LENNON, A. M., ALI, S. Z., LAHERU, D., HRUBAN, R. H., IACOBUZIO-DONAHUE, C. A., HERMAN, J. M. & WOLFGANG, C. L. 2016. Reliable Detection of Somatic Mutations in Fine Needle Aspirates of Pancreatic Cancer With Next-generation Sequencing: Implications for Surgical Management. *Ann Surg,* 263**,** 153-61.

VAN DEN BROECK, A., SERGEANT, G., ECTORS, N., VAN STEENBERGEN, W., AERTS, R. & TOPAL, B. 2009. Patterns of recurrence after curative resection of pancreatic ductal adenocarcinoma. *Eur J Surg Oncol,* 35**,** 600-4.

VAN ROESSEL, S., KASUMOVA, G. G., VERHEIJ, J., NAJARIAN, R. M., MAGGINO, L., DE PASTENA, M., MALLEO, G., MARCHEGIANI, G., SALVIA, R., NG, S. C., DE GEUS, S. W., LOF, S., GIOVINAZZO, F., VAN DAM, J. L., KENT, T. S., BUSCH, O. R., VAN EIJCK, C. H., KOERKAMP, B. G., ABU HILAL, M., BASSI, C., TSENG, J. F. & BESSELINK, M. G. 2018. International Validation of the Eighth Edition of the American Joint Committee on Cancer (AJCC) TNM Staging System in Patients With Resected Pancreatic Cancer. *JAMA Surg***,** e183617.

VILLARROEL, M. C., RAJESHKUMAR, N. V., GARRIDO-LAGUNA, I., DE JESUS-ACOSTA, A., JONES, S., MAITRA, A., HRUBAN, R. H., ESHLEMAN, J. R., KLEIN, A., LAHERU, D., DONEHOWER, R. & HIDALGO, M. 2011. Personalizing cancer treatment in the age of global genomic analyses: PALB2 gene mutations and the response to DNA damaging agents in pancreatic cancer. *Mol Cancer Ther,* 10**,** 3-8.

VON HOFF, D. D., ERVIN, T., ARENA, F. P., CHIOREAN, E. G., INFANTE, J., MOORE, M., SEAY, T., TJULANDIN, S. A., MA, W. W., SALEH, M. N., HARRIS, M., RENI, M., DOWDEN, S., LAHERU, D., BAHARY, N., RAMANATHAN, R. K., TABERNERO, J., HIDALGO, M., GOLDSTEIN, D., VAN CUTSEM, E., WEI, X., IGLESIAS, J. & RENSCHLER, M. F. 2013. Increased survival in pancreatic cancer with nab-paclitaxel plus gemcitabine. *N Engl J Med,* 369**,** 1691-703.

WADDELL, N., PAJIC, M., PATCH, A. M., CHANG, D. K., KASSAHN, K. S., BAILEY, P., JOHNS, A. L., MILLER, D., NONES, K., QUEK, K., QUINN, M. C., ROBERTSON, A. J., FADLULLAH, M. Z., BRUXNER, T. J., CHRIST, A. N., HARLIWONG, I., IDRISOGLU, S., MANNING, S., NOURSE, C., NOURBAKHSH, E., WANI, S., WILSON, P. J., MARKHAM, E., CLOONAN, N., ANDERSON, M. J., FINK, J. L., HOLMES, O., KAZAKOFF, S. H., LEONARD, C., NEWELL, F., POUDEL, B., SONG, S., TAYLOR, D., WADDELL, N., WOOD, S., XU, Q., WU, J., PINESE, M., COWLEY, M. J., LEE, H. C., JONES, M. D., NAGRIAL, A. M., HUMPHRIS, J., CHANTRILL, L. A., CHIN, V., STEINMANN, A. M., MAWSON, A., HUMPHREY, E. S., COLVIN, E. K., CHOU, A., SCARLETT, C. J., PINHO, A. V., GIRY-LATERRIERE, M., ROOMAN, I., SAMRA, J. S., KENCH, J. G., PETTITT, J. A., MERRETT, N. D., TOON, C., EPARI, K., NGUYEN, N. Q., BARBOUR, A., ZEPS, N., JAMIESON, N. B., GRAHAM, J. S., NICLOU, S. P., BJERKVIG, R., GRUTZMANN, R., AUST, D., HRUBAN, R. H., MAITRA, A., IACOBUZIO-DONAHUE, C. A., WOLFGANG, C. L., MORGAN, R. A., LAWLOR, R. T., CORBO, V., BASSI, C., FALCONI, M., ZAMBONI, G., TORTORA, G., TEMPERO, M. A., GILL, A. J., ESHLEMAN, J. R., PILARSKY, C., SCARPA, A., MUSGROVE, E. A., PEARSON, J. V., BIANKIN, A. V. & GRIMMOND, S. M. 2015. Whole genomes redefine the mutational landscape of pancreatic cancer. *Nature,* 518**,** 495-501.

WANG, S., HUANG, S. & SUN, Y. L. 2017. Epithelial-Mesenchymal Transition in Pancreatic Cancer: A Review. *Biomed Res Int,* 2017**,** 2646148.

WATANABE, I., SASAKI, S., KONISHI, M., NAKAGOHRI, T., INOUE, K., ODA, T. & KINOSHITA, T. 2004. Onset symptoms and tumor locations as prognostic factors of pancreatic cancer. *Pancreas,* 28**,** 160-5.

WEBER, A. M. & RYAN, A. J. 2015. ATM and ATR as therapeutic targets in cancer. *Pharmacol Ther,* 149**,** 124-38.

WHITE, R. R., KATTAN, M. W., HANEY, J. C., CLARY, B. M., PAPPAS, T. N., TYLER, D. S. & BRENNAN, M. F. 2006. Evaluation of preoperative therapy for pancreatic cancer using a prognostic nomogram. *Ann Surg Oncol,* 13**,** 1485-92.

WILKERSON, M. D. & HAYES, D. N. 2010. ConsensusClusterPlus: a class discovery tool with confidence assessments and item tracking. *Bioinformatics,* 26**,** 1572-3.

WILLIAMSON, C. T., MILLER, R., PEMBERTON, H. N., JONES, S. E., CAMPBELL, J., KONDE, A., BADHAM, N., RAFIQ, R., BROUGH, R., GULATI, A., RYAN, C. J., FRANCIS, J., VERMULEN, P. B., REYNOLDS, A. R., REAPER, P. M., POLLARD, J. R., ASHWORTH, A. & LORD, C. J. 2016. ATR inhibitors as a synthetic lethal therapy for tumours deficient in ARID1A. *Nat Commun,* 7**,** 13837.

WINOGRAD, R., BYRNE, K. T., EVANS, R. A., ODORIZZI, P. M., MEYER, A. R., BAJOR, D. L., CLENDENIN, C., STANGER, B. Z., FURTH, E. E., WHERRY, E. J. & VONDERHEIDE, R. H. 2015. Induction of T-cell Immunity Overcomes Complete Resistance to PD-1 and CTLA-4 Blockade and Improves Survival in Pancreatic Carcinoma. *Cancer Immunol Res,* 3**,** 399-411.

WITKIEWICZ, A. K., MCMILLAN, E. A., BALAJI, U., BAEK, G., LIN, W. C., MANSOUR, J., MOLLAEE, M., WAGNER, K. U., KODURU, P., YOPP, A., CHOTI, M. A., YEO, C. J., MCCUE, P., WHITE, M. A. & KNUDSEN, E. S. 2015. Whole-exome sequencing of pancreatic cancer defines genetic diversity and therapeutic targets. *Nat Commun,* 6**,** 6744.

YACHIDA, S. & IACOBUZIO-DONAHUE, C. A. 2013. Evolution and dynamics of pancreatic cancer progression. *Oncogene,* 32**,** 5253-60.

YACHIDA, S., JONES, S., BOZIC, I., ANTAL, T., LEARY, R., FU, B., KAMIYAMA, M., HRUBAN, R. H., ESHLEMAN, J. R., NOWAK, M. A., VELCULESCU, V. E., KINZLER, K. W., VOGELSTEIN, B. & IACOBUZIO-DONAHUE, C. A. 2010. Distant metastasis occurs late during the genetic evolution of pancreatic cancer. *Nature,* 467**,** 1114-7.

YAGATA, H., NAKAMURA, S., TOI, M., BANDO, H., OHNO, S. & KATAOKA, A. 2008. Evaluation of circulating tumor cells in patients with breast cancer: multi-institutional clinical trial in Japan. *Int J Clin Oncol,* 13**,** 252-6.

YAMAMOTO, T., UCHIDA, Y. & TERAJIMA, H. 2017. Clinical impact of margin status on survival and recurrence pattern after curative-intent surgery for pancreatic cancer. *Asian J Surg*.

YAP, T. A., GERLINGER, M., FUTREAL, P. A., PUSZTAI, L. & SWANTON, C. 2012. Intratumor heterogeneity: seeing the wood for the trees. *Sci Transl Med,* 4**,** 127ps10.

YAP, T. A., KREBS, M. G., POSTEL-VINAY, S., BANG, Y. J., EL-KHOUEIRY, A., ABIDA, W., HARRINGTON, K., SUNDAR, R., CARTER, L., CASTANON-ALVAREZ, E., IM, S. A., BERGES, A., KHAN, M., STEPHENS, C., ROSS, G. & SORIA, J. C. 2018. Phase I modular study of AZD6738, a novel oral, potent and selective ataxia telangiectasia Rad3-related (ATR) inhibitor in combination (combo) with carboplatin, olaparib or durvalumab in patients (pts) with advanced cancers. *European Journal of Cancer,* 69**,** S2.

YAZINSKI, S. A., COMAILLS, V., BUISSON, R., GENOIS, M. M., NGUYEN, H. D., HO, C. K., TODOROVA KWAN, T., MORRIS, R., LAUFFER, S., NUSSENZWEIG, A., RAMASWAMY, S., BENES, C. H., HABER, D. A., MAHESWARAN, S., BIRRER, M. J. & ZOU, L. 2017. ATR inhibition disrupts rewired homologous recombination and fork protection pathways in PARP inhibitor-resistant BRCA-deficient cancer cells. *Genes Dev,* 31**,** 318-332.

ZEMAN, M. K. & CIMPRICH, K. A. 2014. Causes and consequences of replication stress. *Nat Cell Biol,* 16**,** 2-9.

ZHANG, J., DAI, Q., PARK, D. & DENG, X. 2016a. Targeting DNA Replication Stress for Cancer Therapy. *Genes (Basel),* 7.

ZHANG, J., ZHANG, L., LI, C., YANG, C., LI, L., SONG, S., WU, H., LIU, F., WANG, L. & GU, J. 2018. LOX-1 is a poor prognostic indicator and induces epithelial-mesenchymal transition and metastasis in pancreatic cancer patients. *Cell Oncol (Dordr),* 41**,** 73-84.

ZHANG, J. H., CHUNG, T. D. & OLDENBURG, K. R. 1999. A Simple Statistical Parameter for Use in Evaluation and Validation of High Throughput Screening Assays. *J Biomol Screen,* 4**,** 67-73.

ZHANG, Y., LAI, J., DU, Z., GAO, J., YANG, S., GORITYALA, S., XIONG, X., DENG, O., MA, Z., YAN, C., SUSANA, G., XU, Y. & ZHANG, J. 2016b. Targeting radioresistant breast cancer cells by single agent CHK1 inhibitor via enhancing replication stress. *Oncotarget,* 7**,** 34688-702.

ZHANG, Y., VELEZ-DELGADO, A., MATHEW, E., LI, D., MENDEZ, F. M., FLANNAGAN, K., RHIM, A. D., SIMEONE, D. M., BEATTY, G. L. & PASCA DI MAGLIANO, M. 2017. Myeloid cells are required for PD-1/PD-L1 checkpoint activation and the establishment of an immunosuppressive environment in pancreatic cancer. *Gut,* 66**,** 124-136.

ZHAO, Q., RASHID, A., GONG, Y., KATZ, M. H., LEE, J. E., WOLF, R., BALACHANDRAN, A., VARADHACHARY, G. R., PISTERS, P. W., WANG, H., GOMEZ, H. F., ABBRUZZESE, J. L., FLEMING, J. B. & WANG, H. 2012. Pathologic complete response to neoadjuvant therapy in patients with pancreatic ductal adenocarcinoma is associated with a better prognosis. *Ann Diagn Pathol,* 16**,** 29-37.

ZHEN, D. B., RABE, K. G., GALLINGER, S., SYNGAL, S., SCHWARTZ, A. G., GOGGINS, M. G., HRUBAN, R. H., COTE, M. L., MCWILLIAMS, R. R., ROBERTS, N. J., CANNON-ALBRIGHT, L. A., LI, D., MOYES, K., WENSTRUP, R. J., HARTMAN, A. R., SEMINARA, D., KLEIN, A. P. & PETERSEN, G. M. 2015. BRCA1, BRCA2, PALB2, and CDKN2A mutations in familial pancreatic cancer: a PACGENE study. *Genet Med,* 17**,** 569-77.

ZHENG, H., SHAO, F., MARTIN, S., XU, X. & DENG, C. X. 2017. WEE1 inhibition targets cell cycle checkpoints for triple negative breast cancers to overcome cisplatin resistance. *Sci Rep,* 7**,** 43517.

ZHENG, X., CARSTENS, J. L., KIM, J., SCHEIBLE, M., KAYE, J., SUGIMOTO, H., WU, C. C., LEBLEU, V. S. & KALLURI, R. 2015. Epithelial-to-mesenchymal transition is dispensable for metastasis but induces chemoresistance in pancreatic cancer. *Nature,* 527**,** 525-30.

ZILL, O. A., GREENE, C., SEBISANOVIC, D., SIEW, L. M., LENG, J., VU, M., HENDIFAR, A. E., WANG, Z., ATREYA, C. E., KELLEY, R. K., VAN LOON, K., KO, A. H., TEMPERO, M. A., BIVONA, T. G., MUNSTER, P. N., TALASAZ, A. & COLLISSON, E. A. 2015. Cell-Free DNA Next-Generation Sequencing in Pancreatobiliary Carcinomas. *Cancer Discov,* 5**,** 1040-8.